Design, Characterization, Evaluation and Pharmacokinetic Studies of Temozolomide Loaded Lipid Based Nanocarriers for Glioblastoma

THESIS

Submitted in partial fulfillment
of the requirements for the degree of

DOCTOR OF PHILOSOPHY

by

WAGHULE TEJASHREE VILAS ARCHANA

ID: 2017PH460287P

Under the Supervision

of

PROF. R. N. SAHA

and Co-supervision

of

DR. GAUTAM SINGHVI

BITS Pilani
Pilani | Dubai | Goa | Hyderabad

BIRLA INSTITUTE OF TECHNOLOGY AND SCIENCE, PILANI

2023

DECLARATION

I hereby declare that the thesis work entitled **'Design, Characterization, Evaluation and Pharmacokinetic Studies of Temozolomide Loaded Lipid Based Nanocarriers for Glioblastoma'** is an original piece of research work carried out under the guidance of Prof. Ranendra N. Saha and Prof. Gautam Singhvi in the Department of Pharmacy, Birla Institute of Technology and Sciences (BITS PILANI), Pilani campus. This thesis has not been submitted by me for the award of any other degree of any other University/Institute.

Waghule Tejashree Vilas

2017PH460287P

Research scholar

BITS PILANI, Pilani campus

BIRLA INSTITUTE OF TECHNOLOGY AND SCIENCE, PILANI

CERTIFICATE

This is to certify that the thesis entitled **'Design, Characterization, Evaluation and Pharmacokinetic Studies of Temozolomide Loaded Lipid Based Nanocarriers for Glioblastoma'** submitted by **Waghule Tejashree Vilas**, ID. No. **2017PH460287P** for award of Ph.D. degree of the institute, embodies original work done by her under my supervision.

Signature of the Supervisor

Prof. Ranendra N. Saha

Former Vice Chancellor (Acting)

BITS PILANI, pilani campus,

Former Director, BITS PILANI,

Dubai Campus, UAE

Signature of the Co-Supervisor

Prof. Gautam Singhvi

Associate Professor,

Department of Pharmacy,

BITS PILANI, Pilani campus,

Rajasthan

Date:

Acknowledgement

Myself, Tejashree Waghule, a Research scholar from Department of Pharmacy, Birla Institute of Technology and Sciences, Pilani, Rajasthan would like to express my sincere gratitude towards all those who played an important role in completing my thesis.

Behind every successful student is a guide who directs him through the right path to reach his goal. I feel myself blessed to receive the guidance of my supervisors Prof. R. N. Saha, Former Vice Chancellor (Acting) of BITS PILANI, pilani campus; Former Director of BITS Pilani, Dubai Campus, UAE and Dr. Gautam Singhvi, Assistant Professor, BITS PILANI, pilani campus. I express my sincere gratitude to Prof. R. N. Saha for giving me this opportunity and for his guidance and support throughout this time. His energy, enthusiasm and passion for teaching is just admirable. He has always explained the concepts using daily life examples which makes understanding easy for a student. I would like to express my deepest gratitude towards Dr. Gautam Singhvi, my M-pharm and PhD guide, for being my mentor, for believing in me, and for inspiring me. He made me realize my potential, his words always encouraged to work better and my hardwork never went unnoticed. I express my deepest gratitude to Prof. R. N. Saha and Dr. Gautam Singhvi for helping me understand my potential, for guiding to focus on solutions rather than problems, for teaching me to manage multiple tasks and making me able to face the challenges in all aspects of career and life. Inspite of being busy, they have always given time to students and brought the best out of them. They have always given us the freedom thus making learning a wonderful experience.

I would like to express my gratitude towards Dr. Krishna Iyer, Professor of Bomaby College of Pharmacy, my B-pharm teacher. Apart from teaching the basic concepts during B-pharm, it were his words which motivated me to pursue PhD.

I would like to express my sincere gratitude towards Prof. Souvik Bhattacharyya, Vice Chancellor, and Prof. Sudhirkumar Barai, Director, BITS PILANI for providing me the opportunity to pursue my doctoral research work in the institute. I also thank the Registrar, Dean and Associate Dean (AGSRD) of BITS PILANI for their timely support. I would like to thank Prof. Shamik Chakraborty for helping me with the process of vertical transfer in the institute.

I wish to express my gratitude towards Dr. Anil Gaikwad, Head of pharmacy department, Prof. Hemant Jadhav and Dr. Atish Paul, Former Head for their support during various stages of my

research. I am really thankful towards Dr. Aniruddha Roy and Dr. Anil Jindal, Doctoral Advisory Committee (DAC) members for their suggestions in the improvement of my thesis. I would also like to thank Dr. Aniruddha Roy for his support in using microfluidics and in the cell line studies. I express my gratitude towards Dr. Anil Jindal, Doctoral Research Committe Convener for his support during my PhD. I appreciate all the faculty members of BITS PILANI for sharing their valuable knowledge and experience. I am thankful to Dr. Sushil Kumar Yadav for supporting in animal studies. I also appreciate the kind support of non-teaching staff, Mr. Puran, Mr. Ram Suthar, Mr. Lakshman, Mr. Tarachand, Mr. Naveen, Mr. Abhishek, Mr. Sandeep, Mr. Vishal, Mr. Mukesh, Mr. Shyam Sunder and Mr. Shiv Kumar during this work.

I would like to express my special thanks to my seniors Mr. Vamshi Krishna and Ms. Srividya for always supporting and encouraging me, helping me find the solutions, for their valuable suggestions and helping me with the operation of the instruments. I appreciate Mr. Vamshi Krishna for helping me find solutions even after completion of his PhD. I appreciate Ms. Srividya for being a patient listener when I used to share my problems. Being an amazing teammate, she helped me with managing the academic work load whenever required. I am happy to thank Ms. Sakshi and Ms. Yashika, my juniors who have recently joined. In a short span, we have developed a great bonding. They have always been helpful whenever required and eager to learn new things from us.

I am happy to express my gratitude towards my senior, Dr. Archana Khosa, for providing her support and resources whenever required. Without her support, the journey would have become more difficult.

I am also thankful to all the other research scholars for helping me whenever in need. I would always remember the time spent in the campus and all the fun we had together. I am extremely grateful to Ms. Moumita and Ms. Geetika, my seniors and also my roommates, for creating such a homely environment in the room and also for their care whenever I was sick. Because of their company, the lock down period went peacefully. I would specially like to thank Ms. Kavyashree for helping me with microfluidics; Ms. Swetha for helping me in cell line studies; Mr. Atharva, Mr. Prashant, Ms. Geetika, Ms. Srividya, Ms. Sakshi and Ms. Yashika for helping me in animal studies. I would like to acknowledge Manisha, Ajinath and Atharva for their help, all the fun and sarcasm. I am really thankful to Prashant for his help whenever in need, for the motivation and support during the most difficult times of research. I will always remember the

time spent with Vaibhavi, Kaushal, Neha and Arisha, my juniors and M-pharm students. I would also like to thank Ms. Shalini and Mr. Vishal, my M-pharm seniors. They are the ones with whom I started my research journey.

I would like to express my gratitude towards Biophore India Pharmaceuticals Pvt Ltd (Hyderabad) for supplying a gift sample of temozolomide; VAV Life Sciences Pvt Ltd, Mumbai for gifting Leciva DSPC, DPPC and DMPC; Lipoid GmbH for supplying DSPE-PEG 2000, Mohini Organics Pvt. Ltd. for providing Glyceryl monooleate (Monegyl-O100); BASF (India) for providing a gift sample of Pluronic 127 for this research study.

Most importantly, I would like to thank God, the Almighty, for his blessings and always showing me the right path, for giving me the strength and courage to remain strong in the most difficult situations. I would like to thank my parents for always supporting me in every decision of my career, for trusting me, motivating me, for always trying to make me independent, and for allowing me to pursue my higher studies. Thanks to my younger brother for being my best friend always.

I thank Department of Pharmacy, BITS PILANI for providing all the facilities required for completion of this thesis work.

Besides this, I would also acknowledge several other people who have helped me knowingly or unknowingly in successful completion of this work.

Finally, I express my gratitude towards the innocent rats who sacrificed their lives for this research study.

Tejashree Waghule
2017PH460287P
Research Scholar
Department of Pharmacy
BITS PILANI, Pilani campus, Rajasthan

Abstract

Background and rationale:

Glioblastoma is an abnormal proliferation of the glial cells in brain and has the highest mortality rate. Among the few drugs like carmustine, lomustine, everolimus, bevacizumab, and temozolomide approved for the treatment of glioblastoma, temozolomide (TMZ) is considered a first choice. TMZ is a small molecule and amphiphilic in nature. TMZ is administered by intravenous and oral routes. It attains 100 % bioavailability when administered orally. Despite the high permeability through the blood-brain barrier, only 20-30 % brain bioavailability is achieved. This prodrug undergoes non-enzymatic modification at plasma pH. The resulting active metabolites cannot cross the blood-brain barrier due to their hydrophilic nature. The short half-life of TMZ limits the therapeutic efficacy. The limitations of conventional therapies can be tackled with nanomedicine. Lipid-based nanocarriers have gained much attention due to their biocompatible nature. The objective of the present work was to investigate lipid-based nanocarriers to prolong the plasma circulation time of TMZ and enhanced availability in brain. The nanocarriers would protect TMZ from outside pH, delay its conversion to metabolites, and control the release of TMZ. Further coating of these nanocarriers with hydrophilic lipids would prevent their opsonisation and prolong the plasma circulation of the nanocarriers. Translation of nanoformulations from lab scale to large-scale production (bench-to-bedside) is a major challenge. Thus, it is necessary to investigate the effect of various material and process parameters on the characteristics of the nanocarriers. Quality by design is a useful tool that fastens and assists in translation. A method of preparation that is organic solvent-free, involves a minimum number of steps, which is highly reproducible and industrially feasible is the present need.

Methodology:

Initially, analytical and bioanalytical methods were developed and validated for the quantification of TMZ in formulation, release, plasma, and tissue samples. A few preformulation studies were conducted to assist in the formulation. Two lipid-based nanocarriers, liposomes, and lyotropic liquid crystals were selected for investigation. A quality target product profile was designed. Critical quality attributes, material attributes, and process parameters were identified using the principles of Quality by Design. Various methods of preparation were investigated and compared. The effect of various material attributes and process parameters on critical quality attributes were investigated in detail. The designed

nanocarriers were characterized for particle size, size distribution, zeta potential, morphology, entrapment efficiency, reproducibility, drug release, hemolysis, cell cytotoxicity, cell uptake, pharmacokinetics, and biodistribution.

Results and discussion:

The developed analytical methods using UV-visible spectroscopy and HPLC were found to be reproducible, accurate, precise, and suitable for the estimation of TMZ in lipid-based nanocarriers and release samples with % RSD < 2 %. The bioanalytical method using HPLC was also found to be accurate and precise for the estimation of TMZ in plasma and tissue samples with extraction efficiency > 95 %. The stability and degradation rate kinetics revealed that TMZ was found to be unstable in alkaline pH conditions. The conversion of TMZ to AIC in alkaline pH was confirmed using UV-visible spectroscopy. Acetate buffer pH 4.5 was found to be appropriate to ensure TMZ stability and as a dissolution medium. Storage in refrigerated conditions was found to be suitable to ensure drug stability. Before starting with the formulation process, various critical quality attributes, critical material attributes, and critical process parameters were identified using the principles of quality by design. Out of the various methods screened, industrially feasible membrane extrusion and modified hot melt emulsification techniques were utilized during the formulation. Liposomes and LLCs in the particle size range of 80-120 nm were obtained with entrapment efficiency up to 50 %. The nanocarriers were found to show a prolonged release of up to 72 h. The cytotoxicity studies in glioblastoma cell lines revealed a ~ 1.6-fold cytotoxicity in comparison to free TMZ. PEGylated Liposomes and PEGylated LLCs were found to show a 3.47 and 3.18-fold less cell uptake in macrophage cell lines as compared to uncoated Liposomes and LLCs respectively. A 1.25 and 2-fold increase in the plasma $t_{1/2}$ was observed with PEGylated Liposomes and PEGylated LLCs respectively in comparison to the TMZ when administered intravenously. A 1.3 and 1.8-fold reduction in the clearance was observed with PEGylated Liposomes and PEGylated LLCs respectively in comparison to the TMZ.

It is essential to investigate the effect of various parameters on the characteristics of nanocarriers. The cell uptake and pharmacokinetics studies confirmed that PEGylation of nanocarriers successfully reduced the clearance rate from the plasma. Overall, the observed improved pharmacokinetics and biodistribution of TMZ revealed the potential of these PEGylated nanocarriers in the efficient treatment of glioblastoma.

List of Tables

List of Figures

Abbreviations and Symbols

%	Percentage
<	Less than
≤	Less than equal to
=	Equal to
>	More than
≥	More than equal to
°C	Degree Celsius
µg	Microgram
µM	micromolar
Adeq	Adequate
Adj	Adjusted
AIC	5-amino-imidazole-4-carboxamide
AIC	Akaike Information Criteria
ANOVA	Analysis of variance
API	Active pharmaceutical ingredient
ATR-FTIR	Attenuated total reflectance Fourier transform infrared
AUC	Area under concentration
BBB	Blood brain barrier
BBD	Box–Behnken design
C	Carbon
Cl	Clearance
cm	Centimetre
CMA	Critical material attributes
C_{max}	Maximum concentration
CMC	Critical micelle concentration
CPP	Critical process parameters
CQA	Critical quality attributes
DAPI	4′,6-diamidino-2-phenylindole
DL	Drug loading
DLS	Dynamic light scattering
DMEM	Dulbecco's modified Eagle's medium
DMPC	Dimyristoylphosphatidylcholine
DMSO	Dimethyl sulfoxide

DNA	Deoxyribonucleic acid
DoE	Design of experiment
DPPC	Dipalmitoylphosphatidylcholine
DSPC	Distearoylphosphatidylcholine
DSPE-PEG 2000	1,2-Distearoyl-sn-glycero-3-phosphoethanolamine-N-[methoxy(polyethylene glycol 2000]
EDTA	Ethylenediamine tetraacetic acid
EE	Entrapment efficiency
FBS	Fetal bovine serum
FESEM	Field Emission Scanning Electron Microscopy
FMEA	Failure mode evaluation and analysis
g/mol	Gram per mole
GBM	Glioblastoma
GMO	Glycerol monooleate
h	Hour
H	Hydrogen
HCl	Hydrochloric acid
HLB	Hydrophilic-lipophilic balance
HOMO	Highest occupied molecular orbital
HPLC	High-pressure liquid chromatography
IC_{50}	Inhibitory concentration
ICH	The International Council for Harmonisation of Technical Requirements for Pharmaceuticals for Human Use
IS	Internal standard
IUPAC	International Union of Pure and Applied Chemistry
kDa	Kilo Dalton
kg	Kilogram
L	Litre
LLC	Lyotropic liquid crystals
LOD	Limit of detection
LOQ	Limit of quantification
LUMO	Lowest unoccupied molecular orbital
M	Molar
mg	milligram
min	Minutes

mL	Millilitre
mm	Millimetre
mM	Millimolar
MQC	Middle-quality control
MRT	Mean residence time
MSC	Model Selection Criteria
MTIC	3-methyl-(triazen-1-yl) imidazole-4-carboxamide
MTT	3-(4,5-dimethylthiazol-2-yl)-2,5-diphenyl tetrazolium bromide
mV	Millivolts
N	Nitrogen
NaOH	Sodium hydroxide
ng	Nanogram
Nm	Nanometre
nM	Nanomolar
O	Oxygen
PC	Phosphatidylcholine
PDI	Poly dispersity index
PEG	Polyethylene glycol
PF	Pluronic
Pred	Predicted
PRESS	Predicted residual error sum of squares
PTT	Phase transition temperature
QbD	Quality by design
QTPP	Quality target product profile
RBCs	Red Blood Cells
REM	Risk Estimation Matrix
rpm	Revolutions per minute
RPN	Risk Priority Number
RRMA	Relative risk-based matrix analysis
RSD	Relative standard deviation
RSM	Response surface methodology
SD	Standard deviation
sec	Seconds
SM	Sphingomyelin
$t_{1/2}$	Half-life

T_{max}	Time taken to reach maximum concentration
TMZ	Temozolomide
USFDA	United States Food and Drug Administration
UV	Ultra-violet
V_d	Volume of distribution
w/v	Weight per volume
w/w	Weight per weight
α	Alpha
β	Beta
γ	Gamma
λ_{max}	Lambda max
µL	Microliter
µm	Micrometer

Table of Content

Chapter 1

Introduction

1.1 Glioblastoma

Cancers are the most challenging to treat and have a very high rate of morbidity and mortality. Out of the different cancers, brain cancer is the most difficult to treat and cure. Approximately 19 in 0.1 million people are diagnosed with brain tumors every year around the world. The most aggressive and common brain tumor is the one that arises in the glial cells of the brain [1]. Out of all brain tumors, 80 % are gliomas. About 90% of the cases are of primary glioblastoma and only 5 % are of secondary glioblastoma. The survival rate of the patients is very less from a few months to a year [2]. The median survival rate of primary and secondary glioblastoma patients was found to be 4.7 months and 7.8 months respectively. After conventional therapy, there is only a 25 % chance of the survival of glioblastoma patients for 2 years [3].

1.2 Current therapy and limitations

The brain comprises about 100 billion capillaries and thus is a highly perfused organ. Proper functioning of the vasculature is essential for brain function. The protective blood-brain barrier ensures the correct functioning of the brain. Glioblastoma (GBM) is a challenge to treat because of its unique features like indistinct tumor margins, a higher degree of endothelial cell hyperplasia, and vascular proliferation. The current therapy involves surgical resection followed by radiotherapy and chemotherapy [4]. The highly infiltrative nature of glioblastomas may cause the migration of the cancer cells to the other tissues, thus increasing the chances of tumor reoccurring even after surgery. The major barrier is the tight junctions lining the blood vessels of the brain which is the blood-brain barrier (BBB). This lining is highly selective in nature. This layer allows only nutrients, oxygen and hydrophobic molecules to pass through thus preventing the entry of drugs, neurotoxins, or microorganisms. The various transport mechanisms followed through the blood-brain barrier are represented in **Figure 1.1**. But in the diseased condition, the BBB is disrupted and the function is altered [5,6]. The GBM cells easily infiltrate, migrate and accumulate around the other blood vessels thus developing into a tumor. Moreover, there are multidrug resistance proteins like P-glycoprotein which efflux the drug out of the cell thus preventing its accumulation at the site. Also, the blood-brain barrier eventually gets transformed into the blood-brain tumor barrier on tumor deterioration [1].

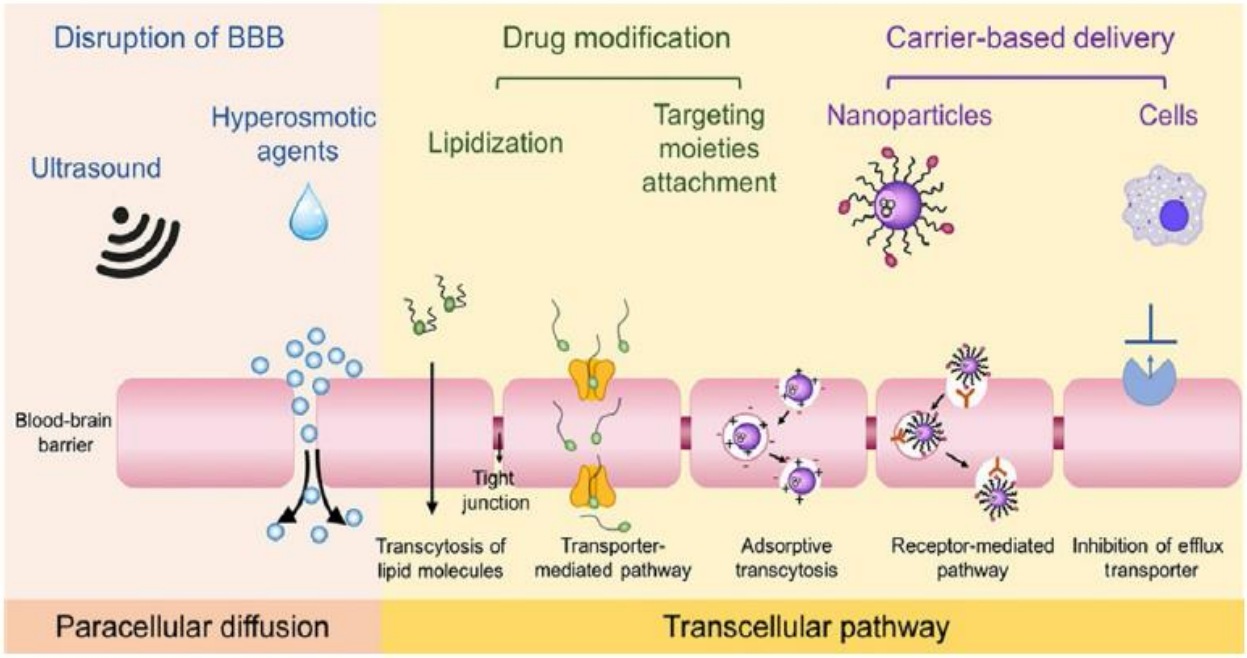

Figure 1.1. Transport mechanisms and strategies for drug delivery through the blood-brain barrier [7]

Only a selected number of drugs have been approved for treating brain cancers like carmustine, lomustine, everolimus, bevacizumab, and temozolomide. Various physicochemical properties of the drug decide the effectiveness of the chemotherapy. Only lipid-soluble drug molecules with a molecular weight of less than 400 Da can conveniently cross the BBB by transcellular diffusion. A log P value of the drug also affects the permeation through the BBB. Lipophilic drugs can easily cross the BBB, but highly lipophilic drugs can cause non-specific toxicity and more distribution of the drug. If the targeted drug delivery is not achieved, then the diffusion of the drug to the other sites can affect the healthy tissues. Most chemotherapeutic drugs act on the rapidly dividing cells and destroy them. But along with the tumor cells, normal cells that are rapidly dividing are also affected thus giving rise to various side effects like immunosuppression, hair loss, and organ dysfunction. Other neurological complications like neurodegeneration, neuropathy, paralysis, seizures, and memory loss are also common. Thus the administered drugs are not able to achieve the desired therapeutic effect. Improving the drug targeting to the brain can help reduce these side effects and complications. This can be achieved by designing a novel drug delivery system that can target the drug to its site of action without affecting the normal cells and reduce the side effects [6,8,9].

1.3 Nanoparticle drug delivery system

Nanopharmaceuticals have caught the eye for the last few decades to overcome the challenges of conventional formulations. As time and cost of new drug development have increased heavily, due to strong regulatory control for safety, research directed to the design of novel drug delivery systems to overcome the drawbacks of existing drugs. It is certainly the golden age of pharmaceutical nanocarriers. In the past few years, various types of nanoparticles have been developed and studied to target the drugs to their site of action like inorganic, polymeric, and lipid-based nanoparticles. Encapsulation of the drug in the nanocarrier provides various benefits like increasing the solubility and permeability of the drugs, protecting the drug from various pH conditions and digestive enzymes, targeting the drug to its site of action, and enhancing cellular internalization. Nanoparticles cannot cross the normal blood vessels. In a diseased condition like GBM, the BBB is disrupted thus tumor cells have leaky vasculature and less lymphatic drainage. Due to this, nanoparticles can enter the tumor cells and accumulate inside thus showing enhanced permeation and retention effect. Nanoparticles of size 80-100 nm are thought to be the best candidates for brain delivery because of longer circulation times as they are capable of avoiding opsonisation by macrophages [8,10]. The surface of the nanoparticles can be modified by different surface coating agents like polysorbate 80, poloxamer 188, chitosan, and polyethylene glycol. These surface-modified nanoparticles have the ability to prevent opsonisation by the reticuloendothelial system, target the drug to the brain, enhance drug uptake by the brain, prevent efflux pump activities, and enhance the stability of nanoparticles and enhance the circulation time. The cell membrane is negatively charged thus cationic nanoparticles are reported to show more BBB permeability through adsorptive mediated endocytosis [11]. Thus nanoparticles can enhance the efficiency of the drug delivery to the tumor cells through passive and active targeting.

1.4 Lipid-based nanoparticles

Pharmaceutical products containing lipids have successfully completed the clinical trials and entered the market. A few examples of such products are Doxil®, Cleviprex®, DaunoXome®, Valium®, Silybin®, Lipo-NSAID®, and Phytosome®. The entry of such products into the market encourages their further investigation and research in the pharmaceutical area. The extensive literature available on lipid-based nanoformulations has proved their potential in treating several diseases including different types of cancers, skin diseases, metabolic and brain disorders. These have shown feasibility in administration by different routes. Most important, as they are already the components of the human cell membrane, they provide excellent

biocompatibility [12]. The lipid-based formulations provide numerous advantages like enhanced solubility, protection of the drug from degradation, modified release, improved bioavailability, enhanced circulation time, improved therapeutic index, reduced side effects, and reduced dosing frequency. These lipids are highly biocompatible and easily metabolized by the body thus showing reduced toxicity as compared to the polymeric-based systems. Hydrolysis or oxidation of the lipids during storage and instability in the gastrointestinal tract are some of the limitations associated with phospholipid-based carriers. Various lipid-based formulations which have been developed are represented in **Figure 1.2**. Distinctive properties of lipids like solubility, surface charge, polymorphism, critical packing parameter, hydrophilic-lipophilic balance (HLB), hydrophilic-lipophilic difference (HLD), critical micelle concentration (CMC), and phase transition temperature play a crucial role in formation and stability of these formulations [13].

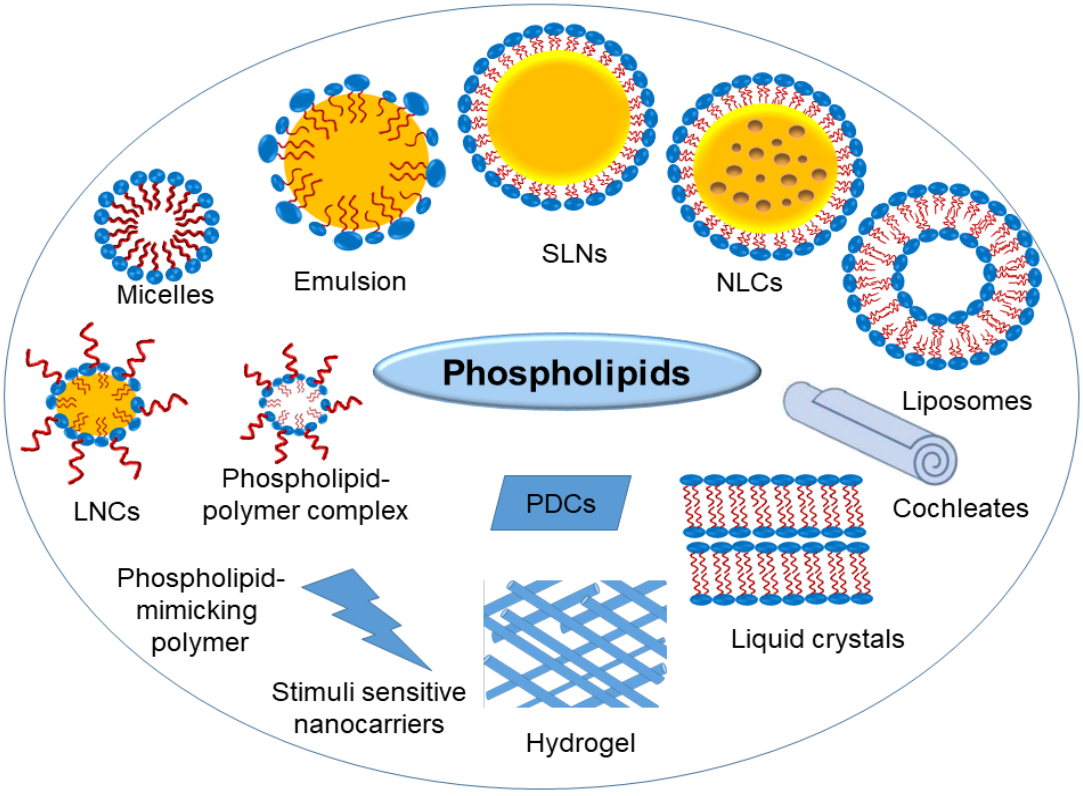

Figure 1.2. Different types of nanocarriers formed using phospholipids. *SLNs: Solid lipid nanoparticles; NLCs: Nanostructured lipid carriers; PDCs: Phospholipid-drug conjugates* [14]

1.5 Theories and driving forces involved in lipids self-assembly

When lipids are added to the water, initially these align themselves at the water-air interface with polar heads into the water and hydrophobic tails aligning towards the air. When the

concentration of lipids increases further, there is no further space to accommodate these molecules at the interface, thus they start moving inside the water phase. When the critical micelle concentration (equilibrium) is reached, individual lipid molecules start aligning as micelles/ bilayer vesicles eventually. The concentration of these aggregates is close to zero below the critical micelle concentration and increases linearly above it with the addition of more lipid molecules as represented in **Figure 1.3**.

Various thermodynamic parameters like enthalpy, entropy, heat capacity, and Gibbs free energy play a vital role in the transfer of lipids from the air-water interface to the water phase and the formation of micellar/vesicular structure. The combined average effect of the electrostatic, hydrogen bonding, and van der Waals forces is mainly responsible for the lipid bilayer formation. There are two opposing forces (polar head group repulsions and fatty acid side chains association) that compete with each other and are imparted by hydrophobic tails and hydrophilic heads. The hydrophobic effect is imparted by the fatty acid side chains while the polar head groups are responsible for the stability of the membrane formed. When a micelle or vesicle is formed, the fatty acid side chain is shielded from the outer aqueous environment due to its hydrophobic nature. The hydrophobic tails on the verge of hiding from the water associate with each other. The surrounding pH or salt concentration can significantly modify the thermodynamics involved in the self-assembly of phospholipids. The critical micelle concentration of negatively charged lipids is much lower in the presence of salts like sodium chloride. It is reported that the formation of lipid micelle is unaffected by temperature in the range of 5 to 50^{o}C. Destabilization of the membranes can lead to various functional consequences like lipid exchange, membrane fission, and fusion [15,16]. Few reports revealed the effect of temperature, moisture content, oxidation products, and free fatty acids on the critical micelle concentration of lipids [17,18].

1.6 Liposomes

Among the various nanocarriers, liposomes have become the popular drug carrier systems due to their biocompatibility, improved efficacy of treatment, controlled drug release, and reduced toxicities. Liposomes were first discovered by Bangham in the 1960s. He found that when phospholipids come in contact with water, they form spherical structures. These were further investigated to encapsulate drugs [19].

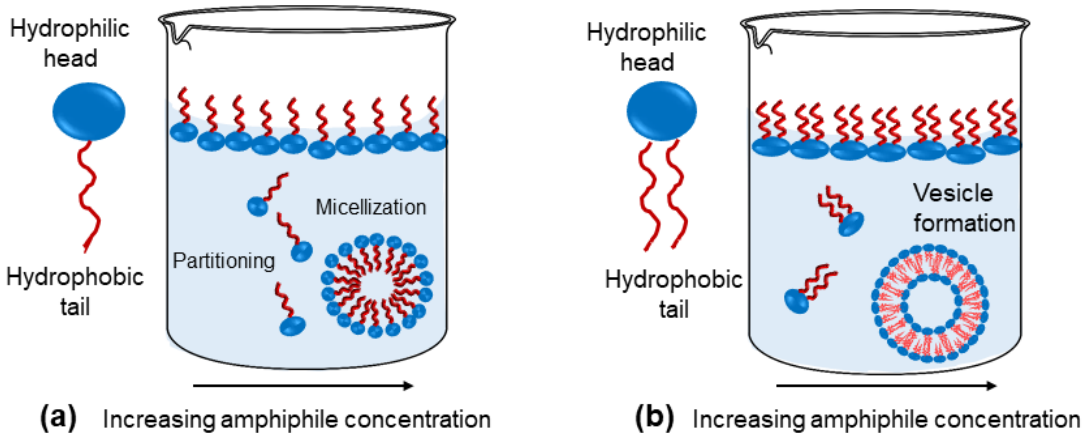

Amphiphile shape and CPP value		Self-organized structure	Curvature	Phospholipids
	< 1/3 Cone	Spherical micelle	+	Lysophospholipids with large head groups
	1/3 < 1/2 Truncated cone	Cylindrical micelle/ Hexagonal phase		Lysophospholipids with small head groups
	1/2 < 1 Truncated cone	Hollow spherical bilayer vesicle		Double chain lipids with large head groups (PC, PS, PG, PI, SM)
	1 Cylinder	Lamellar	0	Double chain lipids with small head groups, lipids with saturated chains, anionic lipids in high salt concentration (PE)
(c)	>1 Inverted Truncated cone	Reverse Cylindrical micelle/ Hexagonal	−	Double chain lipids with small head groups, lipids with polyunsaturated chains

Figure 1.3. (a) Formation of micelles on addition of single chain phospholipid to a solvent (b) Formation of vesicles on addition of two chains containing phospholipids to a solvent (c) Formation of different phospholipid self-assemblies based on the critical packing parameter (CPP) [14]

The first product based on nanotechnology was approved by FDA in 1995. Doxil® (Doxorubicin liposomal injection) was based on PEGylated phospholipid bilayer and was found to passively target the drug to the tumors [20]. It was found to reduce toxicity and offer an effective treatment. Thus liposomes are the first delivery system based on nanotechnology to get approved for treating brain cancer. Further studies revealed that the coated liposomes could increase the circulation time of the drug. The other marketed liposomal products are Ambisome® (Amphotericin B) and Depocyt® (Cytarabine) [21,22].

Liposomes are the concentric bilayered vesicles with phospholipid bilayer encapsulating an aqueous core. The phospholipid bilayer resembles the biological cell membranes. These can encapsulate hydrophilic, lipophilic, and amphiphilic drugs. Liposomes are non-toxic, biocompatible, and biodegradable and provide various advantages like targeted and controlled drug delivery, increased efficacy and therapeutic index, protection of drugs from pH and enzyme degradation, can be prepared in varied sizes, and can be administered through various routes. They also possess certain limitations like less stability, oxidation and hydrolysis, high production costs, and leakage of drugs [23,24].

1.6.1 Composition

1.6.1.1 Phospholipids

Phospholipids are lipids containing phosphate radical along with carbon, hydrogen, and oxygen. The structure consists of a glycerol backbone which is esterified with fatty acid chains on positions 1 and 2 while the 3rd position is occupied with a phosphate group further esterified with polar moiety (alcohol). The polar head groups confer hydrophilicity while the fatty acid chains attached confer hydrophobicity to a phospholipid molecule (non-polar region). Thus phospholipids are amphiphilic in nature. The four different functional groups attached to the second carbon of the glycerol moiety confer chirality to phospholipid molecules. Variation in the attached polar head groups, backbone, and the fatty acid side chains lead to a large array of phospholipids with differing properties [12,25].

Phospholipids can be classified based on the source or structure. Different types of phospholipids have been summarized in **Figure 1.4**. The backbone can be either glycerol or sphingosine. The polar heads when attached to phosphatidic acid form the respective phospholipids like phosphatidylcholine (PC), phosphatidylethanolamine (PE),

phosphatidylserine (PS), phosphatidylinositol (PI), or phosphatidylglycerol (PG). Sphingosine forms the sphingomyelins (SM) class of phospholipids. Some of the fatty acid chains which can be attached are disteroyl (DS), dipalmitoyl (DP), dimyristoyl (DM), and dioleoyl (DO). The fatty acid chains can be either saturated or unsaturated [12,25].

The phospholipid properties like phospholipid chain length, degree of saturation, charge on polar heads, and phase transition temperature can affect the characteristics of liposomes. The length of the fatty acid side chains is likely to affect the volume of the hydrophobic cavity. Liposomes containing ester and amide bonds have more biodegradability and lower toxicity when compared to those containing ether bonds [26]. SM and PC bilayers have different properties. SM can form intermolecular and intramolecular hydrogen bonds. SM interacts strongly with cholesterol as compared to PC as the highly saturated fatty acid chain can form strong bonds with the steroid. Thus, SM containing cholesterol bilayers possess high compressibility and low permeability to water. The rigidity of the liposome bilayer affects the stability/rupture of vesicles and the extent of prolonged drug release. The rigidity/fluidity/elasticity of the liposome bilayer is entirely dependent on the composition and the phase transition temperature of the selected phospholipids. The fluidity and stability of the liposome bilayer can be altered by the addition of different molecules like sterols (cholesterol, sodium taurocholate, sodium glycolate, sodium deoxycholate, sodium cholate) and short-chain alcohols (ethanol) [12]. The liposome structure is highly versatile and can be modified by the addition of other substances like non-ionic surfactants (niosomes/transferosomes), ethosomes (ethanol), phytochemical (herbosomes/phytosomes), photolysase (photosomes), virus glycoprotein (virosomes), enzyme complexes (proteasomes), and many more [27].

The temperature at which phospholipids transform from the gel (highly ordered) to the liquid crystalline phase (disordered) is called the phase transition temperature. It is dependent on the polar head group, length of the fatty acid side chains, degree of saturation in fatty acid side chains, and the purity of the phospholipid. Those with PE head groups have higher PTT than those containing PC or PG head groups which is related to stronger head group interactions. Those with longer side chains have higher PTT as more energy is required to break the bonds as compared to those with shorter side chains. Similarly, saturated phospholipids show higher PTT. Phospholipids consisting of polyunsaturated side chains may show PTT even below 0°C. Phospholipid bilayer assemblies (liposomes) made from low PTT lipids (below 37°C) are reported to be in a leaky state prone to uptake by macrophages when in the blood. Thus if

longer circulation time and controlled release are expected from these nanoparticles, preferentially lipids with high PTT need to be selected.

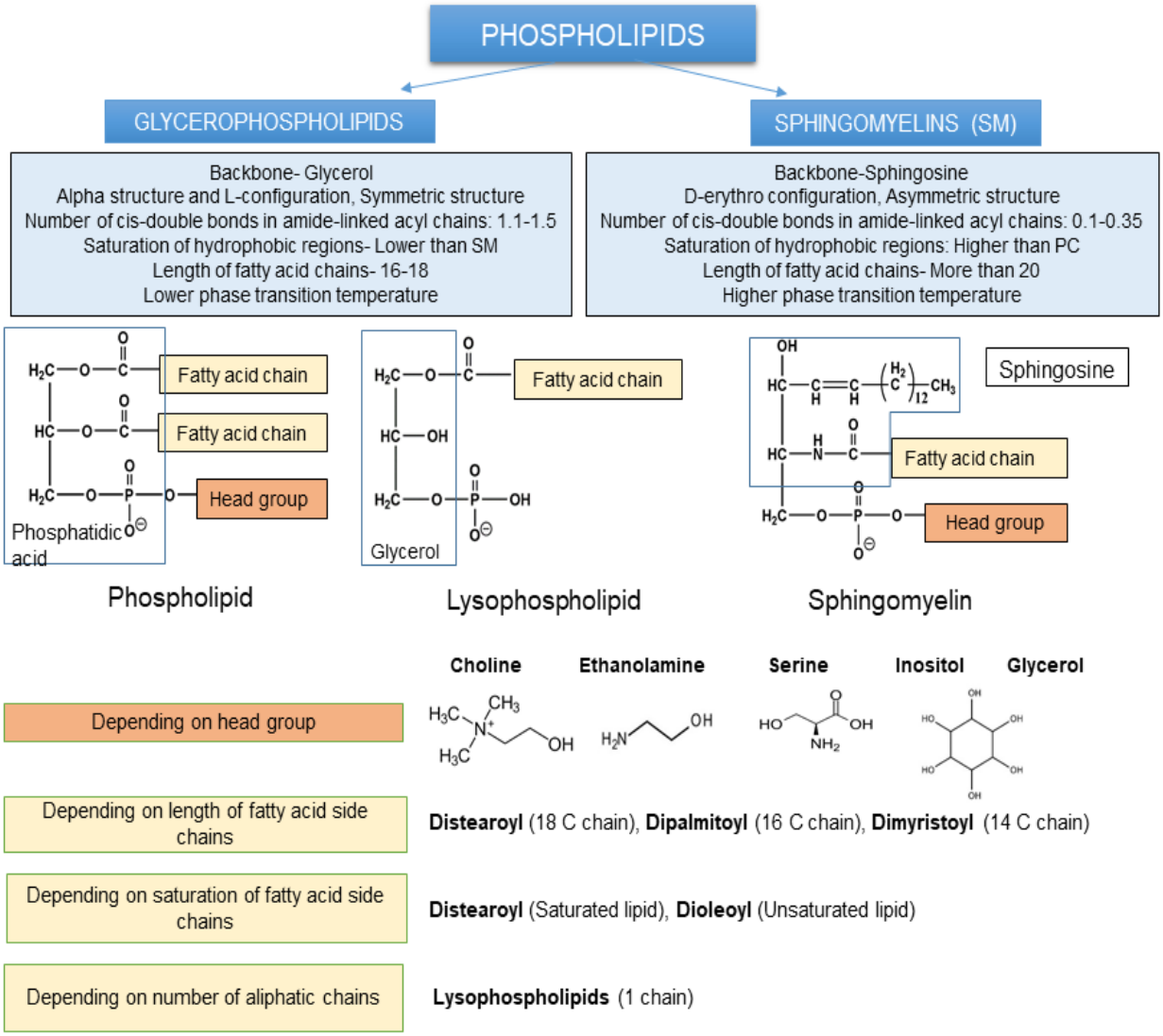

Figure 1.4. Structural features and different types of phospholipids *(SM: Sphingomyelin, PC: Phosphatidylcholine, C: Carbon)* [14]

In the case of topical preparations, phospholipid bilayers with higher PTT lipids will remain rigid at a skin temperature of 32°C (preferred for topical drug delivery) while those with lower PTT will remain in elastic, very flexible bilayer structures that can easily squeeze through the corneocyte cells deeper into the skin layers providing transdermal delivery [28,29]. Vesicles formed from phospholipids with PTT below 37°C are more prone to disruption by bile salts in the gastrointestinal environment when delivered through the oral route as compared to those formed from phospholipids with higher PTT [30].

The surface charge acquired by phospholipids when dispersed in water depends on the polar head group and the pH of the medium. At pH 7, phospholipids containing PC and PE head groups possess a neutral charge (zwitterionic) while those with PS, PI, and PG head groups acquire a negative charge. Cationic charge on the phospholipid head promotes the attraction of nanoparticle towards the cell membrane and improve the cell incorporation rate. The skin cells possess a negatively charged cell membrane, thus nanoparticles with a positive surface charge (as provided by PE at skin pH) are attracted towards them providing enhanced skin permeation [31]. It is reported that nanoparticles with a neutral charge (as provided by PC) show longer circulation time at plasma pH when in the blood due to less binding to plasma proteins. Charged nanoparticles are cleared faster due to uptake by the lungs, liver, and spleen. Thus, surface charge affects the interaction with cells, uptake by macrophages, escape from lysosomes, clearance rate of nanoparticles, and cytotoxicity [32,33].

1.6.1.2 Steroids

Cholesterol and its derivatives improve the phospholipid bilayer stability and fluidity. Liposomes without cholesterol are found to be less stable. Cholesterol orients itself between the fatty acid hydrocarbon chains of the phospholipids [34]. Instead of cholesterol other bile salts like sodium taurocholate, sodium deoxycholate and sodium glycholate can be incorporated into the liposomal structure to protect the liposomes from enzymatic degradation and to improve the stability of the liposomal structure [35,36].

1.6.2 Classification

Liposomes are classified based on the number of vesicles present, based on the method of preparation, and the composition as summarized in **Tables 1.1**, **1.2**, and **1.3** respectively.

Table 1.1. Classification of liposomes based on the structure

Type	**Size**
Small Unilamellar vesicles (SUV) Medium Unilamellar vesicles (MUV)	20-100 nm
Large Unilamellar vesicles (LUV)	> 100 nm
Giant Unilamellar vesicles (GUV)	> 1 µm
Oligolamellar vesicles (OLV)	0.1-1 µm
Multilamellar vesicles (MLV)	> 0.5 µm
Multivesicular vesicles (MVV)	> 1 µm

Table 1.2. Classification of liposomes based on the method of preparation

Type	**Specification**
SUV- REV	Unilamellar vesicle prepared by reverse-phase evaporation technique
MLV- REV	Multilamellar vesicle prepared by reverse-phase evaporation
Stable plurilamellar vesicles (SPLV)	Multilamellar vesicle with relatively less osmotic gradient
Freeze-Thaw MLV	Liposomes prepared by alternate freeze and thaw cycles
VET	Vesicles by extrusion technique
DRV	Liposomes prepared by dehydration-rehydration method

Table 1.3. Classification of liposomes based on the composition

Type	**Characteristics**
Conventional liposomes	Composed of neutral or negatively charged phospholipids
Immunoliposomes	Liposome attached with a monoclonal antibody with or without PEG chains
Long circulating liposomes	Liposome surface coated with a hydrophilic agent
Cationic liposomes	Composed of positively charged phospholipid
pH-sensitive liposomes	Liposomes destabilize on change in external pH
Fusogenic liposomes	Liposome displaying Sendai virus-derived proteins

1.6.3 Methods of preparation

Various methods used for the preparation of liposomes are the thin-film hydration technique, ether injection method, ethanol injection method, reverse phase evaporation method, French pressure cell extrusion, and freeze-thaw method. Detergent removal method, dialysis method, microfluidization technique, and proliposome technique can be used for large-scale industrial production of liposomes [37,38]. The most commonly used techniques are discussed below and compared in **Table 1.4.**

1.6.3.1 Thin film hydration technique (Conventional method)

Phospholipids are first dissolved in the organic solvents to form a homogeneous solution. The selection of solvents depends on the solubility of the lipid in the different solvents. The most commonly used solvents are chloroform and methanol in a 2:1 ratio. The solvent is evaporated to form a thin lipid layer. Liposomes are formed on the hydration of the lipid layer with aqueous

media. The drug can be incorporated into the lipid phase or the aqueous media depending on its nature [39]. This method is simple and most commonly used for the preparation of liposomes and can be used for all different lipid mixtures. Liposomes prepared by this method have variable sizes thus a wide size distribution. The main limitation of this method is less encapsulation efficiency. This method cannot be used for large-scale production of liposomes and thus has less industrial applicability [40].

1.6.3.2 Proliposome technique

In order to overcome the limitations of the conventional methods, a novel carrier-based proliposome technique was invented. Proliposomes are a dry, free-flowing product that immediately forms liposomes on hydration with water or a biological fluid in the body. In this method, a thin lipid film is deposited on the surface of a water-soluble carrier [41]. The presence of a carrier increases the surface area. The carrier molecule should be insoluble in the lipid solution and have high water solubility. The various water-soluble carriers used are Maltodextrin, Sorbitol, Microcrystalline cellulose, Mannitol, and Spray-dried lactose. Sorbitol, lactose monohydrate, and sucrose pose problems in the coating as these are soluble in the organic lipid mixture. These form viscous slurries upon evaporation of the solvents while others form free-flowing powders [42]. Proliposomes can be prepared by various techniques like carrier deposition, spray drying, and the fluidized bed method [43]. Proliposomes are relatively cheap and easy to prepare, provide high entrapment of hydrophilic drugs, overcome the stability issues, and are easy to scale up [44].

1.6.3.3 Membrane extrusion technique

The size of the liposomes obtained by the thin-film hydration method can be reduced further following the membrane extrusion technique. Membrane extrusion is a common technique used for most of the commercially available liposomes. A membrane extruder consists of a pump and a membrane filter of defined pore size. Liposomal suspension is forced through a filter using a pump to achieve monodispersed liposomes of the desired size. As the larger phospholipid vesicles pass the narrow cylindrical pores in the filter, they break down into smaller vesicles. The size of the liposomes majorly depends on the number of extrusion cycles and the membrane filter pore size [45,46].

1.6.3.4 Microfluidics

All other liposome preparation techniques produce polydispersed liposomes with larger diameters and require several post-processing steps like sonication or extrusion to obtain uniform small-sized liposomes. A new method based on the microfluidics principle was explored to obtain small highly reproducible liposomes (a few hundred nanometers) in a minimum number of steps. In this method, phospholipids are dissolved in an alcoholic solution and a stream is forced through a narrow micron channel in a microfluidic device constructed with a cross-flow or T-junction geometry. Two lateral streams of water/aqueous buffers flow around this lipid stream. Self-assembly of phospholipids occurs at the liquid interfaces following the controlled mixing and diffusion of molecular species between the alcohol and water [47,48].

Table 1.4. Comparison of different methods of preparation of liposomes

Thin-film hydration	**Proliposome technique**	**Microfluidics**	**Membrane extrusion technique**
Multilamellar spherical structures composed of phospholipids	Lipid and drug-coated on a water-soluble carrier to form a free-flowing granular product	Liposomes formed by micro-mixing in a microfluidic device	Liposomal suspension extruded through a membrane filter
Tendency to aggregate, susceptible to hydrolysis	Improved storage stability	Highly reproducible, homogenous, liposomes of the desired size are achieved; Minimum number of steps	Highly reproducible, homogenous, liposomes of desired size are achieved
Lyophilisation needed, High production costs	No requirement of lyophilisation thus less time consuming process, Ease of handling, scalability and industrial application	Lyophilisation needed, High production costs, Chances of clogging of channels when high lipid concentrations are used	Lyophilisation needed, High production costs, Chances of clogging of filter pores when high lipid concentrations are used

1.7 Liquid crystalline nanoparticles

Liquid crystals are an intermediate state between a solid and a liquid also called as a mesophase. These possess orderly arrangement and optical properties like a solid crystal and also fluidity, surface tension, and viscosity like a liquid. They have a relatively higher surface area (which ultimately translates to higher bioavailability) than other lipid-based nanocarriers and possess the ability to encapsulate both hydrophobic and hydrophilic moieties These nanoparticles can be formed in a very small size range of 100-200 nm. Due to their unique structural assembly, they can encapsulate a large amount of drug thus offering an advantage over liposomes. The honeycomb-like structure consisting of multiple layers provides sustained delivery of the drug. The advantages of these have proved them effective to target the blood-brain barrier due to increased permeability and uptake in the brain. Certain limitations of these systems are a requirement of a specific type of lipid, scalability, and safety issues [49,50].

1.7.1 Composition

Liquid crystalline nanoparticles are made of amphiphilic lipids like glycerol monooleate (GMO), glycerol dioleate (GDO), phytantriol (PT), phospholipids, glycolipids, and monolinolein. These lipids are polar in nature and water-insoluble but form mesophase when in contact with water. In presence of excess water these form thermodynamically stable colloidal dispersions. Surfactants like poloxamer can be added. Stabilizing agents like pluronic, and polyvinyl alcohol (PVA) are incorporated to stabilize the mesophase and avoid particle aggregation [51].

1.7.2 Classification

Liquid crystals are of two types- thermotropic liquid crystals formed due to changes in temperature and lyotropic liquid crystals formed in the presence of a solvent. Lyotropic liquid crystals have found application as a drug delivery system. These are formed by the addition of an amphiphilic molecule (solute) containing the hydrophilic head and hydrophobic tail into a solvent (water). The amphiphilic molecules arrange themselves as micelles with head groups outside and tail inside. On further increasing the concentration of solute these arrange themselves into hexosomes, cubosomes, and lamellar liquid crystals. The further increase shows reverse condition with head groups inside and tail outside, thus forming reverse cubosomes, reverse hexosomes and reverse micelles. The different types of liquid crystalline nanoparticles have been represented in **Figure 1.5** [52].

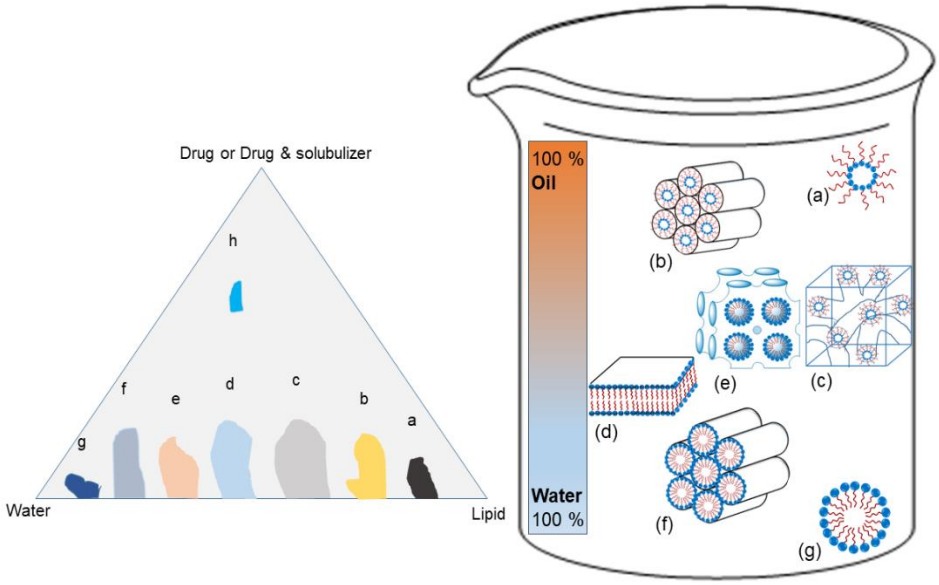

Figure 1.5. Different types of liquid crystalline nanoparticles and ternary phase diagram illustrating different phases. *(a) Reverse micelles; (b) Reverse Hexagonal; (c) Reverse Bicontinuous Cubic; (d) Lamellar; (e) Normal Discontinuous Cubic; (f) Hexagonal; (g) Normal micelles; (h) Microemulsion* [53]

1.7.3 Methods of preparation

Lyotropic liquid crystals are prepared by two main methods. The top-down approach includes the addition of the oil phase to the aqueous phase and providing high energy (ultrasonication or homogenization). The bottom-up approach includes the addition of a hydrotrope (solubilizes water-insoluble lipid) to the oil phase. This phase is then added to the aqueous phase with stirring or vortex. The spray drying technique can also be used. The oil phase is spray dried to get the precursor (in dried form) which on hydration forms liquid crystals (**Figure 1.6**) [50,52].

1.8 Quality by design approach

According to the FDA, pharmaceutical quality is attained when the product delivers clinical performance as mentioned in the label claim, no additional risk is introduced due to unexpected contaminants, and a robust manufacturing system is ensured. To ensure this, the FDA brought in the concept of "quality by design" (QbD) in the early 2000s. This concept came into being when it was realized that increased testing does not mean the enhanced quality of the product. Albeit, quality must be built into the pharmaceutical product [54].

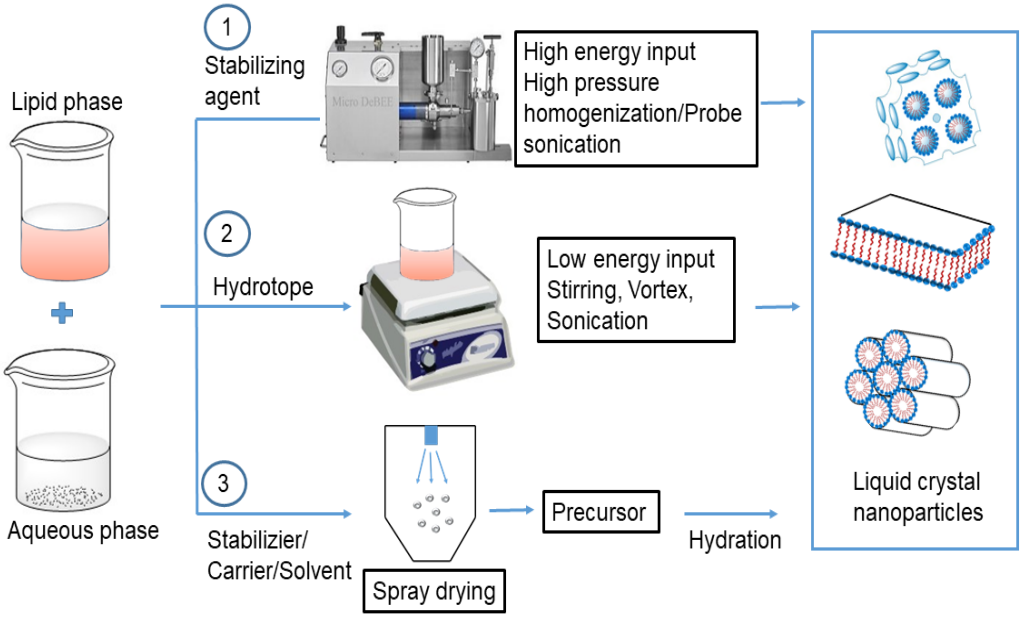

Figure 1.6. Different preparation methods of Liquid crystalline nanoparticles (1) Top-down approach (2) Bottom-up approach (3) Spray drying technique [53]

QbD is gradually becoming the norm in the pharmaceutical field. Pharmaceutical QbD advanced with the issuance of ICH guidelines Q8 (R2) (Pharmaceutical Development), Q9 (Quality Risk Management or QRM), Q10 (Pharmaceutical Quality System), and Q11 (Development and Manufacture of Drug Substance). These guidelines provide direction about the applications and scope of QbD [55]. FDA defines QbD as a "systematic approach to development that begins with predefined objectives and emphasizes product and process understanding and process control, based on sound science and quality risk management". QbD helps in the generation of robust processes. It helps in understanding the product and process in a better way, thus helping the lifecycle management of the pharmaceutical product. QbD offers various advantages to the generic industry including reduction of batch failures, better risk understanding, fewer recalls, and timely launch of the product [55,56]. The various elements of QbD have been summarized in **Figure 1.7**.

Quality target product profile (QTPP) is a potential summary of the characteristics of a product affecting the product quality. It is determined before initiating the QbD approach. It must be identified to assure the product quality. For this, the safety and efficacy of the product are taken into account. In essence, QTPP determines "what we want in our final product". It serves as a road map, which we need to follow to reach our destination (high-quality product). QTPP includes the dosage form, dose, route of administration, physical attributes, drug release,

pharmacokinetics, shelf life, sterility, and container closure system. For a novel drug product, QTPP is decided based on the information in various pharmacopeias and regulatory guidelines. For a generic drug product, QTPP is similar to that of the innovator, and all the requirements of pharmaceutical equivalence, bioequivalence, and patient compliance must be met [57–60].

Critical quality attributes (CQAs) are identified from QTPP. CQA is "a physical, chemical, biological, or microbiological property that should be within an appropriate limit or range to assure the product quality". The screening of CQAs from QTPP is based on impact and severity analysis. Impact analysis is related to changes in formulation material attribute or formulation parameter. Severity analysis is related to the safety and efficacy of the drug product [60–62].

Critical material attributes (CMAs) and critical process parameters (CPPs) are derived from CQAs using risk assessment. CMAs and CPPs are likely to cause variation in the CQAs. The CMAs including physicochemical, biopharmaceutical, or microbiological properties of materials should be within an appropriate specification limit to assure the final product quality. The CPPs are linked with the preparation process of the product. CMAs and CPPs are identified using various methods, such as the Ishikawa diagram, and process mapping [63–65].

Risk assessment is done to evaluate the impact of any variable (either related to API/excipient/process) on the CQAs of a product. Based on the impact, each attribute/parameter is distinguished into low, medium, and high risk. The attributes having higher chances of risk are further investigated in order to minimize the risk. Various methods are used for risk assessment such as failure mode effects analysis (FMEA), and relative risk-based matrix assessment (RRMA) [60,66–68].

Design of experiments (DoE) is used to screen or optimize variables experimentally. DoE is utilize various mathematical models using computer-aided process design. Various types of models are available. Factorial design, Box-Behnken, Plackett-Burman, and Taguchi design are names of a few designs. Design space provides a range of inputs producing the desired outputs. The change within the design space is not considered as a change [57,64,69,70].

Control strategy ensures the consistent development of desired quality products by implementing continuous quality improvement. It includes control of the initial materials, predefined product specifications, and CPPs; real-time release testing (RTRT), and an overall monitoring program [55,58,71].

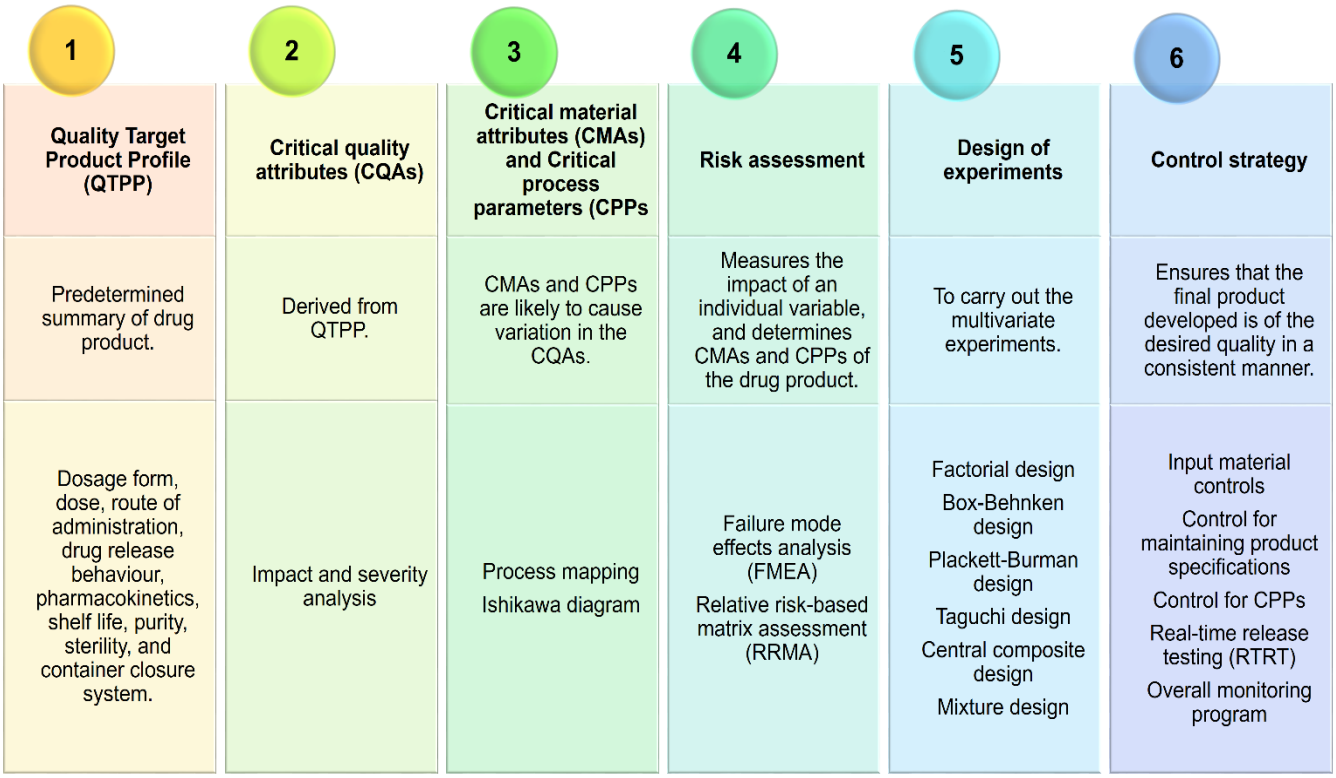

Figure 1.7. Various elements of QbD [66]

1.9 Gaps in existing research

As discussed earlier, present treatment of glioblastoma with post-surgery chemotherapy and radiotherapy, poses several challenges and is not very effective. Out of the few drugs approved for the treatment of glioblastoma, temozolomide (TMZ) is a drug of choice as it is a small molecule and amphiphilic in nature. It has 100 % oral bioavailability and believed to penetrate the blood-brain barrier relatively easily. Despite 100 % oral bioavailability, only 20-30 % of the drug is available to the brain due to its pH-dependent instability and short half-life (1.8 h). Thus, a higher dose of the drug needs to be administered, which also leads to myelosuppression, thrombocytopenia, or neutropenia. Moreover, current temozolomide therapy involves multiple dosing [72–74]. Therefore, there is a need to develop a novel formulation to overcome the existing challenges.

Nanoparticulate systems for TMZ using phospholipids, lipids, polymers or any other form can provide controlled release, longer circulation time, enhance plasma concentrations and improve its concentration in the brain. Enhanced concentration in brain and better therapeutic efficacy may result in reduction of the dose, lower toxic or side effects and improved patient compliance. Although various nanoformulations like polymeric nanoparticles, solid lipid nanoparticles, nanostructured lipid carriers, and liposomes have been investigated [75,76],

complex composition, sophisticated process, and poor entrapment of TMZ within these nanoparticles remain a challenging task. Nanoparticles within a size range of 80-120 nm are reported to show longer plasma circulation time when administered through the parenteral route. Most of the nanoformulations investigated, reported either a particle size >150 nm or used organic solvents in large amounts which poses a safety concern. The studies have reported difficulty in TMZ entrapment in polymeric nanoparticles or solid lipid nanoparticles resulting in low drug loading. High affinity towards water led to the leaching of the drug through these nanoparticles. The stability of TMZ in these nanoformulations is another major concern due to its pH-dependent stability. Hence, still further research needs to be done to overcome the limitations of the existing therapies [75,77–79].

In the course of time, nanoproducts gained significant importance but they had to face numerous challenges before reaching the market such as complex preparation techniques involving multiple steps, stability issues, reproducibility, large scale manufacturing, and regulatory barriers. Most of the manufacturing methods used for the preparation of the nanoformulations are feasible only at the lab scale, prepared by time-consuming and costly processes, utilize organic solvents, and are difficult to scale up. All of these, limit the translation of nanotechnologies for clinical application. It is a challenge to scale-up nanoformulations from lab scale to industrial scale maintaining the necessary properties of the designed nanoparticles [80,81]. Therefore, information related to various factors causing variability needs to be adequately understood by investigating the manufacturing process in detail throughout the development process. Several material or process parameters affecting the final characteristics of the product need to be identified. The relationship between input variables (material/ process) and nanocarrier characteristics is complicated and an elaborate investigation of the effect of individual variable is essential to ensure the successful scale-up. Also, an adequate understanding of the biophysical and chemical interactions of nanoformulations is essential [82–85].

1.10 Objective of the work

Based on the existing gap and challenges of delivery of TMZ for effective and long term therapy with better patient compliance, it was planned to design and formulate TMZ-loaded lipid-based nanoparticulate systems of liposomes and lyotropic liquid crystals. These could prolong the plasma circulation time of TMZ, provide selective and enhanced delivery of the drug to the brain with reduced side effects and improve the efficacy of the treatment with better

patient compliance. Liposomes and lyotropic liquid crystals were selected to be investigated as these have shown great potential to entrap amphiphilic drugs. In order to achieve longer plasma circulation, it was planned to coat nanocarriers with a polymer. DSPE-PEG 2000 is a non-ionic polymer, soluble in aqueous and organic medium, biocompatible, biodegradable, and non-toxic. It is expected to modify the surface energies of the nanocarrier, prevent their macrophage uptake/opsonization and hence prolong the plasma circulation time further.

Quality by design is an important tool which helps gain process understanding, reduce chances of failure in later stages of product development and help shorten the translation process. Hence, it was planned to optimize the selected lipid based nanocarriers using the principles of Quality by Design which would include investigating the effect of various critical material attributes, and process parameters on the critical quality attributes of lipid based nanocarriers. As TMZ has a high affinity toward the water phase (although amphiphilic in nature), it is likely to pose several challenges during the formulation process. Thus, it was planned to study the effect of various critical formulation and process parameters on the particle size and the entrapment of this molecule inside lipid based nanocarriers. Also, it was planned to compare the potential of different methods of preparation to entrap TMZ. A method of preparation that does not require organic solvent, involves minimum number of steps, which is highly reproducible and industrial feasible was planned to be selected. The optimized lipid based nanocarriers were further characterized for particle size distribution, morphology, surface charge, entrapment efficiency, drug release kinetics, cell line studies, pharmacokinetic and biodistribution studies to confirm the potential of these nanocarriers for better therapeutic efficacy.

Additionally, to achieve these objectives, it was planned to develop an analytical method using UV-visible spectroscopy and HPLC to quantify TMZ in the formulation and release samples, a bioanalytical method to estimate TMZ in plasma and tissue samples and to conduct a few preformulation studies to assist in this research endeavour.

References:

1. Ganipineni LP, Danhier F, Préat V. Drug delivery challenges and future of chemotherapeutic nanomedicine for glioblastoma treatment. J Control Release. 2018;281:42–57.

2. Messaoudi K, Clavreul A. Toward an effective strategy in glioblastoma treatment . Part I : resistance mechanisms and strategies to overcome resistance of glioblastoma to temozolomide. Drug Discov Today. 2015;20(7):899–905.

3. Ohgaki H, Kleihues P. Genetic Pathways to Primary and Secondary Glioblastoma. Am J Pathol. 2007;170(5):1445–53.

4. Tellingen O Van, Yetkin-arik B, Gooijer MC De, Wesseling P, Wurdinger T, Vries HE De. Overcoming the blood – brain tumor barrier for effective glioblastoma treatment. Drug Resist Updat. 2015;19:1–12.

5. Gao H. Progress and perspectives on targeting nanoparticles for brain drug delivery. Acta Pharm Sin B. 2016;6(4):268–86.

6. Khosa A, Saha RN, Singhvi G. Drug delivery to the brain. In: Grumezescu AM, editor. Nanomaterials for Drug Delivery and Therapy. Elsevier Inc.; 2019. 461–514.

7. Li G, Shao K, Umeshappa CS. Recent progress in blood-brain barrier transportation research. In: Gao H, Gao X, editors. Brain Targeted Drug Delivery Systems: A Focus on Nanotechnology and Nanoparticulates. Elsevier Ltd.; 2018. 33–51.

8. Comoglu T, Arisoy S, Akkus ZB. Nanocarriers for Effective Brain Drug Delivery. 2017;1490–506.

9. Nsairat H, Khater D, Odeh F, Al-adaileh F, Al-taher S. Lipid nanostructures for targeting brain cancer. Heliyon. 2021;7:e07994.

10. Masserini M. Nanoparticles for Brain Drug Delivery. 2013;2013.

11. Zhou Y, Ning Q, Yu D, Li W, Deng J. Improved oral bioavailability of breviscapine via a Pluronic P85-modified liposomal delivery system. 2014;903–11.

12. Li J, Wang X, Zhang T, Wang C, Huang Z, Luo X, et al. A review on phospholipids and their main applications in drug delivery systems. Asian J Pharm Sci. 2015;10(2):81–98.

13. Mohanta B, Palei NN, Surendran V, Dinda SC. Lipid Based Nanoparticles: Current Strategies for Brain Tumor Targeting. 2019; 4(2): 84-100

14. Waghule T, Saha RN, Alexander A, Singhvi G. Tailoring the multi-functional properties of phospholipids for simple to complex self-assemblies. J Control Release. 2022;349:460–74.

15. Alipour E, Halverson D, McWhirter S, Walker GC. Phospholipid Bilayers: Stability and Encapsulation of Nanoparticles. Annu Rev Phys Chem. 2017;68(1):261–83.

16. Marsh D. Thermodynamics of phospholipid self-assembly. Biophys J. 2012;102(5):1079–87.

17. Kim JS, Kim MJ, Lee JH. The critical micelle concentration of lecithin in bulk oils and medium chain triacylglycerol is influenced by moisture content and total polar materials. Food Chem. 2018;261:194–200.

18. Lehtinen OP, Nugroho RWN, Lehtimaa T, Vierros S, Hiekkataipale P, Ruokolainen J, et al. Effect of temperature, water content and free fatty acid on reverse micelle formation of phospholipids in vegetable oil. Colloids Surfaces B Biointerfaces. 2017;160:355–63.

19. Allen TM, Cullis PR. Liposomal drug delivery systems : From concept to clinical applications. Adv Drug Deliv Rev. 2013;65(1):36–48.

20. Barenholz YC. Doxil ® — The fi rst FDA-approved nano-drug : Lessons learned. J Control Release. 2012;160(2):117–34.

21. Nekkanti V, Kalepu S. Recent Advances in Liposomal Drug Delivery : A Review. Pharm Nanotechnol. 2015;3(1):35–55.

22. Bulbake U, Doppalapudi S, Kommineni N, Khan W. Liposomal Formulations in Clinical Use : An Updated Review development. Pharmaceutics. 2017;9(12):1–33.

23. Chandra D, Yadav KK, Singh VK, Patel A. AN OVERVIEW : THE NOVEL CARRIER FOR VESICULAR DRUG DELIVERY. World J Pharm Res. 2014;3(6):1299–322.

24. Akbarzadeh A, Rezaei-sadabady R, Davaran S, Joo SW, Zarghami N. Liposome : classification , preparation , and applications. Nanoscale Res Lett. 2013;8:102.

25. Van Hoogevest P, Wendel A. The use of natural and synthetic phospholipids as pharmaceutical excipients. Eur J Lipid Sci Technol. 2014;116(9):1088–107.

26. Li M, Du C, Guo N, Teng Y, Meng X, Sun H, et al. Composition design and medical application of liposomes. Eur J Med Chem. 2019;164:640–53.

27. Bansal S, Prasad Kashyap C, Aggarwal G, Harikumar S. A Comparative Review on Vesicular Drug Delivery System and Stability Issues. Int J Res Pharm Chem. 2012;2(3):704–13.

28. Van Hoogevest P, Fahr A. Phospholipids in Cosmetic Carriers. In: Cornier J., Keck C. V de VM, editor. Nanocosmetics. Springer, Cham; 2019. 95–140.

29. Miaorong Yu, Wenyi Song, Falin Tian, Zhuo Dai, Quanlei Zhu, Ejaj Ahmad, Shiyan Guo CZ. Temperature-and rigidity-mediated rapid transport of lipid nanovesicles in hydrogels. Biophys Comput Biol. 2019;116(12):5362–9.

30. He H, Lu Y, Qi J, Zhu Q, Chen Z, Wu W. Adapting liposomes for oral drug delivery. Acta Pharm Sin B. 2019;9(1):36–48.

31. Ternullo S, Gagnat E, Julin K, Johannessen M, Basnet P, Vanić Ž, et al. Liposomes augment biological benefits of curcumin for multitargeted skin therapy. Eur J Pharm Biopharm. 2019;144:154–64.

32. Krasnici S, Werner A, Eichhorn ME, Schmitt-Sody M, Pahernik SA, Sauer B, et al. Effect of the surface charge of liposomes on their uptake by angiogenic tumor vessels. Int J Cancer. 2003;105(4):561–7.

33. Sercombe L, Veerati T, Moheimani F, Wu SY, Sood AK, Hua S. Advances and challenges of liposome assisted drug delivery. Front Pharmacol. 2015;6:286.

34. Deshmukh RR, Gawale SV, Bhagwat MK. A REVIEW ON : LIPOSOMES. 2016;5(03):506–17.

35. Andrieux K, Forte L, Lesieur S, Paternostre M, Ollivon M, Grabielle-madelmont C. Solubilisation of dipalmitoylphosphatidylcholine bilayers by sodium taurocholate : A model to study the stability of liposomes in the gastrointestinal tract and their mechanism of interaction with a model bile salt. Eur J Pharm Biopharm. 2009;71(2):346–55.

36. Andrieux K, Forte L, Lesieur S, Paternostre M, Ollivon M, Grabielle-madelmont C. Insertion and Partition of Sodium Taurocholate into Egg Phosphatidylcholine Vesicles. 2004;21(8).

37. Wagner A, Vorauer-uhl K. Liposome Technology for Industrial Purposes. 2011;2011.

38. Patil YP, Jadhav S. Novel methods for liposome preparation. Chem Phys Lipids. 2014;177:8–18.

39. Srivastava D, Ansari VA, Singh SP, Ali S, Akhtar J. Journal of Chemical and Pharmaceutical Research , 2016 , 8 (2): 834-838 Review Article Development of liposomal cosmeceuticals. 2016;8(2):834–8.

40. Al-rubaie MS, Abdullah TS. Multi Lamellar Vesicles (Mlvs) Liposomes Preparation by Thin Film Hydration Technique. 2014;32(3):3–4.

41. Of I, Stability V. in Pharmaceutical and Nano Sciences PROLIPOSOMES AS A NOVEL DRUG DELIVERY SYSTEM FOR THE IMPROVEMENT OF VESICULAR STABILITY. 2014;3(4):326–36.

42. Akhilesh D, Faishal G, Kamath J V. Review Article Comparative Study of Carriers Used in Proniosomes. 2012;1(1):164–73.

43. Khan I, Yousaf S, Subramanian S, Korale O, Albed M, Ahmed W, et al. Proliposome powders prepared using a slurry method for the generation of beclometasone dipropionate liposomes. Int J Pharm. 2015;496(2):342–50.

44. Kumara BC, Parthiban S. PROLIPOSOME : A NOVEL APPROACH TO CARRIER DRUG. Int J Biopharm. 2015;6(2):98–106.

45. Gim S, Ong M, Chitneni M, Lee KS, Ming LC, Yuen KH. Evaluation of Extrusion Technique for Nanosizing Liposomes. Pharmaceutics. 2016;8(36):1–12.

46. Clerc SG, Thompson TE. A possible mechanism for vesicle formation by extrusion. Biophys J. 1994;67(1):475–6.

47. Carugo D, Bott E, Owen J, Stride E, Nastruzzi C. Liposome production by microfluidics : potential and limiting factors. Sci Rep. 2016;16(1):1–15.

48. Jahn A, Vreeland WN, Devoe DL, Locascio LE, Gaitan M. Microfluidic directed

formation of liposomes of controlled size. Langmuir. 2007;23(11):6289–93.

49. Hegmann T, Qi H, Marx VM. Nanoparticles in Liquid Crystals : Synthesis , Self-Assembly , Defect Formation and Potential Applications. J. Inorg. Organomet. Polym. Mater. 2007;17 (3): 483-508.

50. Anbarasan B, X FG, Shanmuganathan S. AN OVERVIEW OF CUBOSOMES - SMART DRUG DELIVERY SYSTEM. 2015;8(1):1–4.

51. Jahn A, Kim D, Jahn A, Cho J, Kim JS, Ki M, et al. Lyotropic liquid crystal systems in drug delivery: a review. J. Pharm. Investig. 2014;45(1): 1-11.

52. Guo C, Wang J, Cao F, Lee RJ, Zhai G. Lyotropic liquid crystal systems in drug delivery. Drug Discov Today. 2010;15(23–24):1032–40.

53. Rapalli VK, Waghule T, Hans N, Mahmood A, Gorantla S, Dubey SK, et al. Insights of lyotropic liquid crystals in topical drug delivery for targeting various skin disorders. J Mol Liq. 2020;315:113771.

54. Sangshetti JN, Deshpande M, Zaheer Z, Shinde DB, Arote R. Quality by design approach: Regulatory need. Arab J Chem. 2017;10:S3412–25.

55. Yu LX, Amidon G, Khan MA, Hoag SW, Polli J, Raju GK, et al. Understanding pharmaceutical quality by design. AAPS J. 2014;16(4):771–83.

56. Rapalli VK, Khosa A, Singhvi G, Girdhar V, Jain R, Dubey SK. Application of QbD Principles in Nanocarrier-Based Drug Delivery Systems. In: Sarwar Beg MSH, editor. Pharmaceutical Quality by Design. Academic Press; 2019: 255–96.

57. International Conference on Harmonisation (ICH). Quality risk management Q9. ICH Harmonised Tripartite Guideline. 2005: 1–19.

58. Lionberger RA, Lee SL, Lee L, Raw A, Yu LX. Quality by design: concepts for ANDAs. AAPS J. 2008 Jun;10(2):268–76.

59. International Conference on Harmonisation (ICH). Pharmaceutical Development Q8(R2). ICH Harmonised Tripartite Guideline. 2009: 1–28.

60. Barshikar R. Quality by Design (QbD) and its implementation in Pharma Industry. Express Pharma. 2020: 1–9.

61. Balasaheb Jadhav J, Namdeogirawale N, Chaudhari RA. Quality by Design (QBD) Approach used in Development of Pharmaceuticals. Int J pure Appl Biosci. 2014;2(5):214–23.

62. Bansal S, Beg S, Asthana A, Garg B, Asthana GS, Kapil R, et al. QbD-enabled systematic development of gastroretentive multiple-unit microballoons of itopride hydrochloride. Drug Deliv. 2016;23(2):437–51.

63. Mahmood A, Rapalli VK, Waghule T, Gorantla S, Singhvi G. Luliconazole loaded lyotropic liquid crystalline nanoparticles for topical delivery: QbD driven optimization, in-vitro characterization and dermatokinetic assessment. Chem Phys Lipids. 2021;234:e105028.

64. Srinivas NSK, Verma R, Kulyadi GP, Kumar L. A quality by design approach on polymeric nanocarrier delivery of gefitinib: Formulation, in vitro, and in vivo characterization. Int J Nanomedicine. 2017;12:15–28.

65. Bei D, Marszalek J, Youan BC. Formulation of Dacarbazine-loaded Cubosomes — Part II : In fl uence of Process Parameters. AAPS PharmSciTech. 2009;10(3):1040–7.

66. Waghule T, Dabholkar N, Gorantla S, Rapalli VK, Saha RN, Singhvi G. Quality by design (QbD) in the formulation and optimization of liquid crystalline nanoparticles (LCNPs): A risk based industrial approach. Biomed Pharmacother. 2021;141.

67. Javed MN, Kohli K, Amin S. Risk Assessment Integrated QbD Approach for Development of Optimized Bicontinuous Mucoadhesive Limicubes for Oral Delivery of Rosuvastatin. AAPS PharmSciTech. 2018;19(3):1377–91.

68. Fahmy R, Kona R, Dandu R, Xie W, Claycamp G, Hoag SW. Quality by Design I: Application of Failure Mode Effect Analysis (FMEA) and Plackett–Burman Design of Experiments in the Identification of “Main Factors” in the Formulation and Process Design Space for Roller-Compacted Ciprofloxacin Hydrochloride Immediat. AAPS PharmSciTech. 2012 Dec;13(4):1243–54.

69. Garg NK, Sharma G, Singh B, Nirbhavane P, Tyagi RK, Shukla R, et al. Quality by Design (QbD)-enabled development of aceclofenac loaded-nano structured lipid carriers (NLCs): An improved dermatokinetic profile for inflammatory disorder(s). Int J Pharm. 2017;517(1–2):413–31.

70. Waghule T, Rapalli VK, Singhvi G, Manchanda P, Hans N, Dubey SK, et al. Voriconazole loaded nanostructured lipid carriers based topical delivery system: QbD based designing, characterization, in-vitro and ex-vivo evaluation. J Drug Deliv Sci Technol. 2019;52:303–15.

71. von Stosch M, Schenkendorf R, Geldhof G, Varsakelis C, Mariti M, Dessoy S, et al. Working within the design space: Do our static process characterization methods suffice? Pharmaceutics. 2020;12(6):1–15.

72. Lopes IC, De Oliveira SCB, Oliveira-Brett AM. Temozolomide chemical degradation to 5-aminoimidazole-4-carboxamide - Electrochemical study. J Electroanal Chem. 2013;704:183–9.

73. Danson SJ, Middleton MR. Temozolomide : a novel oral alkylating agent. Expert Rev Anticancer Ther. 2001;1(1):13–9.

74. Newlands ES, Blackledge GRP, Slack JA, Rustin GJS, Smith DB, Stuart NSA, et al. Phase I trial of temozolomide (CCRG 81045 : M & B 39831 : NSC 362856). Bristish J Caner. 1992;65:287–91.

75. Qu J, Zhang L, Chen Z, Mao G, Gao Z, Qu J, et al. Nanostructured lipid carriers , solid lipid nanoparticles , and polymeric nanoparticles : which kind of drug delivery system is better for glioblastoma chemotherapy ? Nanostructured lipid carriers , solid lipid nanoparticles , and polymeric nanoparticles. Drug Deliv. 2016;23(9):3408–16.

76. Gao J, Wang Z, Liu H, Wang L, Huang G. Liposome encapsulated of temozolomide for the treatment of glioma tumor : preparation , characterization and evaluation. Drug Discov Ther. 2015;9(3):205–12.

77. Clemente N, Ferrara B, Gigliotti CL, Boggio E, Capucchio MT, Biasibetti E, et al. Solid lipid nanoparticles carrying temozolomide for melanoma treatment. Preliminary in vitro and in vivo studies. Int J Mol Sci. 2018;19(2).

78. Ananta JS, Paulmurugan R, Massoud TF. Temozolomide-loaded PLGA nanoparticles to treat glioblastoma cells: A biophysical and cell culture evaluation. Neurol Res. 2016;38(1):51–9.

79. Khosa A, Krishna K V, Dubey SK. Chapter 15: Lipid Nanocarriers for enhanced

delivery of temozolomide to the brain. In: Jain KK, editor. Drug Delivery Systems, Methods in Molecular Biology. Springer Science+Business Media; 2020:285–98.

80. Muthu MS, Wilson B. Challenges posed by the scale-up of nanomedicines. Nanomedicine. 2012;7(3):307–9.

81. Mu Q, Yu J, Mcconnachie LA, Kraft JC, Gao Y, Gaurav K, et al. Translation of combination nanodrugs into nanomedicines: lessons learned and future outlook. J Drug Target. 2017;26(5–6):435–47.

82. Agrahari V, Agrahari V. Facilitating the translation of nanomedicines to a clinical product : challenges and opportunities. Drug Discov Today. 2018;23(5):974–91.

83. Dormont F, Rouquette M, Mahatsekake C, Gobeaux F, Peramo A, Brusini R, et al. Translation of nanomedicines from lab to industrial scale synthesis : The case of squalene-adenosine nanoparticles. J Control Release. 2019;307:302–14.

84. Agrahari V. Challenges associated and approaches for successful translation of nanomedicines into commercial products. 2017;12:819–23.

85. McIntosh TJ, Simon SA, Needham D, Huang C hsien. Structure and Cohesive Properties of Sphingomyelin/Cholesterol Bilayers. Biochemistry. 1992;31(7):2012–20.

86. Waghule T, Rapalli VK, Singhvi G, Gorantla S, Khosa A, Dubey SK, et al. Design of temozolomide-loaded proliposomes and lipid crystal nanoparticles with industrial feasible approaches: comparative assessment of drug loading, entrapment efficiency, and stability at plasma pH. J Liposome Res. 2020;31(2):158–68.

Chapter 2

Drug Profile

2.1 Introduction

Temozolomide (TMZ) is chemically 3-methyl-4-oxoimidazo [5, 1-d] [1, 2, 3, 5] tetrazine-8-carboxamide. This second-generation imidazotetrazine derivative was approved by the United States Food and Drug Administration (USFDA) for the treatment of refractory anaplastic astrocytoma in 1999 and the treatment of glioblastoma in 2005. TMZ, a broad-spectrum prodrug, has been found effective in the treatment of glioma, sarcoma, melanoma, leukemia, and carcinoma. It is the only chemotherapeutic drug in the first-line treatment of glioblastoma [1,2].

TMZ is an N-methyl congener of mitozolomide which was the first drug discovered in the class of imidazatetrazines. These compounds were found to show high antitumor potential attributed to the presence of three adjacent nitrogen atoms in comparison to the bicyclic triazenes. The clinical trials for metozolomide showed severe myelosuppression. However, TMZ was found to show a different toxicological profile [3]. This novel drug has action and efficacy similar to dacarbazine. TMZ does not require hepatic activation unlike dacarbazine and can be given orally. It is a small molecule amphiphilic in nature and can cross the blood-brain barrier efficiently. Due to these reasons, TMZ remains a drug of choice for treating brain tumors [4]. TMZ is well tolerated when administered orally showing 100% systemic bioavailability. Despite these advantages, the brain bioavailability of TMZ is only 20-30 % when administered orally or intravenously. This has been attributed to its pH-dependent conversion to 3-methyl-(triazen-1-yl) imidazole-4-carboxamide (MTIC) above pH 6. TMZ undergoes conversion when in plasma and brain, it is expected that brain concentration at any time is 20 % of the systemic concentration. MTIC is a metabolite that rapidly converts to 5-amino-imidazole-4-carboxamide (AIC) and methyl diazonium ion which methylates the O^6 and N^7 position of guanine residues of the DNA resulting in DNA damage. However, these active metabolites have poor permeation through the blood-brain barrier. Only TMZ which crosses the blood-brain barrier is responsible for the therapeutic effect after conversion to MTIC and AIC [4,5].

2.2 Drug properties

IUPAC name:	3-methyl-4-oxoimidazo [5, 1-d] [1, 2, 3, 5] tetrazine-8-carboxamide
Brand names:	Temodar (capsules and injection), Temodal (capsules) and Temcad (capsules)

Drug class:	Anti-cancer alkylating agent
Molecular Formula:	$C_6H_6N_6O_2$
Structure:	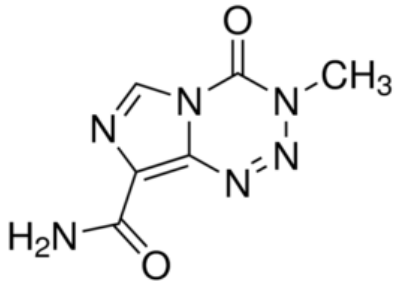
Molecular Weight:	194.154 g/mol
Nature of molecule:	Amphiphilic
Physical description:	Solid/ white light pink/ tan colour
Melting point:	212^{o}C (decomposes)
Solubility:	Slightly soluble in water (3.1 mg/mL), DMSO- > 20 mg/mL
Log P:	- 1.15
pKa:	No pKa as not ionised
BCS class:	Class I
Stability:	Stable below pH 5, start decomposing at pH 7, and completely decomposed at pH 9

2.3 Pharmacodynamic profile

2.3.1 Mechanism of action

TMZ is a prodrug having little to no pharmacological activity. After administration, in presence of water and physiological pH, it undergoes rapid, non-enzymatic hydrolysis at the highly electropositive C4 position. This is followed by the opening of the ring and the release of carbon dioxide to convert to the MTIC. This metabolism takes place at all sites including plasma and brain. The pH of intracellular tumor tissue is alkaline (7.2-7.4) which favors TMZ conversion. MTIC has a short half-life (~ 2.5 mins) and thus rapidly converts to AIC and methyl diazonium ions (**Figure 2.1**). The methyl diazonium ions cause methylation of DNA at the O^6 and N^7 positions of guanine, and O^3 position of adenine. The failure to find a complementary

base for methylated guanine and adenine results in long-lived nicks in the DNA. Also, a complex of proteins is formed which bind to and remove the methylated bases. The DNA replication is inhibited due to subsequent apoptotic cell death, thus preventing tumor proliferation [3,4].

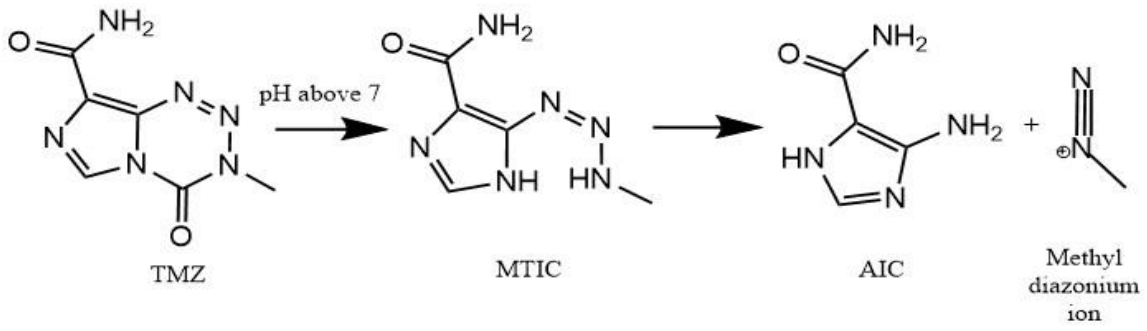

Figure 2.1. Conversion of TMZ at physiological pH to its metabolites

2.3.2 Therapeutic Use

TMZ is used as a first-line treatment for glioblastoma multiforme and advanced metastatic malignant melanoma. It is indicated, along with radiotherapy, to adult patients newly diagnosed with glioblastoma and is followed by maintenance therapy. TMZ is also used as a second-line treatment for refractory anaplastic astrocytoma in patients who have experienced progression of the disease even after use of other chemotherapeutic drugs like nitrosourea and procarbazine [3].

2.3.3 Contraindications

Contraindicated in patients with hypersensitivity to any of the excipients of the capsule or a history of hypersensitivity to DTIC.

2.3.4 Resistance mechanisms

The major problem associated with TMZ therapy is that tumors in a few patients may develop resistance to TMZ. Resistance is an outcome of multiple molecular events including alteration of DNA alkylating proteins expression, DNA repair enzymes, and alterations in cell signaling pathways. It is proposed that the DNA methylated by the active metabolite of TMZ can be removed by base excision. Also, the DNA mismatch repair pathways work to remove any wrongly paired bases. Tumors resistant to TMZ were found to have higher expression of the O^6 methyl guanine methyl transferase/ alkyl guanine transferase protein which repairs the methylation of the guanine. Other pathways of TMZ resistance include decreased levels of nuclear factor-kappa B pathway modulator Tumor necrosis factor-alpha-induced protein 3,

upregulation of microRNAs, upregulation of phosphorylated p65, upregulation of glucose/citrate/choline/creatine levels, and increased c-Jun N-terminal kinase (JNK) signaling pathway [1,5,6].

2.4 Pharmacokinetic data [3,7,8]

Absorption:	Rapid and complete absorption (almost 100%) from the gastrointestinal tract. Peak plasma concentrations are achieved in 1 h. The presence of food affects the rate and extent of absorption. Taking TMZ along with food decreases the maximum plasma concentration by around 33% and increases T_{max} by 2 fold.
Volume of Distribution:	0.4 L/kg (independent of the dose)
Metabolism:	Not metabolized by liver enzymes Hydrolyzed at physiological pH to MTIC (in blood and tissues). MTIC further degrades to AIC and methylhydrazine ions.
Route of Elimination:	Maximum of the drug metabolites are excreted by the renal route. From the total administered TMZ total radioactive dose (mainly comprising of the metabolites) about 37.7% is found in urine and 0.8% in faeces after 7 days. It is estimated that 6 % of the total recovered dose is the unchanged TMZ.
Clearance:	5.5 L/hr/m^2
Biological Half-Life:	Approximately 1.8 h
Protein Binding:	15%
T_{max}:	1 h
CNS bioavailability:	20-30 % of the plasma concentration
Drug interactions:	No major drug interactions. Co-administration with valproic acid is likely to decrease the clearance of TMZ
Side effects and toxicity:	The common side effects are nausea, vomiting, fatigue, headache, anorexia, and constipation. The drug is genotoxic, teratogenic, and fetotoxic. Bone marrow suppression is

observed in some patients. Other adverse reactions are myelodysplastic syndrome, lymphoblastic leukaemia, non-Hodgkin's lymphoma, immunosuppression, aplastic anaemia, hepatotoxicity, pulmonary fibrosis, and diabetes insipidus

B. Diez *et al* [9] investigated the efficacy and safety of TMZ by intravenous and oral routes. Equivalence was found to be attained between a 90 min intravenous infusion and oral delivery of TMZ. Similar Cmax, AUC, and $t_{1/2}$ values were observed for intravenous and orally administered TMZ. Also, a low inter-subject variability was revealed. Intravenous administration of TMZ was generally well tolerated. The pharmacokinetic profile of TMZ was found to be independent of the route of administration.

2.5 Pharmaceutical data

2.5.1 Dosing

The dosing of TMZ consists of multiple schedule-dependent doses. The daily dose is calculated based on the patient's body surface area (BSA) and rounded off to the nearest 5 mg. According to the clinical trials, the recommended dose of TMZ is 750-1000 mg/m^2 which is divided into 5 consecutive days on a 28-day cycle. For newly diagnosed glioblastoma, the initial loading dose of 75 mg/m^2 is given for 42 days along with the radiotherapy. After 4 weeks, 150 mg/m^2 is given as a maintenance dose for 5 days, thereafter for 23 days, no treatment is given. For the following cycles, the dose may be increased to 200 mg/m^2. The dosage must be modified on the basis of the previous cycle neutrophil and platelet counts [9,10].

2.5.2 Storage

Store at 20- 25ºC

2.6 Marketed formulations

TMZ is marketed as oral capsules or powder to be reconstituted for intravenous infusion. Both are marketed with Temodar® as the brand name. The New Drug Application was filed by Merck Sharp Dohme company. Capsules are available in 5, 20, 100, 140, 180, and 250 mg strength. Along with TMZ, the capsules contain lactose anhydrous, sodium starch glycolate, colloidal silicon dioxide, tartaric acid, and stearic acid. Sterile pyrogen-free TMZ lyophilized powder is available as 100 mg/vial. Along with TMZ (100 mg), the vial consists of mannitol (600 mg),

sodium citrate dihydrate (235 mg), L-threonine (160 mg), hydrochloric acid (160 mg) and polysorbate 80 (120 mg). Each vial has to be reconstituted with 41 mL of sterile water for injection (2.5 mg/mL TMZ solution). During infusion, 40 mL is transferred to a 250 mL empty infusion bag. Capsules are also marketed by other generic companies like Accord Healthcare, Sun Pharma, Ani Pharms, Amneal Pharms, Chemi S.p.A, Chartwell, and Zydus Pharms [11].

References:

1. Lee SY. Temozolomide resistance in glioblastoma multiforme. Genes Dis. 2016;3(3):198–210.

2. Herbener VJ, Burster T, Goreth A, Pruss M, Bandemer H von, Baisch T, et al. Considering the experimental use of Temozolomide in glioblastoma research. Biomedicines. 2020;8(6):1–29.

3. Danson SJ, Middleton MR. Temozolomide : a novel oral alkylating agent. 2001;13–9.

4. Friedman HS, Kerby T. Temozolomide and Treatment of Malignant Glioma 1. Clin cancer Res. 2000;6:2585–97.

5. Kingdom U, Corporation S. Temozolomide, a Novel Alkylating Agent with Activity in the Central Nervous System , May Improve the Treatment of Advanced Metastatic Melanoma. Oncologist. 2000;5:144–51.

6. Kaina B. Temozolomide in Glioblastoma Therapy : Role of Apoptosis, Senescence and Autophagy. Comment on Strobel et al., Temozolomide and Other Alkylating Agents in Glioblastoma Therapy. Biomedicines 2019,7,69. Biomedicines. 2019;7(90):4–8.

7. Newlands ES, Blackledge GRP, Slack JA, Rustin GJS, Smith DB, Stuart NSA, et al. Phase I trial of temozolomide (CCRG 81045 : M & B 39831 : NSC 362856). 1992;287–91.

8. Yung WKA. Future directions for temozolomide therapy. Semin Oncol. 2001;28(4 SUPPL. 13):43–6.

9. Schwarz M, Guadalupe ÆM, Fabio PÆ. Evaluation of the exposure equivalence of oral versus intravenous temozolomide. 2010;727–34.

10. Chua J, Nafziger E, Leung D. Evidence-Based Practice: Temozolomide Beyond

Glioblastoma. Curr Oncol Rep. 2019;21(4):1–9.

11. Sun T. CHMP assessment report. Vol. 44. 2011.

Chapter 3

Analytical methods development and validation

3.1 Introduction

A simple and accurate analytical method is necessary for routine analysis and estimation of the selected drug in the complex formulations, drug release studies, and pharmacokinetic studies. Sometimes it can be a reported method or need to be developed. The developed method needs to be validated to ensure reliable and reproducible results. The excipients used in the preparation of formulation should not interfere with the estimation of the drug, thus the developed method should be sensitive and specific. Even using reported method needs validation in the laboratory. ICH and USFDA (United States Food and Drug Administration) provide guidelines on developing and validating the analytical methods. Analytical methods for TMZ estimation using UV (ultraviolet)-Visible spectroscopy have been reported in phosphate buffer pH 2 and 0.1 N HCl [1,2]. However, these methods are either not validated as per ICH guidelines or are not suitable for routine analysis. Recently, a fully validated analytical method for the estimation of TMZ has been reported in 0.1 N HCl [3]. However, the reported method has not been explored for the suitability for lipid-based nanoformulations (planned in this project), drug release, and quantification of conversion of TMZ to MTIC and AIC. The suitability of an alternate analytical method for the estimation of TMZ and the application of the developed method in various aspects can be explored further. There is a requirement to continuously develop new spectroscopic method. A method that is easy to use, easily accessible, solvent-free, and utilizes non-toxic inexpensive chemicals would prove beneficial.

An analytical method using UV-Visible spectroscopy was developed and fully validated. Our team has already developed and fully validated the analytical and bioanalytical (for estimation in plasma samples) methods for estimation of TMZ using HPLC (High-Performance Liquid Chromatography) in our previous studies. The same methods were used subject to some minor modifications like a change in linearity range and column. According to the ICH and USFDA guidelines, these methods were partially validated to ensure accuracy and reproducibility.

3.2 Chemicals and reagents

Temozolomide was obtained as a gift sample from Biophore India Pharmaceuticals Pvt Ltd, Hyderabad, India. 5-Aminoimidazole-4-carboxamide (AIC) was purchased from Toronto Research Chemicals INC, Canada. Sodium acetate (SRL: 99%), glacial acetic acid extra pure (S D Fine-Chem Limited: 99.5%), hydrochloric acid (Central Drug House Pvt Ltd: 35-38%), sodium chloride (Central Drug House Pvt Ltd: 99.5 %), potassium chloride (Qualigens Fine

Chemicals: 99.5%), disodium hydrogen phosphate (Central Drug House Pvt Ltd: 99.5 %), potassium dihydrogen phosphate (S D Fine-Chem Limited: 99.5%), perchloric acid (70 %, Fisher Scientific), formic acid (98 %, CDH), EDTA (99.5 %, Himedia), diethylether (Molychem) were the lab chemicals used. Ganciclovir was obtained as a gift sample from Ranbaxy Laboratories Limited, Gurgaon, India. Milli Q water purified by Merck Millipore systems was used during the entire analysis.

3.3 Analytical method development and validation of TMZ using UV-visible spectroscopy

3.3.1 Instrumentation

The method development and validation were carried out using the ultra-violet visible spectrophotometer (Jasco, Model V-750) connected to a computer loaded with Spectra Manager (Version 2) software. Matched micro quartz cuvettes with 10 mm path length were used for the measurements. Absorption spectra were recorded from 200 to 800 nm at medium scanning speed and 1 nm bandwidth using the Spectrum mode. Quantitative analysis was conducted using the Fixed wavelength mode.

3.3.2 Selection of media and determination of λ_{max}

An appropriate media was selected based on the solubility and stability of TMZ in the media. The analytical method was established for the quantification of TMZ using the selected media. The method was validated as per ICH guidelines [4,5].

Precisely weighed TMZ (10 mg) was dissolved in 10 mL of the selected media to prepare a strength of 1 mg/mL primary stock solution. From this primary stock, a 100 µg/mL secondary stock solution was prepared. The secondary stock solution was diluted further to get a 10 µg/mL solution. The 10 µg/mL solution was scanned from 200-800 nm using ultraviolet spectroscopy to determine the λ_{max} (wavelength of maximum absorption) of TMZ in the selected media. Similarly, a 10 µg/mL solution of AIC (a final metabolite of TMZ) was scanned to determine the λ_{max} of AIC [6].

3.3.3 Linearity and range

The linearity in the analytical procedure provides absorbency directly proportional to the concentration of an analyte. Range determines the interval between the lower and higher concentration of an analyte which is proportional. Lower and upper concentration values were

selected to cover the absorbance range from 0.2 to 1.2 according to Beer Lambert's Law. For the determination of linearity, six solutions of different concentrations (4, 8, 12, 16, 20, 24 µg/mL) in the selected media were prepared respectively. The absorbance of these solutions was analyzed at the λ_{max} of TMZ using the UV spectrophotometer. With the help of the data obtained, the calibration curve was plotted. The regression equation and regression coefficient were determined from the curve. The experiment was performed in triplicate. Standard deviation and % Relative standard deviation (% RSD) were calculated for the obtained data. The Limit of detection (LOD) and Limit of quantification (LOQ) were determined using the equations 3.1 and 3.2

$$LOD = 3.3 (\sigma / S) \ldots\ldots\ldots (3.1)$$

$$LOQ = 10 (\sigma / S) \ldots\ldots\ldots (3.2)$$

where, σ and S are standard deviation and slope of the calibration curve respectively [6,7]

3.3.4 Precision

Precision evaluates the closeness of agreement between a series of measurements from multiple sampling of the same solution. Precision was determined in terms of repeatability, intra-day, and inter-day precision. Different drug quality controls (QC), namely low-quality control (LQC: 6 µg/mL), medium quality control (MQC: 14 µg/mL), and high-quality control (HQC: 22 µg/mL) were selected and made. The repeatability of the method was determined by analyzing the absorbance of the MQC (14 µg/mL) solution six times. Intra-day precision was determined by analyzing the absorbance of LQC, MQC, HQC solutions 3 times a day in triplicate. Inter-day precision was evaluated by analyzing the absorbance of these solutions on three consecutive days in triplicates. Further, the % RSD was calculated [3,5].

3.3.5 Accuracy

Accuracy, also termed as trueness, is the degree to which a measured value conforms to the true value. Accuracy was determined using the quality controls (low, medium, and high) and the standard addition method. For the standard addition method, a known amount of standard stock solution was added to the 50 %, 100%, and 150% of the pre-analyzed solution (4 µg/mL) of TMZ. Using the calibration curve, the concentration of the samples was determined and % recovery was calculated [1,8].

3.3.6 Specificity and Selectivity

Specificity was evaluated to assess the ability of the developed analytical method to detect

TMZ in the presence of other components (metabolites and excipients) that are likely to be present and interfere with the absorbance of the drug. TMZ undergoes conversion to MTIC and AIC. The metabolite MTIC has a short half-life (~ 2.5 min) and immediately converts to AIC. Thus, only AIC is quantifiable. In order to confirm that AIC does not show interference at drug wavelength, a known amount of TMZ concentration (10 µg/mL) was added to AIC solution (AIC dissolved in water, 10 µg/mL). In-order to check the interference of excipients, placebo formulations were spiked with a known amount of drug. The drug-containing dispersion was vortexed to ensure uniform mixing. Methanol (800 µL) was added to 200 µL of this dispersion and centrifuged at 10,000 rpm for 10 minutes at 4^{o}C to settle the lipids. The supernatant was analyzed by the developed UV method after appropriate dilutions. The % of drug recovered in presence of metabolite and excipients was calculated [6,9].

3.3.7 Results and discussion

3.3.7.1 Selection of media and determination of λ_{max}

Based on solubility, stability, and feasibility of use, 0.1 N HCl (pH 1.2) and acetate buffer (pH 4.5) were selected as media for method development and validation of TMZ. In the spectrum of TMZ, three characteristic peaks were observed in both 0.1 N HCl and acetate buffer as seen in **Figure 3.1**. In 0.1 N HCl, two peaks with maximum intensity were observed at 329 and 210.5 nm while a medium intensity peak was observed at 254 nm. In pH 4.5, peaks were observed at 329, 254, and 218 nm. The first peak at 329 nm is attributed to HOMO to LUMO ($\pi \rightarrow \pi^*$) transitions. The peaks at 329 and 254 nm were similar in both the media however a difference in the third peak was observed which showed maximum absorption at 210.5 nm in 0.1 N HCl and 218 nm in acetate buffer. The final stable converted compound, AIC, was found to show maximum absorbance at 267 nm (**Figure 3.1**) which also indicated that AIC does not show any absorbance at drug wavelength (329 nm). Thus a non-separative method can also be suitable for the estimation of TMZ [10–12].

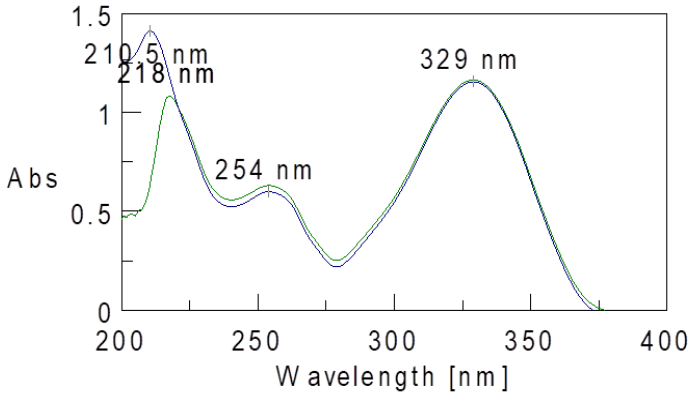

(a)

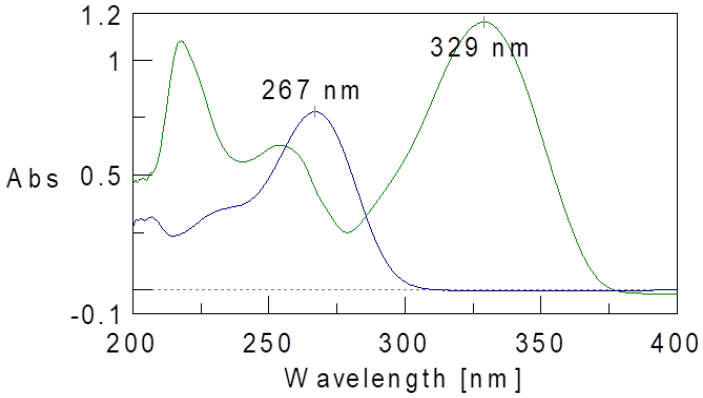

(b)

Figure 3.1. (a) Spectrum of TMZ in 0.1 N HCl (blue) and pH 4.5 (green) acetate buffer (25 µg/mL). (b) Overlay of Spectrum of TMZ (green) and metabolite AIC (blue)

3.3.7.2 Linearity and range

The linearity range of TMZ in both the media was found to be 4-24 µg/mL. The linearity curve obtained is represented in **Figure 3.2**. The regression coefficient (R^2) value of 0.9999 and 0.9997 was obtained. The LOD and LOQ for TMZ in 0.1 N HCl were found to be 0.036 µg/mL and 0.109 µg/mL respectively. The LOD and LOQ for TMZ in acetate buffer were found to be 0.047 µg/mL and 0.144 µg/mL respectively[8,13].

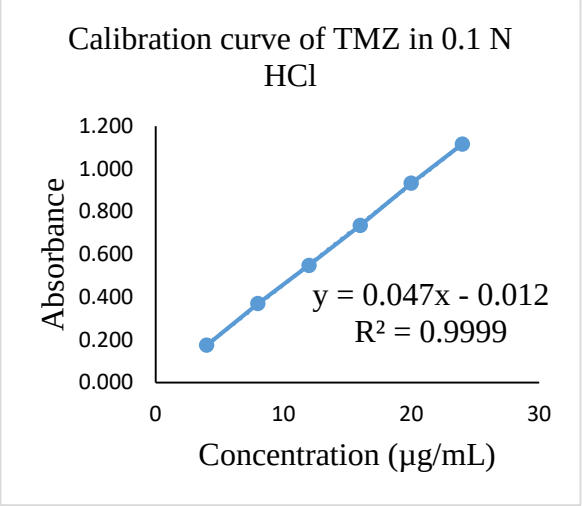

(a)

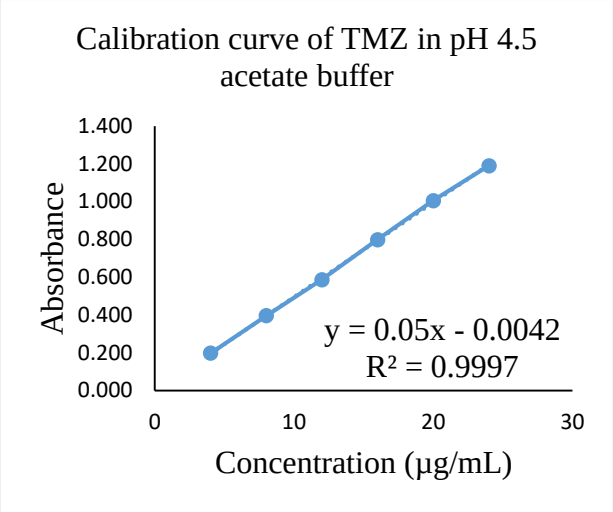

(b)

Figure 3.2. Linearity and range of TMZ in (a) 0.1 N HCl and (b) pH 4.5 acetate buffer using UV-visible spectroscopy

3.3.7.3 Precision

The results obtained for repeatability, intra-day, and inter-day precision for TMZ in 0.1 N HCl and acetate buffer are mentioned in **Table 3.1**. The % RSD of less than 2 % was obtained when the precision was evaluated in terms of repeatability, intra-day, and inter-day precision in both the media. This confirmed the reliability of the developed analytical methods. TMZ was stable in both the selected media [9,14].

3.3.7.4 Accuracy

The results obtained for accuracy in 0.1 N HCl and acetate buffer are summarized in **Table 3.2**. The RSD of less than 1.5 % was obtained in all the cases indicating the accuracy of the developed methods. The recovery in the range of 99.801 to 101.089 % was obtained [5,15].

Table 3.1. Repeatability, Intra-day and Inter-day precision for TMZ using UV analytical method in 0.1 N HCl and pH 4.5 acetate buffer (measurements were done at λ :329 nm)

Repeatability					
Media	Concentration (µg/mL)	Absorbance (Mean ± SD) n=6		% RSD	
0.1 N HCl	14	0.659 ± 0.010		1.495	
pH 4.5 acetate buffer	14	0.693 ± 0.008		1.277	
Media	Concentration (µg/mL)	**Intra-day precision**		**Inter-day precision**	
		Absorbance (Mean ± SD) n=9	% RSD	Absorbance (Mean ± SD) n=9	% RSD
0.1 N HCl	6	0.285 ± 0.004	1.40	0.289 ± 0.002	0.993
	14	0.653 ± 0.002	0.42	0.656 ± 0.004	0.658
	22	1.006 ± 0.011	1.18	1.021 ± 0.018	1.810
pH 4.5 acetate buffer	6	0.298 ± 0.002	0.772	0.295 ± 0.002	0.793
	14	0.690 ± 0.008	1.207	0.666 ± 0.010	1.505
	22	1.022 ± 0.015	1.484	1.012 ± 0.007	0.781

Table 3.2. Accuracy for TMZ using the (low, medium, high) quality controls and the standard addition method for the UV analytical method (measurements were done at λ :329 nm)

	Using Quality controls			**Using the standard addition method**		
Media	Conc. (µg/mL)	% Recovery (Mean ± SD) n=3	% RSD	Amount added (%)	% Recovery (Mean ± SD) n=3	% RSD
0.1 N HCl	6	100.000 ± 0.354	0.354	50	100.733 ± 0.892	0.885
	14	101.089 ± 0.423	0.418	100	100.816 ± 1.074	1.066
	22	100.000 ± 0.730	0.730	150	99.801 ± 0.683	0.685
pH 4.5 acetate buffer	6	100.156 ± 0.429	0.472	50	100.733 ± 0.334	0.330
	14	100.219 ± 0.719	0.717	100	100.55 ± 0.661	0.657
	22	100.986 ± 0.378	0.374	150	100.640 ± 0.871	0.866

3.3.7.5 Specificity and Selectivity

The amount of TMZ recovered in presence of AIC was 100 ± 0.078 %. The placebo formulation containing glyceryl monooleate, poloxamer 127, and PEG 200 was found to show absorbance at the drug wavelength (Figure 3), thus TMZ estimation in these formulations was done using the HPLC analytical method developed in section 3.4. The amount of TMZ recovered in presence of phospholipids (DSPC, DPPC, DMPC) and cholesterol was 99.029 ± 0. 974 % indicating that these excipients did not interfere with the TMZ estimation (**Figure 3.3**). Thus, the TMZ estimation in these formulations was done using the developed UV analytical method. The statistical data summary obtained for UV-visible spectroscopy method has been summarized in **Table 3.3** [9,16].

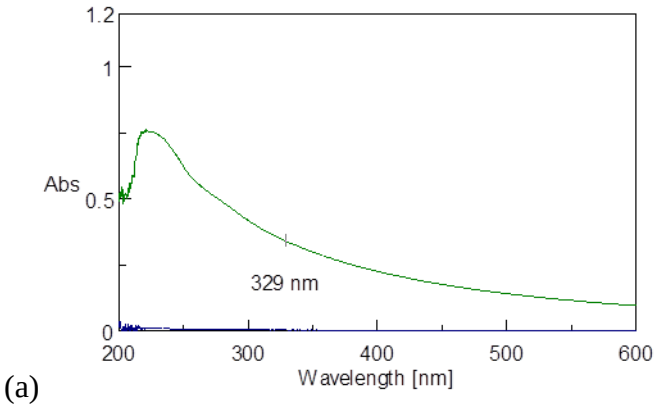

(a)

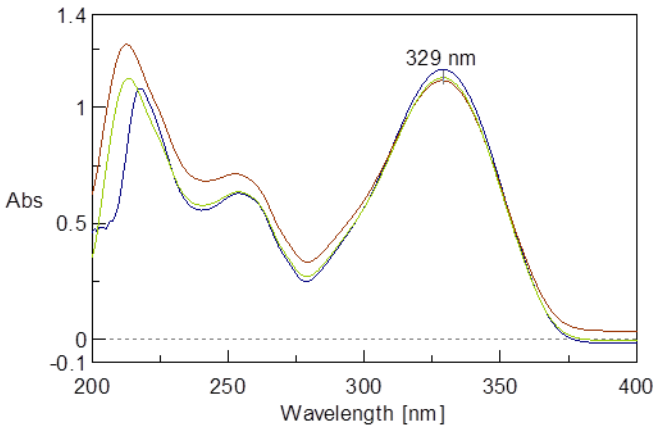

(b)

Figure 3.3. (a) Spectrum of a placebo formulation containing glyceryl monooleate, poloxamer 127 and PEG 200 (b) Spectrum of placebo formulations containing DSPC and cholesterol, DPPC and cholesterol and DMPC and cholesterol spiked with a standard TMZ concentration (10 µg/mL)

Table 3.3. Statistical data summary for UV spectroscopy method

Parameters	Results	
	0.1 N HCl	pH 4.5 acetate buffer
Calibration range (µg/mL)	4-24 µg/mL	4-24 µg/mL
Regression equation	Y=0.047 X – 0.012	Y= 0.05 X – 0.004
Linearity (Regression coefficient)	0.9999	0.9997
Accuracy (% Recovery)	99.801 – 101.089	100.156 – 100.986
Precision (% RSD) Repeatability Intermediate precision	 < 1.495 < 1.810	 < 1.277 < 1.505
Limit of detection (µg/mL)	0.036	0.047
Limit of quantification (µg/mL)	0.109	0.144

(λ_{max} **:**329 nm)

3.4 Analytical method development and validation of TMZ using HPLC

3.4.1 Instrumentation and chromatographic conditions

The Shimadzu HPLC system (LC-2010CHT) connected to a computer with LC solutions software was utilized for developing the analytical method. The system consisted of a quaternary pump, autosampler, and UV-visible detector. The SUPELCO C18 column (250 mm x 4.6 mm x 5 µm) was used for the drug estimation. The mobile phase consisted of 0.5 % glacial acetic acid and methanol which were pumped in an isocratic mode in the ratio of 9:1. The glacial acetic acid (0.5 %) solution was prepared, filtered through a 0.22 µm pore size membrane filter, and degassed using a bath sonicator. The mobile phases were purged before starting the analysis. The column temperature was set at 30ºC. The flow rate was 1mL/min. The system pressure was 120 ± 20 kgf/cm^2. The autosampler sampling speed was 15 µL/sec. The sample volume of 20 µL was injected through the system for analysis. Detection was done at a wavelength of 329 nm. The run time was kept as 10 mins [17,18].

3.4.2 Preparation of stock and calibration standards

A stock solution of TMZ was prepared by dissolving 5 mg of the drug in 5 mL of methanol (1 mg/mL). From this stock solution, 100 µg/mL solution was prepared using acetate buffer (pH 4.5) as diluting solvent which was further used for the preparation of calibration standards.

Calibration standards of 0.1, 0.5, 1, 2, 4, 6, 8, and 10 µg/mL were prepared after appropriate dilutions of the stock solution. The calibration standards were prepared in triplicates [17].

3.4.3 System suitability

System suitability was determined to check the suitability of the system and autosampler to produce reproducible results. A standard concentration (8 µg/mL) was injected 6 times through the system. Parameters like peak area, retention time, capacity factor (k'), tailing factor, and the number of theoretical plates (HETP) were determined and compared [19].

3.4.4 Linearity and range

The calibration standards were analyzed using HPLC with the described chromatographic conditions on three different days. The respective chromatographic peaks and the peak areas were obtained. The calibration curve was produced by plotting peak areas against the concentration (µg/mL). The data was analyzed using the least-squares linear regression. A calibration equation and regression coefficient were generated. The LOD and LOQ were determined using the equations 3.1 and 3.2 [8]

3.4.5 Precision

Precision was determined in terms of intra-day and inter-day precision. LQC (0.75 µg /mL), MQC (3 µg/mL) and HQC (7 µg/mL) were selected as the quality controls. For intra-day precision, the quality control standards were analyzed three different times a day (morning, afternoon, and evening) in triplicates. For inter-day precision, the quality control standards were analyzed on three consecutive days in triplicates. For all the samples, % RSD was determined [20,21].

3.4.6 Accuracy

Accuracy was determined using the quality control standards and the placebo spiking method. The quality control standards (LQC, MQC, and HQC) were analyzed in triplicates. For the placebo spiking method, a standard placebo concentration was added to the quality control standards. Accuracy was determined as % Recovery and % Bias (Equations 3.3 and 3.4) [17].

$$\%\ Recovery = (Predicted\ concentration/Actual\ concentration) * 100 \quad \text{.....(3.3)}$$

$$\%\ Bias = \frac{(Predicted\ concentration - Actual\ concentration)}{Actual\ concentration} * 100 \quad \text{.....(3.4)}$$

3.4.7 Specificity

Specificity studies were conducted to determine the interference of the excipients used in the formulation (liquid crystal nanoparticles as discussed in chapter 6). A Lysis of nanoparticles was carried out by adding methanol to the placebo formulation. This was centrifuged at 15,000 rpm, 4^{o}C for 10 mins to settle the excipients. The supernatant was collected and analyzed using HPLC to check for any interference at the drug wavelength. To the supernatant, a standard drug concentration (8 µg/mL) was added and the sample was analyzed using HPLC. Specificity was confirmed in terms of % recovery [6].

3.4.8 Forced degradation and stability studies

In our previous studies [22], forced degradation studies were conducted, where in, TMZ was exposed to acidic (0.1 N HCl), alkaline (0.1 N NaOH), oxidative (5% hydrogen peroxide) stress conditions, and UV radiation. Thus, these studies were not repeated again. As drug is likely to be exposed to heat during formulation process, heat stability was evaluated. A standard TMZ concentration was exposed to 80^{o}C up to 4 h and the TMZ concentration was estimated at 1, 1.5, 2 and 4 h respectively. Also, the drug stability at pH 7.4 (plasma pH) was evaluated where in the TMZ and AIC (metabolite) peaks were estimated [23,24]

3.4.9 Results and discussion

3.4.9.1 System suitability

The observed system suitability parameters are summarized in **Table 3.4**. The system suitability parameters were highly reproducible indicated by the low standard deviation values. The peak symmetry was indicated by the tailing factor. The tailing factor was found to be ~ 1.2 which is within the acceptable range (0.8 – 1.5). The number of theoretical plates was greater than 2000 [25].

Table 3.4. System suitability parameters for HPLC analytical method

Concentration	8 µg/mL
Area	59785.20 ± 459.32
Retention time (mins)	5.038 ± 0.002
Tailing factor	1.235 ± 0.001
Number of theoretical plates (N)	9348.236 ± 20.040
Height equivalent to theoretical plate (HETP)	16.045 ± 0.034

3.4.9.2 Linearity and range

Linearity was observed in the range of 0.1 to 10 µg/mL. The calibration curve obtained is represented in **Figure 3.4**. The regression coefficient was found to be 0.9997. From the calibration curve, the calculated LOD and LOQ values were 0.0004 µg/mL and 0.014 µg/mL.

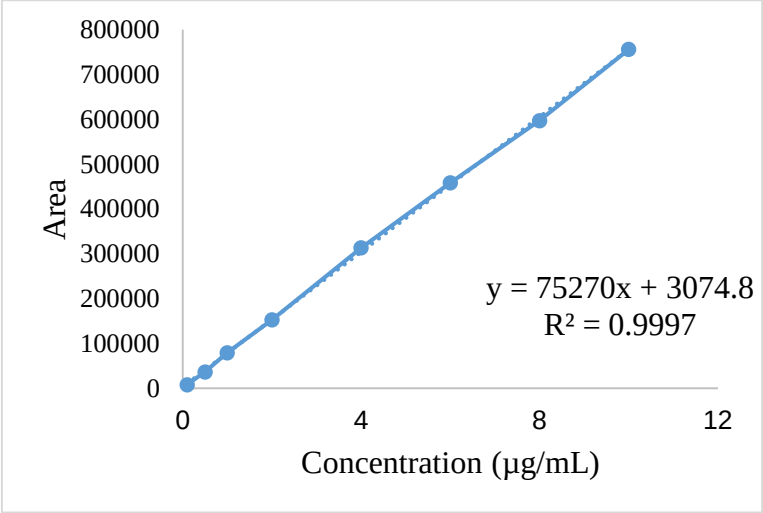

Figure 3.4. Linearity and range of TMZ using HPLC

3.4.9.3 Precision, Accuracy and Specificity

The intra-day and inter-day precision were determined in terms of % RSD which was found to be less than 2 % for all the quality control standards (**Table 3.5**). The accuracy of the method was determined in terms of % recovery and % bias. The % recovery for all the quality control standards was in the range of 99.874 to 101.527 % which was within the acceptable range (95-105 %). The % recovery in quality control samples spiked with placebo formulation was found to be in the range of 99.294 to 100.958 % which confirmed that there was no interference of the excipients with drug estimation. The precision and accuracy data are summarized in Table 3.6. The overlay of HPLC peak of LQC (0.75 µg/mL), MQC (3 µg/mL), and HQC (7 µg/mL) of TMZ are represented in Figure 3.5 [17,26].

Table 3.5. Intra and inter-day precision using HPLC analytical method

Quality control	**Intra-day precision** % RSD (n=9)	**Inter-day precision** % RSD (n=27)
LQC (0.75 µg/mL)	1.237	1.143
MQC (3 µg/mL)	1.899	1.368
HQC (7 µg/mL)	0.954	1.823

Table 3.6. Accuracy data using HPLC analytical method

Accuracy using quality control standards				
Quality control	Predicted concentration (µg/mL) (n=9) Average ± SD	% Recovery Average ± SD	% RSD	% Bias
LQC (0.75 µg/mL)	0.754 ± 0.010	100.577 ± 1.386	1.378	0.577
MQC (3 µg/mL)	3.071 ± 0.059	101.527 ± 1.900	1.871	0.402
HQC (7 µg/mL)	7.059 ± 0.144	99.874 ± 0.451	0.452	-0.45
Accuracy by placebo spiking method				
Quality control	Predicted concentration (µg/mL) (n=3) Average ± SD	% Recovery Average ± SD	% RSD	% Bias
LQC (0.75 µg/mL)	0.754 ± 0.001	100.511 ± 1.198	0.197	0.511
MQC (3 µg/mL)	2.979 ± 0.0002	99.294 ± 0.009	0.009	-0.706
HQC (7 µg/mL)	7.067 ± 0.008	100.958 ± 1.123	0.122	0.958

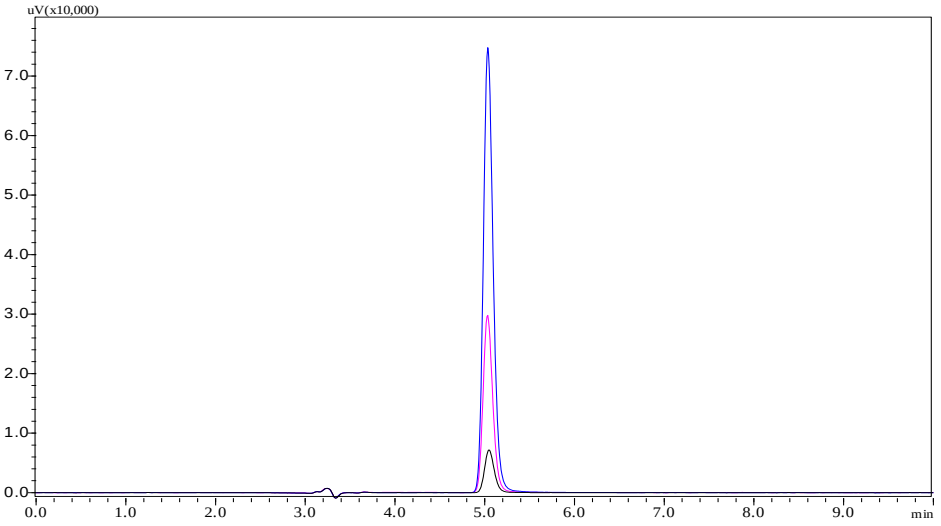

Figure 3.5. Overlay of HPLC peak of LQC (0.75 µg/mL), MQC (3 µg/mL), and HQC (7 µg/mL) of TMZ

The excipients used in lyotropic liquid crystals did not show any interference in TMZ estimation. The overlay of HPLC peak of placebo formulation and standard drug concentration (8 µg/mL) spiked with placebo formulation is represented in **Figure 3.6.**

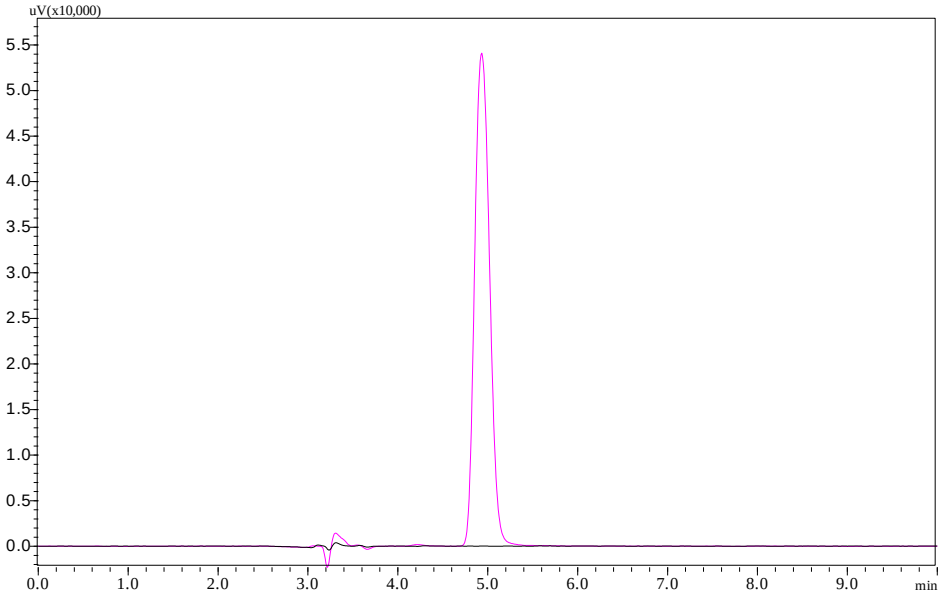

Figure 3.6. Overlay of HPLC peak of placebo formulation and standard drug concentration (8 µg/mL) spiked with placebo formulation

3.4.9.4 Forced degradation and stability studies

As per our previous studies [22], the forced degradation studies revealed that in all stress conditions, except base hydrolysis, the recovery was more than 95 %. When exposed to extreme heat conditions for longer time, TMZ concentration was found to decrease. The % recovery when exposed to heat (80^{o}C) for 1, 1.5, 2 and 4 h was 100.353 ± 0.329, 97.558 ± 0.398, 75.051 ± 1.373 and 37.900 ± 0.281 % respectively. Thus, exposing TMZ to extreme heat conditions for more than 1.5 h should be avoided during the formulation process. During HPLC analysis, TMZ was found to show maximum absorbance at 328 nm (retention time 5.2 mins) whereas its final converted compound (AIC) was found to show maximum absorbance at 272 nm (retention time 3.3 mins). When exposed to alkaline conditions, initially, a high intensity TMZ drug peak was observed at 328 nm as shown in **Figure 3.7**. After 12 h, it was observed that the intensity of drug peak at 328 nm decreased whereas a new peak was observed at 272 nm indicating the conversion of the drug in alkaline conditions. After 24 h, it was observed that the drug peak almost disappeared and high intensity metabolite peak was prominent, indicating that more than 95 % of the TMZ was converted to its metabolite. This conforms with the reports stating that TMZ converts to MTIC (half-life: 2.5 mins) above pH 7, which rapidly get converted to a stable AIC. The study also confirmed that the developed HPLC method could distinguish between the AIC and TMZ and there was no interference at the retention time. The AIC did not show any absorbance at 328 nm. The AIC peak at 272 nm

was found to show interference with the solvent peak. It eluted out early due to its highly hydrophilic nature. The stability indicating potential of the developed method was also confirmed [27–29].

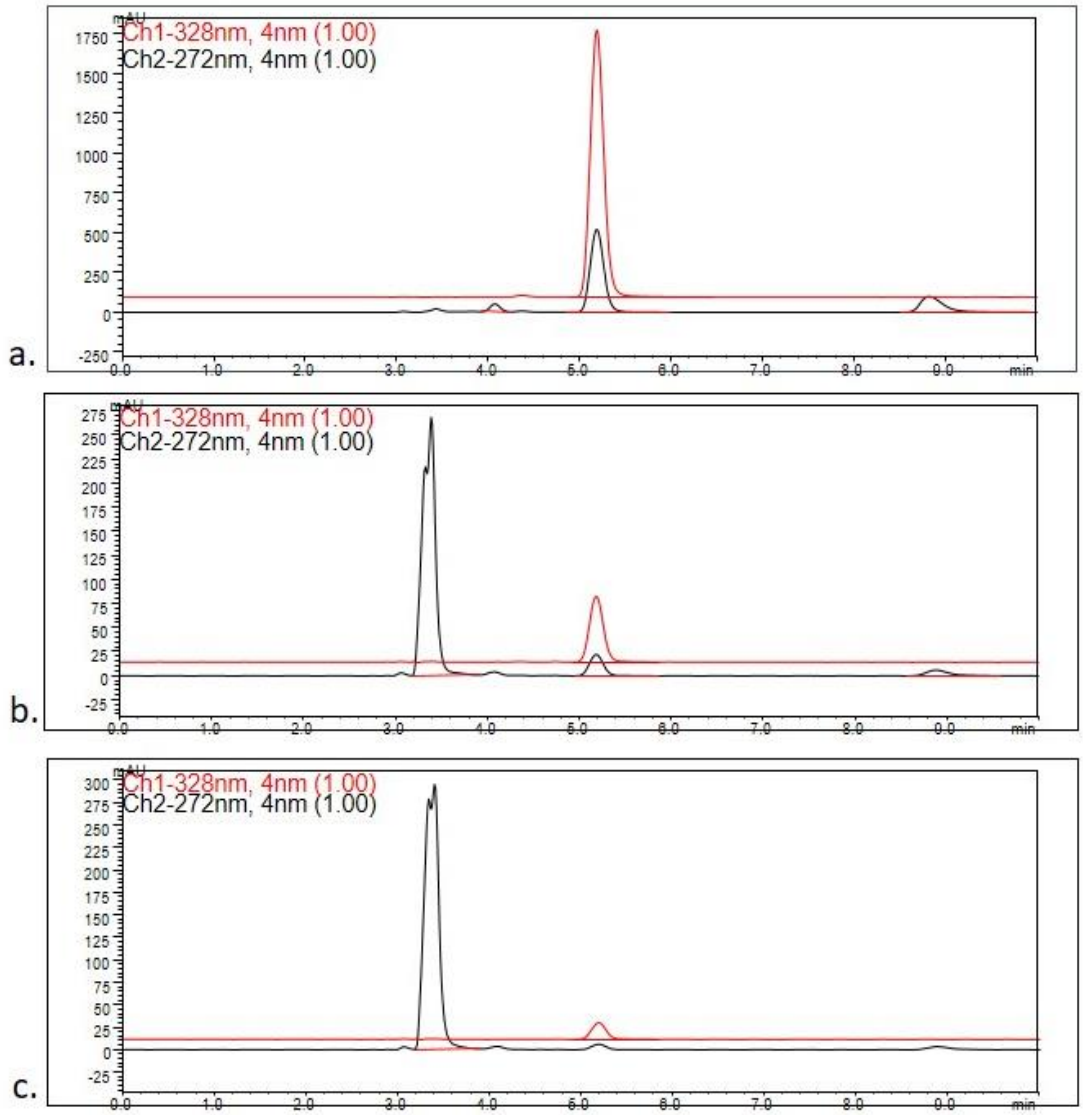

Figure 3.7. HPLC chromatogram showing TMZ peak at 328 nm and metabolite peak at 272 nm after (a) 0 h (b) 12 h (c) 24 h indicating base hydrolysis.

3.5 Bioanalytical method development and validation of TMZ using HPLC

3.5.1 Instrumentation and chromatographic conditions

The same instrument, column and procedure as described in section 3.4.1 were used. In bioanalytical method, the mobile phase consisted of 0.5 % glacial acetic acid and methanol which were pumped in an isocratic mode in the ratio of 98:2. The sample volume of 50 µL was

injected. Detection was done at a dual-wavelength of 310 and 329 nm. The run time was kept as 15 min.

3.5.2 Collection of plasma and tissue homogenates

The study protocol (Protocol No. IAEC/RES/28/13) was approved by the Institutional Animal Ethics Committee (IAEC), BITS PILANI. Healthy male Wistar rats were obtained from the facility and kept in standard plastic cages kept under controlled conditions (23 ± 2^{o}C, 60 ± 5% RH, and 12 h dark-light cycle). The animals were provided standard laboratory pellet food with water ad libitum. Blood was collected from the retro-orbital sinus of the rats in the centrifuge tubes containing 50 µL of 10% w/v EDTA. The blood was centrifuged at 8000 rpm for 10 mins at 4^{o}C. The supernatant plasma was collected and stored at -20^{o}C till further use. The rats were anesthetized and the tissues (brain, kidney, liver, lungs, spleen, and heart) were collected following a surgical procedure. The collected tissues were cleaned with ice cold formic acid (4 %) solution. The organs were dried using Whatmann filter paper (no. 40) and weighed individually. According to the weight, 2 mL ice cold formic acid (4 %) solution was added per gram of a tissue in a 50 mL tarson tube. The organs were thereafter homogenized at 20,000 rpm (Polytron® PT 1600E homogenizer by Kinematica). The obtained fine homogenate was centrifuged at 7500 rpm for 30 min. The supernatant was collected and used further [17].

3.5.3 Preparation of stock and calibration standards

A primary stock solution of TMZ was prepared by dissolving 1 mg TMZ in 1mL methanol (1000 µg/mL). A secondary stock solution of 200 µg/mL was prepared by diluting the primary stock solution with 0.5 % glacial acetic acid solution. From this, spiking standard solutions of 1, 2, 10, 20, 100, and 200 µg/mL were prepared. Calibration solutions (50, 100, 500, 1000, 5000, and 10,000 ng/mL) were prepared by spiking 10 µL of the spiking standard solutions to 190 µL of rat plasma and tissue samples. The plasma samples were stabilized by the addition of 100 µL 1M formic acid solution. Ganciclovir was taken as the internal standard (IS). A primary stock solution of IS was prepared by dissolving 1 mg in 1mL water (1000 µg/mL). A secondary stock solution of 500 µg/mL was prepared by diluting the primary stock solution with water. From this, 50 µg/mL of solution was prepared. This solution (100 µL) was spiked into the plasma and tissue samples. TMZ was extracted from the samples using the protein precipitation method. For extraction, 100 µL of 10% perchloric acid solution was added to the plasma samples and vortex mixed for 5 min. The samples were centrifuged at 15,000 rpm for

30 mins at 4^{o}C. The clear supernatant was collected and analyzed by the HPLC using the developed method [17,30].

3.5.4 Linearity and range

The calibration standards were prepared freshly and analyzed in triplicates. Linearity was obtained by plotting the peak area ratio of TMZ/IS for plasma against concentration. The regression equation and regression coefficient were obtained. The calibration curve was also obtained for individual organs [31].

3.5.5 Precision and Accuracy

Precision was studied in terms of intra-day and inter-day precision. To evaluate the precision, four quality control standards were prepared at a lower limit of quantitation (LLOQ-50 ng/mL), low-quality control (LQC-150 ng/mL), medium-quality control (MQC-4000 ng/mL), and high-quality control (HQC-8000 ng/mL). The quality control standards were prepared in five replicates on three consecutive days and analyzed. Precision was calculated as % RSD. To determine accuracy, the obtained peak area ratios were substituted in the obtained regression equation. Accuracy was studied in terms of % bias [32]

3.5.6 % Extraction efficiency

To evaluate the % extraction efficiency, the quality control standards were prepared in plasma and without plasma. The TMZ and IS were extracted from the plasma by the discussed method. The peak area ratios of extracted samples were compared with the unextracted samples of the respective concentrations [17].

3.5.7 Results and discussion

The overlay of HPLC peaks of blank plasma, plasma spiked with IS and plasma spiked with IS and TMZ at 310 and 329 nm has been represented in **Figure 3.8**. The linearity was obtained within the range of 50 to 10,000 ng/mL. The data obtained and the calibration curve has been represented in **Figure 3.9**. The calibration curve equations obtained for the organs is represented in **Table 3.7**. The % recovery from the plasma extracted quality control standards were found to be in the range of 94.995 to 96.934 with % RSD less than 5 % (**Table 3.7**). The % RSD obtained for intra-day and inter-day precision was less than 15 % (**Table 3.8**). The precision and accuracy data confirmed the reproducibility of the method. The overlay of HPLC peak of LQC, MQC and HQC in plasma samples has been represented in **Figure 3.10.**

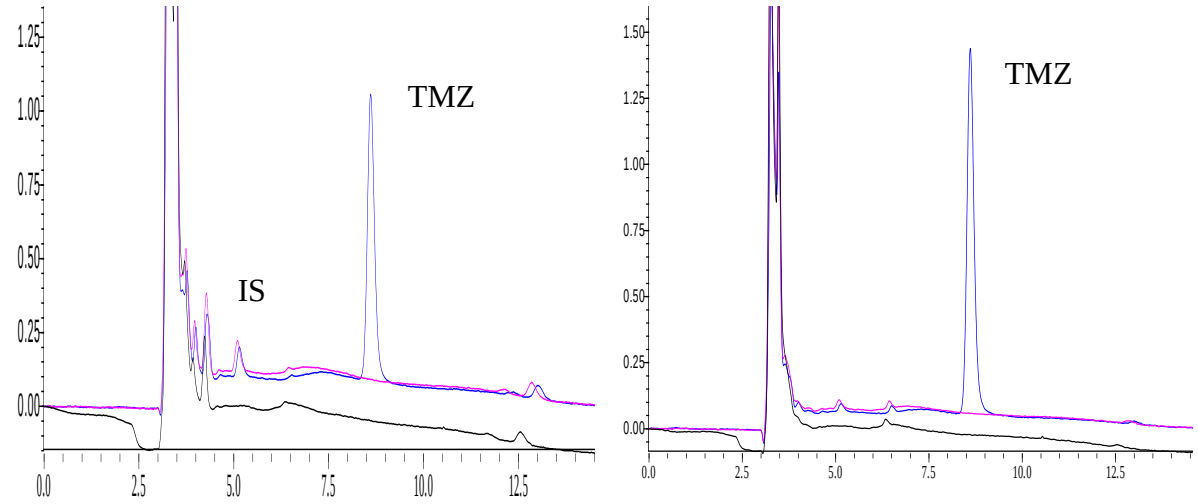

Figure 3.8. Overlay of HPLC peaks of blank plasma, plasma spiked with IS and plasma spiked with IS and TMZ at (a) 310 and (b) 329 nm respectively.

Concentration (ng/mL)	TMZ peak area/ IS peak area (± SD)	%RSD
50	0.246 ± 0.0461	15.721
100	0.437 ± 0.0405	9.272
500	2.249 ± 0.0835	3.711
1000	4.766 ± 0.352	7.401
5000	24.732 ± 1.382	5.589
10,000	52.986 ± 5.641	12.422

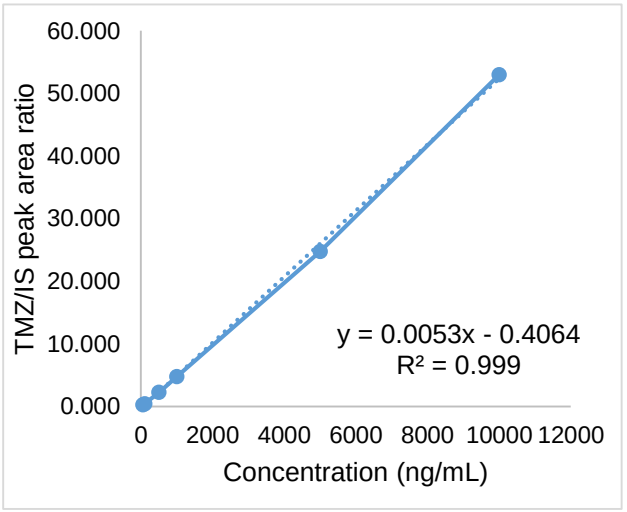

Figure 3.9. Calibration curve data and regression equation for bioanalytical method

3.6 Conclusion

An analytical method was successfully developed and validated using UV-visible spectroscopy. The method was simple, precise, accurate and did not use any organic solvents. The developed method was successfully used for estimation of TMZ in purity, stability study, formulation, and dissolution samples. The analytical and bioanalytical methods, using HPLC, were successfully validated which confirmed the reproducibility and accuracy of our previously developed methods and thus can be used for further estimation of TMZ in stability, formulation, release and tissue samples. Above methods have been used successfully for further work.

Table 3.7. Calibration curve equations obtained for individual organs

Organs	Calibration equation	Regression coefficient
Brain	y = 0.0032x + 0.174	0.9999
Liver	y = 0.0042x + 0.125	0.9988
Kidney	y = 0.0035x - 0.105	0.9989
Lungs	y = 0.0039x + 0.142	0.9988
Spleen	y = 0.0027x + 0.103	0.9991
Heart	y = 0.0035x - 0.002	0.9998

Table 3.8. % Extraction efficiency

Quality control standard	% Recovery (± SD)	%RSD
LLOQ	96.934 ± 1.238	1.277
LQC	96.755 ± 3.979	4.112
MQC	95.647 ± 1.618	1.691
HQC	94.995 ± 2.122	2.234

Table 3.9. Precision and accuracy data for bioanalytical method

Quality control standard	Precision (% RSD)		Accuracy (% Bias)	
	Intra-day	Inter-day	Intra-day	Inter-day
LOQQC (50 ng/mL)	14.251	10.665	-9.947	-10.101
LQC (150 ng/mL)	6.796	6.388	6.495	4.870
MQC (4000 ng/mL)	5.859	4.662	-5.136	-6.860
HQC (8000 ng/mL)	10.357	12.220	1.568	-5.651

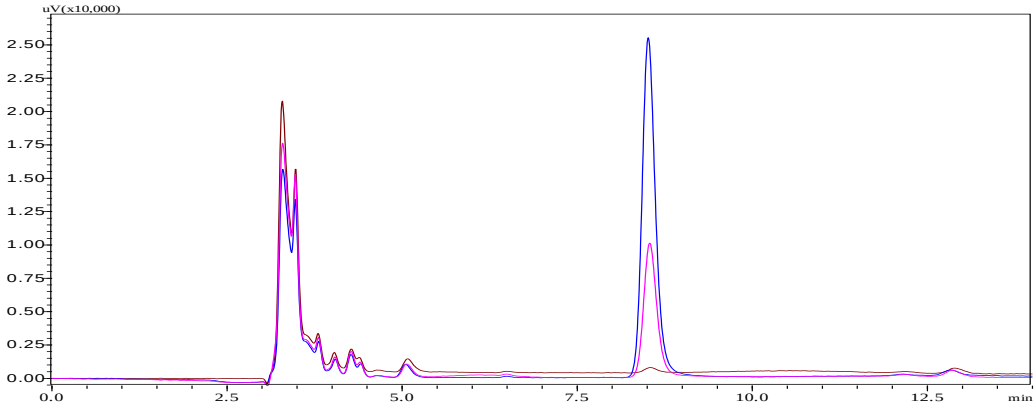

(a)

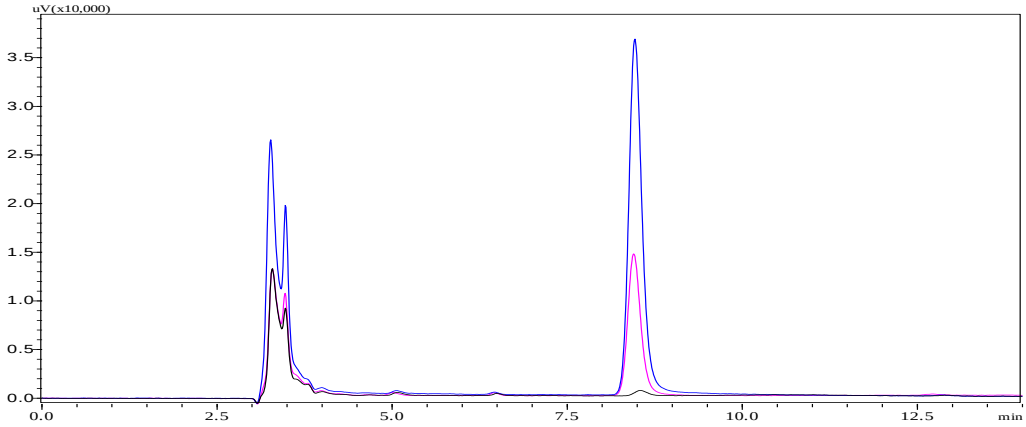

(b)

Figure 3.10. Overlay of HPLC peak of LQC, MQC and HQC in plasma samples at (a) 310 and (b) 329 nm respectively.

References:

1. B Mohammed I, Hindustan AA, Shaik M, S P, B F. Analytical Method Development and Validation for the Estimation of Temozolomide in Phosphate Buffer Ph 2.0 As a Solvent By Uv Spectroscopy. Int Res J Pharm. 2014;4(1):17–20.

2. A. Abdul Razak, SK Masthanamma, B. Omshanthi, V. Suresh PO. Development and validation of UV spectrophotometric method of temozolomide in bulk and capsule formulation. Int J PharmTech Res. 2013;4(4):1419–23.

3. Khosa A, Sinha S, Reddi S, Saha RN. Simple, rapid and sensitive uv spectrophotometric method for determination of temozolomide in poly-ε-caprolactone nanoparticles. Asian J Chem. 2018;30(4):868–72.

4. Mahmood A, Rapalli VK, Waghule T, Gorantla S, Dubey SK, Saha RN, et al. UV spectrophotometric method for simultaneous estimation of betamethasone valerate and tazarotene with absorption factor method: Application for in-vitro and ex-vivo characterization of lipidic nanocarriers for topical delivery. Spectrochim Acta - Part A Mol Biomol Spectrosc. 2020;235:118310.

5. Ravichandran V, Shalini S, Sundram KM, Rajak H. Validation of analytical methods - Strategies & importance International Journal of Pharmacy and Pharmaceutical Sciences. Int J Pharm Pharm Sci. 2010;2(3):18–22.

6. Rapalli VK, Kaul V, Gorantla S, Waghule T, Dubey SK, Pandey MM, et al. UV Spectrophotometric method for characterization of curcumin loaded nanostructured lipid nanocarriers in simulated conditions: Method development, in-vitro and ex-vivo applications in topical delivery. Spectrochim Acta Part A Mol Biomol Spectrosc. 2020;224:117392.

7. Singh S, Saini M, Malik JK, Kumar A. Analytical Method Development and Validation for Estimation of Silymarin in Tablet Dosage form by HPLC. Asian J Appl Chem Res. 2020;(04):22–31.

8. Nita Yadav AG. Method development and validation of Teneligliptin in pharmaceutical dosage form by UV spectrophotometric methods. Int J Pharm Chem Anal. 2017;4(3):54–8.

9. Singh S, Sharma N, Kanojia N, Kaur G, Arora S. Development and validation of UV-spectrophotometer method for analysis of Fluvastatin sodium in polyethylene glycol 6000 and polyvinyl pyrollidone K30 solid dispersions. Plant Arch. 2020;20(1):3365–71.

10. Khalilian MH, Mirzaei S, Taherpour AA. The simulation of UV spectroscopy and electronic analysis of temozolomide and dacarbazine chemical decomposition to their metabolites. J Mol Model. 2016;22(11):270.

11. Lopes IC, De Oliveira SCB, Oliveira-Brett AM. Temozolomide chemical degradation to 5-aminoimidazole-4-carboxamide - Electrochemical study. J Electroanal Chem. 2013;704:183–9.

12. Fotaki N, Brown W, Kochling J, Chokshi H, Miao H, Tang K, et al. Rationale for selection of dissolution media: Three case studies. Dissolution Technol. 2013;20(3):6–

13.

13. Waghule T, Narayan R, Singhvi G. UV spectroscopic method for estimation of temozolomide : Application in stability studies in simulated plasma pH , degradation rate kinetics , formulation design , and selection of disso. Spectrochim Acta Part A Mol Biomol Spectrosc. 2021;258:119848.

14. Gorantla S, Saha RN, Singhvi G. Spectrophotometric method to quantify tofacitinib in lyotropic liquid crystalline nanoparticles and skin layers: Application in ex vivo dermal distribution studies. Spectrochim Acta - Part A Mol Biomol Spectrosc. 2021;255:119719.

15. Singhvi G, Shukla VK, Ukawala R, Gampa G, Saha RN. Development of a new, rapid and sensitive HPTLC method for estimation of Milnacipran in bulk, formulation and compatibility study. Arab J Chem. 2017;10:S2417–23.

16. Rapalli VK, Kaul V, Gorantla S, Waghule T, Dubey SK, Pandey MM, et al. UV Spectrophotometric method for characterization of curcumin loaded nanostructured lipid nanocarriers in simulated conditions: Method development, in-vitro and ex-vivo applications in topical delivery. Spectrochim Acta - Part A Mol Biomol Spectrosc. 2020;224:117392.

17. Khosa A, Krishna K V., Saha RN, Dubey SK, Reddi S. A simplified and sensitive validated RP-HPLC method for determination of temozolomide in rat plasma and its application to a pharmacokinetic study. J Liq Chromatogr Relat Technol. 2018;41(10):692–7.

18. Kapçak E, Şatana-Kara EH. Development and full validation of a stability-indicating HPLC method for the determination of the anticancer drug temozolomide in pharmaceutical form. Turkish J Pharm Sci. 2018;15(3):271–7.

19. Bose, Anirbandeep , Acharya BR. HPLC Calibration Process Parameters in Terms of System Suitability Test. Austin Chromatogr. 2014;1(2):1–4.

20. Gorantla S, Saha RN, Singhvi G. Design of experiment-driven stability-indicating RP-HPLC method for the determination of tofacitinib in nanoparticles and skin matrix. Futur J Pharm Sci. 2021;7(1):1-12.

21. Sun H, Liu S, Gao X, Xiong Z, He Z, Zhao L. Study on degradation kinetics of epalrestat in aqueous solutions and characterization of its major degradation products under stress degradation conditions by UHPLC-PDA-MS/MS. J Pharm Anal. 2019;9(6):423–30.

22. Philosophy DOF, Khosa A. Design , Characterization and Evaluation of Lipid Based Nanoparticulate Temozolomide for Enhanced Delivery to the brain. BITS PILANI, pilani campus; 2018.

23. Rapalli VK, Singhvi G, Gorantla S, Waghule T, Dubey SK, Saha RN, et al. Stability indicating liquid chromatographic method for simultaneous quantification of betamethasone valerate and tazarotene in in vitro and ex vivo studies of complex nanoformulation. J Sep Sci. 2019;42(22):3413–20.

24. Zhou D, Porter WR, Zhang GGZ. Drug stability and degradation studies. Developing Solid Oral Dosage Forms: Pharmaceutical Theory and Practice: Second Edition. Elsevier Inc.; 2017. 113–149.

25. Syed HK, Liew K Bin, Loh GOK, Peh KK. Stability indicating HPLC-UV method for detection of curcumin in Curcuma longa extract and emulsion formulation. Food Chem. 2015;170:321–6.

26. Rapalli VK, Singhvi G, Gorantla S, Waghule T, Dubey SK, Saha RN, et al. Stability indicating liquid chromatographic method for simultaneous quantification of betamethasone valerate and tazarotene in in vitro and ex vivo studies of complex nanoformulation. J Sep Sci. 2019;42:3413–20.

27. Baker SD, Wirth M, Statkevich P, Reidenberg P, Alton K, Sartorius SE, et al. Absorption, metabolism, and excretion of 14C-temozolomide following oral administration to patients with advanced cancer. Clin Cancer Res. 1999;5(2):309–17.

28. Andrasi M, Bustos R, Gaspar A, Gomez FA, Klekner A. Analysis and stability study of temozolomide using capillary electrophoresis. J Chromatogr B Anal Technol Biomed Life Sci. 2010;878(21):1801–8.

29. Waghule T, Rapalli VK, Singhvi G, Gorantla S, Khosa A, Dubey SK, et al. Design of temozolomide-loaded proliposomes and lipid crystal nanoparticles with industrial feasible approaches: comparative assessment of drug loading, entrapment efficiency, and stability at plasma pH. J Liposome Res. 2020;31(2):158–68.

30. Tijare LK, Rangari NT, Mahajan UN. A review on bioanalytical method development and validation. Asian J Pharm Clin Res. 2016;9:6–10.

31. Krishna KV, Saha RN, Singhvi G, Dubey SK. Pre-clinical pharmacokinetic-pharmacodynamic modelling and biodistribution studies of donepezil hydrochloride by a validated HPLC method. RSC Adv. 2018;8(44):24740–9.

32. Singhvi G, Kumar V, Ukawala R, Saha RN. Development of Bioanalytical HPLC Method for Estimation of Milnacipran Hydrochloride in Rabbit Plasma Using Solid Phase Extraction Technique and its Application in Pharmacokinetic Investigation. Curr Pharm Anal. 2017;13(6):574–80.

Chapter 4

Preformulation studies

4.1 Introduction

Formulation development is an extensive and expensive process. Every drug has different characteristics and properties which should be well known or studied for making effective formulation or delivery system. The formulation process involves several steps and knowledge of drug characteristics are essential. Each step requires adequate conditions and parameters to be maintained. Before beginning with the formulation development of any drug, adequate information about the physicochemical properties of the drug molecule need to be gathered either from literature or a few preformulation studies. Preformulation studies guide in selecting appropriate excipients, proper manufacturing process and storage conditions required during the formulation. The challenges faced during formulation development can be reduced with adequate knowledge about drug [1,2]. The physicochemical properties of TMZ are available in the literature. A few additional preformulation studies can provide a rationale for the selection of excipients. Appropriate conditions can be maintained during formulation preparation. These studies can help in designing the proposed lipid-based nanoparticles.

4.2 Materials

Temozolomide was obtained as a gift sample from Biophore India Pharmaceuticals Pvt Ltd, Hyderabad, India. DSPC (Distearoylphosphatidylcholine) was obtained as a gift sample from VAV Life Sciences Pvt Ltd, Mumbai, India. Cholesterol (Minimum assay: 95%) was purchased from Central Drug House (P) Ltd, Bombay. Glyceryl monooleate (GMO) was received as a gift sample from Mohini Organics Pvt. Ltd. Pluronic 127 was acquired as a gift sample from BASF (Mumbai), Polyethylene glycol 200 (PEG 200) was purchased from CDH Fine Chemicals (New Delhi). DSPE-PEG 2000 (1,2-Distearoyl-sn-glycero-3-phosphoethanolamine-N-[methoxy(polyethylene glycol 2000)] was obtained as a gift sample from Lipoid GmbH. Sodium acetate (SRL: 99%), glacial acetic acid extra pure (S D Fine-Chem Limited: 99.5%), hydrochloric acid (Central Drug House Pvt Ltd: 35-38%), sodium chloride (Central Drug House Pvt Ltd: 99.5 %), potassium chloride (Qualigens Fine Chemicals: 99.5%), disodium hydrogen phosphate (Central Drug House Pvt Ltd: 99.5 %), and potassium dihydrogen phosphate (S D Fine-Chem Limited: 99.5%) were the lab chemicals used. Milli Q water purified by Merck Millipore systems was made in the lab and used during the entire analysis.

4.3 Instruments/Equipment

Denver Instruments Monolithic Analytical balance TB-215D, UV visible spectrophotometer (Jasco, Model V-750), Shimadzu HPLC system (LC-2010CHT), REMI Laboratory Centrifuge R8C, Temperature controlled centrifuge (Centrifuge 5430R, Eppendorf, Germany), Toshiba Bath Sonicator (Laboratory Testing Instruments, Delhi, India), Differential Scanning Calorimeter (DSC-60, Shimadzu, Japan), Bruker ATIR spectrophotometer (OPUS software), Tarsons Multispin Motorless Magnetic Stirrer, and Tarsons Spinot Digital Magnetic Stirrer were the instruments and equipment used.

4.4 Methods

4.4.1 Bulk characterization

The physical properties of TMZ like appearance and colour were identified visually. The functional groups in TMZ were identified using ATIR. The IR spectrum was obtained in the range of 400 – 4000 nm^{-1}. The melting point of TMZ was determined using DSC. Approximately 2 mg of TMZ was filled in an aluminum pan which was covered with the lid and sealed. The sealed pan was placed in the sample holder against the reference pan. The inert environment was maintained by purging nitrogen at a 30 mL/min flow rate. The heating rate was maintained at 10^{o}C/min. Thermogram was obtained in the range of 30-300^{o}C [3,4].

4.4.2 Solubility studies

The solubility of TMZ in various aqueous and organic solvents was determined using the shake flask method. Excess of TMZ was added to 2 mL of each solvent and kept under constant stirring. After 24 hours, the concentration of TMZ was determined using the developed analytical methods [5,6].

4.4.3 Stability studies and degradation rate kinetics

Stability studies were conducted to evaluate the effect of environmental factors on the quality of the drug. These can be utilized for the prediction of shelf-life, deciding the appropriate storage conditions, and formulation design [7]. To study the solution state degradation rate kinetics, TMZ (5 mg) was dissolved completely in 20 mL of 0.1 N HCl (pH 1.2), acetate buffer (pH 4.5) and phosphate buffer (pH 7.4) respectively to get 250 µg/mL solution. These were divided as 1 mL solution into Eppendorf tubes. The tubes were analyzed sequentially at different time intervals (0, 3, 6, 9, 12, 24, 36, 48, 60, and 72 h) using the developed UV spectroscopic method for TMZ concentration after appropriate dilutions. In the case of pH 7.4

solutions, dilutions and analysis were done using pH 4.5 acetate buffer. The concentration of TMZ at different time intervals was calculated using the respective developed methods. The kinetics and conversion rate of TMZ in different pH media was analyzed and t_{90} (time taken for 10% of the drug to degrade) was calculated. As the proposed formulation was supposed to be reconstituted in an appropriate media suitable for parenteral administration, the degradation rate kinetics and stability of TMZ in Water for injection, acetate buffer pH 4.5 (10 mM), citrate buffer pH 4.5 (10 mM), 0.9 % Normal saline, and 5 % Dextrose injection was also evaluated [4,8,9].

4.4.4 Partition coefficient

A stock solution of TMZ (1 mg/mL) was prepared in acetate buffer (pH 4.5). Lipid (glycerylmonooleate, 500 mg) was weighed and melted at 70^{o}C. TMZ stock solution (2 mL) was added to the melted lipid and kept under stirring for 2 h at 70^{o}C. TMZ stock solution (2 mL) kept under the same conditions was considered as a control. The samples were cooled and centrifuged at 10,000 rpm for 30 min. The supernatant was analyzed using the HPLC method. The lipid/water partition coefficient was determined using equation 4.1 [10].

$$Partition\ coefficient = \frac{Concentration\ of\ TMZ\ added - Concentration\ of\ TMZ\ in\ aqueous\ phase}{Concentration\ of\ TMZ\ in\ aqueous\ phase} \quad \text{.....(4.1)}$$

4.4.5 Drug-excipient compatibility studies

Drug excipient compatibility was determined by HPLC analysis. A physical mixture of TMZ and various excipients (GMO, PF 127, PEG 200, phospholipids, cholesterol, and DSPE-PEG 2000) mixed in a 1:2 ratio was formed by uniform mixing. The physical mixtures were stored at room temperature (30^{o}C) and refrigerated conditions (4^{o}C). During analysis, the physical mixtures were dissolved in 1 mL methanol and further diluted with acetate buffer (pH 4.5). These were further centrifuged at 15,000 rpm for 10 min. The supernatant was analyzed by the developed HPLC method for drug assay after 1, 2, and 3 months respectively. The mixtures were also observed visually for any changes in colour or lump formation [11,12].

4.4.6 Selection of appropriate dissolution medium

In-vitro drug release studies were carried out in two different media with pH 4.5 and pH 7.4 respectively to study the effect of pH of the dissolution media on the TMZ dissolution. The dissolution of TMZ was studied in three ways (i) TMZ was dissolved in acetate buffer pH 4.5

and dissolution was studied with acetate buffer pH 4.5 as dissolution medium (ii) TMZ was dissolved in acetate buffer pH 4.5 and dissolution was studied with phosphate buffer saline pH 7.4 as dissolution medium (iii) TMZ was dissolved in 0.9 % Normal saline and dissolution was studied with phosphate buffer saline pH 7.4 as dissolution medium. In each case, TMZ solution (1 mL equivalent to 1 mg TMZ) was filled in a dialysis bag. The bag was inserted in 30 mL dissolution media and kept under stirring at 80 rpm. The temperature was maintained at 37±0.5^{o}C. Aliquots (0.5 mL) were taken at different time intervals (0.5, 1, 2, 4, 8, 12, and 24 h respectively). The media was replenished with an equal volume of the respective dissolution media each time. The samples were analyzed using the developed UV analytical method after appropriate dilutions [13–15].

4.5 Results and discussion

4.5.1 Bulk characterization

The pure TMZ appears as a light cream colour powder. The FTIR spectrum obtained for the pure drug is shown in **Figure 4.1**. The characteristic strong peak for carbonyl amide was found at 1680-1630 cm^{-1} thus confirming the presence of amide. The N-H band for secondary amide was observed at 3300 cm^{-1}. The N-H stretch for primary amide was seen as a doublet in the range of 3350 and 3180 cm^{-1}. The N-H bending band at 1640-1620 cm^{-1} is found to partially overlap the carbonyl band. Other bands like N=N stretching at 1577 cm^{-1} and C-N stretching at 1400 cm^{-1} were also observed.

The exothermic peak for TMZ was obtained at 215.3^{o}C which is close to the reported melting point of the drug 212^{o}C. The sharp symmetric peak indicates the relative purity of the sample. A broadening or asymmetric peak indicates the presence of impurities.

4.5.2 Solubility studies

The solubility of TMZ in water and aqueous buffers (pH 1-6) was found to be 4.604 ± 0.22 mg/mL. Above pH 7, the drug is found to show pH dependent stability as revealed in the stability studies. A similar solubility was found in organic solvents like methanol, acetonitrile and acetone. A solubility of less than 2 mg/mL was observed in solvents like ethanol, isopropyl alcohol and ethyl acetate. A solubility of 10 ± 2.530 mg/mL was observed in dicloromethane. A higher solubility (25.023 ± 3.120 mg/mL) was observed in DMSO [6].

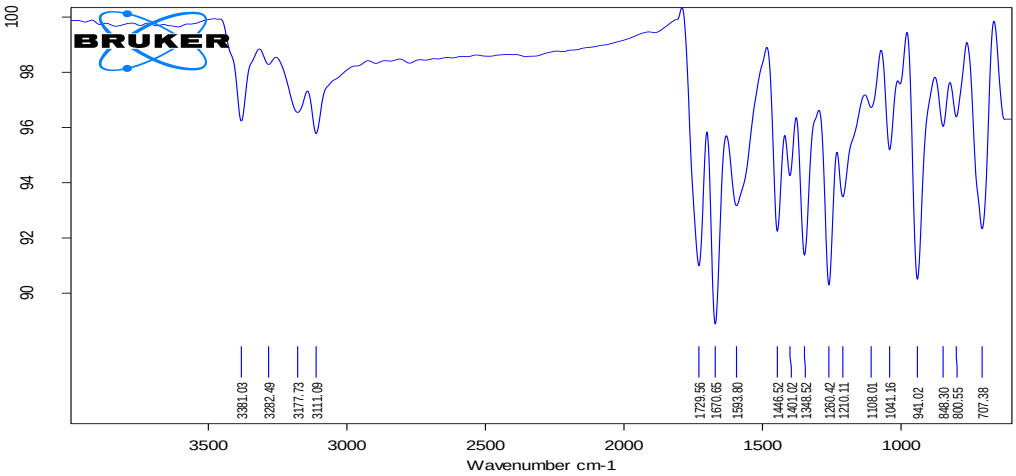

(a) FTIR spectrum of TMZ

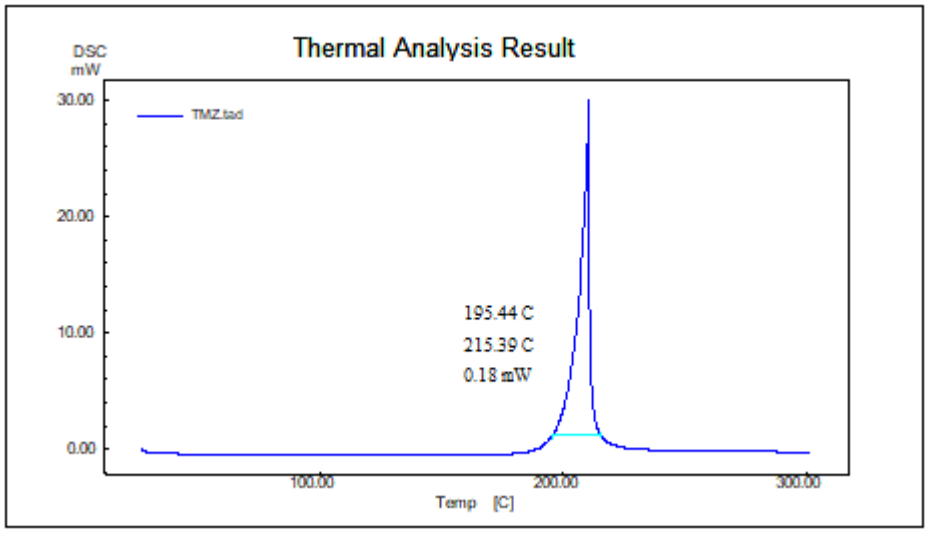

(b) DSC thermogram of TMZ

Figure 4.1. FTIR spectrum and DSC thermogram of TMZ

4.5.3 Stability studies and degradation rate kinetics

The stability studies revealed pH-dependent stability of TMZ which is also in accordance with the reported literature [16]. The pH-dependent stability is attributed to the protonated and non-protonated state of TMZ in acidic and alkaline conditions. The protonated form present at lower pH conditions decreases the rate of conversion but does not halt it completely [17]. An overlay of the spectrum of TMZ in pH 1.2, pH 4.5, and pH 7.4 after 24 h respectively is represented in **Figure 4.2**. After 24 h, the spectrum of TMZ at pH 1.2 and pH 4.5 remained unchanged. However, the spectrum of TMZ in pH 7.4 showed a decrease in absorption intensity at the λ_{max} 329 nm (attributed to the urea group present in TMZ) and an appearance of a new peak at 264 nm (attributed to the amide group) indicating the conversion of TMZ to its AIC metabolite (**Figure 4.2**) [18,19]. The second peak at 254 nm gradually shifted to 264 nm in the course of

time while the third peak near 215 nm decreased in intensity. The spectra of TMZ at pH 1.2 and pH 4.5 remain unchanged up to 144 h (**Figure 4.3**). The conversion of TMZ to its metabolite was found to follow first-order rate kinetics as represented in **Figure 4.4**. The conversion rate of TMZ in pH 1.2, pH 4.5, and pH 7.4 was found to be 0.0011, 0.0011, and 0.0453 h^{-1} respectively. The $t_{90\%}$ in pH 1.2, pH 4.5, and pH 7.4 were found to be 91.51 h, 91.51 h, and 2.32 h respectively. The TMZ was found to be stable in all the parenteral solutions indicated by more than 90 % drug remaining up to 48 h. Thus, the reconstituted nanoformulation dispersions should not be stored in these parenteral solutions for more than 48 h before administering to the paitent The degradation profile obtained in parenteral solutions is represented in **Figure 4.5** [7,16].

4.5.4 Partition coefficient

The partition coefficient of TMZ in GMO and water was found to be 0.311 which revealed affinity of TMZ towards water.

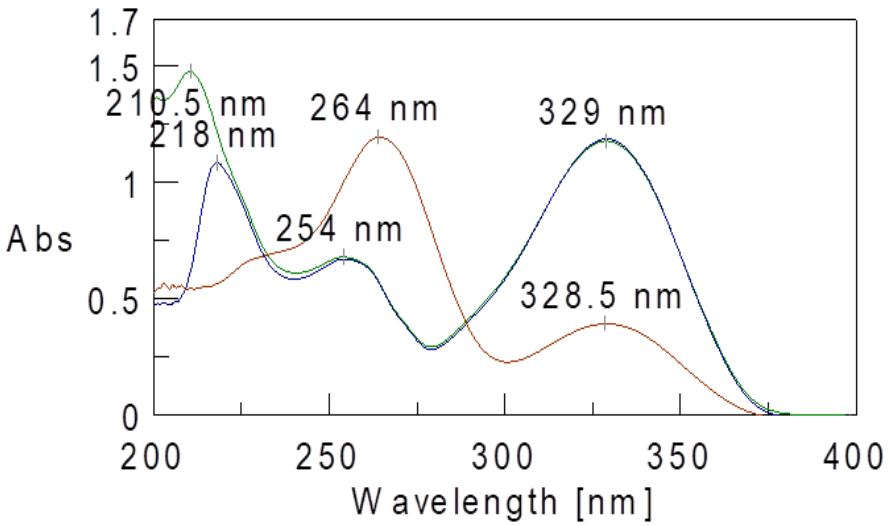

Figure 4.2. Overlay of spectra of TMZ in pH 1.2 (green), 4.5 (blue) and 7.4 (red) after 24

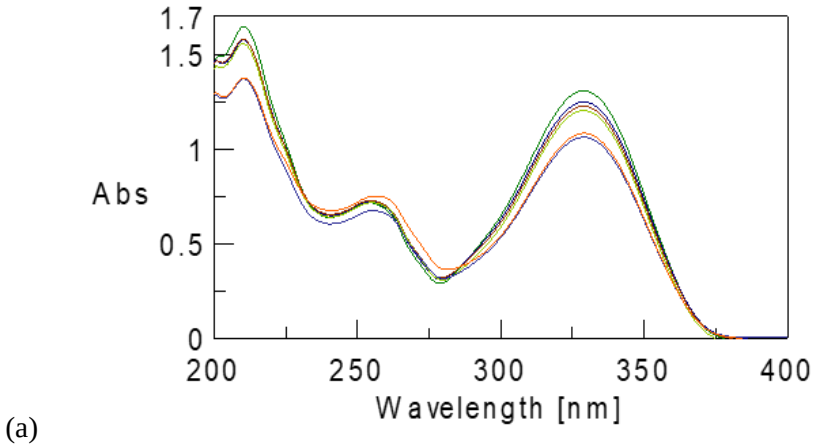

(a)

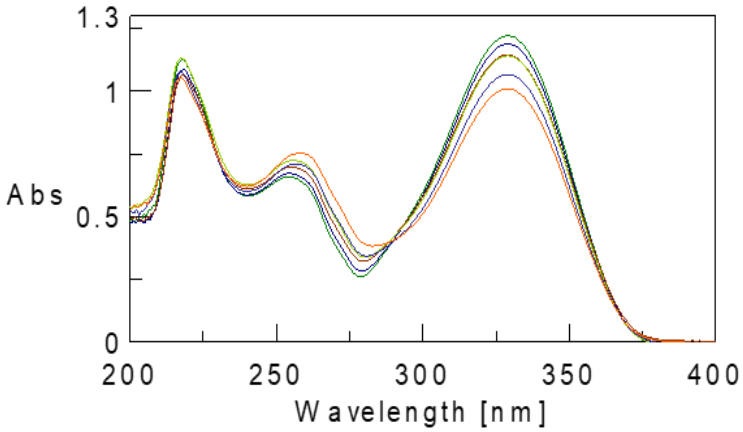

(b)

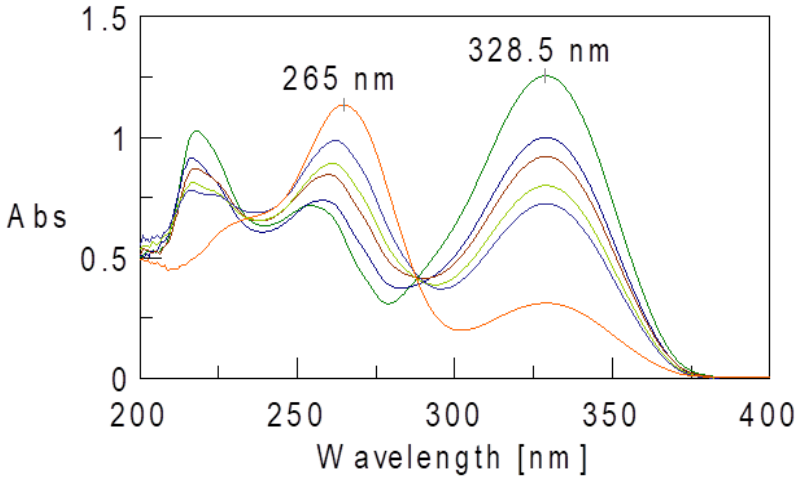

(c)

Figure 4.3. Overlay of spectra of TMZ in (a) pH 1.2, and (b) pH 4.5 at 0, 24, 48, 72, 96 and 144 h respectively (c) Overlay of spectra of TMZ in pH 7.4 at 0, 3, 6, 9, 12, 24 h respectively.

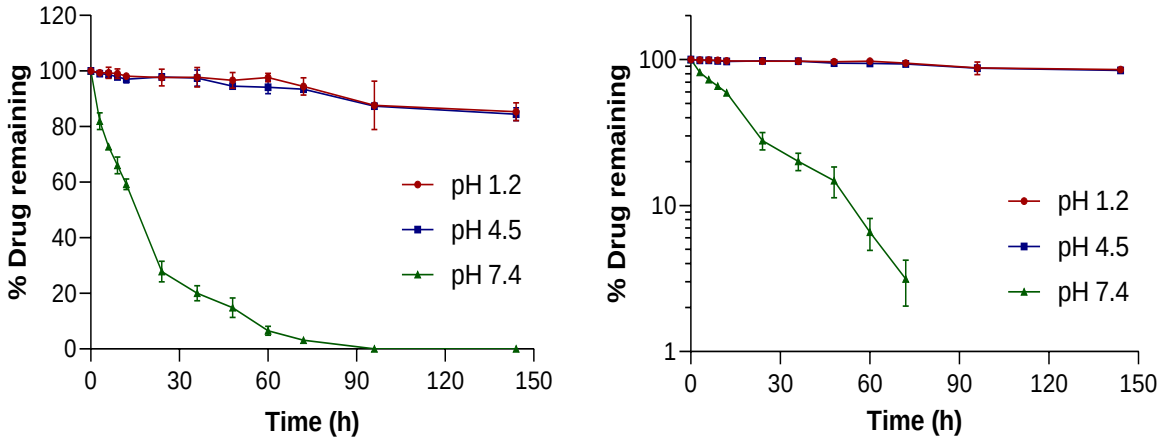

Figure 4.4. Degradation kinetic profile of TMZ in pH 1.2, pH 4.5, and pH 7.4 respectively (n=3)

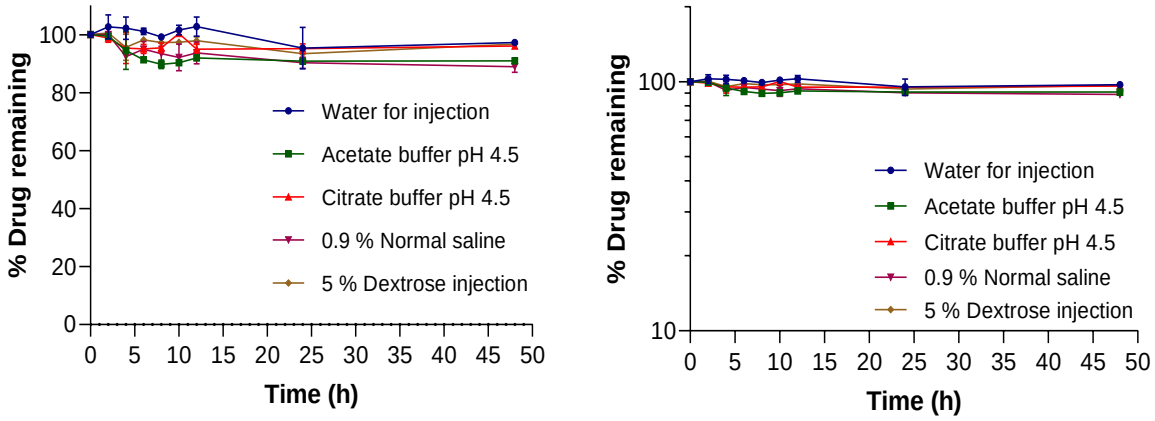

Figure 4.5. Degradation kinetic profile of TMZ in parenteral solutions (Water for injection, acetate buffer pH 4.5 (10 mM), citrate buffer pH 4.5 (10 mM), 0.9 % Normal saline, and 5 % Dextrose injection respectively, n=3)

4.5.5 Drug-excipient compatibility studies

The results obtained for drug excipient compatibility study (% assay and visual appearance after 1, 2 and 3 months has been represented in **Table 4.1 and 4.2**. The TMZ was found to degrade when stored along with PEG 200 at 30 ^{o}C. This could be attributed to hydrolysis of the drug. However, the % assay was more than 95 % when stored at refrigerated conditions. TMZ did not show any incompatibility with other excipients. TMZ is reported to show temperature dependant stability thus a gradual colour change from tan to dark brown colour is observed when exposed to extreme temperature conditions. Storage in refrigerated conditions was found to be suitable to ensure drug stability.

Table 4.1. Drug excipient compatibility study when stored at room temperature (30ºC)

Excipient	% Assay and visual appearance		
	1 month	**2 months**	**3 months**
GMO	97.357 ± 0.398 No colour change, sticky sample	97.412 ± 0.132 No colour change, sticky sample	94.523 ± 0.22 No colour change, sticky sample
PF 127	100.954 ± 0.127 No colour change, free flowing	96.613 ± 0.006 No colour change, free flowing	92.445 ± 0.110 No colour change, free flowing
PEG 200	99.049 ± 0.069 Slightly yellow colour	37.325 ± 0.047 Brown colour	29.648 ± 1.361 Brown colour
Phospholipid	100.786 ± 0.016 No colour change, free flowing	96.489 ± 0.031 No colour change, free flowing	97.425 ± 0.083 No colour change, free flowing
Cholesterol	97.831 ± 0.144 No colour change, free flowing	96.733 ± 0.073 No colour change, free flowing	94.704 ± 3.866 No colour change, free flowing
DSPE-PEG 2000	100.784 ± 0.008 No colour change, free flowing	99.924 ± 0.089 No colour change, free flowing	93.638 ± 0.023 No colour change, free flowing

Table 4.2. Drug excipient compatibility study when stored at refrigerated conditions (4ºC)

Excipient	% Assay and visual appearance		
	1 month	**2 months**	**3 months**
GMO	98.502 ± 0.987 No colour change, sticky sample	100.087 ± 0.038 No colour change, sticky sample	100.061 ± 0.090 No colour change, sticky sample
PF 127	100.817 ± 0.050 No colour change, free flowing powder	100.069 ± 0.027 No colour change, free flowing powder	98.255 ± 0.062 No colour change, free flowing powder
PEG 200	96.618 ± 0.960 Slightly yellow colour	100.262 ± 0.095 Slightly yellow colour	96.233 ± 0.153 Slightly yellow colour
Phospholipid	96.241 ± 0.070 No colour change, free flowing powder	100.174 ± 0.045 No colour change, free flowing powder	95.307 ± 3.565 No colour change, free flowing powder
Cholesterol	103.596 ± 0.107 No colour change, free flowing powder	97.752 ± 0.053 No colour change, free flowing powder	96.910 ± 3.240 No colour change, free flowing powder
DSPE-PEG 2000	100.538 ± 0.041 No colour change, free flowing powder	99.989 ± 0.098 No colour change, free flowing powder	99.454 ± 3.904 No colour change, free flowing powder

4.5.6 Selection of appropriate dissolution medium

The obtained dissolution profiles are represented in **Figure 4.6**. The dissolution profile of TMZ in acetate buffer pH 4.5 indicated more than 90 % dissolution in initial 2 h. After 100 % drug dissolution, the drug concentration was maintained which indicates that acetate buffer pH 4.5 ensures drug stability and can be a suitable dissolution medium for TMZ which was also indicated by the stability studies. The dissolution profile in phosphate buffer pH 7.4 revealed an increasing concentration up to 2 h after which the drug concentration was found to decrease. This could be attributed to the degradation of TMZ in alkaline conditions. Similar profiles were obtained when TMZ was dissolved in acetate buffer pH 4.5 and 0.9 % Normal saline. The internal medium (containing TMZ) of the proposed nanoparticles was supposed to be acidic (pH 4.5) to ensure drug stability during longer circulation when administered in plasma. The acetate buffer might be unsuitable for parenteral administration; thus the nanoparticles need to be dispersed in a medium suitable for parenteral administration (0.9 % Normal saline having pH around 5). This study confirmed that acetate buffer pH 4.5 ensures TMZ stability and can be used during the formulation process, and as a dissolution medium [15].

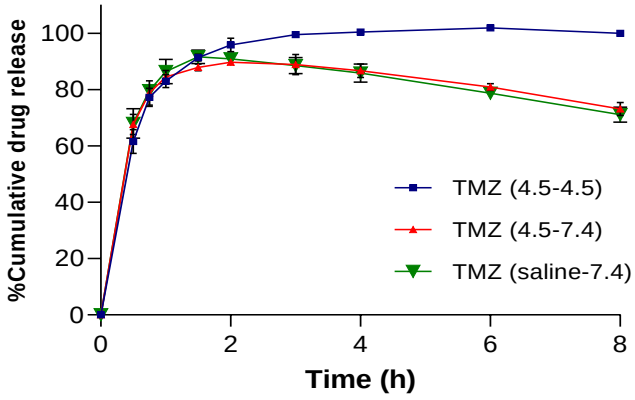

Figure 4.6. Dissolution profiles of TMZ in different dissolution media (n=3)

4.6 Conclusion

The API received from Biophore India Pharmaceuticals was found to be TMZ and was pure. The solubility of TMZ in aqueous solvents below pH 6 was found to be approximately 5 mg/mL. TMZ has a pH dependent stability. It gets converted to its metabolites in alkaline conditions. Thus, an appropriate pH needs to be maintained during formulation development. From the dissolution studies, it was concluded that an appropriate dissolution medium need to be selected considering the drug properties as well as the type of formulation selected. The

acetate buffer (pH 4.5) was found to be an appropriate dissolution medium for TMZ. Preformulation studies confirmed the characteristics of the TMZ, and helped in selection of appropriate excipients. It also provided significant information to assist in formulation development and characterization.

References

1. Jones TM. Preformulation studies. In: Tovey GD, editor. Pharmaceutical Formulation: The Science and Technology of Dosage Forms. London, UK: The Royal Society of Chemistry; 2018: 173–233.

2. Zhou D, Porter WR, Zhang GGZ. Drug stability and degradation studies. Developing Solid Oral Dosage Forms: Pharmaceutical Theory and Practice: Second Edition. Elsevier Inc.; 2017. 113–149.

3. Waghule T, Patil S, Rapalli VK, Girdhar V, Gorantla S, Kumar Dubey S, et al. Improved skin-permeated diclofenac-loaded lyotropic liquid crystal nanoparticles: QbD-driven industrial feasible process and assessment of skin deposition. Liq Cryst. 2020;47:1–19.

4. Waghule T, Rapalli VK, Singhvi G, Gorantla S, Khosa A, Dubey SK, et al. Design of temozolomide-loaded proliposomes and lipid crystal nanoparticles with industrial feasible approaches: comparative assessment of drug loading, entrapment efficiency, and stability at plasma pH. J Liposome Res. 2020;31(2):158–68.

5. Baka E, Comer JEA, Takács-Novák K. Study of equilibrium solubility measurement by saturation shake-flask method using hydrochlorothiazide as model compound. J Pharm Biomed Anal. 2008;46(2):335–41.

6. Philosophy DOF, Khosa A. Design , Characterization and Evaluation of Lipid Based Nanoparticulate Temozolomide for Enhanced Delivery to the brain. BITS PILANI, pilani campus; 2018.

7. Bajaj S, Singla D, Sakhuja N. Stability testing of pharmaceutical products. J Appl Pharm Sci. 2012;2(3):129–38.

8. Ofokansi K, Uzor P. Stability studies and degradation kinetics of some commercially available metronidazole suspensions in Nigeria. J Pharm Allied Sci. 2012;8(3):1379-86

9. Sun H, Liu S, Gao X, Xiong Z, He Z, Zhao L. Study on degradation kinetics of epalrestat

in aqueous solutions and characterization of its major degradation products under stress degradation conditions by UHPLC-PDA-MS/MS. J Pharm Anal. 2019;9(6):423–30.

10. Hodges G, Eadsforth C, Bossuyt B, Bouvy A, Enrici MH, Geurts M, et al. A comparison of log K ow (n-octanol–water partition coefficient) values for non-ionic, anionic, cationic and amphoteric surfactants determined using predictions and experimental methods. Environ Sci Eur. 2019;31(1):1–18.

11. Bansal S, Beg S, Asthana A, Garg B, Asthana GS, Kapil R, et al. QbD-enabled systematic development of gastroretentive multiple-unit microballoons of itopride hydrochloride. Drug Deliv. 2016;23(2):437–51.

12. Abioye AO, Issah S, Kola-Mustapha AT. Ex vivo skin permeation and retention studies on chitosan-ibuprofen-gellan ternary nanogel prepared by in situ ionic gelation technique - A tool for controlled transdermal delivery of ibuprofen. Int J Pharm. 2015;490(1–2):112–30.

13. Waghule T, Rapalli VK, Singhvi G, Manchanda P, Hans N, Dubey SK, et al. Voriconazole loaded nanostructured lipid carriers based topical delivery system: QbD based designing, characterization, in-vitro and ex-vivo evaluation. J Drug Deliv Sci Technol. 2019;52:303–15.

14. Kianvash N, Bahador A, Pourhajibagher M, Ghafari H, Nikoui V, Rezayat SM, et al. Evaluation of propylene glycol nanoliposomes containing curcumin on burn wound model in rat: biocompatibility, wound healing, and anti-bacterial effects. Drug Deliv Transl Res. 2017;7(5):654–63.

15. Fotaki N, Brown W, Kochling J, Chokshi H, Miao H, Tang K, et al. Rationale for selection of dissolution media: Three case studies. Dissolution Technol. 2013;20(3):6–13.

16. Lopes IC, De Oliveira SCB, Oliveira-Brett AM. Temozolomide chemical degradation to 5-aminoimidazole-4-carboxamide - Electrochemical study. J Electroanal Chem. 2013;704:183–9.

17. Mirzaei S, Khalilian MH, Taherpour AA. Mechanistic study of the hydrolytic degradation and protonation of temozolomide. RSC Adv. 2015;5(51):41112–9.

18. Babu NJ, Sanphui P, Nangia A. Crystal engineering of stable temozolomide cocrystals. Chem - An Asian J. 2012;7(10):2274–85.

19. Ward SM, Skinner M, Saha B, Emrick T. Polymer-Temozolomide Conjugates as Therapeutics for Treating Glioblastoma. Mol Pharm. 2018;15(11):5263–76.

Chapter 5
Formulation and characterization of TMZ loaded Liposomes

5.1. Introduction

Liposomes have gained much attention as a drug delivery system since their first discovery by Bangham and colleagues in the 1960s and the approval of the first nanotechnology-based product (Doxil®) approved by FDA in 1995. Among the various nanocarriers, liposomes have become the popular drug carrier systems due to their biocompatibility, improved efficacy of treatment, variable sizes (30 nm to micrometers), protection of drugs from pH and enzyme induced degradation, controlled/sustained drug release, and versatility to be administered through various routes. Further studies revealed that the coated liposomes could increase the plasma circulation time of the drug. Despite these outstanding properties, only a few liposomal products like DaunoXome® (Daunorubicin), Ambisome® (Amphotericin B), Depocyt® (Cytarabine), Exparel (Bupivacaine), and Marqibo (Vincristine sulfate) were successfully commercialized [1,2]. Certain limitations like complex preparation techniques, stability issues due to lipid oxidation and hydrolysis, high production costs due to low entrapment, leakage of drugs and reproducibility issues, and lack of information related to process parameters and regulatory burden are the various challenges faced by liposomal products [3,4]. Liposomes are traditionally prepared using the thin film hydration technique. Other methods of preparation include reverse-phase evaporation, solvent injection method, detergent removal method, dialysis method, and freeze-thaw method. Membrane extrusion technique, microfluidization technique, and proliposome technique can be used for large-scale industrial production of liposomes [5]. Several material and process parameters can significantly affect the final product characteristics of liposomes. The relationship of process parameters and liposomal properties is complicated and an elaborate investigation of the effect of individual variable is essential to ensure the scale-up [6,7]. This can be easily evaluated using the principles of Quality by Design (QbD). Various critical and non-critical parameters affecting the critical quality attributes can be systematically identified and studied using risk-based assessment. With the help of QbD, quality can be built into the product from the early development stages itself. A manufacturing process that is robust and consistently produces the intended product can be designed [8,9].

5.2. Materials

Lipoid S75 and Phospholipon®90 H were received as a gift sample from Lipoid GmbH. Lipoid S75 contains fat-free soybean phospholipids with 70 % Phosphatidylcholine, the remaining 30% consists of phosphatidylethanolamine, lysophospholipids, phosphatidylinositol, and triglycerides.

Phospholipon®90 H is granulated hydrogenated soybean phospholipid containing 90 % Phosphatidylcholine and the remaining 10% is composed of lysophosphatidylcholine and triglycerides. DSPC (Distearoylphosphatidylcholine), DPPC (Dipalmitoylphosphatidylcholine), and DMPC (Dimyristoylphosphatidylcholine) were obtained as a gift sample from VAV Life Sciences Pvt Ltd, Mumbai, India. Cholesterol was purchased from Fisher Scientific India Pvt Ltd (Mumbai). DSPE-PEG 2000, Temozolomide, Sodium acetate, glacial acetic acid extra pure, hydrochloric acid, sodium chloride, potassium chloride, disodium hydrogen phosphate and potassium dihydrogen phosphate used were as mentioned in **section 4.2**. Milli Q water purified by Merck Millipore systems was used during the entire analysis.

5.3. Instruments/ equipment

Denver Instruments Monolithic Analytical balance, UV visible spectrophotometer, REMI Laboratory Centrifuge R8C, Temperature controlled centrifuge, and Toshiba Bath Sonicator were used as mentioned in **section 4.3**. Rotary Evaporator R210 (Buchi, Switzerland), (Laboratory Testing Instruments, Delhi, India), REMI motor Mechanical stirrer with speed regulator (REMI Elektrotechnik Ltd. Vasai, India), Zetasizer (Zetasizer Nano-ZS ZEN 3600, Malvern), Field emission Scanning Electron Microscope **(**FESEM) with Apreo Switch XT microscope, Lyophilizer (Freezone 2.5, Labconco, USA), ZEISS Fluorescence microscope, Membrane extruder (Avanti® Mini-extruder) were the lab instruments/equipment used.

5.4 Methods

5.4.1 Screening of different phospholipids and preparation methods

Different phospholipids like Lipoid S75, Leciva S95, Phospholipon H90, DSPC, DPPC, and DMPC were screened. Phospholipids were selected based on the stability of the dispersion and the obtained entrapment efficiency. Different methods of preparation were explored for the formulation of liposomes. A few preliminary trials were taken using methods like ethanol injection method, thin-film hydration, proliposome method, reverse phase evaporation, and microfluidics. Size reduction techniques like probe sonication, homogenization, and membrane extrusion technique were used. A suitable method was selected based on the obtained particle size, entrapment efficiency, drug loading, the stability of the drug and the formulations [4,10].

5.4.2 Defining and identifying Quality Target Product Profile and Critical Quality Attributes

The first step of pharmaceutical product development using QbD involves establishing a Quality Target Product Profile (QTPP). It is a summary of all the characteristics which need to be targeted in the final intended product along with a justification. In the next step, these characteristics were distinguished as critical and non-critical attributes based on the impact and severity analysis. Critical quality attributes (CQAs) are those characteristics from the QTPP which are likely to have a significant impact on the quality of the final product and are expected to be within an appropriate range to ensure the overall quality of the final product. Once the CQAs are identified, the formulation scientist can investigate them further in detail [11,12].

5.4.3 Quality risk management

Quality risk management helps to review, assess and evaluate risks to the quality of the product so that they can be controlled in the early stages. Various factors including the material attributes and the process parameters were identified and summarized following the ICH guidelines 8,9, and 10. This was done using tools like Process mapping and Ishikawa fish-bone diagram. Various steps in the preparation of liposomes were identified through prior knowledge, literature review, and a few preliminary trials. A process flow was designed. Using process mapping, a flow chart of the preparation process was prepared and the various material and process parameters that are likely to affect the product characteristics at each step were identified. A cause-effect relationship was obtained using the Fish-bone diagram [13,14].

5.4.4 Identifying Critical Material Attributes (CMAs) and Critical Process Parameters (CPPs)

Once various material attributes and process parameters were identified, the CMAs and CPPs were analyzed and evaluated qualitatively and quantitatively using the Relative risk-based matrix analysis (RRMA) and Failure Mode Effect Analysis (FMEA) tools respectively. This was done utilizing the information obtained through the literature review, prior scientific knowledge, and preliminary trials. Using RRMA, the risk contributed by the material attributes and process parameters was differentiated as low, medium, and high risk. Using FMEA, the risk was assessed quantitatively based on the probability of occurrence (P), severity (S), and detectability (D). Scores were assigned on a scale of 1 to 5 and the risk priority numbers (RPN score) were assigned using

the equation 5.1. The parameters with scores higher than 25 were considered to be critical for the CQAs [15,16].

$$RPN\ score = Occurrence\ x\ Severity\ x\ Detectability \quad \text{……..(5.1)}$$

5.4.5 Investigating the effect of various formulation and process variables on the critical quality attributes of TMZ-loaded liposomes

5.4.5.1 Formulation of liposomes using Microfluidics

Acetate buffer (pH 4.5) was considered as the aqueous phase to ensure TMZ stability in the dispersion. It was pumped through pump A of the microfluidic device (Dolomite Mitos syringe pump). The specified quantity of lipid (5 mg/mL) and drug (1.25 mg/mL) was dissolved in organic solvent and pumped through pump B. The pipe through the organic phase pump was directly connected to the glass chip. The pipe through an aqueous phase pump was divided into two pipes (described as T-junction geometry), these two pipes were connected to a glass chip, one below the organic phase channel and one above the organic phase channel. The chip started with these three channels which finally fused into one channel which continued in a zig-zag manner through the glass chip (Dolomite Part no. 3200401). The glass chip involved micro mixing channels with an internal channel cross-section of 125 µm x 350 µm and 50 µm x 125 µm (depth x width). The total flow rate and flow rate ratio were set in the device. When inside the chip, mixing and diffusion takes place and liposomes are formed through nanoprecipitation. The formed liposomal dispersion was collected through the outlet and characterized. The effect of process parameters was studied further [17,18].

5.4.5.2 Formulation of liposomes using Membrane extrusion technique

A weighed quantity of phospholipid and cholesterol mixture was transferred into a clean and dry round bottom flask. The lipids were dissolved in 4 mL of chloroform. The round bottom flask was attached to the rota-evaporator (Buchi Rotary Evaporator R210). The temperature of the water bath was kept 5-10^{o}C above the phase transition temperature of the phospholipid. The organic solvent was evaporated until a thin film was formed. The formed film was kept for drying overnight and hydrated with 10 mL of TMZ solution (1mg/mL) containing acetate buffer (pH 4.5). The buffer was used to ensure the stability of the drug during formulation. This was further bath sonicated for 10 min to ensure complete hydration of the film and formation of a dispersion. The

formed liposomal dispersion was extruded through a membrane extruder (Avanti® Mini-extruder) using a 0.1 μ polycarbonate filter to obtain a homogenous liposomal dispersion. The effect of the number of extrusion cycles on particle size and entrapment efficiency was investigated. Also, the effect of various formulation variables like type of phospholipid (DSPC, DPPC, DMPC), phospholipid to cholesterol ratio, and phospholipid to drug ratio was investigated. Further to achieve longer plasma circulation time, PEGylated phospholipid (DSPE-PEG 2000) was incorporated along with other phospholipid during the liposome formulation. The effect of phospholipid to PEGylated phospholipid ratio was also investigated [19,20].

After the separation of the free drug, the optimized Liposomal dispersion was further freeze-dried to convert the dispersion into dry form and to improve the shelf-life. Trehalose (10%) was added to the dispersion as a lyoprotectant, the vials were sealed with parafilm and allowed to freeze for 12 h at –20^{o}C. The sample was subjected to drying using Labconco-Freezone 2.5 at –50^{o}C and vacuum pressure of 0.06 mBar. After 24 h the freeze-dried sample was stored under refrigerated conditions.

5.4.6 Characterization of TMZ-loaded Liposomes

5.4.6.1 Particle size distribution, Zeta potential, and morphology

The particle size, polydispersity index, and surface charge of the liposomal dispersions were measured using Zetasizer (Malvern Nano-ZS ZEN 3600) based on the dynamic light scattering technique. It used a red laser (633 nm wavelength) and 173^{o} scattering angle. The liposomal dispersions were diluted 20 times with Milli-Q water before the analysis. Particle size was reported as Z-average (nm). Similarly, the zeta potential was measured using the cuvettes with in-built electrodes. The measurements were done in triplicates at 25^{o}C [21]. Liposome morphology was studied using different techniques. Initially, the proliposome powder (phospholipid layer coated on a carrier-mannitol) was observed under the optical microscope. The process of liposome vesicle formation after hydration was confirmed by observation under the Fluorescence microscope. The thin film formed after solvent evaporation was hydrated with acetate buffer by manual shaking. Immediately after the addition of buffer, a drop of dispersion was positioned on a glass slide along with a cover slip and observed using Fluorescence microscopy. The images were obtained using the ZEISS software. Further, the liposomal dispersion was bath sonicated for 10 min. The liposomal dispersion formed was observed under Fluorescence microscopy to confirm the

formation of vesicles. The morphology of liposomes after membrane extrusion was analyzed using the Field Emission Scanning Electron Microscopy (FESEM) (Apreo Switch XT microscope, USA). A drop of liposomal dispersion was uniformly spread on a cover slip. This was vacuum dried to form a thin film. The thin film formed was coated with gold (Gold sputter module, Quorum ES, UK) and observed under the FESEM microscope [22,23].

5.4.6.2 Entrapment efficiency (% EE) and Drug Loading (% DL)

The entrapment efficiency was analyzed using the dialysis bag method. Dialysis also favored removal of methanol used during preparation of liposomes by microfluidics technique. A 1 mL liposomal dispersion was filled into a dialysis bag (molecular cutoff – 12–14 kDa, Himedia) and tied at both ends. The bag was inserted into 50 mL of acetate buffer (pH 4.5) and kept under stirring at 80 rpm. The dialysis was continued for 35 min to separate the free drug. Thereafter, the liposomal dispersion was removed from the bag. Methanol was added to break the liposomal structure. The dispersion was centrifuged at 15000 rpm for 10 min. The supernatant was further diluted with acetate buffer (pH 4.5) and analyzed for the drug concentration using the in-house developed UV analytical method. The amount of drug entrapped and drug loading in the TMZ-loaded Liposomes was determined by equations 5.2 and 5.3, respectively [24].

$$\%\ Entrapment\ efficiency = \frac{Amount\ of\ drug\ entrapped}{Total\ amount\ of\ drug\ added} * 100 \quad \text{..... (5.2)}$$

$$\%\ Drug\ Loading = \frac{Amount\ of\ drug\ entrapped}{Total\ weight\ of\ excipients} * 100 \quad \text{..... (5.3)}$$

5.4.6.3 Drug release and release kinetics

In-vitro drug release was studied with the dialysis bag technique. Initially, the studies were carried out in three different media with pH 1.2, pH 4.5, and pH 7.4 respectively to study the effect of pH of the dissolution media on the release of TMZ from the liposomes and to select an appropriate dissolution medium. Liposomal dispersion (1 mL equivalent to 2 mg TMZ) was filled in a dialysis bag. The bag was inserted in 30 mL dissolution media and kept under stirring at 80 rpm. The temperature was maintained at 37±0.5^{o}C. Aliquots (0.5 mL) were taken at different time intervals (30 min, 1, 2, 4, 8, 12, and 24 h respectively). The media was replenished with an equal volume

of the respective dissolution media each time. The samples were analyzed using the developed UV analytical method after appropriate dilutions.

Further, the effect of various formulation variables on drug release was studied. Initially, the study was conducted in acetate buffer (pH 4.5) to ensure drug stability and to get an idea of time taken for the complete release of TMZ from the liposomes. The drug stability and sink conditions were ensured during the entire study. Initially, the time taken for 100 % TMZ diffusion was evaluated by filling the TMZ solution (1 mg/mL) into the dialysis bag (molecular cutoff – 12-14 kDa, Himedia). To study the effect of cholesterol concentration and drug loading on drug release, liposomal formulations with different phospholipid: cholesterol mol % ratios (100, 70:30, 55:45) and different drug loading (1.5, 2.5, and 3.5 % w/w relative to phospholipid) were prepared. The respective liposomal dispersion (1 mL) was filled into the dialysis bag and tied on both ends. The bag was placed in the 30 mL of appropriate dissolution medium and kept under stirring at 80 rpm. Aliquots (0.5 mL) were taken at different time intervals and replenished with the same volume of the medium. The study was similarly performed for optimized TMZ-loaded Liposomes and TMZ-loaded PEGylated Liposomes to study the effect of PEGylation on drug release. The samples were analyzed for drug concentration after appropriate dilutions using the in-house developed UV analytical method. A plot of % cumulative drug release and time was obtained [22,25]. The obtained data was further studied for release kinetics using DDSolver software (Excel Add-In). The best fit release model was identified based on the high R^2 value, highest MSC (Model Selection Criteria) value, and lowest AIC (Akaike Information Criterion) value. The corresponding $t_{25,}$ $t_{50,}$ and t_{75} values were also obtained [26–28].

Following the same methodology, the drug release of TMZ and the optimized PEGylated liposomes was studied in phosphate buffer saline (pH 7.4) to evaluate the potential of PEGylated Liposomes to protect the drug at plasma pH [29].

5.4.6.4 Reproducibility

As the Miniextruder allowed extrusion of only 1 mL formulation at a time, the reproducibility was confirmed by measuring the particle size of each 1 mL extruded formulation individually. It is expected that Liposomes need to be diluted with suitable media for intravenous delivery in the form of infusion. The stability on dilution is a critical factor for intravenous delivery. The prepared

Liposomal formulation was diluted 50, 100, 500, and 1000 times. The change in particle size and PDI was studied thereafter [30,31].

5.4.6.5 In-vitro cytotoxicity study

In-vitro cytotoxicity of the formulations was analyzed against U87 (a human glioblastoma astrocytoma) cells. U87 cells were cultured in DMEM media (Gibco) supplemented with 10% fetal bovine serum (FBS, Himedia), penicillin (50 units/mL), and streptomycin (50 mg/mL, Thermo Fisher Scientific) maintained at 37 °C and 5% CO_2. Trypsin–EDTA (Thermo Fisher Scientific) solution (0.05%) was used to detach cells. The cytotoxicity of TMZ, blank Liposomes, TMZ loaded Liposomes and PEGylated Liposomes was evaluated using the MTT (3-(4,5-dimethylthiazol-2-yl)-2,5-diphenyl-2H-tetrazolium bromide) assay. The glioma cells were seeded in 96 well plates at a density of 2 x 10^3 cells per well. The cells were incubated at 37^{o}C for 24 h to permit cell attachment. Thereafter, the cells were treated with TMZ, and Liposomal formulations with TMZ concentrations equivalent to 0.04, 0.2, and 1 mM. TMZ (10 mg/mL) stock solution was prepared in dimethyl sulfoxide (DMSO). Untreated cells were taken as control. After treatment for 48 h with formulations, the cells were incubated with MTT dye (5mg/mL in culture media) for 4 h. DMSO (200 µL) was added to the formed formazan crystals and the absorbance was measured at 570 and 630 nm using the BioTek Epoch Microplate reader (Gen5^{TM} 1.11 software). The % cell viability was calculated using equation 5.4 [32,33].

$$\%\ Cell\ viability = \frac{Sample_{abs}\ 570\ nm - Sample_{abs} 630\ nm}{Control_{abs} 570 nm - Control_{abs} 630\ nm} * 100 \quad \text{.....(5.4)}$$

5.4.6.6 Cell uptake study

The optimized formulations (Liposomes and PEGylated Liposomes) were prepared by loading Dil (a fluorescent lipophilic indocarbocyanine dye). The uptake by U87 (glioblastoma cell lines) and RAW (macrophage cell lines) cells was analyzed using Confocal microscopy. The respective cells were seeded on coverslips at a density of 50000 cells per well. The coverslips were placed in 6 well plates with 2 mL media. After incubation for 24 hours, the cells were treated with dye-loaded nanocarriers. After 4 h, the cells were washed three times using phosphate buffer saline (PBS). Thereafter, ice-cold methanol was added for the fixation of the cells. The cells were again washed three times using PBS. The cells were then treated with DAPI (1 µg/ml) containing PBS for 15 min followed by washing with PBS. The coverslips were then mounted on the glass slides. The

slides were observed under a confocal microscope at 63x magnification and the images were obtained. The fluorescence intensity of the Liposomes and PEGylated Liposomes were obtained using the ImageJ 1.53k software and was compared to evaluate the effect of PEGylation on cell uptake [34,35].

5.4.6.7 Storage stability

The optimized freeze-dried TMZ loaded PEGylated Liposomes dispersion was stored at refrigerated conditions and room temperature upto 2 months. The particle size, PDI and drug content were evaluated after 1 and 2 months to ensure the stability of the formulation and the drug.

5.5 Results and Discussion

5.5.1 Screening of different phospholipids and preparation methods

Particle sizes in the size range of 0.5-2 µm were obtained with methods like thin-film hydration, proliposomes, ethanol injection, and reverse phase evaporation. The particle sizes were not found reproducible using these methods. Also, methods like ethanol injection and reverse phase evaporation were found to be unsuitable for ensuring the stability of TMZ. No significant difference was found in the entrapment efficiency when TMZ was added either in the lipid phase or aqueous phase. Hence, incorporation of TMZ during the film formation was avoided in methods like thin-film hydration and proliposome to ensure the stability of the drug.

Liposomes with small particle size (50- 250 nm) and narrow PDI (< 0.2) were obtained in a reproducible manner when the liposomes were formulated using the microfluidics technique. Particle sizes in the range of 300-500 nm were achieved after size reduction with probe sonication or homogenization following the thin film hydration process. Thin film hydration followed by downsizing using membrane extrusion generated liposomes with reproducible particle size less than 200 nm and PDI <0.2. Thus, microfluidics and membrane extrusion techniques were selected for further optimization. Criteria used for the selection of phospholipids was the composition of the marketed products, the composition of the phospholipids, the phase transition temperature of phospholipid, and suitability for intravenous delivery. Based on the literature survey on the properties of different phospholipids and the entrapment efficiency obtained in the trials, synthetic phospholipids (DSPC, DPPC, and DMPC) were selected for further optimization.

5.5.2 Defining and identifying Quality Target Product Profile and Critical Quality Attributes

The Quality target product profile of TMZ-loaded liposomes was defined concerning the target final product and its application as summarized in **Table 5.1**. From the profile, the critical quality attributes were identified as represented in **Table 5.2**. The dosage form and route of administration are already predefined. The physical attributes, osmolarity, labeling, packaging, and storage are taken care of for a parenteral product. Thus, these parameters were not considered for further investigation [15,24].

Table 5.1. Quality Target Product Profile of TMZ loaded Liposomes

Quality attribute	Target	Justification
Dosage design	Liposomes and PEGylated Liposomes	Liposomes are biocompatible and are suitable for entrapping amphiphilic drugs. Liposomes release the drug in a prolonged manner thus helping to improve in-vivo circulation time. PEGylation helps improve the plasma circulation time of liposomes.
Dosage form	Lyophilized powder to be reconstituted	Ensures stability of drug during storage
Route of administration	Intravenous	Pharmaceutical equivalence: Same route as Reference Listed Drug (RLD)
Physical attributes	White powder	-
Assay	95-115 %	To ensure the therapeutic effectiveness
pH	Near to plasma pH (4-6)	Required to prevent drug degradation, maintain isotonicity, and prevent hemolysis
Osmolality	290±20 mOsm/kg	To maintain blood osmolarity and prevent hemolysis
Biocompatibility	Non-hemolytic and non-toxic	To prevent hemolysis and reduce toxicity

Particle size	80-150 nm	Recommended to prolong plasma circulation time and reduce clearance rate
Zeta potential	Near to neutral	Avoids protein binding and uptake by organs like the liver and lungs
% Entrapment efficiency	Maximum	To obtain maximum therapeutic efficiency
% Drug loading	Optimum	Affects drug release patterns, patient compliance, and the cost of the product
Drug release	Prolonged release compared to free drug	Provide longer plasma circulation time of drug and improved brain bioavailability
Pharmacokinetics	Longer circulation time, higher brain bioavailability and reduced clearance rate in comparison to free drug.	Required to achieve an improved therapeutic effect and patient compliance
Stability	No visible signs of instability during preparation and storage	Ensures stability of drug during shelf-life and required for marketing approval
Storage	Store between 2^{o}C to 8^{o}C	Required to ensure the stability of the drug and the lipid carrier
Container closure system	Air-tight glass vial	Ensure protection of drug and the excipients
Administration/ Labeling	Reconstitute with sterile water for injection/ Normal saline before administration Store at room temperature and use within 14 hours	Required to ensure the stability of the drug and therapeutic use

Table 5.2. Critical Quality Attributes of TMZ loaded Liposomes

Quality Target Product Profile (QTPP)	Impact analysis	Severity analysis	Critical or not?	Justification
Dosage design	No	Yes (But is Already decided)	No	-
Dosage form	No	No (Is already decided)	No	-
Route of administration	No	Yes (But is Already decided)	No	-
Dosage strength	Yes	Yes	Yes	Affects the therapeutic effectiveness
Physical attributes	No	No	No	-
Assay	Yes	Yes	Yes	Affects the therapeutic effectiveness
pH of product	Yes	Yes	Yes	Affects the stability of the drug and is essential for parenteral administration
Particle size	Yes	Yes	Yes	Affects drug release rate, plasma circulation, and clearance rate
Zeta potential	Yes	Yes	Yes	Affects formulation stability, plasma circulation, protein binding, and uptake by organs
% Entrapment efficiency	Yes	Yes	Yes	Affects therapeutic effect
% Drug loading	Yes	Yes	Yes	Affects release rate and patient compliance
Drug release	Yes	Yes	Yes	Affects therapeutic effect and pharmacokinetic parameters
Pharmacokinetics	No	No	No	It is dependent on the other quality attributes
Stability	Yes	Yes	Yes	Affects therapeutic effect
Storage	No	Yes	No	-
Container closure system	No	Yes	No	-
Administration/ Labelling	No	Yes	No	-

**Does a change in formulation/process parameter affect the quality attribute of a product?*
***Does failure to meet the quality attribute severely affect the efficacy and safety of the product in a patient?*

5.5.3 Quality risk management

Based on the screening of various preparation methods and the quality target set, to achieve particle size within a size range of 80-150 nm, membrane extrusion and microfluidics techniques were selected. Various input material attributes and process parameters likely to affect the particular CQAs at each step were identified and the process flow map was created for microfluidics and membrane extrusion techniques as described in **Figures 5.1** and **5.2** respectively. The process flow map gave an overview of the entire liposome formulation process and the factors/causes likely to create variability in the quality attributes of the product. This may assist in finding the probable problem (s) and its solution at each step of the formulation process. For the preparation of the Fish-bone diagram, TMZ-loaded liposomes were considered as an effect/outcome. All the probable causes likely to affect this outcome were gathered and structured on the bones of the fish as represented in **Figure 5.3** [36].

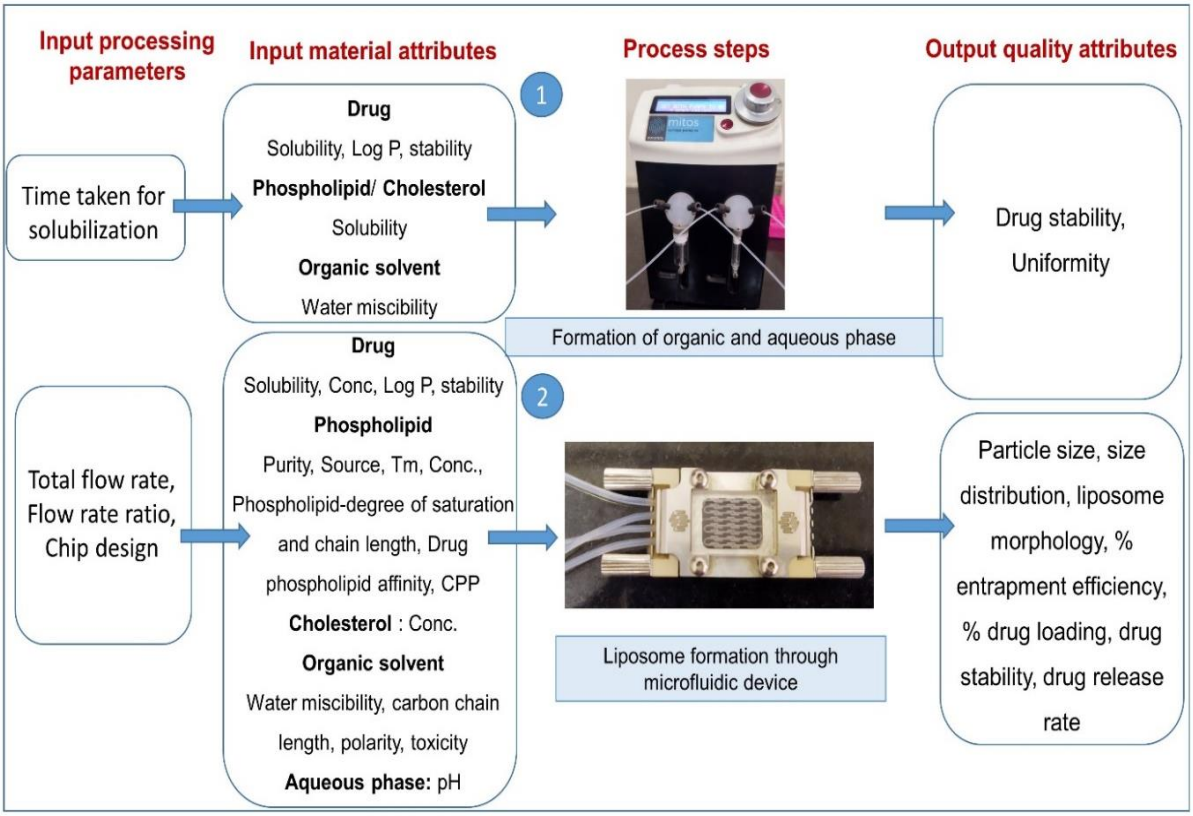

Figure 5.1. Process flow map for TMZ-loaded liposomes prepared using microfluidics *(Conc.: Concentration, CPP: Critical packing parameter, Tm: Phase Transition Temperature)*

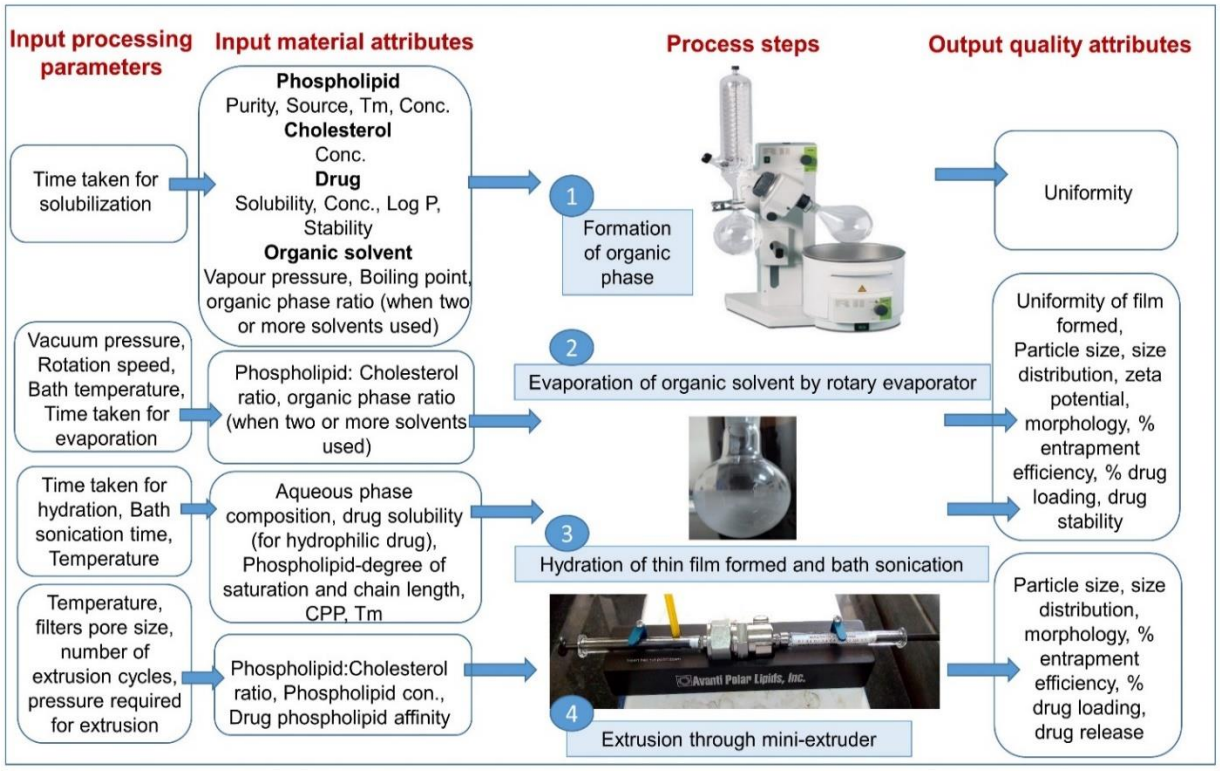

Figure 5.2. Process flow map for TMZ loaded liposomes using membrane extrusion technique.

(Conc.: Concentration, CPP: Critical packing parameter, Tm: Phase Transition Temperature)

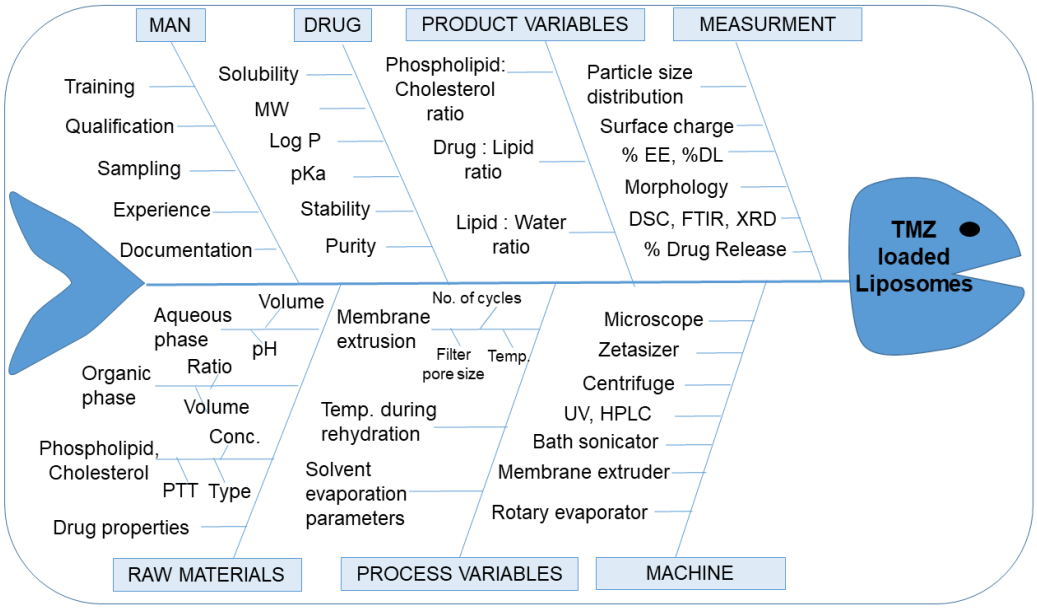

Figure 5.3. Ishikawa fish-bone diagram (cause-effect analysis) for TMZ-loaded liposomes prepared using the Membrane extrusion technique. *(PTT: Phase transition temperature)*

5.5.4 Identifying Critical Material Attributes (CMAs) and Critical Process Parameters (CPPs)

After identifying all the material attributes and process parameters, these were linked to the CQAs using RRMA (**Table 5.3-5.6**). The risk was also assessed quantitatively using FMEA (**Table 5.7-5.10**). Parameters likely to cause high risk to the CQAs were identified as CMAs and CPPs (critical parameters). The solubility and chemical stability were found to be the CMAs related to TMZ (**Table 5.7**). The solubility in solvents and lipids was found to be a critical factor as it majorly affects the entrapment efficiency and drug release. TMZ has pH-dependent stability, thus chemical stability needs to be ensured during formulation and storage. Choosing a suitable organic solvent is essential while formulating liposomes using microfluidics **(Table 5.8)**. An organic solvent with high water miscibility, high lipid solubility, and low toxicity need to be selected. The organic solvents with short carbon chains consist of more polar OH groups allowing them to form hydrogen bonds with water molecules and thus have high water miscibility. The most commonly preferred organic solvents are methanol, ethanol, and isopropanol. Factors like concentration of lipid, total flow rate, and flow rate ratio might significantly affect the particle size, particle size distribution, and entrapment efficiency. The available research on the preparation of nanoparticles indicates that the particle size of a nanoparticle is dependent on the concentration of lipid/ polymer used in the formation of the particle. From the principle of microfluidics, it is clear that the particle size can be tuned by optimizing the two main process parameters (total flow rate and flow rate ratio) [37,38].

For the thin-film hydration and membrane extrusion technique **(Table 5.9-5.10)**, the temperature during the thin film formation, thin-film rehydration, and membrane extrusion need to be maintained above the PTT of the phospholipid used. Above the PTT of the phospholipid, the phospholipid bilayer is less rigid (fluid-like phase), thus the liposome vesicle formation process is favored. The phospholipid chain length, degree of saturation, and charge on polar heads can affect the liposomal properties and biodegradability. The length of the fatty acid side chains is likely to affect the volume of the hydrophobic cavity. Liposomes containing ester and amide bonds have more biodegradability and lower toxicity when compared to those containing ether bonds During membrane extrusion, the membrane filter pore size can be selected based on the target particle size required. The number of extrusion cycles needs to be optimized. In the case of TMZ, maintaining

the pH of the aqueous phase is essential to ensure the stability of the drug during the formulation process. As fewer number of parameters were found to be critical, no experimental design was selected. The effect of parameters was studied individually [20,25,39].

Table 5.3. Linking material attributes (MAs) of TMZ to Critical Quality Attributes (CQAs) of LLCs using relative risk-based matrix analysis

MAs / **CQAs**	Solubility	Particle size	Moisture content	Chemical stability	Impurities
Assay					
pH of product					
Particle size distribution					
Zeta potential					
Entrapment and loading efficiency					
Drug release					
Stability					

Green: Low risk, Yellow: Medium risk, Red: High risk

Table 5.4. Linking material attributes (MAs) and process parameters (PPs) to CQAs of TMZ loaded Liposomes prepared by microfluidics using RRMA

MAs/ PPs / **CQAs**	Type /Composition of phospholipid	Conc. Of Phospholipid/ Cholesterol	Water miscibility of the organic phase	pH of the aqueous phase	Total flow rate	Flow rate ratio
Assay						
pH						
PS and PDI						
Zeta potential						
% EE and % DL						
Drug release						

Green: Low risk, Yellow: Medium risk, Red: High risk; Conc.: Concentration, DL: Drug Loading, EE: Entrapment efficiency, PDI: Polydispersity index, PS: Particle size

Table 5.5. Linking material attributes (MAs) related to excipients to CQAs of TMZ loaded Liposomes prepared by membrane extrusion using RRMA

MAs / **CQAs**	Type /Composition of phospholipid	PTT of Phospholipid	Conc. Of Phospholipid	Conc. of Cholesterol	pH of the aqueous phase	Vapour pressure/ Ratio of organic solvent	MW/ Chain Length of DSPE-PEG2000
Assay							
pH							
PS and PDI							
Zeta potential							
% EE and % DL							
Drug release							

Green: Low risk, Yellow: Medium risk, Red: High risk; Conc.: Concentration, DL: Drug Loading, EE: Entrapment efficiency, MW: Molecular weight, PDI: Polydispersity index, PS: Particle size, PTT: Phase transition temperature

Table 5.6. Linking of process parameters (PPs) to CQAs of Liposomes prepared by thin-film hydration and membrane extrusion technique using RRMA

PPs / **CQAs**	Speed of rotation during evaporation	Temperature during solvent evaporation	Temp. during rehydration	Membrane filter pore size	No. of extrusion cycles	Temp. during extrusion
Assay						
pH						
PS and PDI						
Zeta potential						
% EE and % DL						
Drug release						

Green: Low risk, Yellow: Medium risk, Red: High risk

Table 5.7. FMEA of material attributes of TMZ

Material attribute	Failure mode	Effect on CQAs	P	S	D	RPN
Solubility	Low	Affect entrapment and loading efficiency-Drug release - Efficacy	3	5	2	**30**
Particle size	High	Affect content uniformity- Efficacy	2	2	1	4
Dose	High	Affect pharmacokinetic profile- Safety and Efficacy	3	4	1	12
Moisture content	High	Affect drug stability- Efficacy	2	3	2	12
Chemical Stability	Unstable	Affect assay and pharmacokinetic profile - Efficacy	4	5	2	**40**
Impurities	Present	Affect assay - safety and efficacy	2	4	2	16

Table 5.8. FMEA of the material attributes and process parameters related to the preparation of TMZ-loaded Liposomes using the microfluidics technique

Excipient/ Process	Material attribute/ Process parameter	Failure mode	Effect on CQAs	P	S	D	RPN
Phospholipid	Chain length and degree of saturation	Unsuitable for intravenous delivery	Affect the rigidity of the liposome bilayer- Affect drug release when in plasma- Efficacy	3	4	2	**24**
	Concentration	High	Affect particle size, EE, drug release, and patient compliance- Safety and Efficacy	3	3	2	18
Cholesterol	Concentration	High	Affect rigidity of liposome bilayer- Efficacy	3	3	2	18
Organic solvent	Water miscibility	Low	Affect the process of liposome formation- Efficacy	3	4	2	**24**
Aqueous phase	pH	> 5	Affect drug stability, and assay - Efficacy	3	5	2	**30**
Microfluidics	Total flow rate	Inappropriate	Affect particle size, and EE- Efficacy	3	4	2	**24**
	Flow rate ratio	Inappropriate	Affect particle size, and EE- Efficacy	3	4	2	**24**

Table 5.9. FMEA of the material attributes of the excipients used in the preparation of TMZ-loaded Liposomes using the membrane extrusion technique

Excipient	Material attribute	Failure mode	Effect on CQAs	P	S	D	RPN
Phospholipid	Chain length and degree of saturation	Unsuitable for intravenous delivery	Affect the rigidity of the liposome bilayer- Affect drug release when in plasma- Efficacy	3	4	2	**24**
	Phase transition temperature	Below 37^{o}C	Affect the drug release when in plasma- Efficacy	3	4	2	**24**
	Concentration	High	Affect particle size, entrapment efficiency, drug release, and patient compliance- Safety and Efficacy	3	3	2	18
Cholesterol	Concentration	High	Affect rigidity of liposome bilayer- Efficacy	3	3	2	18
Aqueous phase	pH	> 5	Affect drug stability, and assay - Efficacy	3	5	2	**30**

Table 5.10. FMEA of process parameters involved in the preparation of TMZ loaded Liposomes using membrane extrusion technique

Process	Process parameters	Failure mode	Effect on CQAs	P	S	D	RPN
Thin-film hydration	Temperature during solvent evaporation	Below PTT of phospholipid	Affect film formation - Efficacy	3	3	2	18
	Temperature during film rehydration	Below PTT of phospholipid	Affect particle size distribution-Efficacy	3	3	2	18
Membrane extrusion	Pore size of the filter	Inadequate	Affect particle size and size distribution-Efficacy	2	3	1	6
	Temperature during extrusion	Below PTT of phospholipid	Affect pressure required while extrusion- Efficacy	2	4	2	16
	Number of extrusion cycles	High	Affect particle size and entrapment efficiency- Efficacy	3	4	2	**24**

5.5.5 Investigating the effect of various formulation and process variables on the critical quality attributes of TMZ-loaded liposomes

5.5.5.1 Formulation of liposomes using Microfluidics

Based on the solubility of lipids (DSPC and cholesterol), the solubility of TMZ, and water miscibility, methanol was selected as an organic solvent for the formulation of liposomes using

microfluidics. The results obtained after investigating different formulation and process variables have been summarized in **Figures 5.4 and 5.5**. A slight increase in particle size was observed on increasing the lipid concentration from 3 to 15 mg/mL. A significant decrease in particle size was observed on increasing the total flow rate from 80 to 150 µL/min. Changing the total flow rate also changes the shear forces. When the total flow rate is low, more time is available for the phospholipid molecules to arrange in layers as compared to with high flow rates, thus bigger-sized vesicles are formed with lower flow rate. The mixing time is slow with lower flow rates. As the organic solvent passes through the aqueous phase, due to the less solubility of phospholipids in water, gradually the phospholipids start to self-assemble into bilayers. As they move forward, the bilayers grow into discs. To reduce the surface area of the hydrophobic chains which are exposed to the aqueous phase, the discs tend to grow, bend and eventually fuse into spherical vesicles enclosing the aqueous core inside finally forming the liposomal structure. The other parameters likely to affect the particle size can be the width of the organic phase passing through the aqueous phase in the channels (dependent on the organic to aqueous flow rate ratio), the dimensions of the chip (width, length, internal volume), viscosity and density of the fluid passing through the channel [17,18,40].

The lipid concentration in the formulation can also be tuned by adjusting the organic phase flow rate in the microfluidic device. A significant increase in particle size, zeta potential, % entrapment efficiency, and % drug loading was observed on increasing the organic phase flow rate. PDI remained unaffected on changing the organic: aqueous phase flow rate ratio. As the organic phase flow rate is increased, the lipid concentration is also increased in comparison to the aqueous phase. As the organic phase proportion was increased, an increase in zeta potential was observed which can be attributed to the increased amount of phospholipid. More phospholipid molecules contribute to the higher zeta potential value [41]. As more phospholipid molecules are available, a greater number of vesicles are formed which entrap the drug inside, leading to higher entrapment and drug loading values. When the organic phase proportion is less in comparison to the aqueous phase, the alcohol concentration rapidly decreases, thus decreasing the vesicle closure times leading to the formation of smaller liposomal vesicles [17,18,40].

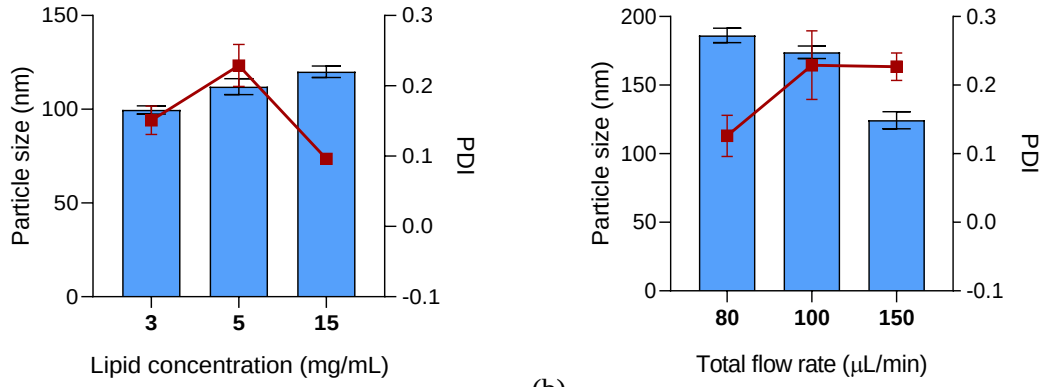

(a) (b)

Figure 5.4. Effect of different lipid concentration and total flow rate on CQAs of TMZ loaded liposomes prepared using microfluidics technique *(a) Effect of lipid concentration (DSPC: cholesterol, 7:3) on particle size and PDI were total flow rate and organic to aqueous phase flow rate ratio were kept 150 µL/min and 1:14 respectively; (b) Effect of total flow rate on particle size and PDI were lipid concentration (DSPC: cholesterol, 7:3) was kept 5 mg/mL (n=3, Mean ± SD). In each figure, the bar chart (blue) refers to the left axis, and the scatter plot (red) refers to the right axis.*

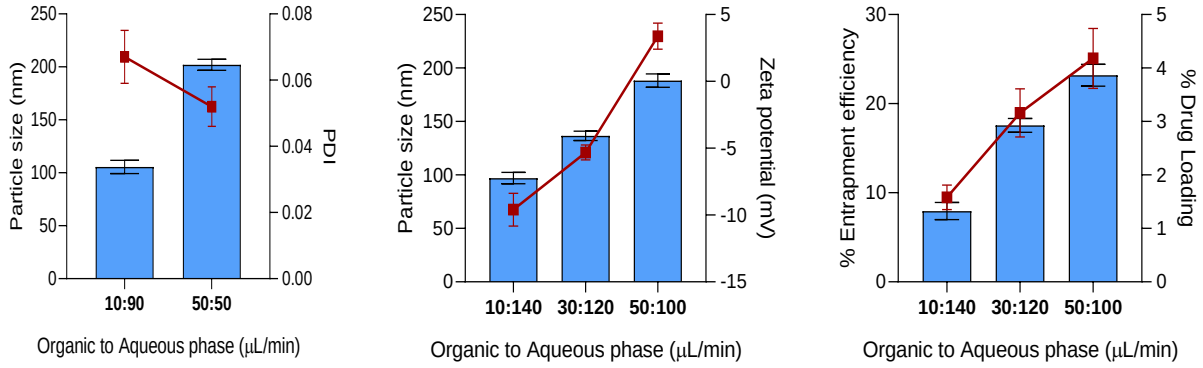

(a) (b) (c)

Figure 5.5. Effect of different process variables on CQAs of TMZ loaded (DSPC: cholesterol, 7:3) liposomes prepared using microfluidics technique *(a) Effect of organic to aqueous phase flow rate on particle size and PDI were lipid concentration and the total flow rate was kept 5 mg/mL and 100 µL/min respectively; (b) Effect of organic to aqueous phase flow rate on particle size and zeta potential were lipid concentration and the total flow rate was kept 5 mg/mL and 150 µL/min; (c) Effect of organic to aqueous phase flow rate on % entrapment efficiency and % drug loading were lipid concentration and the total flow rate was kept 5 mg/mL and 150 µL/min (n=3, Mean ± SD).*

Although microfluidics provided desirable results, this technique was not taken for further characterization due to too dilute liposomal dispersions obtained, time-consuming process, and difficulty in separation and concentration of liposomes.

5.5.5.2 Formulation of liposomes using Membrane extrusion technique

During the formation of thin film, after evaporation of the organic solvent, the phospholipid molecules tend to arrange themselves as parallel sheets with the hydrocarbon tails facing each other. During the rehydration with the aqueous phase, swelling of the phospholipid layers takes place and they tend to fuse and form spherical liposomal vesicles with phospholipid bilayer enclosing an aqueous core. Initially, bigger vesicles are formed which tend to break into smaller vesicles. The process of formation of liposomes was confirmed through microscopy as represented in **Figure 5.6 a**. As initially bigger vesicles were formed and the process was not yet completed, the average particle size obtained was in micron level. Sufficient hydration time needs to be provided to favor the liposome formation and encapsulation of the TMZ inside. After the application of energy during bath sonication, some bigger vesicles reformed into smaller vesicles, thus a non-uniform particle size distribution was observed. Multilamellar liposomes were found to be present along with the small unilamellar liposomes when observed under fluorescence microscopy. This was also confirmed with two particle size populations observed through Zetasizer measurement (**Figure 5.6 b**). A uniform particle size (100 nm) was obtained on completion of 11 extrusion cycles through the membrane filter of defined pore size present in the membrane extruder. The monodispersity was confirmed from the single particle size peak observed through the Zetasizer analysis and the image obtained through FESEM. Uniformly distributed liposomes with a solid outer layer with hollow-core were observed which confirmed the spherical shape and the morphology of the liposomes (**Figure 5.6 c**) [4,23].

Initially, the effect of the number of extrusion cycles on particle size and entrapment efficiency was studied and optimized. The liposomal dispersion was extruded 5, 8, and 11 times through the membrane filter. The particle size of the liposomes was found to decrease on increasing the number of extrusion cycles (**Figure 5.7**). Liposomal particles with an average particle size of 100 nm with narrow size distribution (PDI < 0.3) were obtained on the completion of 11 extrusion cycles. The particle size of 100 nm was achieved as the filter pore size selected was 0.1 µm. The larger vesicles formed after thin film hydration tend to break, fuse and reform in to smaller vesicles when they

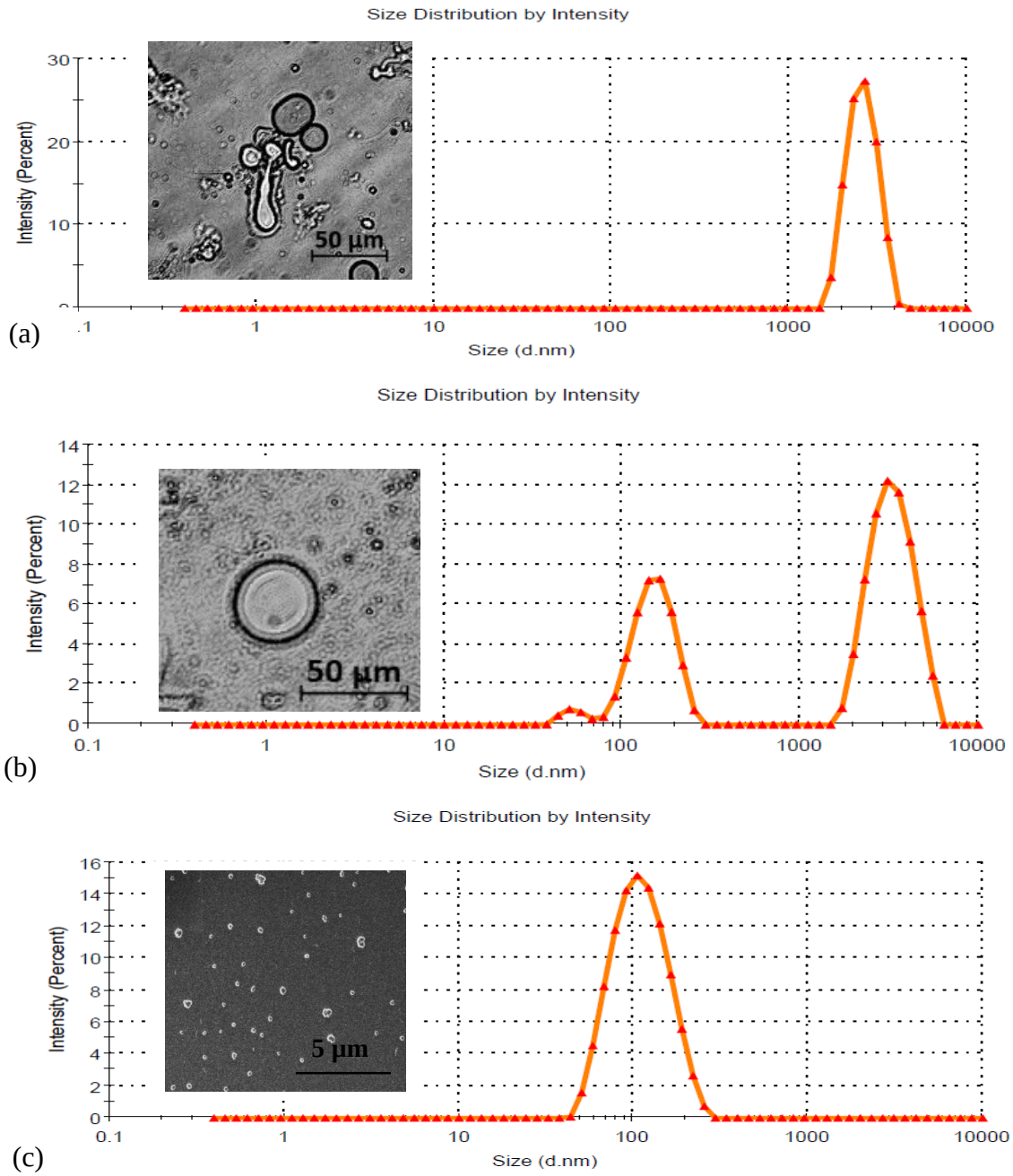

Figure 5.6. Particle size and morphology of liposomes (a) Immediately after rehydration with buffer (b) After bath sonication of 10 min (c) After 11 cycles of extrusion through the membrane extruder

are forced through the pores of the membrane filter. The particle size can be easily altered by the selection of different membrane filter pore sizes and by varying the number of extrusion cycles. Also, a decrease in entrapment efficiency was observed on increasing the number of extrusion cycles as it is dependent on the particle size (**Figure 5.7 a**). The internal to external volume ratio

is less when particle size is less, thus less space for the accommodation of the drug. However, this can be increased by increasing the number of vesicles (increasing the phospholipid concentration) [20,42]. As the membrane filter pore size and number of extrusion cycles were fixed as per the target particle size, the average particle size of all the liposomal formulations prepared further was near 100 nm. Thus, further various factors affecting entrapment efficiency were investigated.

Further, the effect of different phospholipids and concentrations of phospholipids was studied. Three phospholipids (DSPC containing 18 carbon side chain, DPPC containing 16 carbon side chain, DMPC containing 14 carbon side chain) with long chain saturated fatty acid side chains were selected. The highest entrapment efficiency was observed in liposomal formulations prepared using DMPC, followed by DPPC and DSPC. In the case of liposomal formulations prepared with DSPC, no significant increase in the % entrapment efficiency was observed on increasing the lipid concentration. However, an increase in % entrapment efficiency was observed in liposomal formulations prepared using DPPC and DMPC on increasing the phospholipid concentration. A smaller aqueous core is formed when a liposomal bilayer is formed with phospholipids containing a longer fatty acid carbon chain length resulting in less entrapment of a hydrophilic drug. However, for a 100 nm liposome, the decrease in internal volume relative to an increase in membrane thickness resulting from a fatty acid chain length addition of 2 carbon length might be negligible. The difference in entrapment efficiency obtained might be majorly due to the affinity/interaction of the drug with the different phospholipids. A decrease in drug loading was observed on increasing the phospholipid concentration as it is dependent on the phospholipid to drug ratio. Based on the phase transition temperature (higher than the body temperature) and entrapment efficiency obtained, DPPC was selected for further investigation [39,43].

The composition of the liposomes was found to affect the pressure required for extrusion. Liposomes prepared with DSPC required more pressure during extrusion in comparison to liposomes prepared using DMPC. The pressure required during extrusion is directly proportional to the rigidity of the liposomal bilayer. The temperature has to be maintained 5-10^{o}C higher than the phase transition temperature of the phospholipids during the hydration and extrusion process. The phospholipids phase transition temperature is dependent on the fatty acid carbon chain length (DSPC - 55 ^{o}C, DPPC - 41 ^{o}C, and DMPC - 23 ^{o}C). The liposomal vesicles are difficult to reform if hydrated or extruded below the phase transition temperature of the phospholipids due to the

rigidity of the bilayers. However, in the case of TMZ, heating for a longer time (more than 2 h) needs to be avoided because of the instability of the drug at higher temperatures. Compositions containing higher amounts of cholesterol and DSPE-PEG 2000 were hard to extrude in comparison with those containing only phospholipids [39,43].

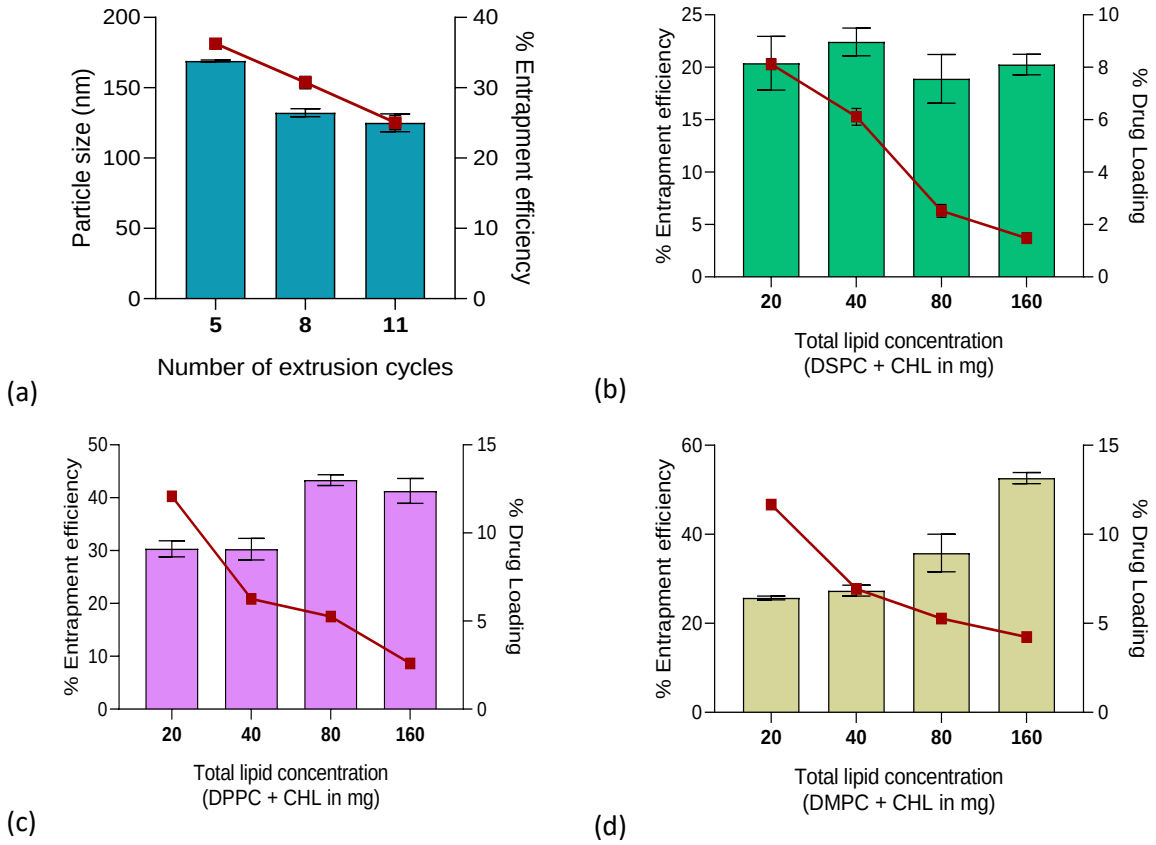

Figure 5.7. Effect of number of extrusion cycles and total lipid concentrations of different phospholipids on characteristics of liposomes prepared using membrane extrusion technique. *(a) Effect of number of extrusion cycles on particle size and entrapment efficiency of TMZ loaded (DSPC: cholesterol, 7:3) liposomes (PDI < 0.3, Zeta potential: 1.18 ± 0.31); Effect of total lipid concentration on % Entrapment efficiency and % Drug loading where different phospholipids (b) DSPC (c) DPPC (d) DMPC were investigated with phospholipid:cholesterol ratio of 7:3, average particle size range 100-130 nm, PDI values < 0.2. (All the measurements were done in triplicates).*

On increasing the concentration of cholesterol from 0 to 45 mol %, a decrease in zeta potential was observed which might be attributed to the negative charge provided by the hydroxyl group present in the cholesterol molecule. When incorporated into the phospholipid bilayer, the hydroxyl group of cholesterol is aligned towards the water on either surface of the phospholipid bilayer

whereas the remaining part of cholesterol stays in contact with the phospholipid hydrocarbon chains within the bilayer. It is considered that the concentration of DPPC, which is slightly positively charged, was reduced by the addition of cholesterol, and thus a decrease in zeta potential was observed (**Figure 5.8 a**). Also, a decrease in entrapment efficiency was observed. The effect of cholesterol on entrapment efficiency is determined by the drug's physicochemical properties, degree of saturation in phospholipids, and concentration of cholesterol. The incorporation of cholesterol into saturated phospholipids increases the fluidity of the membrane which might be responsible for the low entrapment of a hydrophilic drug. Thus, liposome composition consisting of 100 % DPPC was considered for further studies.

Along with DPPC, 5 mole % of PEGylated phospholipid (DSPE-PEG 2000) was added to the composition. Negative zeta potential was observed (**Figure 5.8 b**). The hydroxyl groups on the PEG molecule might contribute to the negative surface charge. A slight decrease in entrapment efficiency was observed on PEGylation [44,45].

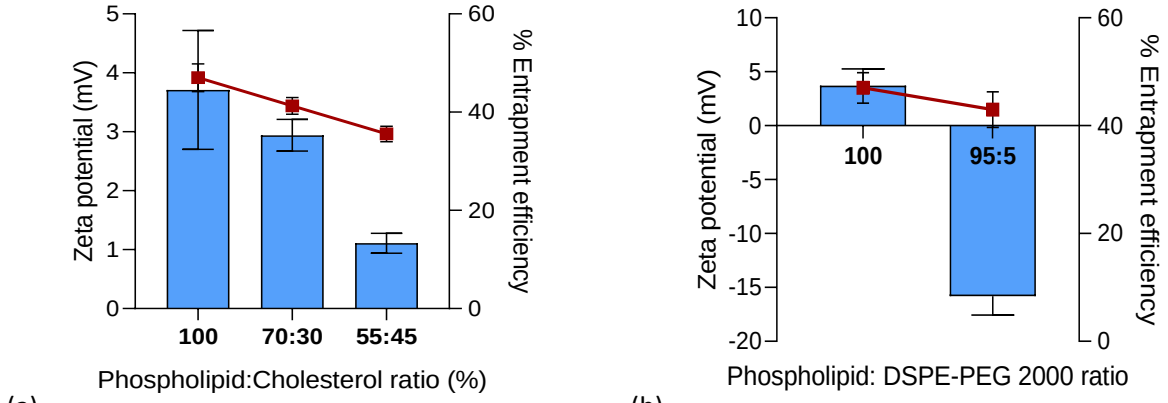

Figure 5.8. (a) Effect of phospholipid (DPPC): cholesterol ratio on zeta potential and % entrapment efficiency of TMZ loaded liposomes (b) Effect of phospholipid (DPPC): DSPE-PEG 2000 on the zeta potential and % entrapment efficiency of TMZ loaded liposomes. *The average particle size range of all the formulations was 100-130 nm with PDI values < 0.3. All the measurements were done in triplicates.*

5.5.6 Characterization of TMZ loaded Liposomes

5.5.6.1 Particle size distribution, Zeta potential, and morphology

The particle size and zeta potential graphs obtained for the optimized TMZ loaded liposomes and PEGylated liposomes are represented in **Figures 5.9.**

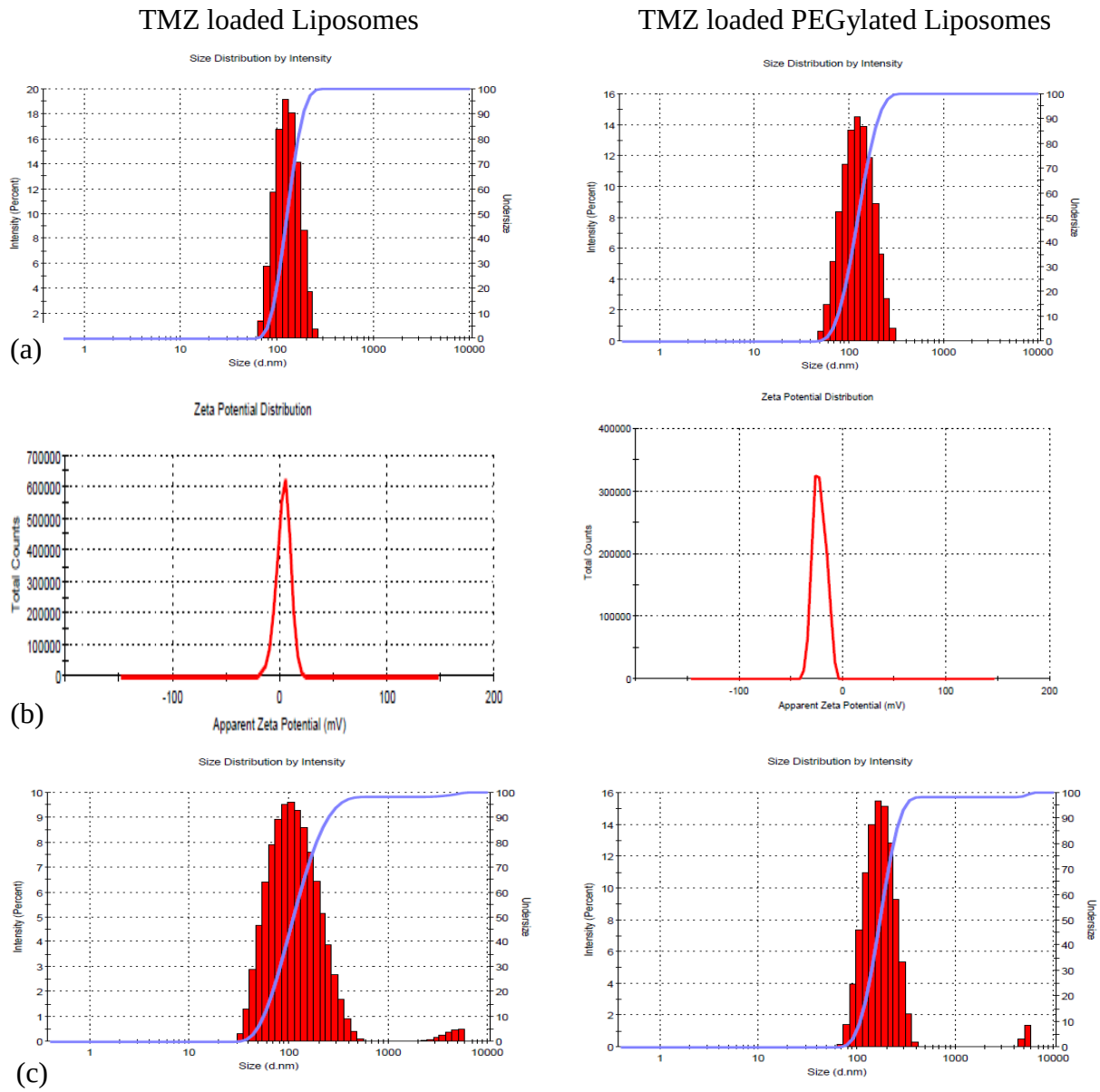

Figure 5.9. (a) Particle size graphs of TMZ loaded Liposomes and TMZ loaded PEGylated Liposomes (b) Zeta potential graphs of TMZ loaded Liposomes and TMZ loaded PEGylated Liposomes (c) Particle size graphs of TMZ loaded Liposomes and TMZ loaded PEGylated Liposomes after reconstitution of freeze-dried form.

The different microscopic images confirming the morphology of liposomes are represented in **Figure 5.10**. When the proliposome powder was observed under an optical microscope, lipid (yellow colour) was found to coat the mannitol crystal (rod-shaped), thus confirming the coating of the carrier molecule on evaporation of the solvents. The formation of vesicles on hydration was

confirmed under a fluorescence microscope. Under an optical microscope, the spherical vesicles were seen. The SEM image confirmed the spherical nature of the nanoparticles formed.

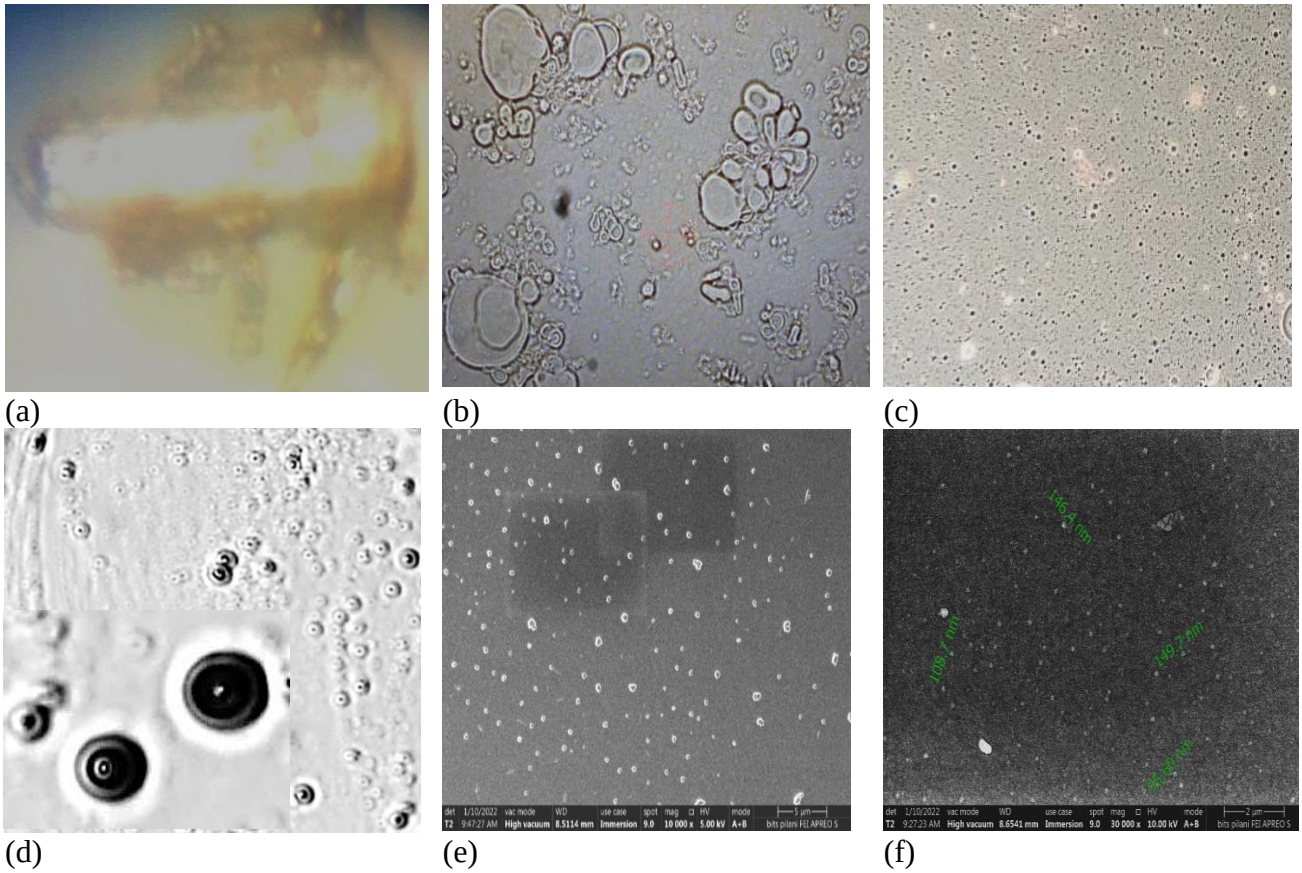

Figure 5.10. Microscopic images of liposomes. *(a) Lipid coated on mannitol after the formation of proliposome powder (Optical microscope- 40x) (b) Initiation of liposome formation on the hydration of proliposome powder/ thin film (Fluorescence microscope- 100x) (c) Liposomes under optical microscope (d) Liposomes under Fluorescence microscope-40x before membrane extrusion (e) Liposomes after membrane extrusion (SEM) (f) PEGylated liposomes after membrane extrusion (SEM)*

5.5.6.2 Drug release and release kinetics

The release profile obtained for TMZ loaded liposomes in different pH media were represented in **Figure 5.11**. The release profile of TMZ in pH 1.2 media showed a 100 % drug release within 2 h itself. This could be attributed to the instability of liposomes in pH 1.2. It is reported that phospholipids are sensitive to extreme pH conditions. The prepared liposomes were formulated using phospholipids. The extreme pH of 1.2 could cause the liposome structure to break and release all the drug. However, drug concentration remained same beyond 2 h, indicating the stability of the TMZ in pH 1.2. There was an increase in the concentration of TMZ released in the initial 1 h

in pH 7.4 media. However, after 1 h, a decrease in the concentration of TMZ was observed. This could be attributed to the conversion of the released TMZ to its AIC. Thus, the release profile of TMZ indicated that pH 1.2 and pH 7.4 phosphate buffer were not suitable as a dissolution medium for the evaluation of TMZ release from the liposomes. The release profile of TMZ in pH 4.5 indicated a burst release in initial 2 h (~ 85 %) followed by a controlled release of TMZ with a 95 % drug release up to 12 h. The liposomes were able to release the entrapped TMZ in a slow and controlled manner. The pH 4.5 acetate buffer could show the controlled release of the TMZ, and thus could be an appropriate dissolution medium. This could provide a rationale for the selection of an appropriate dissolution medium [46].

Cholesterol is likely to affect the drug release rate as observed from the obtained drug release profiles (**Figure 5.12**). A higher drug release rate was observed with the formulations containing cholesterol in comparison to the formulation which contained only phospholipid. The phospholipid used is composed of saturated long-chain fatty acid side chains resembling a cylindrical symmetry. On incorporation of cholesterol, cholesterol occupies space between the fatty acid side chains of the two neighboring phospholipid molecules in the bilayer creating some space. This may lead to faster drug release of the entrapped drug from the liposomes. In the case of phospholipids with unsaturated fatty acid side chains, space is created between two side chains due to the bend created by the double bond. Cholesterol occupies the space between the two fatty acid side chains of a phospholipid molecule, improving the rigidity of the bilayer formed. This may cause a slow release of the entrapped drug through the phospholipid bilayer [44,47].

Drug loading was found to show a significant effect on the drug release rate (**Figure 5.12**). The drug release rate was directly proportional to the drug loading. Less drug loading represents higher phospholipid concentration in comparison to the drug. In this case, a higher concentration of lipid is present which represents a higher number of vesicles formed which can sustain the release of the entrapped drug. Thus, physicochemical properties of the drug, type of phospholipid used, amount of phospholipid, and amount of cholesterol are the various formulation variables significantly affecting the drug release from the liposomes [44,47].

Further, the effect of incorporating DSPE-PEG 2000 on the drug release was studied (**Figure 5.13**). Various release kinetics models were applied to the release data obtained for TMZ, TMZ loaded Liposomes and TMZ loaded PEGylated Liposomes using DDsolver and the best fit model was

identified (**Table 5.11**). TMZ was found to follow first-order kinetics. TMZ loaded liposomes were found to follow Korsmeyer's Peppas model. The release exponent 'n' value less than 0.45 demonstrated diffusion-controlled drug release. The drug release in pH 7.4 demonstrated that the PEGylated liposomes could successfully protect TMZ for a longer period in plasma pH [45].

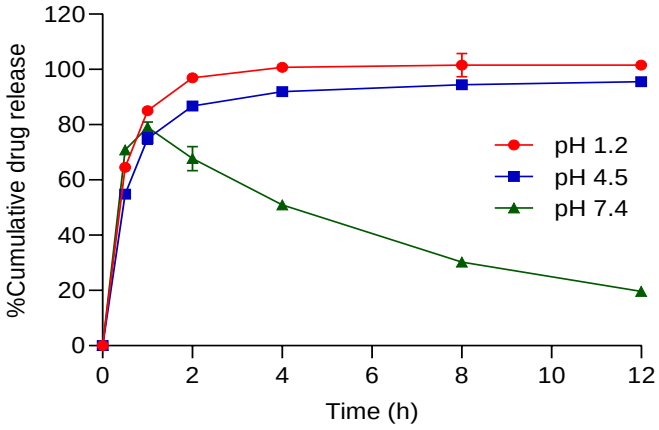

Figure 5.11. Drug release profile of TMZ loaded liposomes in different dissolution media (n=3)

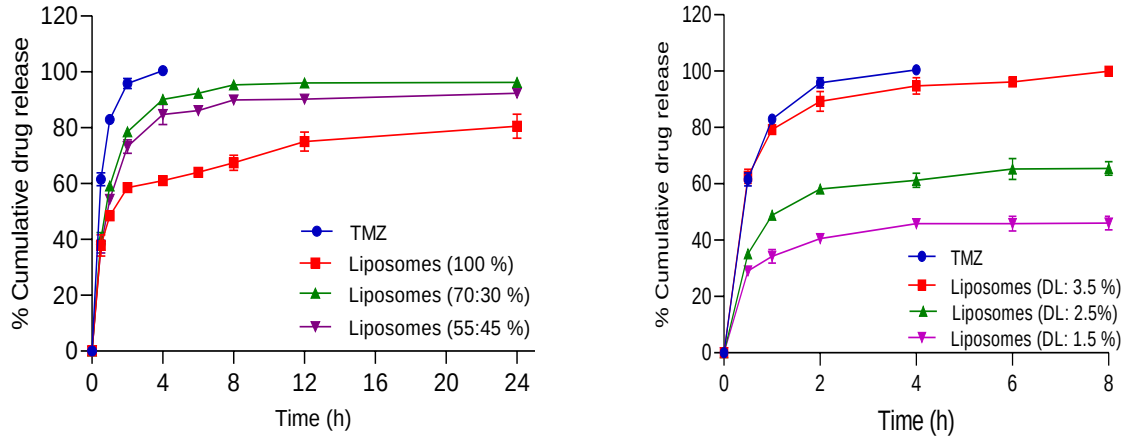

(a) (b)

Figure 5.12. (a) Effect of cholesterol concentration on in-vitro drug release of TMZ from DPPC liposomes (b) Effect of drug loading on in-vitro drug release of TMZ from liposomes. *The average particle size range of all the formulations was 90-110 nm with PDI values < 0.2. All the measurements were done in triplicates.*

Table 5.11. Release kinetics parameters obtained for TMZ, TMZ loaded Liposomes and TMZ loaded PEGylated Liposomes through different models

Model	TMZ			TMZ loaded Liposomes			TMZ loaded PEGylated Liposomes		
	R^2	AIC	MSC	R^2	AIC	MSC	R^2	AIC	MSC
Zero order	0.756	45.831	-1.53	0.694	85.646	-2.078	0.634	88.727	-2.179
First order	**0.999**	**11.017**	**5.432**	0.890	74.252	-0.812	0.953	70.949	-0.204
Higuchi	0.925	38.134	0.009	0.866	74.376	-0.825	0.819	78.363	-1.028
Korsmeyer Peppas	0.992	27.341	2.168	**0.994**	**39.645**	**3.033**	**0.977**	**54.598**	**1.613**
Hixson Crowell	0.975	32.277	1.180	0.584	76.841	-1.099	0.822	79.169	-1.117
Best fit model parameters									
	First order			**Korsmeyer-Peppas**					
K	2.266			47.760			56.022		
N	-			0.171			0.154		
t_{25}	0.127			0.023			0.005		
t_{50}	0.306			1.306			0.479		
t_{75}	0.612			13.895			6.619		

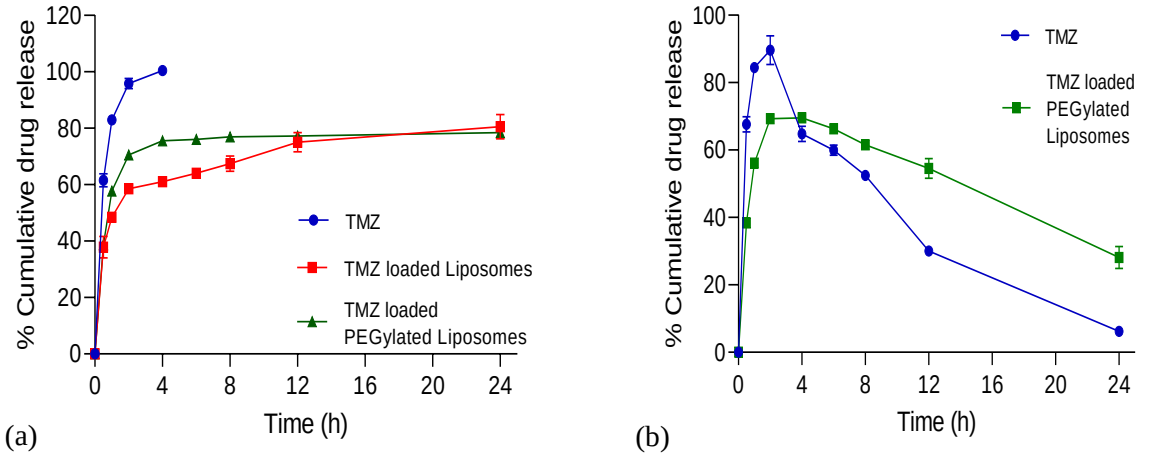

Figure 5.13. The in-vitro drug release profile of (a) TMZ, TMZ loaded Liposomes and TMZ loaded PEGylated Liposomes in acetate buffer pH 4.5 (b) TMZ and TMZ loaded PEGylated liposomes in phosphate buffer pH 7.4 *(n=3 represented as Mean ± SD)*

5.5.6.3. Reproducibility

The average particle size and PDI of 118.833 ± 7.062 and 0.119 ± 0.032 were obtained respectively (n=6, data obtained for six 1 mL formulation extruded individually). The reproducibility between individual extrusions was confirmed. The particle size and PDI of both Liposomes and PEGylated Liposomes were found to be stable even after 1000 times dilution, which revealed that the structure was maintained even after dilution (**Figure 5.14**) [48].

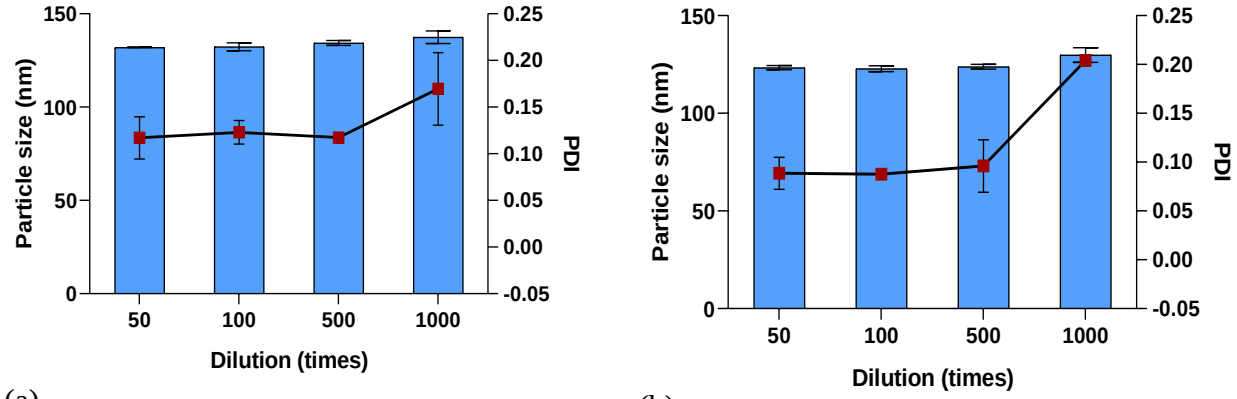

Figure 5.14. Particle size (nm) and PDI of (a) TMZ-loaded Liposomes and (b) PEGylated Liposomes on different dilutions with Milli Q water. *The zeta potential of TMZ-loaded Liposomes and PEGylated Liposomes were found to be 1.52 ± 1.59 mV and -25.05 ± 4.28 mV respectively (n=3 shown as Mean ± SD)*

5.5.6.4 In-vitro cytotoxicity study

MTT assay is one of the colorimetric tests used to assess cell viability. The cellular enzymes metabolize the MTT dye to formazan crystals. Dead cells are not able to metabolize due to the absence of enzymes. When solubilized in DMSO, the formazan crystals produce purple color that has characteristic absorption at 570 nm. The results obtained for cell viability are summarized in **Figure 5.15**. TMZ was found to show dose-dependent cytotoxicity on glioma cells. The IC_{50} value for TMZ was found to be 0.98 mM. TMZ loaded Liposomes were found to show significantly increased cell cytotoxicity. TMZ loaded Liposomes and TMZ loaded PEGylated Liposomes were found to show 1.71 and 1.59 fold more cytotoxicity as compared to TMZ alone. Liposomes enhance the permeability through cells. As the drug concentration increases, the number of

Liposomes also increases, ultimately resulting in higher cytotoxicity. The study revealed that incorporating TMZ into the Liposomes potentiates the cytotoxicity of TMZ [49].

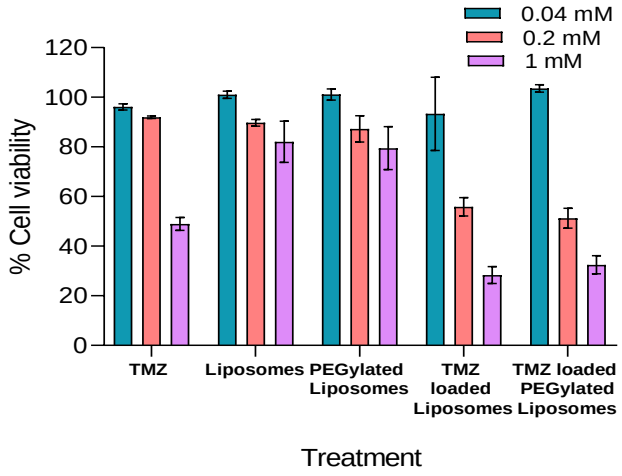

	IC_{50} value
TMZ	0.98 ± 0.049 mM
TMZ loaded Liposomes	0.57 ± 0.112 mM
TMZ loaded PEGylated Liposomes	0.61 ± 0.052 mM

Figure 5.15. In-vitro cytotoxicity assessment of TMZ and TMZ-loaded Liposomes on U87 cells exposed for 48 h. *Data represented as Mean ± SD (n=4, where n represents the number of wells in an experiment)*

5.5.6.5. Cell uptake study

The U87 glioblastoma cell uptake study (**Figure 5.16)** was conducted to evaluate the potential of Liposomes when directly administered to the brain. Certain emerging techniques like convection-enhanced delivery (CED) have shown promising results in the treatment of glioblastoma. This technique involves infusion directly into the brain under a pressure gradient. However, this technique gets limited as most of the drugs have a short half-life and are eliminated quickly from the brain. Few studies have shown hope for the delivery of nanoparticles through this technique, which provides advantages like protection of the drug from the outside environment, controlled and modified drug distribution. PEGylated nanoparticles of small size (up to 150 nm) have been reported to show uniform distribution through the brain after CED as compared to uncoated particles. Although, no significant difference in the fluorescence intensity obtained for U87 cell uptake by Liposomes and PEGylated liposomes was observed, a difference in the cell uptake mechanism was noticed. The confocal images obtained for cell uptake by liposomes demonstrated regions of dark spots indicating endosomal uptake whereas the images obtained for PEGylated liposomes demonstrated a uniform distribution indicating endosomal escape. PEGylated liposomes were found to show a 3.47-fold less cell uptake in macrophage cell lines as

compared to uncoated Liposomes (**Figure 5.17**). When the nanoparticles are administered in to the plasma, they are considered foreign particles and taken up by the macrophages through opsonization followed by phagocytosis. It is known that PEGylation of nanoparticles forms a hydrophilic protective layer around the nanoparticles, prevents opsonization and their uptake by macrophage cells, reduces the clearance rate, and hence provides longer circulation of these particles in plasma. Particle size is another factor affecting cell uptake. Smaller particles (80 to 150 nm) provide a longer plasma circulation time. Longer circulation may lead to more TMZ distribution to brain [50–52].

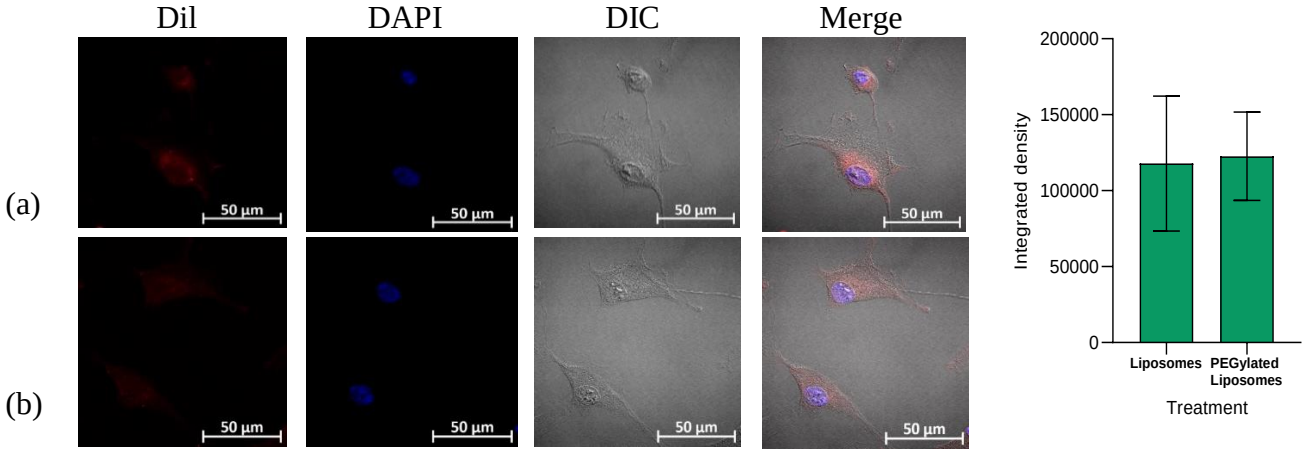

Figure 5.16. Confocal images and fluorescence intensity obtained for cell uptake studies of (a) Dye loaded Liposomes and (b) Dye loaded PEGylated Liposomes in U87 glioblastoma cell lines after treatment of 4 hours *(Data represented as Mean ± SD, n=4).*

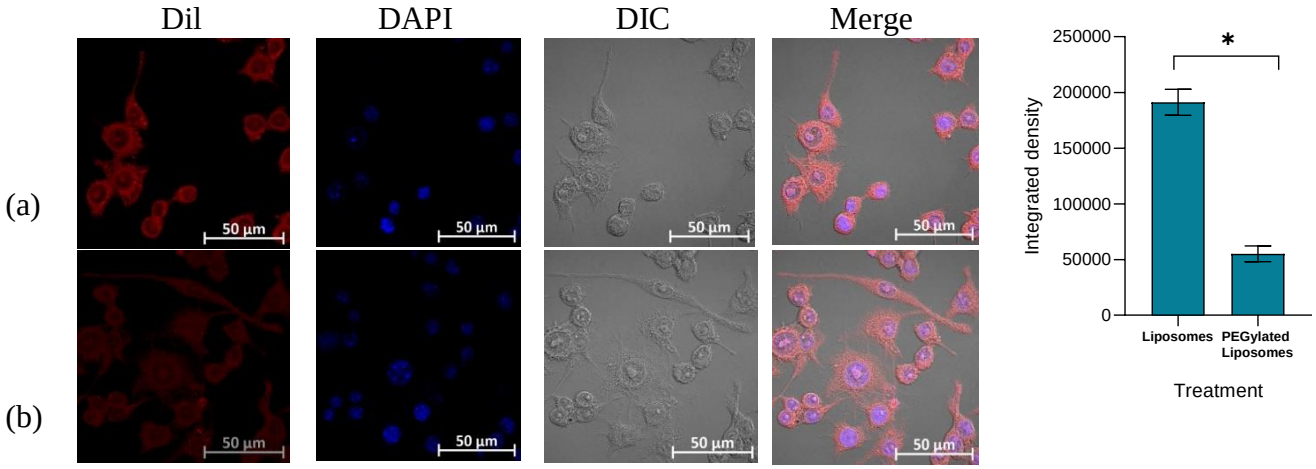

Figure 5.17. Confocal images and fluorescence intensity obtained for cell uptake studies of (a) Dye loaded Liposomes and (b) Dye loaded PEGylated Liposomes in RAW macrophage cell lines after treatment of 4 hours *(Data represented as Mean ± SD, n=4). * statistical significance $p < 0.05$ using t-test*

5.5.6.6. Storage stability

The stability data revealed that TMZ loaded PEGylated Liposomes were stable under refrigerated conditions. A decrease in drug content was observed when stored at room temperature owing to the instability of TMZ at room temperature (**Table 5.12**).

Table 5.12. Storage stability data of freeze-dried TMZ loaded PEGylated Liposomes (n=3)

Months		**0**	**1**	**2**
Refrigerated conditions	Particle size (nm)	111.2 ± 6.924	106.8 ± 3.416	114.55 ± 5.041
	PDI	0.117 ± 0.020	0.119 ± 0.008	0.122 ± 0.018
	Drug content (%)	98.123 ± 0.054	102.058 ± 1.957	98.022 ± 3.330
Room temperature	Particle size (nm)	111.2 ± 6.924	123.95 ± 3.456	124.7 ± 6.647
	PDI	0.117 ± 0.020	0.120 ± 0.042	0.169 ± 0.015
	Drug content (%)	98.123 ± 0.054	57.208 ± 1.760	46.514 ± 1.713

5.6. Conclusion

The principles of QbD helped in the risk assessment and identification of various CMAs and CPPs before starting with the actual formulation process. Liposomes with small, uniform and reproducible particle sizes have been successfully prepared using microfluidics and membrane extrusion techniques. These techniques are suitable for the entrapment of an amphiphilic drug like TMZ. Both the techniques involve a minimum number of critical process parameters which can be optimized as per the target. When the liposomes of the same composition were produced using microfluidics and membrane extrusion, similar particle sizes and entrapment efficiency were obtained. These techniques are suitable for the formulation of dilute liposomal dispersions as too concentrated dispersions might clog the channels in the microfluidic chip or the pores of the membrane filters in the extruder. Using microfluidics, 3-4 times dilute liposomal dispersions were obtained in comparison to membrane extrusion. This is a major drawback of using microfluidics. However, there is the future scope of producing concentrated liposomal dispersions by designing a chip and combining multiple chips together. These techniques have huge scope in the future for producing liposomes with reproducibility. The liposomes were found to show prolonged drug

release and also protect TMZ from plasma pH. PEGylated liposomes were found to prevent macrophage uptake.

References:

1. Barenholz YC. Doxil ® — The first FDA-approved nano-drug : Lessons learned. J Control Release. 2012;160(2):117–34.
2. Liu P, Chen G, Zhang J. A Review of Liposomes as a Drug Delivery System: Current Status of Approved Products, Regulatory Environments, and Future Perspectives. Molecules. 2022;27(4):1372.
3. Chandra D, Yadav KK, Singh VK, Patel A. AN OVERVIEW : THE NOVEL CARRIER FOR VESICULAR DRUG DELIVERY. World J Pharm Res. 2014;3(6):1299–322.
4. Akbarzadeh A, Rezaei-sadabady R, Davaran S, Joo SW, Zarghami N. Liposome : classification , preparation , and applications. Nanoscale Res Lett. 2013;8:102.
5. Bhupendra Pradhan*, Kumar N, Saha S, Roy A. Liposome: Method of Preparation, Advantages, Evaluation and its application. J Appl Pharm Res. 2015;3(2348):01–8.
6. Mishra DK, Shandilya R, Mishra PK. Lipid based nanocarriers : a translational perspective. Nanomedicine Nanotechnology, Biol Med. 2018;14(7):2023–50.
7. Dormont F, Rouquette M, Mahatsekake C, Gobeaux F, Peramo A, Brusini R, et al. Translation of nanomedicines from lab to industrial scale synthesis : The case of squalene-adenosine nanoparticles. J Control Release. 2019;307:302–14.
8. Zhang L, Mao S. Application of quality by design in the current drug development. Asian J Pharm Sci. 2017;12(1):1–8.
9. Sangshetti JN, Deshpande M, Zaheer Z, Shinde DB, Arote R. Quality by design approach: Regulatory need. Arab J Chem. 2017;10:S3412–25.
10. Van Hoogevest P, Wendel A. The use of natural and synthetic phospholipids as pharmaceutical excipients. Eur J Lipid Sci Technol. 2014;116(9):1088–107.
11. Balasaheb Jadhav J, Namdeogirawale N, Chaudhari RA. Quality by Design (QBD)

Approach used in Development of Pharmaceuticals. Int J pure Appl Biosci. 2014;2(5):214–23.

12. Darkunde SL. A review on quality by design. Int J Pharm Chem Anal. 2020;5(1):1–6.

13. Bansal S, Beg S, Asthana A, Garg B, Asthana GS, Kapil R, et al. QbD-enabled systematic development of gastroretentive multiple-unit microballoons of itopride hydrochloride. Drug Deliv. 2016;23(2):437–51.

14. de Barros C, Aranha N, Severino P, Souto EB, Zielińska A, Lopes A, et al. Quality by design approach for the development of liposome carrying ghrelin for intranasal administration. Pharmaceutics. 2021;13(5):686.

15. Németh Z, Pallagi E, Dobó DG, Kozma G, Kónya Z, Csóka I. An updated risk assessment as part of the QbD-based liposome design and development. Pharmaceutics. 2021;13(7):1071.

16. Fahmy R, Kona R, Dandu R, Xie W, Claycamp G, Hoag SW. Quality by Design I: Application of Failure Mode Effect Analysis (FMEA) and Plackett–Burman Design of Experiments in the Identification of "Main Factors" in the Formulation and Process Design Space for Roller-Compacted Ciprofloxacin Hydrochloride Immediat. AAPS PharmSciTech. 2012 Dec;13(4):1243–54.

17. Carugo D, Bott E, Owen J, Stride E, Nastruzzi C. Liposome production by microfluidics : potential and limiting factors. Sci Rep. 2016;16(1):1–15.

18. Lim SWZ, Wong YS, Czarny B, Venkatraman S. Microfluidic-directed self-assembly of liposomes: Role of interdigitation. J Colloid Interface Sci. 2020;578:47–57.

19. Shukla SK, Kulkarni NS, Chan A, Parvathaneni V, Farrales P, Muth A, et al. Metformin-encapsulated liposome delivery system: An effective treatment approach against breast cancer. Pharmaceutics. 2019;11(559):1–25.

20. Gim S, Ong M, Chitneni M, Lee KS, Ming LC, Yuen KH. Evaluation of Extrusion Technique for Nanosizing Liposomes. Pharmaceutics. 2016;8(36):1–12.

21. Bhattacharjee S. DLS and zeta potential - What they are and what they are not? J Control

Release. 2016;235:337–51.

22. Waghule T, Rapalli VK, Singhvi G, Gorantla S, Khosa A, Dubey SK, et al. Design of temozolomide-loaded proliposomes and lipid crystal nanoparticles with industrial feasible approaches: comparative assessment of drug loading, entrapment efficiency, and stability at plasma pH. J Liposome Res. 2020;31(2):158–68.

23. Placzek M, Kosela M. Microscopic methods in analysis of submicron phospholipid dispersions. Acta Pharm. 2016;66(1):1–22.

24. Waghule T, Laxmi Swetha K, Roy A, Narayan Saha R, Singhvi G. Quality by design assisted optimization of temozolomide loaded PEGylated lyotropic liquid crystals: Investigating various formulation and process variables along with in-vitro characterization. J Mol Liq. 2022;352:118724.

25. Waghule T, Narayan R, Singhvi G. UV spectroscopic method for estimation of temozolomide : Application in stability studies in simulated plasma pH , degradation rate kinetics , formulation design , and selection of disso. Spectrochim Acta Part A Mol Biomol Spectrosc. 2021;258:119848.

26. Zhao L, Xiong H, Peng H. PEG-coated lyophilized proliposomes : preparation , characterizations and in vitro release evaluation of vitamin E. Eur Food Res Technol. 2011;232:647–54.

27. Mahmood A, Krishna V, Waghule T, Gorantla S, Kumar S, Narayan R, et al. Spectrochimica Acta Part A : Molecular and Biomolecular Spectroscopy UV spectrophotometric method for simultaneous estimation of betamethasone valerate and tazarotene with absorption factor method : Application for in-vitro and ex-vivo characterization of. Spectrochim Acta Part A Mol Biomol Spectrosc. 2020;235:118310.

28. Zuo J, Gao Y, Bou-Chacra N, Löbenberg R. Evaluation of the DDSolver software applications. Biomed Res Int. 2014;2014.

29. Zhang Y, Huo M, Zhou J, Zou A, Li W, Yao C, et al. DDSolver: An add-in program for modeling and comparison of drug dissolution profiles. AAPS J. 2010;12(3):263–71.

30. Gorantla S, Saha RN, Singhvi G. Exploring the affluent potential of glyceryl mono oleate – myristol liquid crystal nanoparticles mediated localized topical delivery of Tofacitinib: Study of systematic QbD, skin deposition and dermal pharmacokinetics assessment. J Mol Liq. 2021;346:117053.

31. Lu J, Owen SC, Shoichet MS. Stability of self-assembled polymeric micelles in serum. Macromolecules. 2011;44(15):6002–8.

32. Jain V, Swarnakar NK, Mishra PR, Verma A, Kaul A, Mishra AK, et al. Paclitaxel loaded PEGylated gleceryl monooleate based nanoparticulate carriers in chemotherapy. Biomaterials. 2012;33(29):7206–20.

33. Patel BK, Parikh RH. FORMULATION DEVELOPMENT AND EVALUATION OF TEMOZOLOMIDE LOADED HYDROGENATED SOYA PHOSPHATIDYLCHOLINE LIPOSOMES FOR THE TREATMENT OF BRAIN CANCER. Asian J Pharm Clin Res. 2016;9(3):340–340.

34. Rapalli VK, Kaul V, Waghule T, Gorantla S, Sharma S, Roy A, et al. Curcumin loaded nanostructured lipid carriers for enhanced skin retained topical delivery: optimization, scale-up, in-vitro characterization and assessment of ex-vivo skin deposition. Eur J Pharm Sci. 2020 Sep 1;152:105438.

35. Bapat P, Ghadi R, Chaudhari D, Katiyar SS, Jain S. Tocophersolan stabilized lipid nanocapsules with high drug loading to improve the permeability and oral bioavailability of curcumin. Int J Pharm. 2019;560:219–27.

36. Pallagi E, Gabriella D. A Proposed Methodology for a Risk Assessment-Based Liposome Development Process. Pharmaceutics. 2020;12:1164.

37. Cameron Webb, Swapnil Khadke, Signe Tandrup Schmidt, Clara B. Roces, Neil Forbes, Gillian Berrie YP. The Impact of Solvent Selection: Strategies to Guide the Manufacturing of Liposomes Using Microfluidics. Pharmaceutics. 2019;11:653.

38. Waghule T, Patil S, Rapalli VK, Girdhar V, Gorantla S, Kumar Dubey S, et al. Improved skin-permeated diclofenac-loaded lyotropic liquid crystal nanoparticles: QbD-driven industrial feasible process and assessment of skin deposition. Liq Cryst. 2020;47:1–19.

39. Li J, Wang X, Zhang T, Wang C, Huang Z, Luo X, et al. A review on phospholipids and their main applications in drug delivery systems. Asian J Pharm Sci. 2015;10(2):81–98.

40. Zook JM, Vreeland WN. Effects of temperature , acyl chain length , and flow-rate ratio on liposome formation and size in a microfluidic hydrodynamic focusing device. 2010;1352–60.

41. Surianarayanan R, Gurumallappa Shivakumar H, Varma Vegesna NSK, Srivastava A. Effect of sample Concentration on the Characterization of Liposomes using Dynamic light Scattering Technique. Pharm Methods. 2016;7(1):70–4.

42. Clerc SG, Thompson TE. A possible mechanism for vesicle formation by extrusion. Biophys J. 1994;67(1):475–6.

43. Xu X, Khan MA, Burgess DJ. A quality by design (QbD) case study on liposomes containing hydrophilic API: I. Formulation, processing design and risk assessment. Int J Pharm. 2011;419(1–2):52–9.

44. Martinez-Seara H, Róg T, Pasenkiewicz-Gierula M, Vattulainen I, Karttunen M, Reigada R. Interplay of unsaturated phospholipids and cholesterol in membranes: Effect of the double-bond position. Biophys J. 2008;95(7):3295–305.

45. Maritim S, Boulas P, Lin Y. Comprehensive analysis of liposome formulation parameters and their influence on encapsulation, stability and drug release in glibenclamide liposomes. Int J Pharm. 2021;592:120051.

46. Angelova MI, Bitbol AF, Seigneuret M, Staneva G, Kodama A, Sakuma Y, et al. pH sensing by lipids in membranes: The fundamentals of pH-driven migration, polarization and deformations of lipid bilayer assemblies. Biochim Biophys Acta - Biomembr. 2018;1860(10):2042–63.

47. Briuglia M-L, Rotella C, Mcfarlane A, Lamprou DA. Influence of cholesterol on liposome stability and on in vitro drug release. Drug Deliv Transl Res. 2015;5:231–42.

48. Rapalli VK, Sharma S, Roy A, Singhvi G. Design and dermatokinetic evaluation of Apremilast loaded nanostructured lipid carriers embedded gel for topical delivery: A

potential approach for improved permeation and prolong skin deposition. Colloids Surfaces B Biointerfaces. 2021;206:111945.

49. Freag May, Elnaggar, Yosra S R, Abdelmonsif A Doaa AYO. Stealth , biocompatible monoolein-based lyotropic liquid crystalline nanoparticles for enhanced aloe-emodin delivery to breast cancer cells : in vitro and in vivo studies. Int J Nanomedicine. 2016;11:4799–818.

50. Sanchez L, Yi Y, Yu Y. Effect of partial PEGylation on particle uptake by macrophages. Nanoscale. 2017;9(1):288–97.

51. Petithory T, Pieuchot L, Josien L, Ponche A, Anselme K, Vonna L. Size-dependent internalization efficiency of macrophages from adsorbed nanoparticle-based monolayers. Nanomaterials. 2021;11(8):1963.

52. Rodrigues L, Schneider F, Zhang X, Larsson E, Moodie LWK, Dietz H, et al. Cellular uptake of self-assembled phytantriol-based hexosomes is independent of major endocytic machineries. J Colloid Interface Sci. 2019;553:820–33.

Chapter 6

Formulation and characterization of TMZ loaded Lyotropic Liquid Crystals

6.1. Introduction

Lyotropic Liquid Crystals (LLCs) have gained much attraction in recent years in the field of pharmaceutical nanotechnology and drug delivery due to their unique structural properties. LLCs exhibit highly ordered structural alignment and optical properties similar to solid crystals. Additionally, they exhibit fluidity, surface tension, and viscosity like a liquid. LLCs composition consists of lipidic amphiphiles such as glyceryl monooleate (GMO) and lecithin that self-assemble into different three-dimensional structures with aqueous channels when added into excess of the aqueous medium. Stabilizers like Pluronics and polyethylene glycol derivatives are essential for forming stable structures [1,2]. The presence of varying polarities in the LLCs region favors the entrapment of hydrophilic, lipophilic as well as amphiphilic drug molecules [3,4]. The presence of multiple layers of lipids consisting of a honeycomb-like structure allows the entrapped drug to diffuse slowly through the LLCs structure, providing extended drug release. GMO is the most common LLCs forming lipid. It is biocompatible, biodegradable, and classified as GRAS (generally recognized as safe). However, it is reported to cause hemolysis on parenteral administration. Surface coating of the LLCs with polyethylene glycol (PEG) derivatives provides several advantages like improving hemocompatibility, reducing immunogenicity, preventing uptake by the reticuloendothelial system, and providing longer circulation time in plasma [5–7].

6.2. Materials

Glyceryl monooleate (Mono ester content: minimum 35 %, Free Glycerin: maximum 7 %) was received as a gift sample from Mohini Organics Pvt. Ltd. Pluronic 127 was acquired as a gift sample from BASF (Mumbai), Polyethylene glycol 200 (PEG 200) was purchased from CDH Fine Chemicals (New Delhi). DSPE-PEG 2000, Temozolomide, Sodium acetate, glacial acetic acid extra pure, hydrochloric acid, sodium chloride, potassium chloride, disodium hydrogen phosphate and potassium dihydrogen phosphate used were as mentioned in **section 4.2**. Milli Q water purified by Merck Millipore systems was used during the entire analysis.

6.3. Instruments/ equipment

Analytical balance, UV visible spectrophotometer, REMI Laboratory Centrifuge, Temperature controlled centrifuge, Toshiba Bath Sonicator used were as mentioned in **section 4.3.** REMI motor Mechanical stirrer with speed regulator (REMI Elektrotechnik Ltd. Vasai, India), Sonics Vibra

Cell Probe Sonicator, Zetasizer (Zetasizer Nano-ZS ZEN 3600, Malvern), Field emission Scanning Electron Microscope **(**FESEM) with Apreo Switch XT microscope, Lyophilizer (Freezone 2.5, Labconco, USA), ZEISS Fluorescence microscope, X-ray diffractometer (Rigaku- miniflex).

6.4. Methods

6.4.1. Screening of various preparation methods

During the formulation of TMZ-loaded LLCs, various preparation techniques including different size reduction methods were explored to understand the effect on particle size and entrapment efficiency. Initially, the desired quantity of GMO, Poloxamer 127, and PEG 200 were transferred to a clean vial. The lipid phase was melted at around 70 ± 5°C on a hot plate. A weighed quantity of TMZ was dissolved in the aqueous phase (acetate buffer pH 4.5) and heated to the same temperature separately. To study the effect of the order of addition, initially, the aqueous phase was added to the lipid phase under mechanical stirring which was continued for 10 min. Alternatively, the lipid phase was added to the aqueous phase under mechanical stirring which was continued for 10 min [4,8]. To study the effect of the addition of the drug to the lipid or aqueous phase on entrapment efficiency, TMZ was added in lipid phase followed by the process mentioned earlier, and alternatively in the water phase. The effect on entrapment efficiency was determined. To study the effect of solvent used for drug solubilization, initially, acetone (2 mL) was used as a solvent to dissolve TMZ in the lipid phase. It was selected based on drug solubility and low boiling point. The procedure after this was kept the same. In the following method, instead of acetone, water itself was used as a solvent for drug solubilization and mesophase formation. A weighed amount of TMZ was dissolved in a specified quantity of water (20 % of the final dispersion volume) based on the maximum solubility of TMZ in water (5mg/ mL). This was heated to 70 ± 5°C and added drop-wise to the melted lipid phase under magnetic stirring (500 rpm, 5 min). The formed phase was cooled down to room temperature to allow mesophase formation and to achieve entrapment of TMZ within the LLC structure. The remaining quantity of water was added to the formed phase. This was immediately followed by a suitable size reduction method. Various size reduction techniques like magnetic stirring, low-speed mechanical stirring, high-speed mechanical stirring, homogenization, and probe sonication were explored to study the effect on particle size and drug entrapment efficiency [9–11].

6.4.2 Optimization of TMZ loaded LLCs using Quality by Design (QbD) approach

6.4.2.1. Defining and identifying Quality Target Product Profile and Critical Quality Attributes

The QTPP profile and CQAs for TMZ loaded LLCs were defined as discussed in **section 5.4.2**. [12,13].

6.4.2.2. Quality risk management

Risk assessment was conducted similarly as described in **section 5.4.3** [14,15].

6.4.2.3. Identifying Critical Material Attributes (CMAs) and Critical Process Parameters (CPPs)

Screening of various factors was done in the initial preliminary experiments. Various CMAs and CPPs were identified as discussed in **section 5.4.4** [16].

6.4.2.4. Experimental design and data analysis

Independent and response variables were decided based on the literature survey, prior experience, preliminary trials, and risk assessment. Initially, the screening of various process parameters was conducted to distinguish between significant and non-significant factors. Various process parameters involved in the preparation of LLCs which are likely to affect the particle size and polydispersity index were identified. The critical and non-critical factors were found using the Factorial design (Minimum Run Resolution IV) with three center points. The selected process parameters were studied at two levels (low and high) which were decided based on the knowledge obtained from preliminary trials. The Design Expert® software (Version 13, Stat-Ease Inc.) was used to obtain the trials. Accordingly, the formulation trials were taken and characterized. The values obtained were entered into the software as response variables. The effect of various process variables was further studied statistically. Based on the obtained results, variables were selected for further optimization [17].

Further, optimization of the various formulation variables was conducted. Based on the number of variables, the 'Box Behnken' design (BBD) was selected to obtain the optimized formulation and to study the effect of various formulation variables on the response variables. The Box Behnken design helps to predict the actual relation between the factors with a restricted number of

experiments without compromising the resulting quality [18]. The higher and lower levels of the formulation variables were decided based on the preliminary experiments. The Design Expert® software (Version 13, Stat-Ease Inc.) was used to obtain the trials. Accordingly, the formulation trials were taken and characterized. The values obtained were entered into the software as response variables. The effect of various formulation variables was further studied statistically by the software [17].

The software states the significant and non-significant terms based on statistical analysis (F-value and p-value). The non-significant terms were excluded from the model. The best model was selected based on various factors. The values of Predicted R^2 must not be negative. The difference between the Predicted R^2 and Adjusted R^2 should be less than 0.2. The PRESS value helps to select the best model for each response. The Adequate precision value should be more than 4. After obtaining a significant model, Polynomial equations were generated by the software. The equation provides the relationship between the response variable and the independent variable. Further, the data were analyzed using different diagnostic and model graphs [19].

6.4.2.5. Validation of the design and establishment of design space

After obtaining the significant model equations for each response, the target goals were set in the software, and various solutions were obtained. Three random solutions were selected for validating the model equations. The predicted and observed values of the responses were compared. An optimized composition was selected based on the desired particle size, highest entrapment efficiency, low lipid concentration, and the desirability value near to 1 [20,21]. Design space was established to get a range of formulation variables to achieve the desired set of response variables [22].

6.4.3. Preparation of TMZ loaded LLCs by the optimized method

Based on the optimized process and composition using the experimental design, a desired quantity of GMO, Poloxamer 127, PEG 200, and TMZ were transferred to a clean vial. The lipid phase was melted at around 70 ± 5°C on a hot plate. A weighed amount of TMZ was dissolved in a specified quantity of water (10, 20, 30 and 40 % of the final dispersion volume) based on the maximum solubility of TMZ in water (5mg/ mL) in order to study the effect of drug amount on characteristics of LLCs. This was heated to 70 ± 5°C and added drop-wise to the melted lipid phase under

magnetic stirring (500 rpm, 5 min). The formed phase was cooled down to room temperature to allow mesophase formation and entrapment of TMZ within. The remaining quantity of water was added to the formed phase. This was immediately followed by size reduction using probe sonication for 2 min at 20 % amplitude (30 sec Pulse ON and 10 sec Pulse OFF cycle) [4,10].

After separation of free drug, the LLCs dispersion was further freeze-dried as described in **section 5.4.5.2.**

6.4.4. Preparation of PEGylated TMZ loaded LLCs by the optimized method

The optimized formulation was further PEGylated by replacing PEG 200 with DSPE-PEG 2000. Various percentage of DSPE-PEG 2000 (0.05 %, 0.1 %, 0.25 %, 0.5 % and 1 % of the total dispersion) were screened and the effect on size distribution and zeta potential was evaluated. The best formulation was selected based on the hemolysis study [5,23].

6.4.5. Characterization of TMZ loaded LLCs

6.4.5.1. Particle size, Polydispersity index (PDI), and Zeta potential

The dynamic light scattering technique was utilized to measure the size distribution, and surface charge of the prepared TMZ-loaded LLCs. The analysis were conducted as mentioned in **section 5.4.6.1** [24,25].

6.4.5.2. Entrapment efficiency (% EE) and Drug Loading (% DL)

The % EE and % DL of TMZ-loaded LLCs were evaluated as discussed in **section 5.4.6.2**. The amount of drug entrapped and drug loading in the TMZ-loaded LLCs was determined using an in-house developed validated HPLC method as described in chapter 3 [26].

6.4.5.3. Morphology

A thin film of TMZ-loaded LLCs dispersion was formed on a glass slide with the aid of vacuum drying. The thin film of LLCs formed was coated with gold (Gold sputter module, Quorum ES, UK) and observed under Field Emission Scanning Electron Microscopy (FESEM) (Apreo Switch XT microscope, USA). The morphology of TMZ loaded PEGylated LLCs was studied using High Resolution Transmission Electron Microscope (JEOL JEM 2100 PLUS). The dispersion was

loaded on a carbon coated copper grid and allowed to dry for 5 min. The TEM was operated at 200 kV accelerating voltage [27].

6.4.5.4. Confirmation of crystalline structure

The liquid crystalline structure was confirmed under the Polarized light microscope (Olympus: BX53M) with objective 20 x magnification. The LLCs dispersion was placed on the glass slide and covered with a cover slip. The samples were observed under a cross polarizer and without a cross polarizer [28]. X-ray diffractogram of TMZ, physical mixture, and PEGylated TMZ loaded LLCs were obtained using the X-ray diffractometer (Rigaku- miniflex) with Cu (λ=1.54) tube as an anode. The scanning speed was 1^o/min, and the voltage was set at 30 kV. The diffractogram was obtained with a scattering angle (2θ) ranging between 10-40^o [29].

6.4.5.5. Drug release and release kinetics

In-vitro drug release was studied with the dialysis bag technique. The drug stability and sink conditions were ensured during the entire study. Initially, the time taken for 100 % TMZ diffusion was evaluated by filling the TMZ solution (1 mg/mL) into the dialysis bag (molecular cutoff – 12-14 kDa, Himedia). After which, initially, the effect of drug loading on the release rate and the release kinetics was investigated. TMZ loaded LLCs formulation with different drug loading were prepared as discussed in **section 6.4.3**. These were filled in the dialysis bag individually. The dialysis bags were then placed in 30 mL of acetate buffer (pH 4.5, 100 mM) for all the studies. The exposed area of the dialysis bag to the release media was 25 cm^2. The media was kept under magnetic stirring (80 rpm) at 37 ± 0.5^{o}C. Samples (0.5 mL) were withdrawn at predetermined different time points and analyzed using the developed HPLC method to obtain the concentration of TMZ released. The release profile was plotted (time vs. % cumulative drug release), which was further studied for release kinetics using DDSolver software (Excel Add-In). The best fit release model was identified based on the high R^2 value, highest MSC (Model Selection Criteria) value, and lowest AIC (Akaike Information Criterion) value [30–32]. The corresponding $t_{25,}$ $t_{50,}$ and t_{75} values were also obtained [33]. The study was similarly performed for optimized TMZ loaded LLCs and TMZ loaded PEGylated LLCs to study the effect of PEGylation on drug release. Following the same methodology, drug release of TMZ and PEGylated LLCs was studied in phosphate buffer saline (pH 7.4) to evaluate the potential of PEGylated LLCs to protect the drug at plasma pH.

6.4.5.6. Reproducibility and scale-up studies

In order to check the industrial feasibility, reproducibility and scale-up studies were conducted. The optimized batch was repeated 6 times to confirm the reproducibility. The formulation was scaled up to 5 times (50 mL) the initial batch volume (10 mL). For the 10 mL batch, a probe with a 3 mm diameter was used, while for the 50 mL batch probe with a 13 mm diameter was utilized. The process parameters were optimized by keeping the composition constant. The formulations were characterized for particle size and PDI. It is expected that LLCs need to be diluted with suitable media for intravenous administration in the form of infusion. LLCs are self-assembled systems that are likely to dissemble on dilution and release the entrapped drug. The stability on dilution is a critical factor for intravenous delivery. The prepared LLCs formulation was diluted 50, 100, 500, and 1000 times. The change in particle size and PDI was studied thereafter [34,35].

6.4.5.7. Hemolysis study

Nanoparticles administered into the systemic circulation are likely to interact with the blood components. A hemolysis study was conducted to evaluate the hemolytic toxicity of the prepared LLCs. Fresh blood was collected from Wistar rats into Eppendorf tubes containing 10% w/v EDTA (ethylenediamine-tetraacetic acid). The tubes were centrifuged at 1000 rpm for 5 min at 4^{o}C to obtain the red blood cells (RBCs) pellet. The obtained RBCs pellet was washed with 0.9 % normal saline and again centrifuged at 1000 rpm for 5 min. The obtained pellet was resuspended in normal saline (1 mL to 5 mL). The study was conducted to evaluate hemolytic potential of TMZ, LLCs, PEGylated LLCs containing 0.05 %, 0.1 %, 0.25 %, 0.5 % and 1% DSPE-PEG 2000 of the total dispersion. Different dilutions (0, 2, 5, and 10 times) of all formulations were evaluated. 100 µL of each formulation was added to 100 µL of the RBCs suspension in the 1 mL Eppendorf tubes. For positive and negative controls, instead of formulation, 1 % Triton X and normal saline were added to the RBC suspension, respectively. The tubes were incubated at 37^{o}C for 30 mins. After which the volume was made up to 1 mL with normal saline and centrifuged at 1000 rpm for 5 min at 4^{o}C temperature to settle the intact RBCs. The absorbance of the supernatant was measured using the BioTek Epoch Microplate reader (Gen5^{TM} 1.11 software) at 540 nm. The % hemolysis caused was calculated using Equation 6.1 [5,23,36].

$$\%\ Hemolysis = \frac{Sample\ absorbance - Negative\ control\ absorbance}{Positive\ control\ absorbance - Negative\ control\ absorbance} * 100 \ldots\ldots\ldots\ldots (6.1)$$

6.4.5.8. In-vitro cytotoxicity study

The cytotoxicity of TMZ, blank LLCs, TMZ loaded LLCs and PEGylated LLCs was evaluated in U87 glioblastoma cells using the MTT assay as described in **section 5.4.6.5** [23,37].

6.4.5.9. Cell uptake study

The optimized formulations (LLCs and PEGylated LLCs) were prepared by loading Dil (a fluorescent lipophilic indocarbocyanine dye). The uptake of nanocarriers by U87 (glioblastoma cell lines) and RAW (macrophage cell lines) cells was analyzed using Confocal microscopy as per the procedure described in **section 5.4.6.6** [38,39].

6.4.5.10 Storage stability

The storage stability of optimized freeze dried TMZ loaded PEGylated LLCs was evaluated as mentioned in **section 5.4.6.7**.

6.5 Results and Discussion

6.5.1. Screening of various preparation methods

Formulating TMZ-loaded LLCs by various methods revealed that the preparation method significantly affected the particle size and entrapment efficiency. When TMZ was added to the lipid phase, the solvent was required for solubilization of TMZ as it was not soluble in the lipid. The addition of acetone solubilized the drug but provided a lower entrapment value (maximum 12 %). In the next method, acetone was replaced with water as a solvent. TMZ was dissolved in a fixed quantity of water and added to the lipid phase. This also favored the self-assembly of the lipid molecules in presence of water. Allowing this phase to cool down to room temperature favored the formation of the lyotropic mesophase and also the entrapment of the TMZ molecules within. After cooling, this phase was subjected to size reduction. Immediate exposure to size reduction provided lower TMZ entrapment which may be attributed to the insufficient time provided for mesophase formation. Providing sufficient cooling time significantly improved the entrapment efficiency of TMZ in LLCs (up to 30 %). The concentration of water (lipid to water ratio) plays an important role in forming the liquid crystal mesophase [10,40].

The most critical step during the preparation of LLCs was the size reduction technique used. It majorly affects the size, size distribution, and entrapment efficiency. The smallest size was achieved with the probe sonication technique while screening different size reduction techniques. Techniques that provided the smallest to largest particle size were Probe sonication < High-speed mechanical stirring < Homogenization < Magnetic stirring < Low-speed mechanical stirring (**Table 6.1**). No significant difference in entrapment efficiency was observed in all these methods. However, probe sonication provided maximum entrapment value along with the smallest particle size.

Table 6.1. Effect of various size-reduction techniques on particle size, PDI, and entrapment efficiency of TMZ loaded LLCs

	Magnetic Stirring	**High-speed mechanical stirring**	**Low-speed mechanical stirring**	**Homogenization (1000 rpm, 5 min)**	**Probe sonication (5 min)**
Particle Size (Z-average in nm)	171.40 ± 5.23	157.40 ± 4.12	186.60 ± 6.41	169.20 ± 3.21	95.64 ± 5.47
PDI	0.253 ± 0.056	0.259 ± 0.089	0.261 ± 0.124	0.239 ± 0.981	0.165 ± 0.025
% EE	23.19 ± 2.12	22.09 ± 3.45	21.86 ± 1.23	25.33 ± 0.98	25.38 ± 0.54

6.5.2. Optimization of TMZ loaded LLCs using the QbD approach

6.5.2.1. Identifying QTPP and CQAs

The QTPP for TMZ-loaded LLCs was identified as defined in **Table 5.1 and section 5.5.2**. The only difference was the dosage design which would be Lyotropic Liquid crystals in this case. The justification would be LLCs possess a unique structure, small size, can entrap amphiphilic drugs efficiently, and provide controlled release. LLCs can entrap TMZ, protect the drug from degradation and release it in a slow controlled manner thus help improve *in-vivo* circulation time and brain bioavailability. The derived CQAs would be same as defined in **Table 5.2** [12,41].

6.5.2.2. Quality risk management

A process flow chart was prepared using process mapping (**Figure 6.1**). Various material attributes and process parameters identified were represented in the Ishikawa Fish Bone diagram (**Figure 6.2**) [17,42].

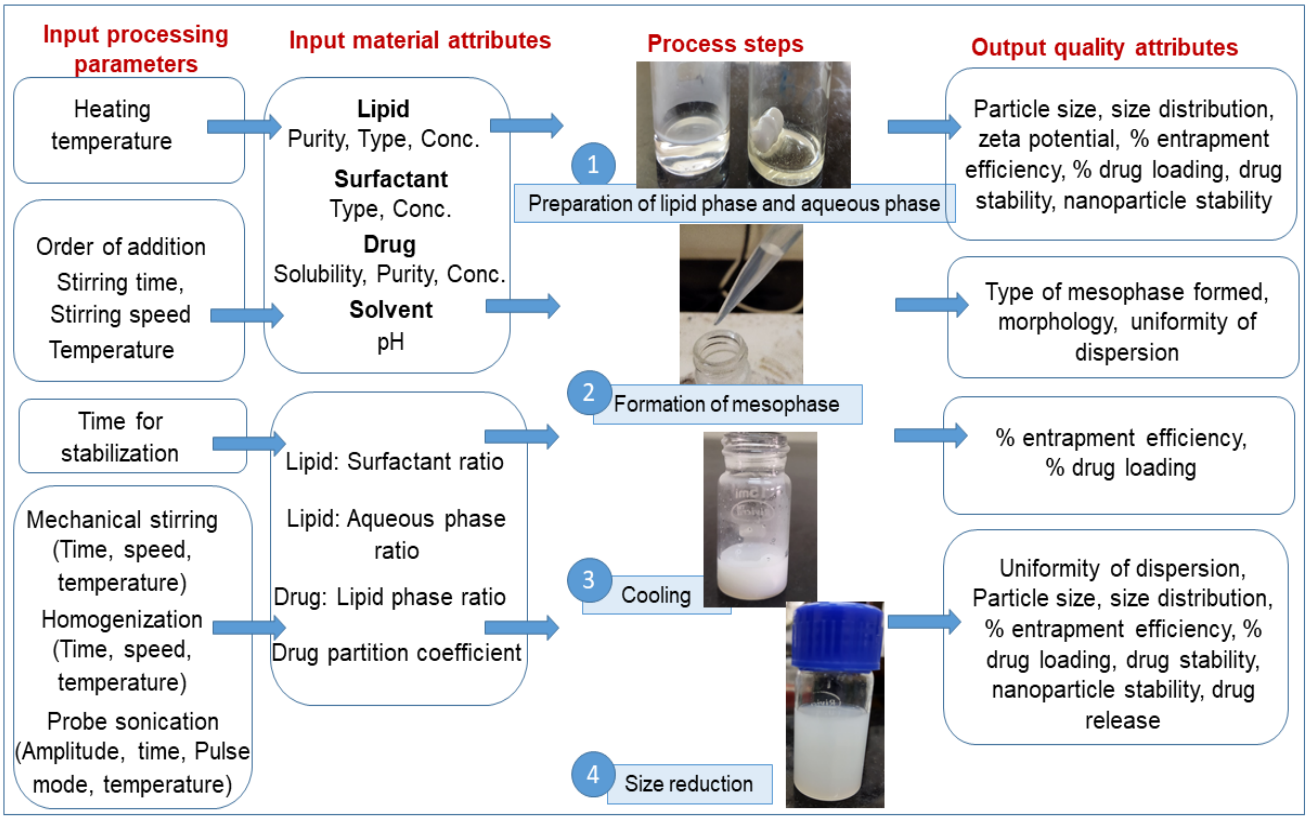

Figure 6.1. A process flow map for preparation of TMZ loaded LLCs

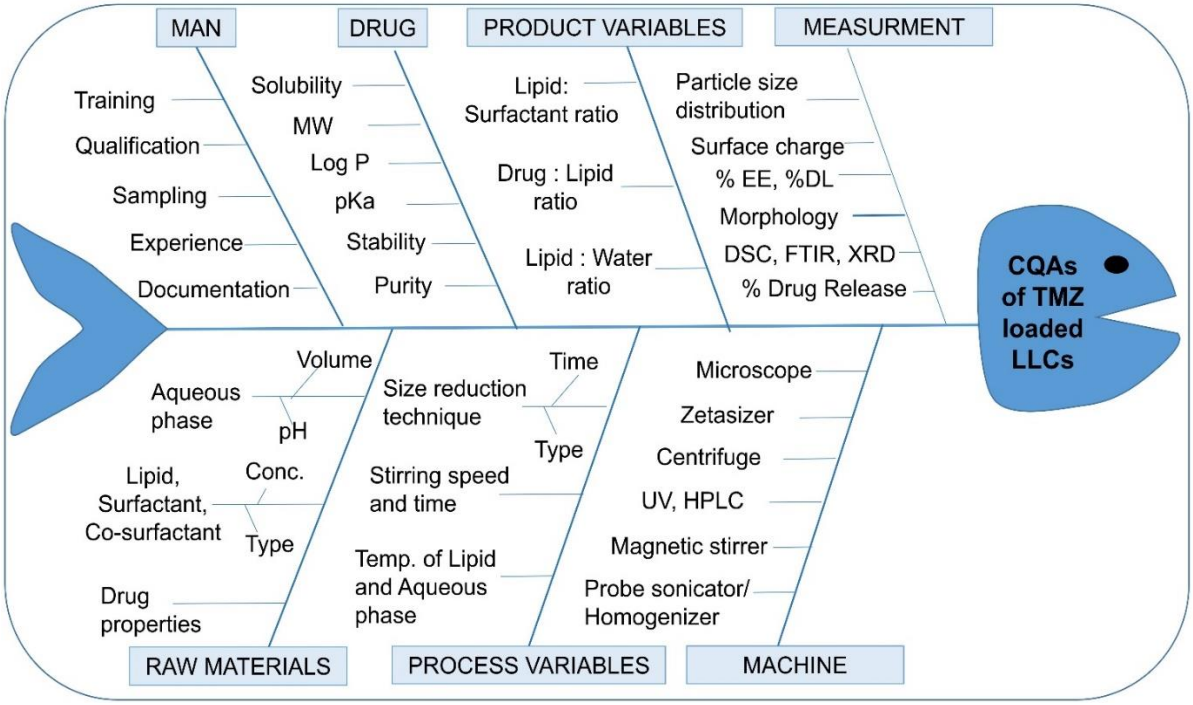

Figure 6.2. Cause-effect analysis of TMZ loaded LLCs using the Fishbone diagram

6.5.2.3. Identifying Critical Material Attributes (CMAs) and Critical Process Parameters (CPPs)

The material attributes and process parameters were linked to the CQAs, and the severity of risk evaluated using the RRMA are represented in **Table 6.2-6.3**. Critical and non-critical factors were distinguished based on the RPN score. The type and concentration of the lipid play a crucial role in forming the liquid crystal phase. The lipid may show concentration-dependent toxicity, which relates to the safety aspects. Surfactant concentration plays an essential role in stabilizing the liquid crystal phase. The CMAs related to excipients are represented in **Table 6.4.** The critical process parameters are represented in **Table 6.5** [34,43].

Table 6.2. Linking material attributes (MAs) related to excipients to Critical Quality Attributes (CQAs) of LLCs using relative risk-based matrix analysis

MAs / **CQAs**	Type of lipid	Hydro-phobicity of lipid	Melting point of lipid	Conc. of lipid	Conc. of surfactant/ stabilizer	pH of aqueous phase
Assay						
pH of product						
Particle size distribution						
Zeta potential						
Entrapment and loading efficiency						
Drug release						
Stability						

Green: Low risk, Yellow: Medium risk, Red: High risk

Table 6.3. Linking of process parameters (PPs) to Critical Quality Attributes (CQAs) of LLCs using relative risk-based matrix analysis

PPs / **CQAs**	Temp. during stirring	Stirring Time	RPM of stirring	Size reduction technique	Parameters during size reduction (Temp., Time, Amplitude/Speed)
Assay					
pH of product					
Particle size distribution					
Zeta potential					
Entrapment and loading efficiency					
Drug release					
Stability					

Green: Low risk, Yellow: Medium risk, Red: High risk

Table 6.4. Failure mode effect analysis of the material attributes of the excipients used in the preparation of TMZ loaded LLCs

Excipient	**Material attribute**	**Failure mode**	**Effect on CQAs**	**P**	**S**	**D**	**RPN**
Lipid	Type	Unsuitable for forming LLCs	Affect the formation of LLC- Surface charge-Safety and Efficacy	3	5	2	**30**
	Hydrophobicity	Low	Affect formation of LLC, and entrapment efficiency- Efficacy	2	4	2	16
	Melting point	Above 70^{o}C	Affect formation of LLC- Efficacy	2	3	1	6
	Concentration	High	Affect particle size, entrapment efficiency, drug release- Safety and Efficacy	3	5	2	**30**
Surfactant/ Co-surfactant/ Stabilizer	Type	Unsuitable for forming LLCs	Affect formation of LLC- Surface charge-Safety and Efficacy	3	4	2	24
	Concentration	High	Affect particle size, entrapment efficiency, drug release, stability- Safety and Efficacy	4	4	2	**32**
Aqueous phase	pH	> 5	Affect drug stability, and assay - Efficacy	3	5	2	**30**
	Volume	Low	Affect formation of LLC, entrapment efficiency, and drug release- Efficacy	3	4	1	12

Table 6.5. Failure mode effect analysis of process parameters involved in the preparation of TMZ loaded LLCs

Process	Process parameters	Failure mode	Effect on CQAs	P	S	D	RPN
Magnetic stirring	Temperature	High	Affect phase formation-Drug degradation - Efficacy	2	4	2	16
	Time	High	Affect particle size distribution-Efficacy	3	2	1	6
	RPM	High	Affect particle size distribution-Efficacy	3	4	2	24
Size reduction technique	Type	Inadequate	Affect particle size distribution-Efficacy	4	4	1	16
	Temperature	High	Affect phase formation-Drug degradation - Efficacy	2	4	1	8
	Time	High	Affect particle size distribution-Efficacy	4	4	2	**32**
	Amplitude/ Pressure/ Speed	High	Affect particle size distribution-Efficacy	4	4	2	**32**

6.5.2.4. Experimental design and data analysis

Effect of various process variables

Our previous experience and risk assessment revealed that mostly 3 formulation variables affect the particle size and entrapment efficiency, thus need to be optimized during the preparation of LLCs. As the method was modified to enhance TMZ entrapment efficiency in LLCs, we decided to identify the critical process parameters using screening studies. Based on the process flow mapping, risk assessment and preliminary trials, 7 process parameters were identified and the low and high levels were set as represented in **Table 6.6**. These when entered into the selected design in the software, 19 runs were obtained as summarized in **Table 6.7**.

Table 6.6. Selected process variables and their levels for screening

Factor	Name	Units	Low level (-1)	High level (+1)
A	Heating Temperature	^{o}C	50	70
B	Initial Volume of water	mL	1	4
C	Stirring speed	rpm	200	600
D	Stirring time	min	2	10
E	Temperature during size reduction	^{o}C	4	70
F	Amplitude during probe sonication	%	20	25
G	Probe sonication time	min	1	4

Table 6.7. Trials of the Factorial design (Minimum resolution IV) and the response variables

Batch	Factor A (^{o}C)	Factor B (mL)	Factor C (rpm)	Factor D (min)	Factor E (^{o}C)	Factor F (%)	Factor G (min)	Response 1 Particle size (nm)	Response 2 PDI
1	50	1	600	10	4	25	1	145.400±0.99	0.2605±0.002
2	50	1	200	10	70	25	4	96.310±0.20	0.1775±0.002
3	50	4	600	10	70	20	1	84.385±0.22	0.113±0.013
4	50	1	600	2	70	20	4	110.900±0.57	0.251±0.001
5	50	4	600	2	4	25	4	107.100±0.14	0.2205±0.013
6	50	1	200	2	4	20	1	138.350±6.72	0.2525±0.010
7	50	4	200	2	70	25	1	87.285±0.47	0.1325±0.014
8	50	4	200	10	4	20	4	171.550±3.75	0.31±0.005
9 (CP)	60	2.5	400	6	37	22.50	2.5	96.065±3.01	0.1555±0.033
10 (CP)	60	2.5	400	6	37	22.50	2.5	104.450±1.77	0.182±0.009
11 (CP)	60	2.5	400	6	37	22.50	2.5	101.250±1.77	0.167±0.031
12	70	1	200	10	70	20	1	91.755±0.16	0.145±0.017
13	70	1	200	2	4	25	4	114.4±2.68	0.224±0.002
14	70	4	600	10	70	25	4	138.1±1.27	0.2615±0.004
15	70	1	600	10	4	20	4	156.25±0.77	0.251±0.021
16	70	4	200	2	70	20	4	88.115±1.71	0.127±0.014
17	70	1	600	2	70	25	1	149.9±4.38	0.269±0.012
18	70	4	600	2	4	20	1	100.305±1.26	0.244±0.033
19	70	4	200	10	4	25	1	106.65±0.21	0.2365±0.010

**CP: Center point*

The obtained data was further analyzed statistically. The critical and non-critical process parameters were identified using the Half-normal and Pareto charts. In Half-normal plots of

particle size and PDI (**Figure 6.3 and 6.4**), the terms which are away from the line (from the right side) were selected one by one until a Shapiro-Wilk value of more than 0.1 and the highest p-value was obtained. This indicates that all the significant terms have been selected and the remaining terms are almost normally distributed (not having any significant effect on particle size). Further, the Pareto chart confirmed the significant factors. In the Pareto chart of particle size and PDI (**Figure 6.3 and 6.4**), orange and blue bars represent the factors having a positive and negative effect on the particle size respectively. The factors crossing the t-value limit line are considered to have a significant effect on the response.

The effects were further studied using the one factor and interaction graphs. **Figure 6.5 (a)** indicated that there was no significant effect of heating temperature within a small range on particle size. Stirring speed affected the particle size to some extent, however, was not much significant **(Figure 6.5 b)**. The temperature during size reduction was found to show a significant effect on particle size (**Figure 6.5 c**). Higher particle sizes were obtained when size reduction was done in cold condition, which might be attributed to the solidification of lipid in cold temperature. Thus, for further studies, room temperature was selected to be kept during size reduction. An interaction effect of heating temperature (factor A) and stirring speed (factor C) was observed at low levels of factor A and low and high levels of factor C indicated by the intersection of the two lines (**Figure 6.5 d**). The black line represented the effect of a low level of factor C at a low and high level of factor A. The red line indicated the effect of a high level of factor C at a low and high level of factor A. This also indicated that lower particle sizes can be achieved by keeping high heating temperature with low stirring speed and also by keeping high stirring speed with low heating temperature. This effect can be seen as heating temperature affects the melting of lipid and stirring speed affect the globule size formed during initial mesophase formation/emulsification process. An interaction effect between initial heating temperature (factor A) and temperature during size reduction (factor E) was observed at high level of factor A and low and high level of factor E indicated by the intersection of two lines (**Figure 6.5 e**). Lower PDI values were obtained with high temperature during size reduction as represented by **Figure 6.5 (f)**. Based on the information obtained, medium levels for all the process parameters were selected for further optimization of formulation variables. No process parameter was taken for optimization design [34,44].

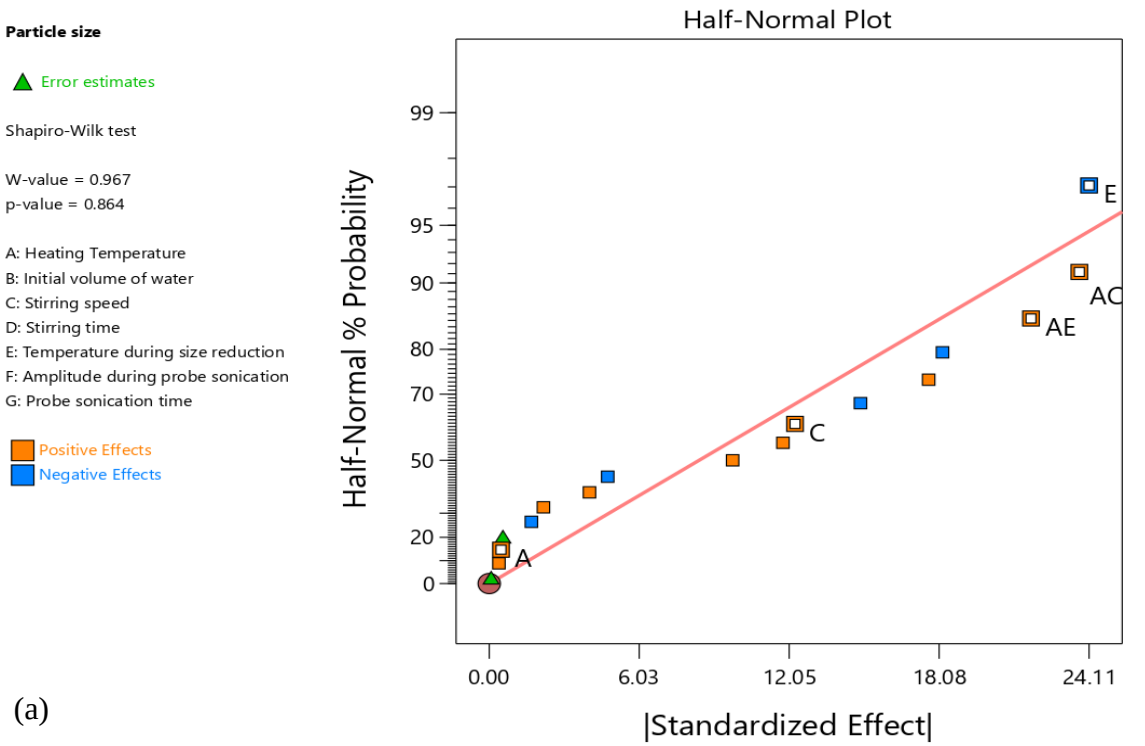

(a)

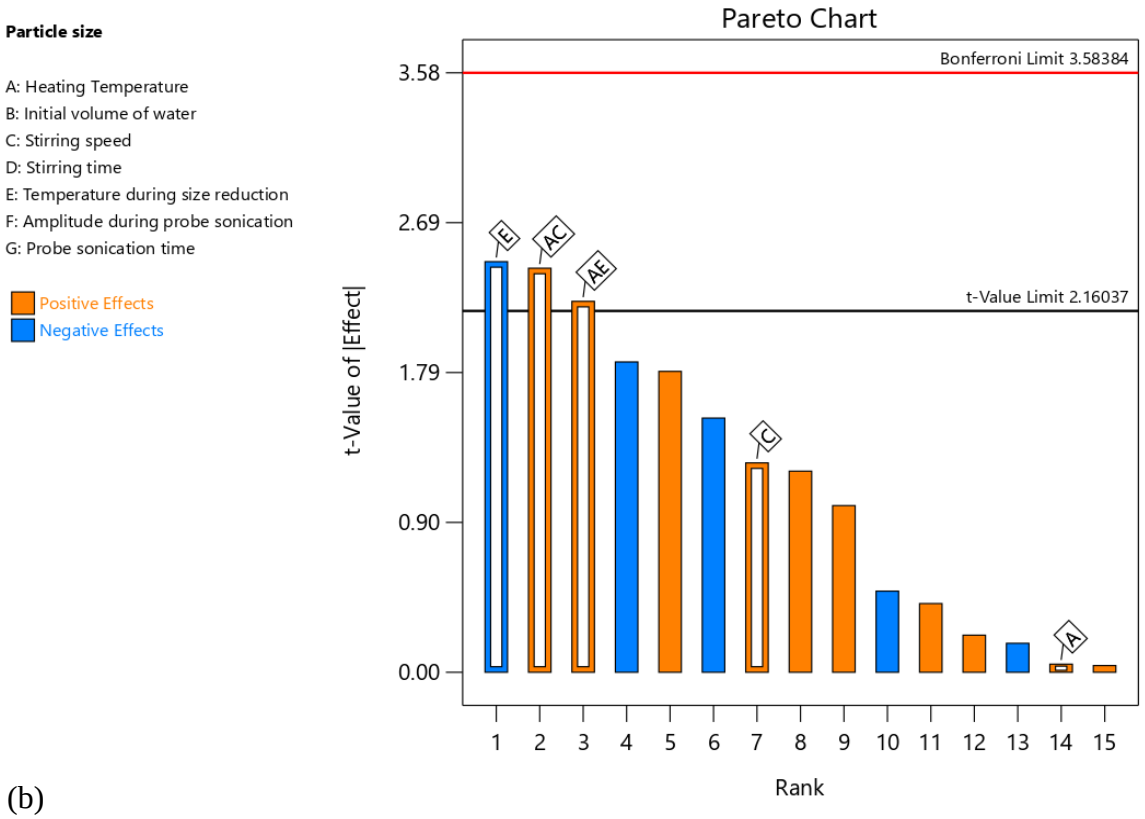

(b)

Figure 6.3. (a) Half-normal and (b) Pareto charts for particle size

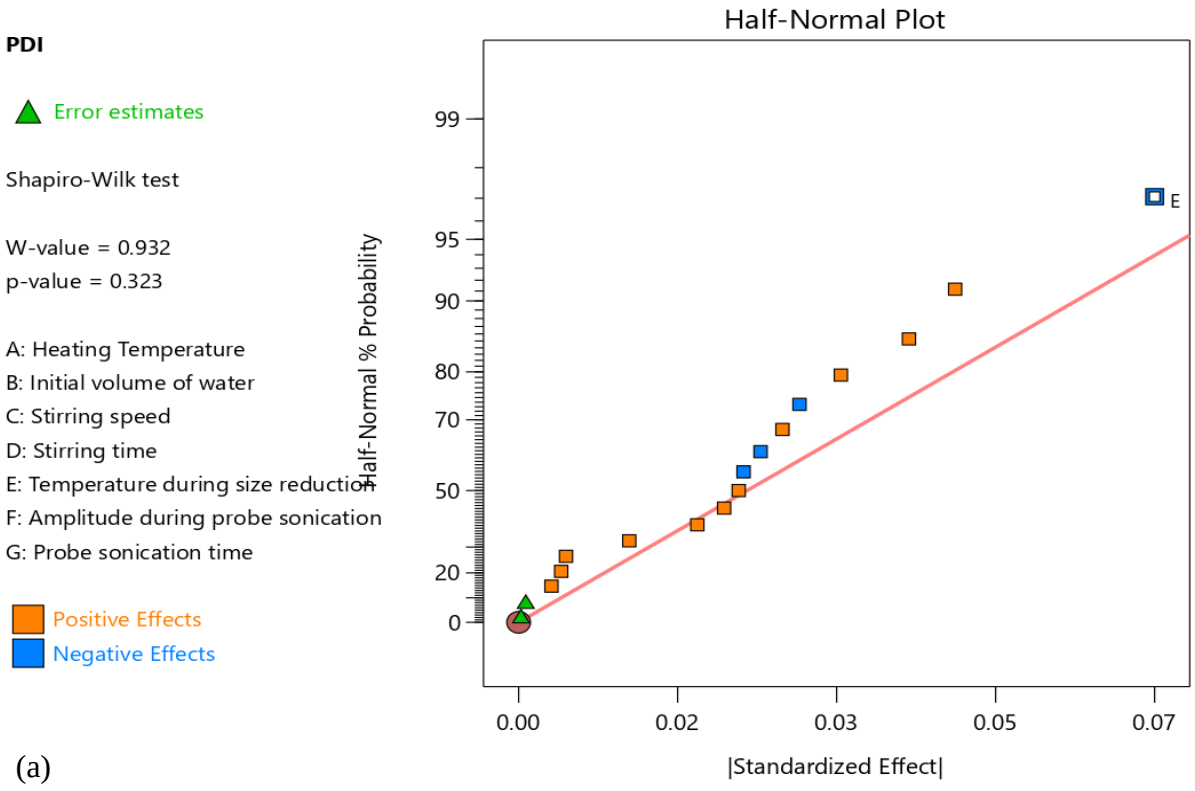

(a)

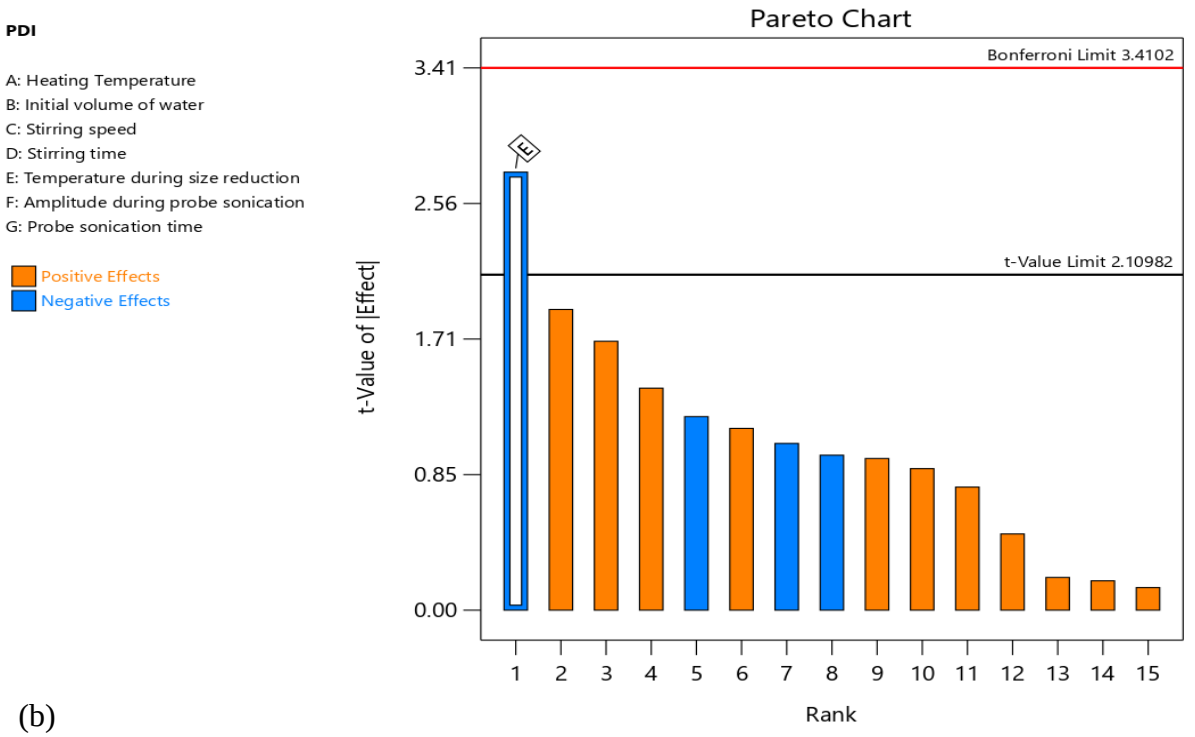

(b)

Figure 6.4. (a) Half-normal and (b) Pareto charts for PDI

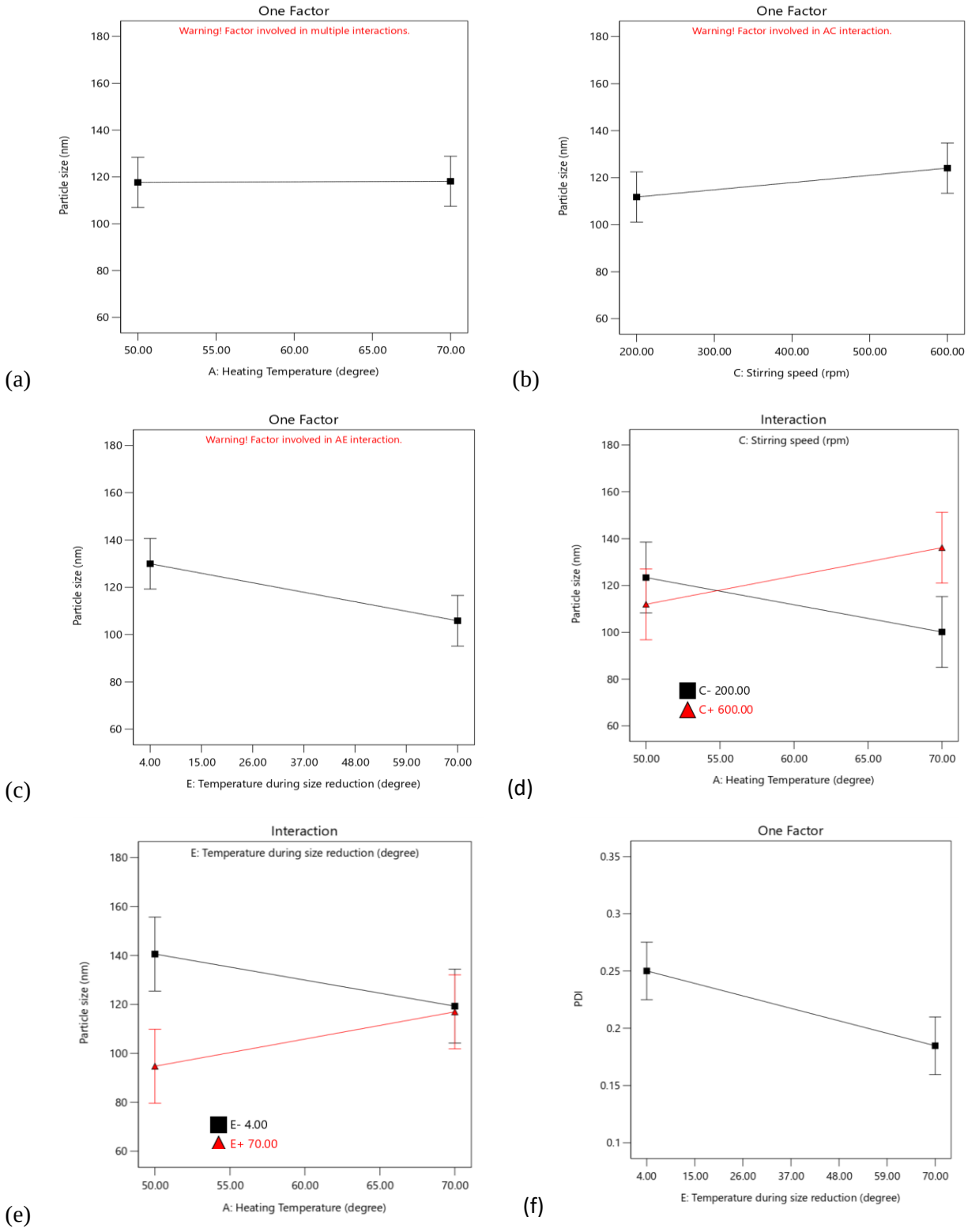

Figure 6.5. Interaction and one factor plots for particle size and PDI

Effect of various formulation variables

Based on the preliminary trials, the variables selected were the amount of GMO (X1), amount of surfactant (X2), and amount of PEG 200 (X3) (**Table 6.8**). The dependent or response variables selected were mean particle size (Y1), PDI (Y2), zeta potential (Y3), % EE (Y4), and % DL (Y5). The variables were entered into the Box-Behnken design for the obtained 15 trials, including the 3 center points (CP) (**Table 6.9**). After statistical analysis, the obtained results were summarized in **Table 6.10**. The obtained respective models for particle size, PDI, zeta potential, % EE, and % DL after excluding the non-significant terms were found to be significant. The Lack of fit for the models was not significant. For all the models, the difference between the Predicted R^2 and Adjusted R^2 was less than 0.2 and the Adequate precision values were more than 4. Thus confirming the significance of the model. All the diagnostic plots (Normal plot of residuals, Residuals vs Predicted, Predicted vs Actual, Cook's distance plot) revealed that there were no outliers in the data. Box-Cox plot revealed that no transformation of the data was required to fit a suitable model. Further, the one factor, perturbation, interaction, and 3-D surface plots were studied [21,41].

Table 6.8. Selected dependent (formulation) variables and the response variables for Box Behnken design

Factors	**Units**	**Low (-1)**	**Medium (0)**	**High (+1)**
GMO concentration (X1)	mg	200	500	800
PF 127 concentration (X2)	mg	50	100	150
PEG 200 concentration (X3)	mL	0.5	1.25	2
Responses and target goals				
Particle size (Y1)	Within range (80-120 nm)			
Polydispersity index (Y2)	Minimum			
Zeta potential (Y3)	Optimum			
% Entrapment efficiency (Y4)	Maximum			
% Drug loading (Y5)	Optimum			

Table 6.9. Trials of Box-Behnken design along with the obtained responses

	X1	X2	X3	Y1	Y2	Y3	Y4	Y5
Batch	**A:GMO (mg)**	**B:PF 127 (mg)**	**C:PEG 200 (mL)**	**Particle size (nm)**	**PDI**	**Zeta potential (mV)**	**% Entrapment efficiency**	**% Drug loading**
1	200	150	1.25	53.157 ± 1.08	0.218 ± 0.02	-14.867 ± 0.96	28.88 ± 0.38	0.753 ± 0.01
2	200	100	0.5	82.103 ± 1.12	0.196 ± 0.00	-13.034 ± 0.32	17.008 ± 0.36	0.594 ± 0.00
3	200	50	1.25	103.667 ± 1.19	0.127 ± 0.02	-9 ± 0.31	19.758 ± 0.63	0.77 ± 0.01
4	200	100	2	88.15 ± 1.72	0.23 ± 0.00	-8.87 ± 0.22	23.425 ± 0.48	0.79 ± 0.00
5 (CP)	500	100	1.25	162.134 ± 2.78	0.161 ± 0.01	-22 ± 0.1	26.87 ± 0.35	0.45 ± 0.00
6	500	150	2	116.67 ± 1.53	0.197 ± 0.00	-19.67 ± 0.28	33.67 ± 1.20	0.483 ± 0.00
7	500	150	0.5	117.8 ± 3.03	0.202 ± 0.00	-12.067 ± 0.15	34.21 ± 0.85	0.49 ± 0.03
8	500	50	0.5	171.467 ± 1.30	0.123 ± 0.02	-18.5 ± 1.13	33.45 ± 1.30	0.54 ± 0.05
9 (CP)	500	100	1.25	156.33 ± 1.76	0.14 ± 0.01	-19.9 ± 0.10	32.12 ± 2.01	0.5 ± 0.06
10 (CP)	500	100	1.25	150.466 ± 0.65	0.149 ± 0.00	-17.634 ± 0.41	28.23 ± 0.12	0.48 ± 0.08
11	500	50	2	164.934 ± 2.81	0.132 ± 0.02	-14.2 ± 1.05	31.673 ± 0.61	0.524 ± 0.01
12	800	100	0.5	182.267 ± 1.59	0.196 ± 0.00	-30.76 ± 0.77	32.19 ± 0.94	0.386 ± 0.02
13	800	100	2	180.033 ± 1.52	0.165 ± 0.01	-19.734 ± 0.32	25.72 ± 2.06	0.303 ± 0.02
14	800	150	1.25	138.434 ± 0.67	0.166 ± 0.02	-23.9 ± 0.88	29.56 ± 8.13	0.296 ± 0.02
15	800	50	1.25	186.5 ± 8.60	0.055 ± 0.05	-25.1 ± 1.12	32.53 ± 0.07	0.388 ± 0.00

Table 6.10. Summary of statistical parameters obtained for the responses

Response	**Significant model terms**	**F value**	**p-value Prob > F**	
Y1 (Particle size)	Model	317.66	< 0.0001	Adj R-Squared: 0.9891 Pred R-Squared: 0.9828 Adeq Precision: 56.279 PRESS: 408.99
	A	871.31	< 0.0001	
	B	270.05	< 0.0001	
	A^2	102.77	< 0.0001	
	B^2	34.31	0.0002	
Y2 (PDI)	Model	16.29	0.0003	Adj R-Squared: 0.8452 Pred R-Squared: 0.7011 Adeq Precision: 13.032 PRESS: 8.554E-003
	A	14.11	0.0045	
	B	47.28	<0.0001	
	C	0.019	0.8924	
	B^2	5.59	0.0423	
	C^2	13.11	0.0056	

Y3 (Zeta potential)	Model	29.04	0.0001	Adj R-Squared: 0.6670 Pred R-Squared: 0.5797 Adeq Precision: 10.436 PRESS: 219.53
	A	29.04	0.0001	
Y4 (% Entrapment efficiency)	Model	17.74	0.0006	Adj R-Squared: 0.8933 Pred R-Squared: 0.8205 Adeq Precision: 13.523 PRESS: 68.67
	A	41.00	0.0004	
	B	3.40	0.1077	
	C	0.24	0.6387	
	AB	12.53	0.0095	
	AC	14.24	0.0070	
	A^2	32.73	0.0007	
	B^2	16.46	0.0048	
Y5 (% Drug loading)	Model	47.15	<0.0001	Adj R-Squared: 0.8683 Pred R-Squared: 0.8201 Adeq Precision: 17.211 PRESS: 0.061
	A	92.73	<0.0001	
	B	1.58	0.2332	

The particle size of TMZ-loaded LLCs was obtained between 53.157 to 186.500 nm. PDI was found to be 0.055 to 0.230. The polynomial equations obtained are represented as equations 6.2 and 6.3, respectively.

$$\text{Particle size (Y1)} = +156.04 + 45.02\ A - 25.06\ B - 22.69\ A^2 - 13.11\ B^2 \quad \text{.....(6.2)}$$

$$\text{PDI (Y2)} = +0.16 - 0.024\ A + 0.043\ B + 0.00087\ C - 0.022\ B^2 + 0.033\ C^2 \quad \text{.....(6.3)}$$

In these equations, terms A, B, and C represent the factors X1, X2, and X3 respectively, '+' sign indicates a positive effect of the respective factor on the response variable while the '-' sign indicates the negative effect. The constant values before each term represent the quantitative effect on the response. Particle size was found to increase on increasing the lipid concentration, also denoted by the '+' sign of term A. Surfactant molecules occupy between the lipid molecules at the lipid water interface thus stabilizing the structure. When lipid concentration increases with a fixed amount of surfactant, fewer surfactant molecules are available per lipid molecule, increasing particle size. The surfactant molecules are not uniformly distributed among the lipid molecules, thus affecting the particle size and size distribution. The increasing number of surfactant molecules reduce the interfacial tension resulting in smaller-sized particles as also indicated by the '-' sign of term B, and C. Particle size was found to be directly proportional to lipid concentration while inversely proportional to surfactant concentration as depicted by the perturbation plot and 3-D

surface plot represented in **Figure 6.6 (a) and Figure 6.7 (a**) respectively. The PEG 200 concentration was found to affect the PDI of the prepared formulations along with the PF127 concentration as represented in the perturbation (**Figure 6.6 b)** and 3-D surface plots (**Figure 6.7 b**) [45,46].

The designed formulations expressed zeta potential in the range of -30.760 to – 8.870 mV. The polynomial equation obtained for zeta potential is represented as equation 6.4.

$$\text{Zeta potential} = -17.95 - 6.72\ A \quad \text{.....(6.4)}$$

The results reflected that zeta potential was majorly dependent on the lipid concentration. GMO itself has a neutral surface charge. Commercial GMO contains free oleic acid that may contribute to the negative zeta potential. Also, the acidic pH of the medium may contribute to the zeta potential as the formulations were prepared in acetate buffer (pH 4.5). The perturbation and 3-D surface plots obtained are represented in **Figure 6.6 (c) and Figure 6.7 (c),** respectively [23,41].

The entrapment efficiency and drug loading of the prepared TMZ loaded LLCs were obtained between 17.008 to 34.210 % and 0.296 to 0.790 %, respectively. The polynomial equations obtained for the same are represented as equations 6.5 and 6.6, respectively.

$$\%\ \text{Entrapment efficiency} = +29.41 + 3.87\ A + 1.11\ B - 0.30\ C - 3.02\ AB - 3.22\ AC - 5.07\ A^2 + 3.60\ B^2 \quad \text{.....(6.5)}$$

$$\%\ \text{Drug Loading} = +0.52 - 0.19\ A - 0.025\ B \quad \text{.....(6.6)}$$

In the above equations, the terms AB and AC represent the presence of the interaction effects between the respective factors. Entrapment efficiency was found to increase on increasing lipid concentration to a specific value, further increasing the lipid concentration demonstrated lower entrapment values (**Figure 6.6 d and Figure 6.7 d**). Interaction between lipid and surfactant concentration was observed as the ratio of both has a significant effect on the particle size, ultimately affecting the entrapment efficiency. Drug loading was majorly dependent on the lipid concentration. As the lipid concentration increases for a fixed amount of drug concentration, more amount of lipid is present for a small amount of drug, thus reducing the % drug loading value (**Figure 6.6 e and Figure 6.7 e**)[34,41].

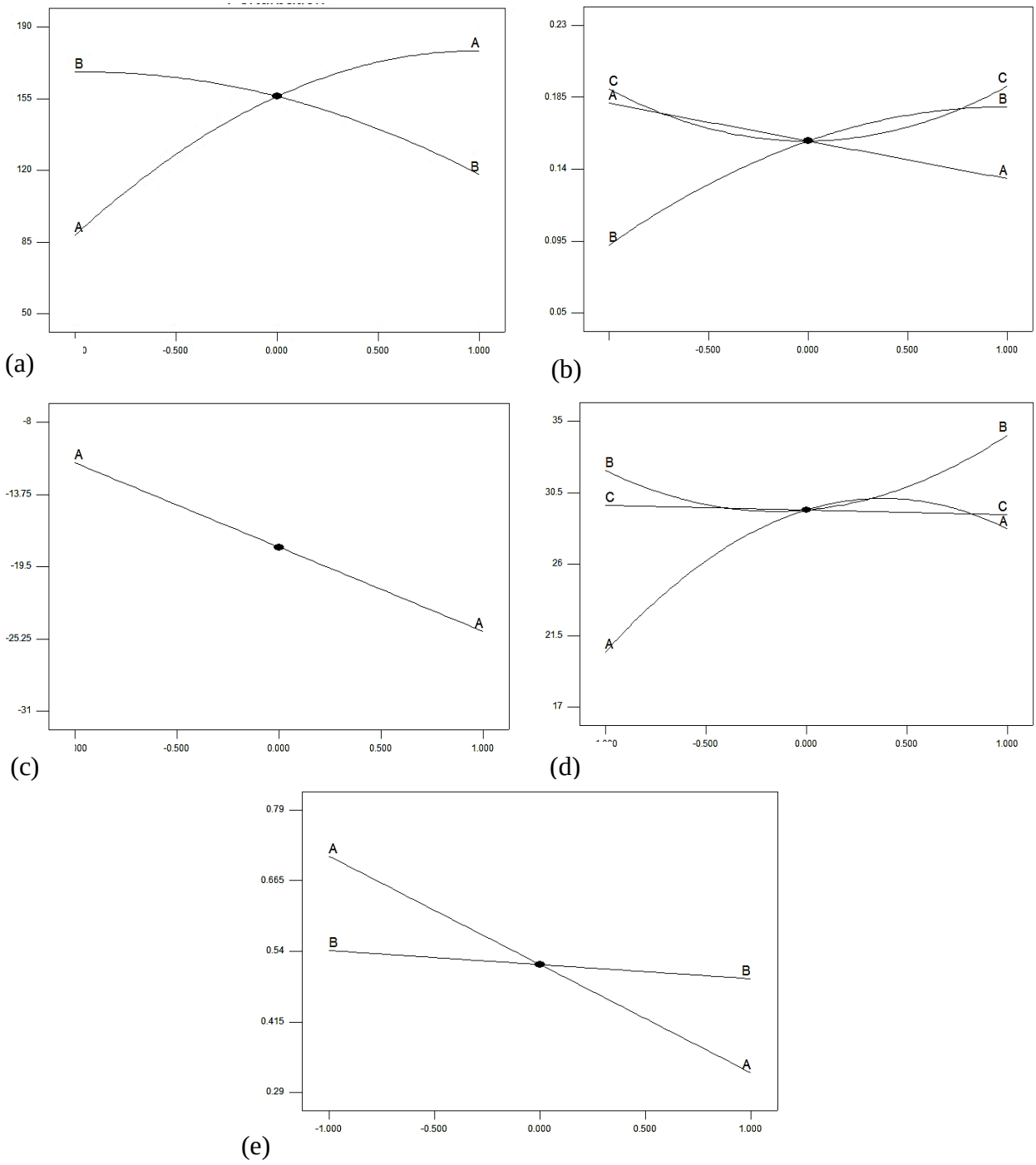

Figure 6.6. Perturbation plots (Interaction plots) (a) Particle size (b) PDI (c) Zeta potential (d) % EE (e) %DL. Y axis represents deviation from reference points.

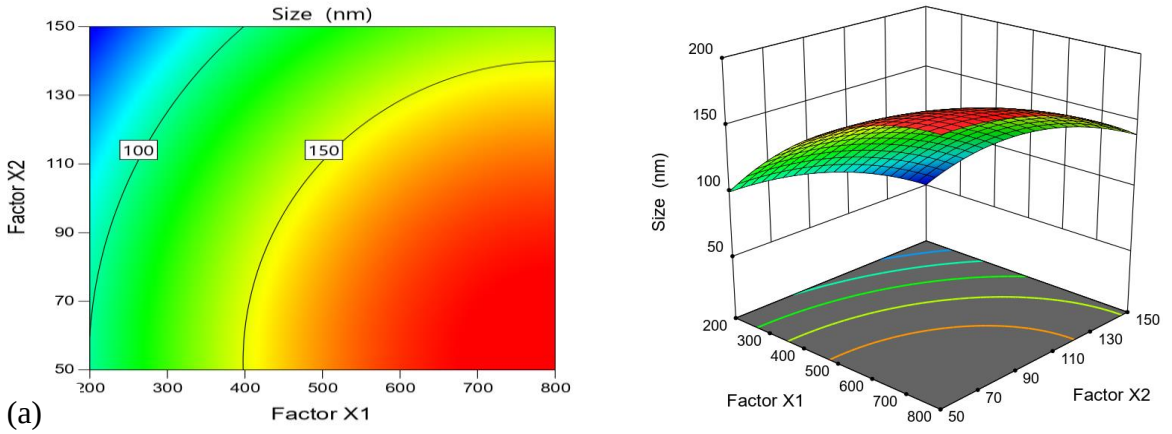
Size (nm)
Factor X2
Factor X1
100
150
Size (nm)
Factor X1
Factor X2

(a)

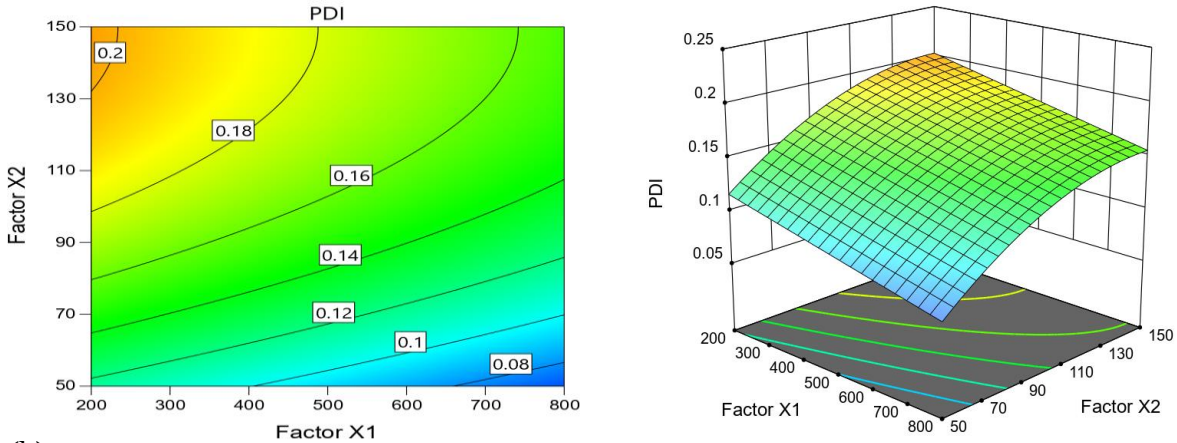
PDI
Factor X2
Factor X1
0.2
0.18
0.16
0.14
0.12
0.1
0.08
PDI
Factor X1
Factor X2

(b)

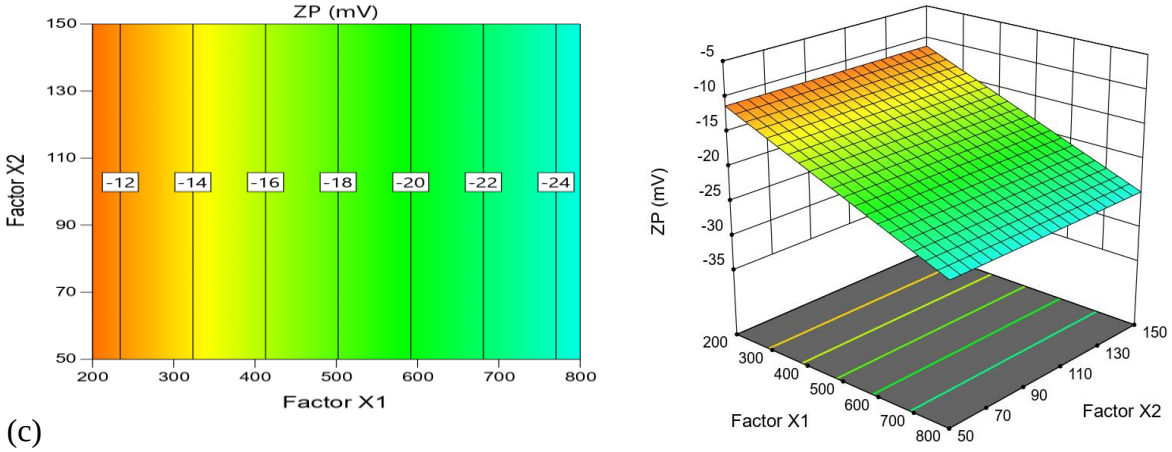
ZP (mV)
Factor X2
Factor X1
-12
-14
-16
-18
-20
-22
-24
ZP (mV)
Factor X1
Factor X2

(c)

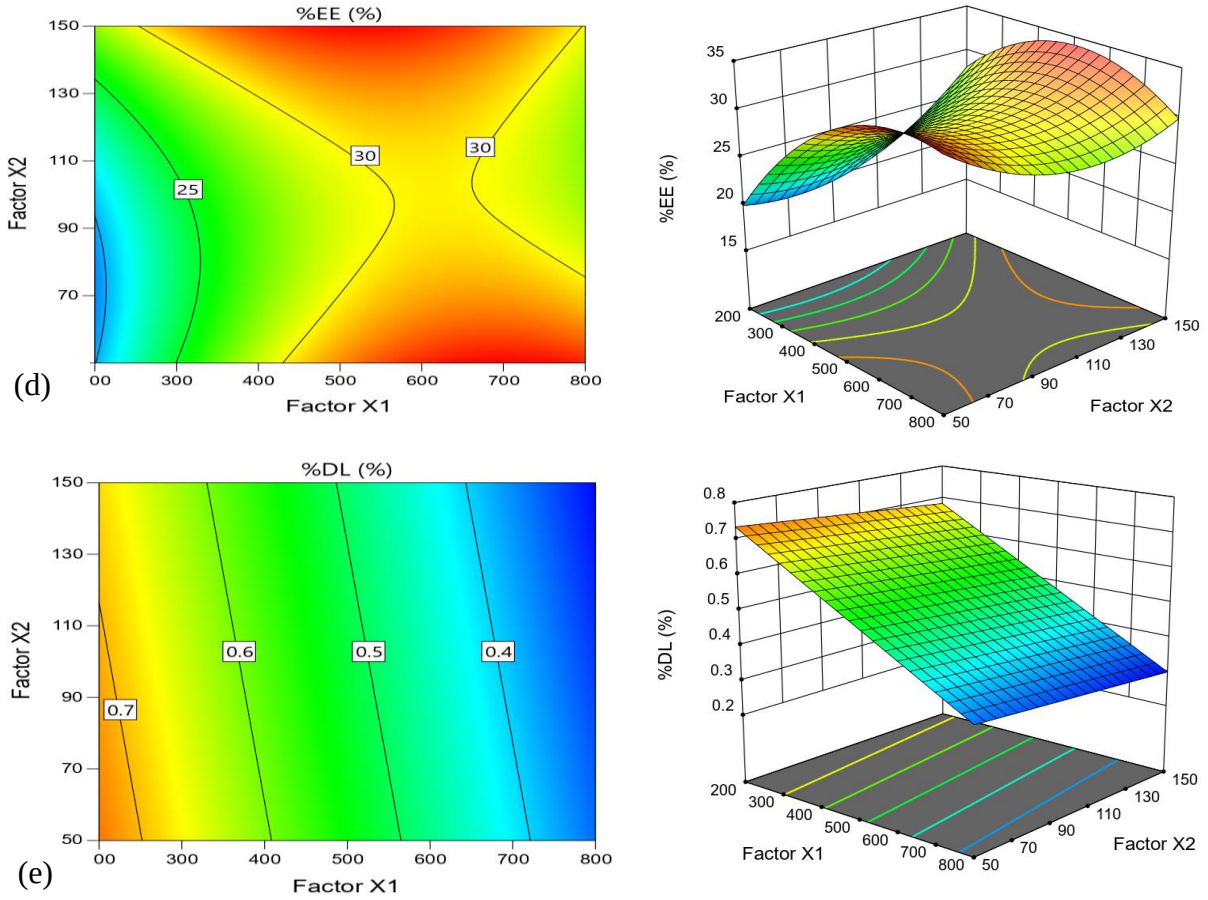

Figure 6.7. Contour and 3D Surface plots (a) Particle size; (b) PDI; (c) Zeta potential; (d) % Entrapment efficiency; (e) % Drug Loading (Factor X1: GMO concentration; Factor X2: PF 127 concentration; All graphs represented at medium level of Factor X3: PEG 200 concentration)

6.5.2.5. Validation of the design and establishment of design space

The composition of the validation batches, predicted, and observed values of the responses were represented in **Table 6.11**. The observed responses were found to be close to the predicted responses thus validating the model equations. The batch with GMO-300 mg, PF 127-150 mg, and PEG 200- 1 mL was selected as the optimized batch for further studies as the highest entrapment and smallest particle size were achieved with the lowest lipid concentration. The design space was successfully established. The overlay plot is represented in **Figure 6.8** [47]

Table 6.11. The composition of the validation batches, predicted, and the observed values.

GMO	270 mg		300 mg		320 mg	
PF 127	120 mg		150 mg		65 mg	
PEG 200	1.98 mL		1 mL		0.56 mL	
	Predicted	Observed	Predicted	Observed	Predicted	Observed
Size (nm)	96.52	119.20 ± 3.25	90	97.7 ± 0.481	132	149 ± 0.77
PDI	0.15	0.18 ± 0.00	0.19	0.18 ± 0.00	0.16	0.14 ± 0.02
% EE	27.46	21.78 ± 1.25	30.37	36.46 ± 1.48	23.47	22.41 ± 0.15

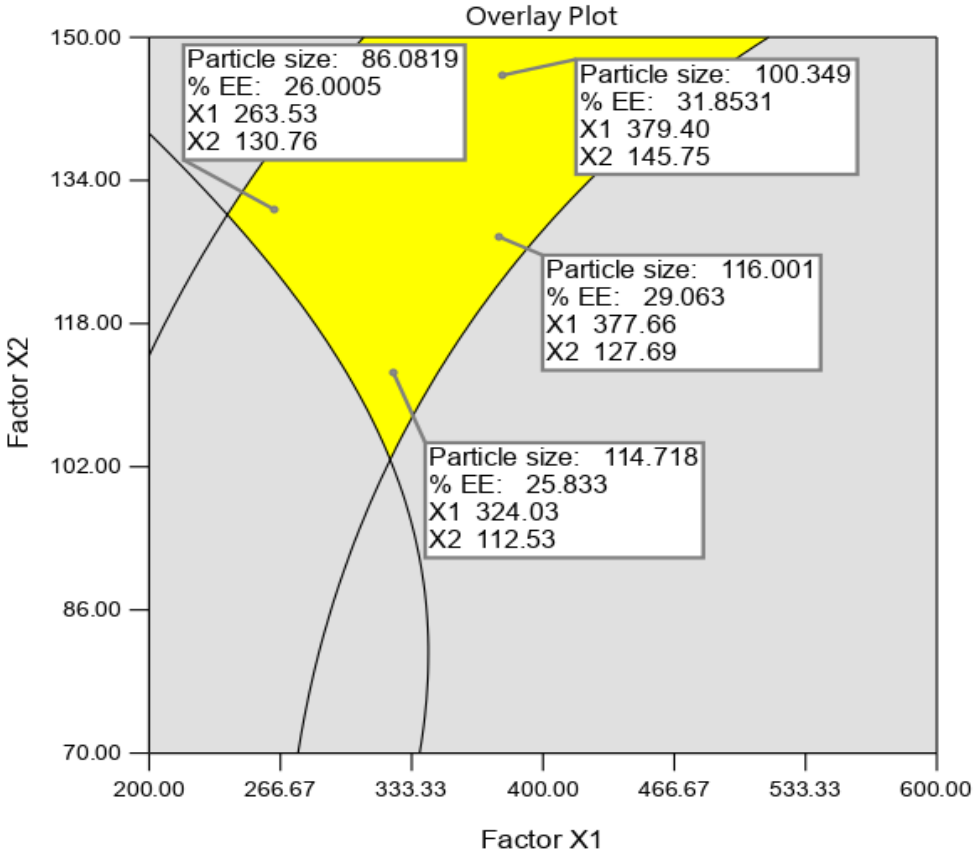

Figure 6.8. Overlay plot representing design space to achieve target responses at medium level of X3 (PEG 200 concentration); Factor X1: GMO concentration; Factor X2: PF 127 concentration; % EE: % Entrapment efficiency

6.5.3. Preparation of TMZ loaded LLCs by the optimized method

TMZ-loaded LLCs were successfully prepared following the optimized method. The TMZ-loaded LLCs with the same composition but varying drug concentrations were prepared as represented in **Table 6.12**. There was no effect on particle size and PDI indicating that it was not dependent on the drug concentration (**Figure 6.9**). No effect on % entrapment efficiency was observed indicating that entrapment of TMZ in LLCs was dependent on the internal to external aqueous phase ratio. A significant effect on drug loading was observed which is dependent on the drug-to-lipid ratio.

Table 6.12. Composition of TMZ loaded LLCs with different drug loading

GMO (mg)	300	300	300	300
PF 127 (mg)	150	150	150	150
PEG 200 (mL)	1	1	1	1
Initial volume of water containing drug (5 mg/mL) Represented as (% v/v) of final dispersion volume	1 mL containing 5 mg drug (10 %)	2 mL containing 10 mg drug (20 %)	3 mL containing 15 mg drug (30 %)	4 mL containing 20 mg drug (40 %)
Volume of water added during probe sonication	9 mL	8 mL	7 mL	6 mL

***** *Final dispersion volume: 10 mL*

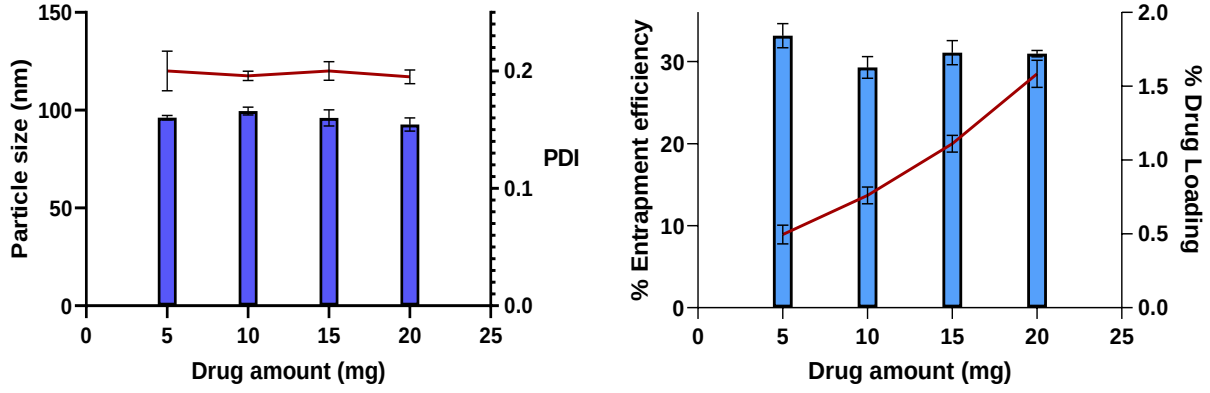

Figure 6.9. Effect of drug amount on particle size, PDI, % entrapment efficiency and % drug loading of TMZ loaded LLCs

6.5.4. Preparation of PEGylated TMZ loaded LLCs by the optimized method

The effect of PEG 200 and DSPE-PEG 2000 was studied by altering their concentration and keeping drug, lipid, and surfactant concentrations constant. The results obtained are summarized in **Table 6.13**. It was found that PEG 200 concentration majorly affected the PDI. The PDI was found to decrease by presence of PEG 200. DSPE-PEG 2000 is also reported to stabilize the LLC structure. PEG 200 was replaced with DSPE-PEG 2000 to overcome the hemolytic potential of GMO and also to improve the plasma circulation time. As the concentration of DSPE-PEG 2000 was increased from 0.05 % to 1 % of the total dispersion, particle size was found to reduce from 101.05 ± 1.202 nm to 85.27 ± 0.240 nm. DSPE-PEG 2000 may act as a surfactant and lower the particle size. PDI was found to increase on increasing concentrations of DSPE-PEG 2000. The negatively charged functional groups in DSPE-PEG 2000 led to a negative surface charge on LLCs [5,48].

Table 6.13. Effect of PEG 200 and DSPE-PEG 2000 on particle size, PDI, and zeta potential of LLCs (Measurements were done in triplicates for each formulation)

GMO (mg)	PF 127 (mg)	PEG 200 (mL)	DSPE-PEG 2000	Size (nm)	PDI	Zeta potential (mV)
300	150	0	0	110.15 ±1.626	0.293 ± 0.013	-4.195 ± 0.134
300	150	1	0	111.05 ± 0.354	0.219 ± 0.013	-1.48 ± 0.474
300	150	0	0.05 %	101.05 ± 1.202	0.241 ± 0.003	-6.29 ± 0.226
300	150	0	0.1 %	94.475 ± 1.817	0.259 ± 0.014	-9.48 ± 0.106
300	150	0	0.25 %	94.785 ± 6.286	0.282 ± 0.003	-11.7 ± 1.768
300	150	0	0.5 %	90.29 ± 1.117	0.359 ±0.001	-16.7 ± 0.283
300	150	0	1 %	85.27 ± 0.240	0.297 ± 0.004	-25.05 ± 1.768

** DSPE-PEG 2000 represented as % (w/v) of the total dispersion (10 mL)*

6.5.5. Characterization of TMZ loaded LLCs

6.5.5.1. Particle size, Polydispersity index (PDI), and Zeta potential

The average particle size of the optimized TMZ-loaded LLCs and TMZ-loaded PEGylated LLCs was in the range of 90 to 120 nm (represented in **Figure 6.10**). PEGylated LLCs were found to show higher PDI values in comparison to non-PEGylated LLCs, however, the PDI values were

less than 0.5. The zeta potential graphs of the optimized formulations are represented in **Figure 6.10**. No significant difference was observed in the particle size and size distribution after freeze-drying.

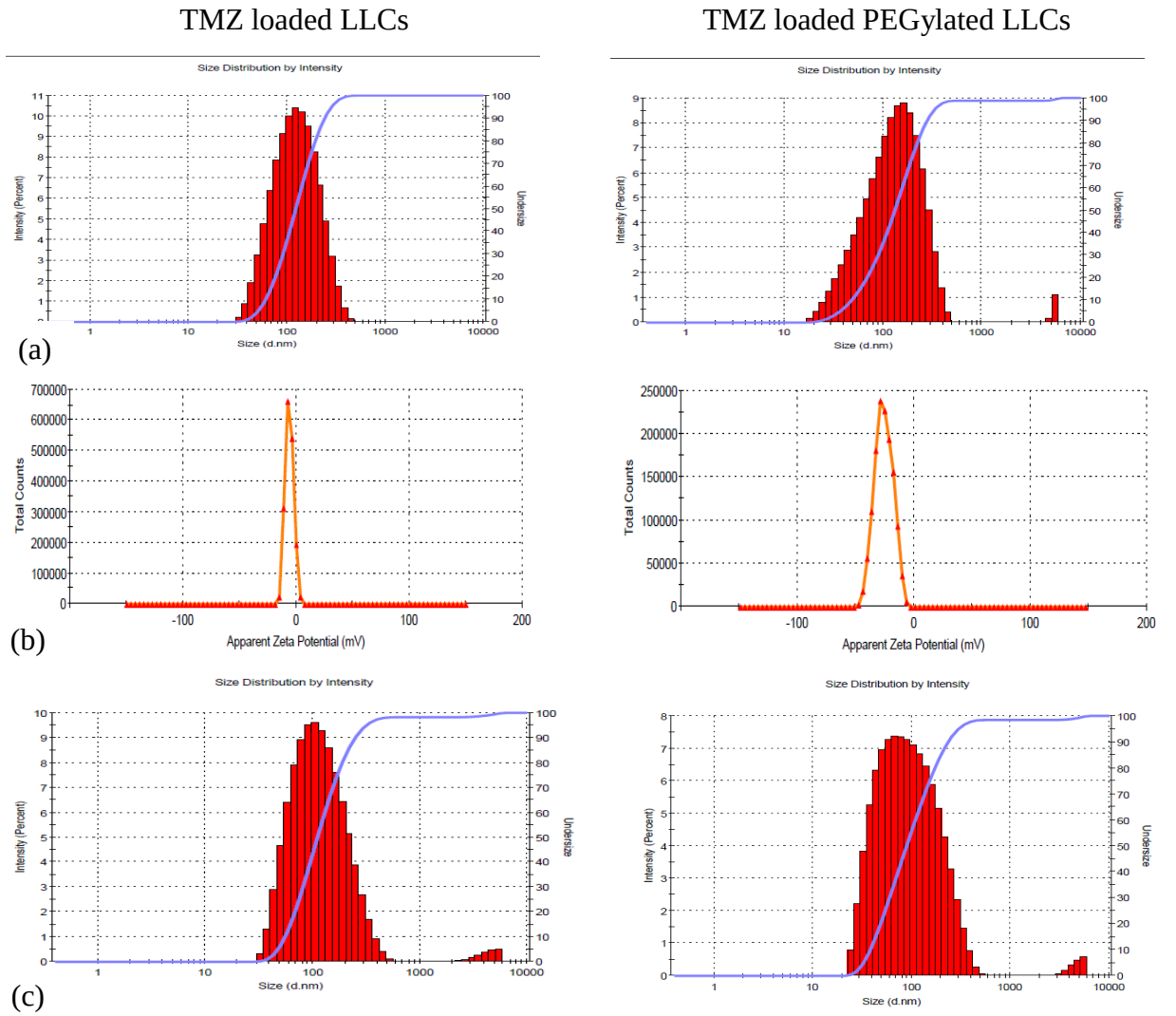

Figure 6.10. (a) Particle size graphs of TMZ loaded LLCs and TMZ loaded PEGylated LLCs (b) Zeta potential graphs of TMZ loaded LLCs and TMZ loaded PEGylated LLCs (c) Particle size graphs of TMZ loaded LLCs and TMZ loaded PEGylated LLCs after reconstitution of freeze-dried form.

6.5.5.3 Morphology

The SEM images confirmed the morphology of the formed LLCs. There was no change in morphology after PEGylation of the LLCs (**Figure 6.11**). The TEM image and the single crystal SAED pattern (Figure 2 c and d) revealed a cubic morphology of the developed PEGylated LLCs [41,49].

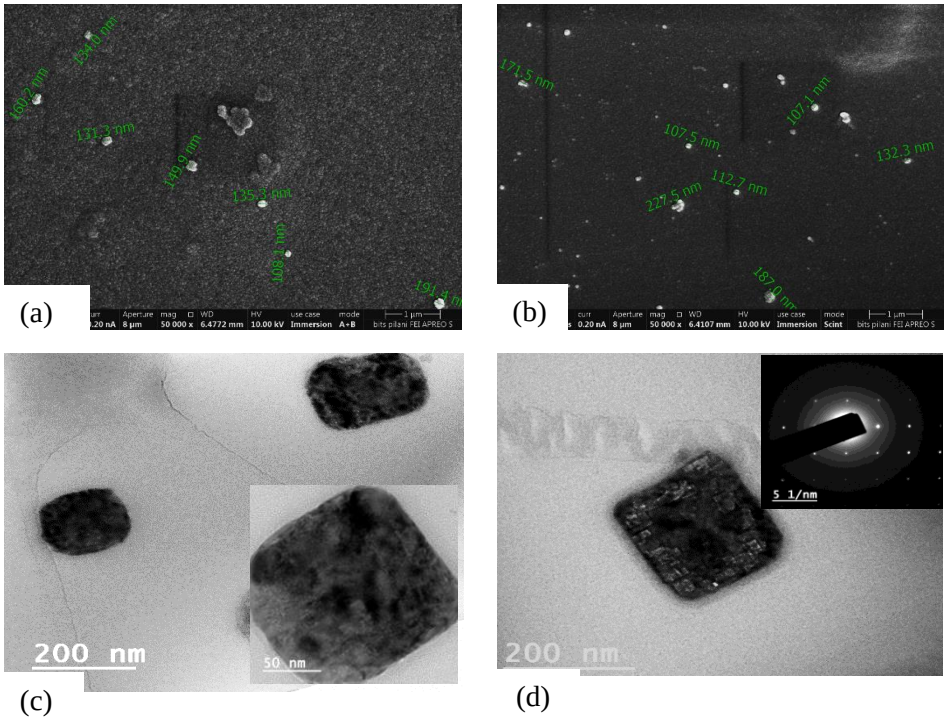

Figure 6. 11. Morphology of LLCs. *(a) SEM image of TMZ loaded LLCs; (b) SEM image of PEGylated TMZ loaded LLCs (c) TEM image of TMZ loaded PEGylated LLCs (d) TEM image with single crystal SAED pattern of TMZ loaded PEGylated LLCs*

6.5.5.4. Confirmation of crystalline structure

The lyotropic liquid crystal formation was confirmed by polarized light microscopy. Crystals have the property of birefringence and the ability to split the cross-polarized light. When we rotate the cross polarizer 90 degrees, the appearance of bright crystals confirms the presence of lyotropic liquid crystals as represented in **Figure 6.12**. The prepared formations had milk-like consistency and appearance depicting liquid nature. Thus the prepared LLCs had both crystalline and liquid-like properties [41,49].

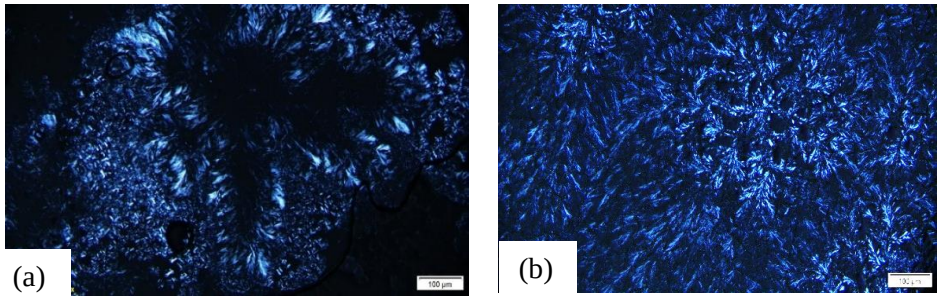

Figure 6.12. Polarized light microscopic images of *(a) TMZ loaded LLCs with the cross polarizer; (b) PEGylated TMZ loaded LLCs with the cross polarizer*

The XRD diffractogram of TMZ, Physical mixture, and TMZ loaded PEGylated LLCs are represented in **Figure 6.13**. Sharp narrow peaks indicate that the substance is crystalline, while broad peaks represent amorphous nature. Sharp peaks were observed at 10.83, 14.63, 17.98, 19.05, 26.49, and 29.80 degrees in the TMZ diffractogram, revealing the crystalline nature of the drug. The intense sharp peaks of TMZ disappeared in the diffractogram of LLCs, indicating drug entrapment inside the LLCs. New sharp peaks at 20.65, 25.46, and 36.39 degrees appeared in the diffractogram of LLCs, revealing the crystalline nature of the LLCs, which confirmed the formation of a liquid crystal structure [41,50].

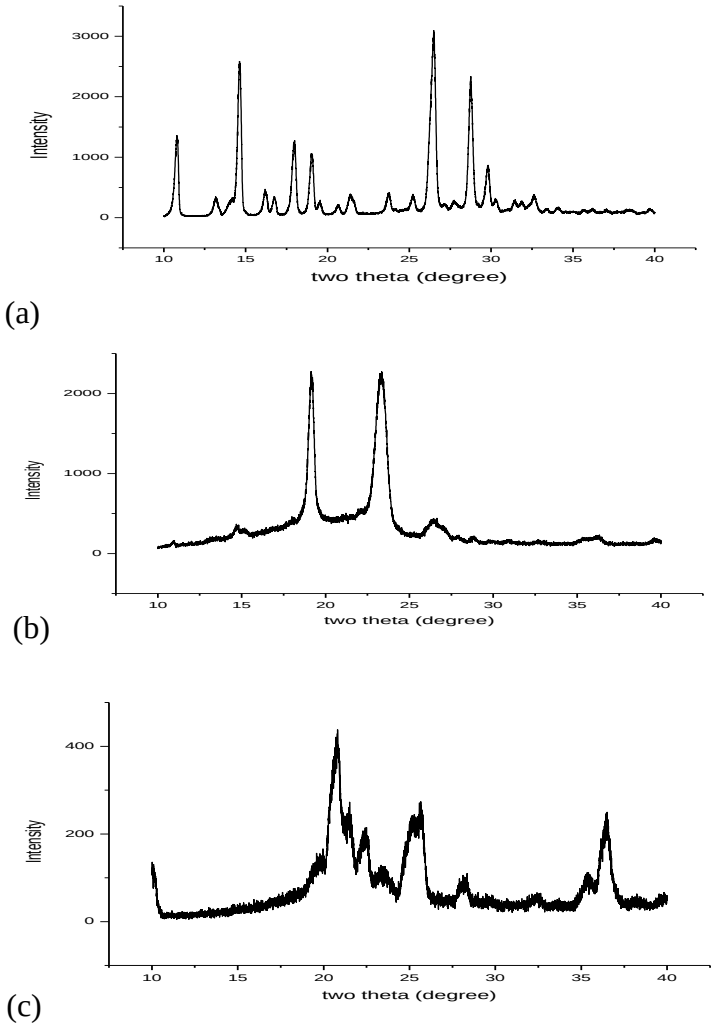

Figure 6. 13. XRD diffractogram of (a) TMZ, (b) Physical mixture, and (c) TMZ loaded PEGylated LLCs

6.5.5.4. Drug release and release kinetics

In-vitro drug release study showed that the free drug diffused out 100 % within 2 h and followed a first-order release kinetics. Initially, the effect of drug loading on drug release was evaluated. The study was conducted on the four formulations with different drug loading, but similar particle size, PDI and entrapment efficiency, as obtained in **section 6.5.3**. TMZ-loaded LLCs exhibited sustained release up to more than 72 h. The drug release profiles obtained are represented in **Figure 6.14**. The drug release rate was found to be proportional to the drug loading. The higher the lipid concentration, the slower the drug release rate as the entrapped drug has to diffuse through the channels of the lipid matrix. The drug crosses multiple layers before reaching the outside media, thus leading to the slow release of the drug [3,41].

The release of TMZ from LLCs could be explained by Korsmeyer's Peppas model. The release exponent 'n' value less than 0.45 demonstrated diffusion-controlled drug release. When the drug release kinetics of TMZ-loaded LLCs and TMZ-loaded PEGylated LLCs was compared, similar drug release rate was observed (**Figure 6.15, Table 6.14**) indicating PEGylation did not alter the release kinetics of LLCs. When the drug release was conducted in phosphate buffer saline (pH 7.4), initially an increase in TMZ concentration was observed, however after 2 h, a decrease in TMZ concentration was observed attributed to the stability of TMZ in alkaline pH (**Figure 6.15**). However, the decrease in TMZ concentration was slower with TMZ-loaded PEGylated LLCs as compared to TMZ alone. As TMZ was entrapped inside the LLCs structure, it was not exposed to the external alkaline pH. Only the released TMZ was exposed and converted to its metabolite. This study indicated that TMZ-loaded PEGylated LLCs had the potential to enhance the plasma circulation time of TMZ, as well as stability when administered intravenously [33,51].

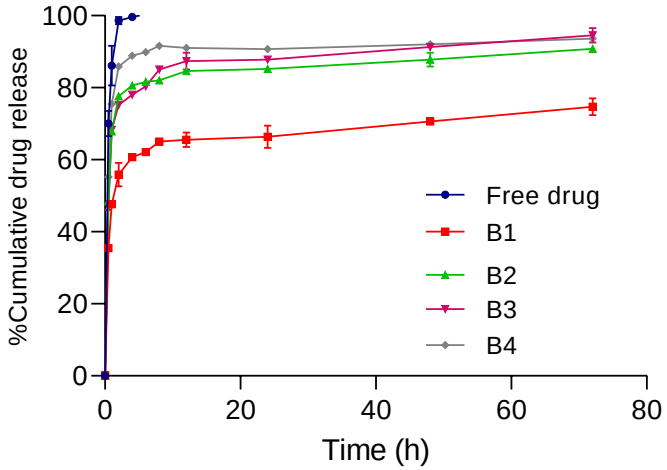

Figure 6.14. Drug release profile of TMZ and TMZ loaded LLCs with different drug loading *(B1- 0.45 %, B2- 0.72 %, B3- 1.00 %, B4- 1.52%) (n=3 represented as Mean ± SD)*

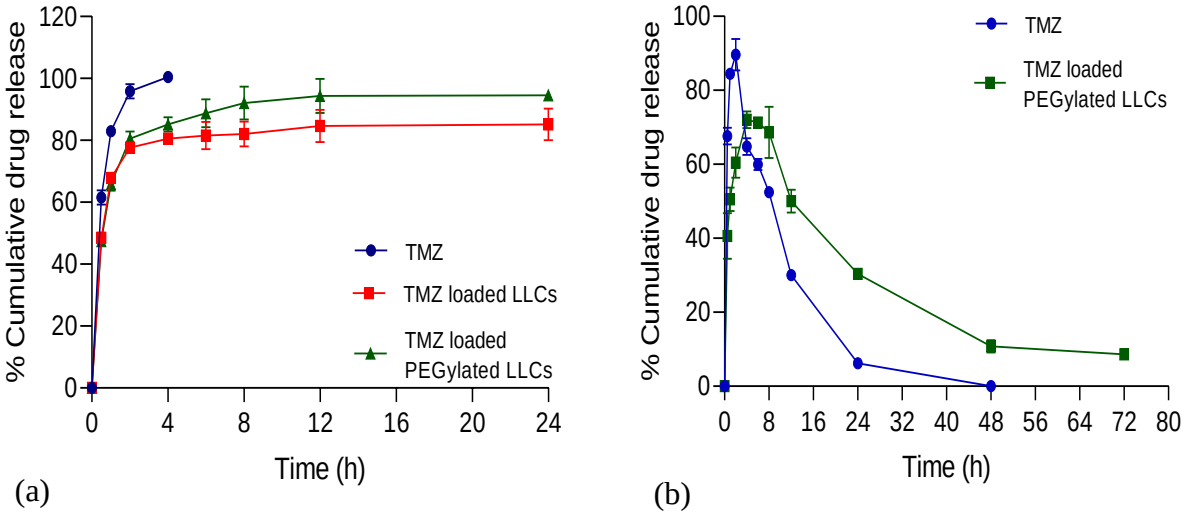

Figure 6.15. The in-vitro drug release profile of (a) TMZ, TMZ loaded LLCs and TMZ loaded PEGylated LLCs in acetate buffer pH 4.5 (b) TMZ and PEGylated LLCs in phosphate buffer pH 7.4 *(n=3 represented as Mean ± SD)*

Table 6.14 Release kinetics parameters obtained for TMZ, TMZ loaded LLCs and TMZ loaded PEGylated LLCs through different models

Model	**TMZ**			**TMZ loaded LLCs**			**TMZ loaded PEGylated LLCs**		
	R^2	AIC	MSC	R^2	AIC	MSC	R^2	AIC	MSC
Zero order	0.756	45.831	-1.53	0.519	91.211	-2.730	0.575	91.441	-2.446
First order	**0.999**	**11.017**	**5.432**	0.975	68.386	-0.194	0.985	62.706	0.747
Higuchi	0.925	38.134	0.009	0.734	82.113	-1.719	0.781	81.641	-1.357
Korsmeyer Peppas	0.992	27.341	2.168	**0.977**	**54.708**	**1.326**	**0.979**	**55.447**	**1.553**
Hixson Crowell	0.975	32.277	1.180	0.749	82.413	-1.753	0.799	81.871	-1.383
Best fit model parameters									
	First order			**Korsmeyer-Peppas**					
k	2.266			65.249			65.269		
n	-			0.106			0.132		
t_{25}	0.127			0.000			0.001		
t_{50}	0.306			0.082			0.133		
t_{75}	0.612			3.712			2.864		

6.5.5.5. Reproducibility and scale-up studies

The average particle size and PDI of the 6 repeated batches were found to be 98.98 ± 7.14 nm and 0.195 ± 0.01, respectively, which confirmed that the process was highly reproducible. In scale up study, to prepare the 50 mL batch, the beaker size and the probe size were increased proportionally, and the sonication time was optimized. The particle size and PDI obtained for the scale-up batch were 120.8 ± 0.70 and 0.219 ± 0.003, respectively. As the process involved a minimum number of steps, it was feasible for scale-up. The particle size and PDI of both LLCs and PEGylated LLCs were found to be stable even after 1000 times dilution, which revealed that the structure was maintained even after dilution (**Figure 6.16**) [20].

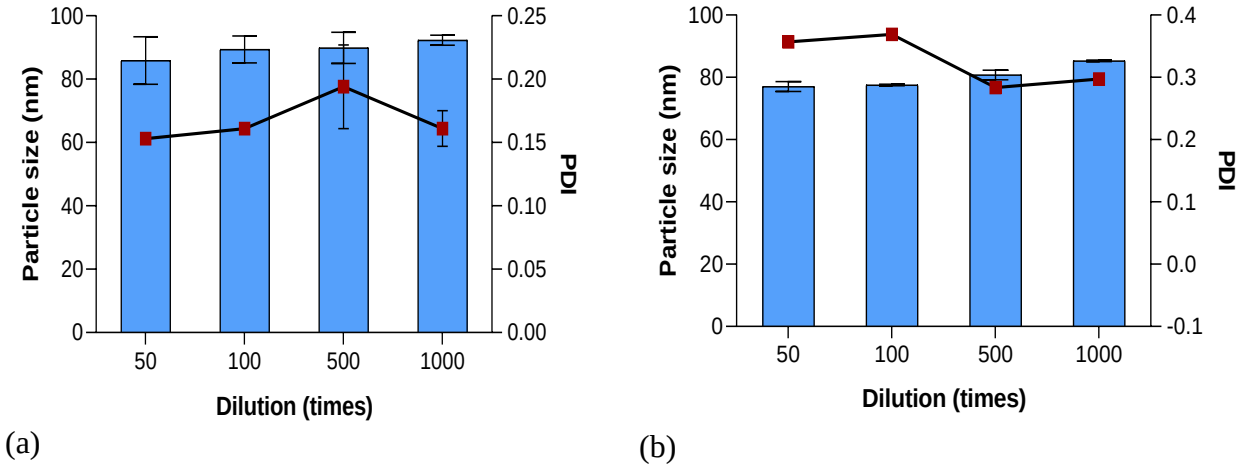

Figure 6.16. Particle size (nm) and PDI of (a) TMZ-loaded LLCs and (b) PEGylated LLCs on different dilutions with Milli Q water. *The zeta potential of TMZ-loaded LLCs and PEGylated LLCs was found to be -6.49 ± 2.19 mV and -18.24 ± 6.42 mV respectively (n=3 shown as Mean ± SD)*

6.5.5.6. Hemolysis study

TMZ was found to show less than 2.5 % hemolysis. GMO-containing LLCs were found to show about 47.42 ± 2.26 % hemolysis (**Figure 6.17**). They were found to show 6.66 ± 1.90 % hemolysis even after 10 times dilution. Few studies have reported that GMO has membrane destabilizing and lipid-mixing properties which is responsible for generating pores in RBC cell membrane and subsequent hemolysis. The extent of hemolysis caused is dependent on the lipid composition and the concentration. In order to overcome the hemolysis caused due to GMO, DSPE-PEG 2000 was added to the formulation [52]. It was observed that on increasing the concentration of DSPE-PEG 2000 from 0.05 % to 1 % significantly reduced the hemolysis of RBCs. LLCs containing 1 % DSPE-PEG 2000 with and without dilution were found to show less than 5 % hemolysis. Also, the TMZ loaded PEGylated (1 %) LLCs were found to show less than 5 % hemolysis. This study proved the potential of PEGylated LLCs containing 1 % DSPE-PEG 2000 for administration into the systemic circulation. PEG 2000 molecules adsorbed on the surface prevent the interaction with the RBCs, thus the reduction of subsequent hemolysis [5,23].

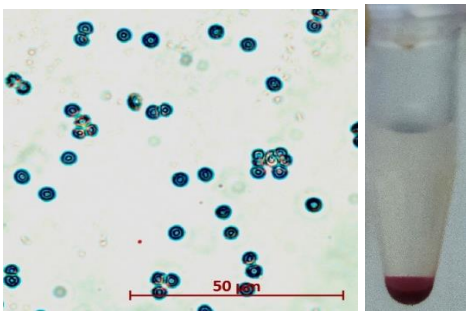

(a) No Hemolysis

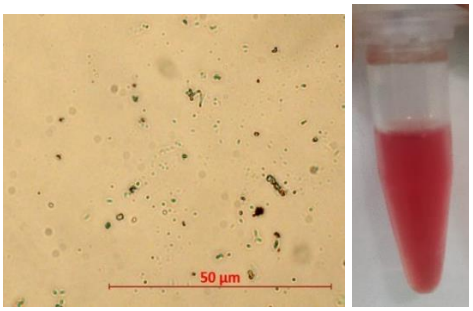

(b) Complete Hemolysis

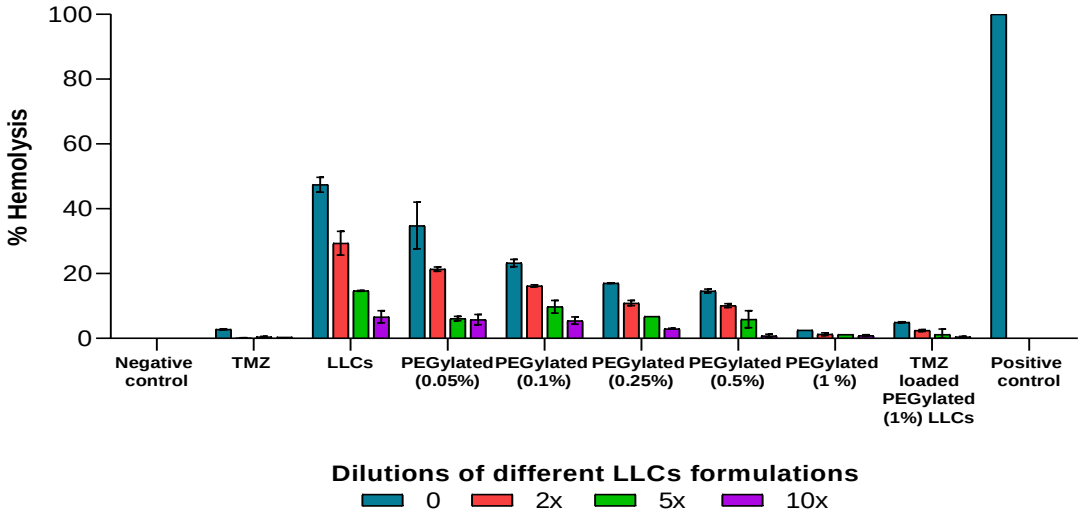

(c) % Hemolysis of different LLCs formulations

Figure 6.17. Fluorescence microscopic image of (a) intact RBCs indicating no hemolysis and (b) RBCs after hemolysis. (c) % Hemolysis of different LLCs formulations. *The % values in brackets represent the DSPE-PEG 2000 % w/v in the PEGylated LLCs. The dilution medium used was normal saline (n=3 represented as Mean ± SD), the undiluted formulation contained 1mg/mL TMZ.*

6.5.5.7. In-vitro cytotoxicity study

The results obtained for cell viability are summarized in **Figure 6.18**. TMZ was found to show dose-dependent cytotoxicity on glioma cells. TMZ-loaded LLCs were found to show significantly increased cell cytotoxicity. TMZ-loaded LLCs and TMZ-loaded PEGylated LLCs were found to show 2.22 and 1.54 fold more cytotoxicity as compared to TMZ alone. The lipidic, bioadhesive, and membrane fusing nature of GMO helps improve cell internationalization. As the drug concentration increases, the number of LLCs also increases, ultimately resulting in higher cytotoxicity. PEGylated LLCs showed less cytotoxicity as compared to LLCs. This may be attributed to the fate of LLCs after taken up by the cells. The PEGylated LLCs might be taken up

by the cells, escape endosomal disruption due to PEGylation and release TMZ slowly in comparison to LLCs. The study revealed that incorporating TMZ into the LLCs potentiates the cytotoxicity of TMZ [5].

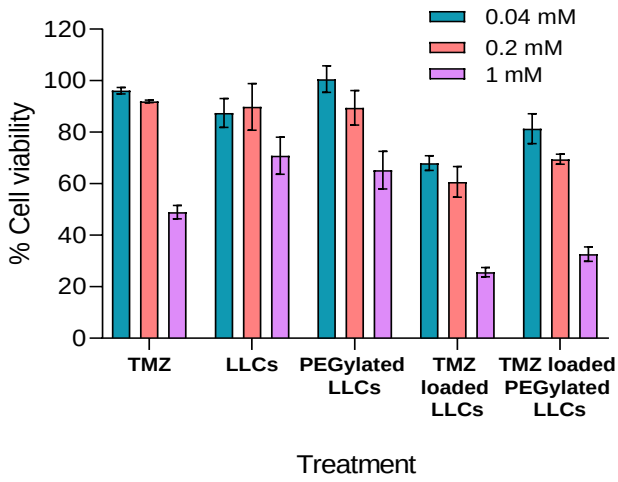

	IC_{50} value
TMZ	0.98 ± 0.049 mM
TMZ loaded LLCs	0.44 ± 0.073 mM
TMZ loaded PEGylated LLCs	0.64 ± 0.072 mM

Figure 6.18. In-vitro cytotoxicity assessment of TMZ and TMZ-loaded LLCs on U87 cells exposed for 48 h. *Data represented as Mean ± SD (n=4, where n represents the number of wells in an experiment)*

6.5.5.8. Cell uptake study

The U87 glioblastoma cell uptake study was conducted to evaluate the potential of LLCs when directly administered in to the brain. **Figure 6.19** represents that PEGylated LLCs were found to show more cell uptake in U87 glioblastoma cell lines as compared to LLCs. Also, a uniform distribution inside the cell was observed with PEGylated LLCs as compared to LLCs indicating that both might have followed different cell uptake mechanisms. Similar observations were obtained in a study, wherein, negatively charged cubosomes were found to be uniformly distributed inside the cell and escaped the endosomal uptake. The cubosomes with near-neutral surface charge were found to show co-localized areas resembling endosomal entrapment [53,54].

When the cell uptake was studied in RAW macrophage cell lines, PEGylated LLCs were found to show a 3.18-fold less cell uptake as compared to uncoated LLCs (**Figure 6.20**). This confirmed that PEGylation of LLCs can provide longer plasma circulation time by escaping uptake by macrophages following opsonization [55–57].

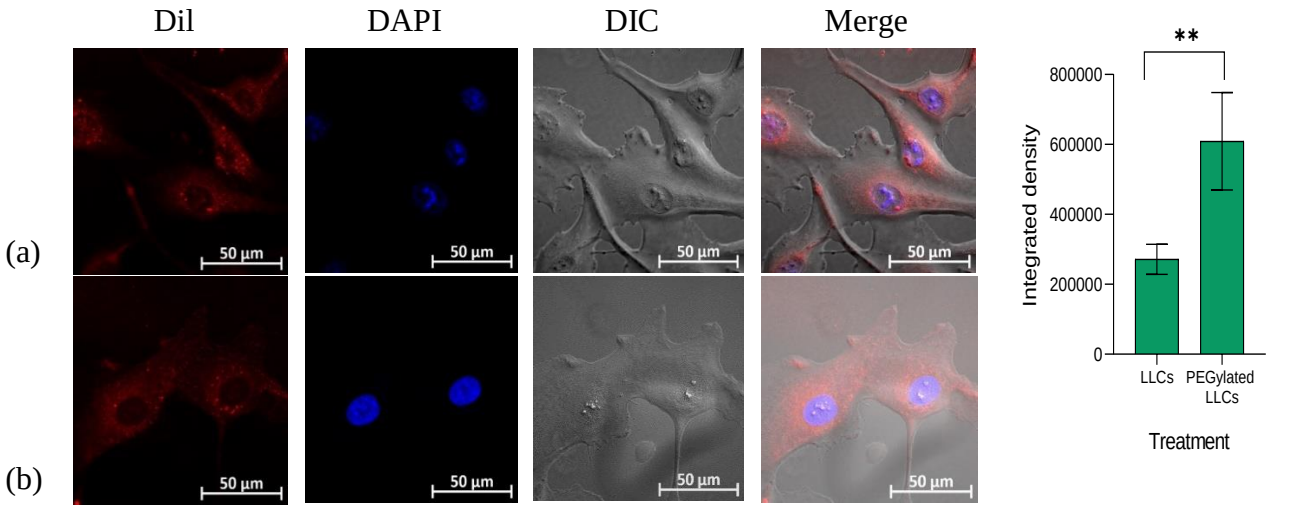

Figure 6.19. Confocal images and fluorescence intensity obtained for cell uptake studies of (a) Dye-loaded LLCs and (b) Dye-loaded PEGylated LLCs in U87 glioblastoma cell lines after treatment of 4 hours *(Data represented as Mean ± SD, n=4), statistical significance calculated using t-test ** < 0.1*

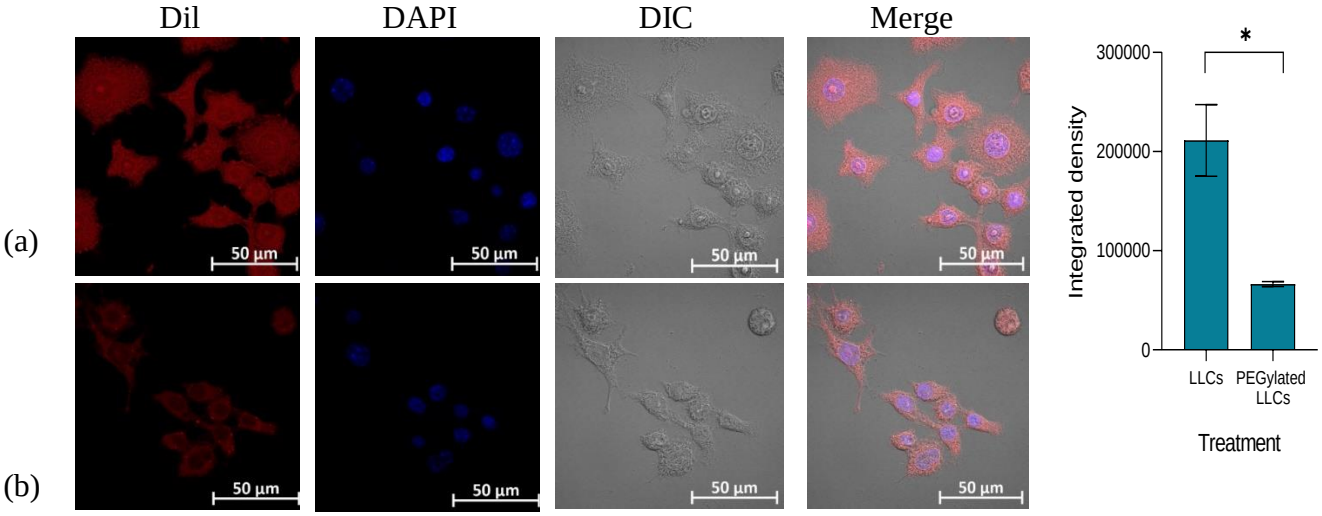

Figure 6.20. Confocal images and fluorescence intensity obtained for cell uptake studies of (a) Dye-loaded LLCs and (b) Dye-loaded PEGylated LLCs in RAW macrophage cell lines after treatment of 4 hours *(Data represented as Mean ± SD, n=4), statistical significance calculated using t-test * p < 0.05*

6.5.5.8. Storage stability

Similar to Liposomes, the TMZ loaded PEGylated LLCs were found to be stable under refrigerated conditions upto 2 months as represented in **Table 6.15**

Table 6.15. Storage stability data of freeze-dried TMZ loaded PEGylated LLCs (n=3)

Months		**0**	**1**	**2**
Refrigerated conditions	Particle size (nm)	97.7 ± 2.970	98.9 ± 4.667	108.1 ± 8.343
	PDI	0.395 ± 0.078	0.306 ± 0.124	0.279 ± 0.086
	Drug content (%)	99.133 ± 0.154	99.774 ± 2.609	98.84 ± 0.564
Room temperature	Particle size (nm)	97.7 ± 2.970	114.25 ± 0.354	104.5 ± 5.547
	PDI	0.395 ± 0.078	0.241 ± 0.004	0.169 ± 0.015
	Drug content (%)	99.133 ± 0.154	42.885 ± 0.169	28.216 ± 0.201

6.6. Conclusion

TMZ-loaded LLCs were successfully optimized using the principles of Quality by Design. Understanding the effect of various material attributes and the process parameters on the critical quality attributes is essential and lowers the risk of product failure. The unique structure of LLCs allows entrapment of amphiphilic drug-like TMZ and provides controlled release. PEGylation of LLCs significantly overcomes the hemolytic potential of GMO. The system has the potential to enhance the plasma circulation time of TMZ. The preparation method involved the minimum number of steps, was highly reproducible and industrially feasible for scale up.

References:

1. Kalyani Ashok C, Ola M, Ramesh DR, Chaudhari VA. Liquid crystals: A review. Int J Creat Innov Res all Stud. 2019;1(12):119–29.

2. Gaballa S, El Garhy O, Abdelkader H. Cubosomes: composition, preparation, and drug delivery applications. J Adv Biomed Pharm Sci. 2020;3:1–9.

3. Waghule T, Rapalli VK, Singhvi G, Gorantla S, Khosa A, Dubey SK, et al. Design of temozolomide-loaded proliposomes and lipid crystal nanoparticles with industrial feasible approaches: comparative assessment of drug loading, entrapment efficiency, and stability at plasma pH. J Liposome Res. 2020;31(2):158–68.

4. Singhvi G, Banerjee S, Khosa A. Lyotropic liquid crystal nanoparticles: A novel improved lipidic drug delivery system. In: Grumezescu AM, editor. Organic Materials as Smart Nanocarriers for Drug Delivery. UK: William Andrew Publishing; 2018. p. 471–517.

5. Freag May, Elnaggar, Yosra S R, Abdelmonsif A Doaa AYO. Stealth , biocompatible monoolein-based lyotropic liquid crystalline nanoparticles for enhanced aloe-emodin delivery to breast cancer cells : in vitro and in vivo studies. Int J Nanomedicine. 2016;11:4799–818.

6. Niu Z, Conejos-Sánchez I, Griffin BT, O'Driscoll CM, Alonso MJ. Lipid-based nanocarriers for oral peptide delivery. Adv Drug Deliv Rev. 2016;106:337–54.

7. Rapalli VK, Waghule T, Hans N, Mahmood A, Gorantla S, Dubey SK, et al. Insights of lyotropic liquid crystals in topical drug delivery for targeting various skin disorders. J Mol Liq. 2020;315:113771.

8. Mo J, Milleret G, Nagaraj M. Liquid crystal nanoparticles for commercial drug delivery. Liq Cryst Rev. 2017;5(2):69–85.

9. Yosra SR Elnaggar, Samar M Etman, Doaa A Abdelmonsif OYA. Novel piperine-loaded Tween-integrated monoolein cubosomes as brain-targeted oral nanomedicine in Alzheimer ' s disease : pharmaceutical , biological , and toxicological studies. Int J Nanomedicine. 2015;10:5459–73.

10. Nasr M, Ghorab MK, Abdelazem A. In vitro and in vivo evaluation of cubosomes containing 5-fluorouracil for liver targeting. Acta Pharm Sin B. 2015;5(1):79–88.

11. Mahmood A, Rapalli VK, Waghule T, Gorantla S, Singhvi G. Luliconazole loaded lyotropic liquid crystalline nanoparticles for topical delivery: QbD driven optimization, in-vitro characterization and dermatokinetic assessment. Chem Phys Lipids. 2021;234:105028.

12. Rapalli VK, Khosa A, Singhvi G, Girdhar V, Jain R, Dubey SK. Application of QbD Principles in Nanocarrier-Based Drug Delivery Systems. In: Sarwar Beg MSH, editor. Pharmaceutical Quality by Design. Academic Press; 2019. p. 255–96.

13. Deborosa Soans, Chandramouli R, Kavitha A N, Roopesh S K SS. APPLICATION OF DESIGN OF EXPERIMENTS FOR OPTIMIZING CRITICAL QUALITY ATTRIBUTES (CQA) IN ROUTINE. J Pharm Res. 2016;15(3):96–100.

14. Javed MN, Alam MS, Waziri A, Pottoo FH, Yadav AK, Hasnain MS, et al. QbD Applications for the Development of Nanopharmaceutical Products. Pharm Qual by Des.

2019;(March):229–53.

15. Srinivas NSK, Verma R, Kulyadi GP, Kumar L. A quality by design approach on polymeric nanocarrier delivery of gefitinib: Formulation, in vitro, and in vivo characterization. Int J Nanomedicine. 2017;12:15–28.

16. Zhang L, Mao S. Application of quality by design in the current drug development. Asian J Pharm Sci. 2017;12(1):1–8.

17. Waghule T, Rapalli VK, Singhvi G, Manchanda P, Hans N, Dubey SK, et al. Voriconazole loaded nanostructured lipid carriers based topical delivery system: QbD based designing, characterization, in-vitro and ex-vivo evaluation. J Drug Deliv Sci Technol. 2019;52:303–15.

18. Ranga S, Jaimini M, Sharma SK, Chauhan BS, Kumar A. A Review on Design OF Experiments (DOE). Int J Pharm Chem Sci. 2014;3(1):216–24.

19. Chaudhary S. A DoE / QbD Optimization Model of "DRY MIXING-DIRECT COMPRESSION" Process using 3^2 Full factorial Design for Solid Oral Dosage Forms. Int J Pharm. 2018;(July).

20. Rapalli VK, Sharma S, Roy A, Singhvi G. Design and dermatokinetic evaluation of Apremilast loaded nanostructured lipid carriers embedded gel for topical delivery: A potential approach for improved permeation and prolong skin deposition. Colloids Surfaces B Biointerfaces. 2021;206:111945.

21. Bei D, Marszalek J, Youan BC. Formulation of Dacarbazine-loaded Cubosomes — Part II : In fl uence of Process Parameters. AAPS PharmSciTech. 2009;10(3):1040–7.

22. Merlo-Mas J, Tomsen-Melero J, Corchero JL, González-Mira E, Font A, Pedersen JN, et al. Application of Quality by Design to the robust preparation of a liposomal GLA formulation by DELOS-susp method. J Supercrit Fluids. 2021;173(October 2020):105204.

23. Jain V, Swarnakar NK, Mishra PR, Verma A, Kaul A, Mishra AK, et al. Paclitaxel loaded PEGylated gleceryl monooleate based nanoparticulate carriers in chemotherapy. Biomaterials. 2012;33(29):7206–20.

24. Bhattacharjee S. DLS and zeta potential - What they are and what they are not? J Control Release. 2016;235:337–51.

25. Zhang P, Jing T, Zhang J. Preparation , characterization , and evaluation of amphotericin B-loaded MPEG-PCL-g-PEI micelles for local treatment of oral Candida albicans. Int J Nanomedicine. 2017;12:4269–83.

26. Pradhan M, Singh D, Murthy SN, Singh MR. Design, characterization and skin permeating potential of Fluocinolone acetonide loaded nanostructured lipid carriers for topical treatment of psoriasis. Steroids. 2015;101:56–63.

27. Kosela M. Microscopic methods in analysis of submicron phospholipid dispersions. Acta Pharm. 2016;66:1–22.

28. Omar S, Ismail A, Hassanin K, Hamdy S. Formulation and Evaluation of Cubosomes as Skin Retentive System for Topical Delivery of Clotrimazole. J Adv Pharm Res. 2019;3(2):68–82.

29. Elisabetta Esposito, Paolo Mariani, Markus Drechsler RC. Structural Studies of Lipid-Based Nanosystems for Drug Delivery: X-ray Diffraction (XRD) and Cryogenic Transmission Electron Microscopy (Cryo-TEM). In: Aliofkhazraei M, editor. Handbook of Nanoparticles. Switzerland: Springer International Publishing; 2015. p. 1–1426.

30. Zhao L, Xiong H, Peng H. PEG-coated lyophilized proliposomes : preparation , characterizations and in vitro release evaluation of vitamin E. Eur Food Res Technol. 2011;232:647–54.

31. Mahmood A, Krishna V, Waghule T, Gorantla S, Kumar S, Narayan R, et al. Spectrochimica Acta Part A : Molecular and Biomolecular Spectroscopy UV spectrophotometric method for simultaneous estimation of betamethasone valerate and tazarotene with absorption factor method : Application for in-vitro and ex-vivo characterization of. Spectrochim Acta Part A Mol Biomol Spectrosc. 2020;235:118310.

32. Zuo J, Gao Y, Bou-Chacra N, Löbenberg R. Evaluation of the DDSolver software applications. Biomed Res Int. 2014;2014.

33. Zhang Y, Huo M, Zhou J, Zou A, Li W, Yao C, et al. DDSolver: An add-in program for

modeling and comparison of drug dissolution profiles. AAPS J. 2010;12(3):263–71.

34. Gorantla S, Saha RN, Singhvi G. Exploring the affluent potential of glyceryl mono oleate – myristol liquid crystal nanoparticles mediated localized topical delivery of Tofacitinib: Study of systematic QbD, skin deposition and dermal pharmacokinetics assessment. J Mol Liq. 2021;346:117053.

35. Lu J, Owen SC, Shoichet MS. Stability of self-assembled polymeric micelles in serum. Macromolecules. 2011;44(15):6002–8.

36. Surve DH, Jirwankar YB, Dighe VD, Jindal AB. Long-Acting Efavirenz and HIV - 1 Fusion Inhibitor Peptide Co-loaded Polymer − Lipid Hybrid Nanoparticles : Statistical Optimization , Cellular Uptake , and In Vivo Biodistribution. 2020;17:3990–4003.

37. Patel BK, Parikh RH. FORMULATION DEVELOPMENT AND EVALUATION OF TEMOZOLOMIDE LOADED HYDROGENATED SOYA PHOSPHATIDYLCHOLINE LIPOSOMES FOR THE TREATMENT OF BRAIN CANCER. Asian J Pharm Clin Res. 2016;9(3):340–340.

38. Rapalli VK, Kaul V, Waghule T, Gorantla S, Sharma S, Roy A, et al. Curcumin loaded nanostructured lipid carriers for enhanced skin retained topical delivery: optimization, scale-up, in-vitro characterization and assessment of ex-vivo skin deposition. Eur J Pharm Sci. 2020 Sep 1;152:105438.

39. Bapat P, Ghadi R, Chaudhari D, Katiyar SS, Jain S. Tocophersolan stabilized lipid nanocapsules with high drug loading to improve the permeability and oral bioavailability of curcumin. Int J Pharm. 2019;560:219–27.

40. Patil S, Kadam C, Pokharkar V. QbD based approach for optimization of Tenofovir disoproxil fumarate loaded liquid crystal precursor with improved permeability. J Adv Res. 2017 Nov;8(6):607–16.

41. Waghule T, Patil S, Rapalli VK, Girdhar V, Gorantla S, Kumar Dubey S, et al. Improved skin-permeated diclofenac-loaded lyotropic liquid crystal nanoparticles: QbD-driven industrial feasible process and assessment of skin deposition. Liq Cryst. 2020;47:1–19.

42. Mahmood A, Rapalli VK, Waghule T, Gorantla S, Singhvi G. Luliconazole loaded lyotropic

liquid crystalline nanoparticles for topical delivery: QbD driven optimization, in-vitro characterization and dermatokinetic assessment. Chem Phys Lipids. 2021;234:e105028.

43. Waghule T, Dabholkar N, Gorantla S, Rapalli VK, Saha RN, Singhvi G. Quality by design (QbD) in the formulation and optimization of liquid crystalline nanoparticles (LCNPs): A risk based industrial approach. Biomed Pharmacother. 2021;141.

44. Beg S, Sandhu PS, Batra RS, Khurana RK, Singh B. QbD-based systematic development of novel optimized solid self-nanoemulsifying drug delivery systems (SNEDDS) of lovastatin with enhanced biopharmaceutical performance. Drug Deliv. 2015;22(6):765–84.

45. Bei D, Marszalek J, Youan BC. Formulation of Dacarbazine-Loaded Cubosomes — Part I : In fl uence of Formulation Variables. AAPS PharmSciTech. 2009;10(3):1032–9.

46. Abdelaziz HM, Elzoghby O, Maged W, Samaha MW, Fang J, May S. Liquid crystalline assembly for potential combinatorial chemo – herbal drug delivery to lung cancer cells. Int J Nanomedicine. 2019;14:499–517.

47. Patel M, Sawant K. A Quality by Design Concept on Lipid Based Nanoformulation Containing Antipsychotic Drug: Screening Design and Optimization using Response Surface Methodology. J Text Sci Eng. 2017;08(03):1000442.

48. Zhai J, Hinton TM, Waddington LJ, Fong C, Tran N, Mulet X, et al. Lipid − PEG Conjugates Sterically Stabilize and Reduce the Toxicity of Phytantriol-Based Lyotropic Liquid Crystalline Nanoparticles. Langmuir. 2015;31:10871–80.

49. Wang X, Zhang Y, Gui S, Huang J, Cao J, Li Z, et al. Characterization of Lipid-Based Lyotropic Liquid Crystal and Effects of Guest Molecules on Its Microstructure: a Systematic Review. AAPS PharmSciTech. 2018;19(5):2023–40.

50. Bansal S, Beg S, Asthana A, Garg B, Asthana GS, Kapil R, et al. QbD-enabled systematic development of gastroretentive multiple-unit microballoons of itopride hydrochloride. Drug Deliv. 2016 Feb;23(2):437–51.

51. Waghule T, Narayan R, Singhvi G. UV spectroscopic method for estimation of temozolomide : Application in stability studies in simulated plasma pH , degradation rate kinetics , formulation design , and selection of disso. Spectrochim Acta Part A Mol Biomol

Spectrosc. 2021;258:119848.

52. Barauskas J, Cervin C, Jankunec M, Špandyreva M, Ribokaitė K, Tiberg F, et al. Interactions of lipid-based liquid crystalline nanoparticles with model and cell membranes. Int J Pharm. 2010 May;391(1–2):284–91.

53. Gaudin A, Song E, King AR, Saucier-sawyer JK, Bindra R, Desmaële D, et al. PEGylated squalenoyl-gemcitabine nanoparticles for thetreatment of glioblastoma. Biomaterials. 2017;105:136–44.

54. Deshpande S, Singh N. Influence of Cubosome Surface Architecture on its Cellular Uptake Mechanism. Langmuir. 2017;33(14):3509–16.

55. Sanchez L, Yi Y, Yu Y. Effect of partial PEGylation on particle uptake by macrophages. Nanoscale. 2017;9(1):288–97.

56. Petithory T, Pieuchot L, Josien L, Ponche A, Anselme K, Vonna L. Size-dependent internalization efficiency of macrophages from adsorbed nanoparticle-based monolayers. Nanomaterials. 2021;11(8):1963.

57. Rodrigues L, Schneider F, Zhang X, Larsson E, Moodie LWK, Dietz H, et al. Cellular uptake of self-assembled phytantriol-based hexosomes is independent of major endocytic machineries. J Colloid Interface Sci. 2019;553:820–33.

Chapter 7
Pharmacokinetics and Biodistribution

7.1. Introduction

Pharmacokinetics involves the study of absorption, distribution, metabolism, and elimination of drugs when administered to an animal or human body. It plays an essential role not only in the drug discovery and formulation development process but also during preclinical and clinical research. The time for which the drug remains in the body, the regions of the body where the drug distributes, and the amount of the drug reaching the target site, as well as rate of these processes can be altered by designing/modifying a suitable dosage form. The particle size, surface charge, morphology, and composition of the developed nanoformulation significantly alter the various pharmacokinetic parameters [1,2]. After the formulation development of a drug, it is essential to evaluate the pharmacokinetics fate of the drug from the designed formulation in the body. It also helps to fix the dosage regimen for the developed dosage form and to predict the human dose. Pharmacokinetics is initially evaluated in animals, preferably rats, prior to humans. This helps to select the best formulation, the dose, and the dosing frequency for the clinical trials in humans. It also assists in in vitro in vivo correlation (IVIVC) and establishing bioequivalence. The pharmacokinetics is evaluated based on various pharmacokinetic parameters generated using mathematical equations and models. The various pharmacokinetic parameters include the C_{max}, Area under the curve (AUC), plasma half-life ($t_{1/2}$), elimination rate constant, volume of distribution (Vd), clearance (CL), and Mean residence time (MRT) [3,4].

7.2. Materials and Instruments

Temozolomide was obtained as a gift sample from Biophore India Pharmaceuticals Pvt Ltd, Hyderabad, India. Perchloric acid (70 %, Fisher Scientific), Formic acid (98 %, CDH), EDTA (99.5 %, Himedia), Diethylether (Molychem), Whatman filter paper, Syringes (1 and 2 mL), and Microcapillary tubes were the lab materials used. Formulations optimized in Chapters 5 and 6 were further evaluated for pharmacokinetics. All the surgical instruments like scissors and forceps were sterilized before use. A high-speed homogenizer (Polytron® PT 1600E homogenizer by Kinematica) was utilized for tissue homogenization. Temperature-controlled centrifuge (Centrifuge 5430R, Eppendorf, Germany), and Vortexer (GeNei^{TM}) were used during sample processing.

7.3. Methods

7.3.1. Animals

Healthy male Wistar rats (250-300 g, 12-15 weeks old) were selected for evaluating the pharmacokinetics and biodistribution of TMZ and TMZ-loaded optimized nanoformulations. The study protocol (Protocol No. IAEC/RES/28/13) was approved by the Institutional Animal Ethics Committee (IAEC), BITS PILANI. The rats were kept in standard plastic cages maintained under controlled conditions (23 ± 2^{o}C, 60 ± 5% RH, and 12 h dark-light cycle) for 1 week. The animals were provided standard laboratory pellet food with water. All the experimental procedures were followed under the guidelines set by the IAEC and Committee for the Purpose of Control and Supervision of Experiments on Animals (CPCSEA), India.

7.3.2. Pharmacokinetic studies

Pharmacokinetic studies were conducted for pure TMZ solution, TMZ loaded liposomes, TMZ loaded PEGylated liposomes and TMZ loaded PEGylated LLCs. Animals were randomly selected, marked, and dosed as per their body weight. The rats were anesthetized for a short period using diethyl ether. The tail was cleaned with water and xylene using cotton. For pure TMZ, a solution was freshly prepared with normal saline. For formulations, the dispersions were also made in normal saline. A single dose of each formulation, equivalent of TMZ (10 mg/kg), was administered through the tail vein. Blood samples (0.5 mL) were collected at 0.08, 0.25, 0.5, 1, 2, 3, 4, 6, 8, 12 and 24 h respectively (n=4) from the retro-orbital sinus of the rat using the capillary tubes. The blood samples were immediately transferred into pre-chilled 2 mL centrifuge tubes containing 10 % w/v EDTA solution (anticoagulant). The tubes were mixed properly and immediately centrifuged at 8000 rpm, 4^{o}C for 10 min. The 200 µL supernatant plasma was collected and transferred to 100 µL of formic acid (1M) containing centrifuge tube. The samples were stored at -20^{o}C till further use. The samples were processed as mentioned in Chapter 3. TMZ concentration in blood plasma was estimated using the developed bioanalytical method and the respective pharmacokinetic profile was obtained [5,6].

7.3.3. Biodistribution studies

For biodistribution studies, after the administration, the rats were anesthetized and sacrificed at 1, 2, 4, and 8 h respectively (n=3) using cervical dislocation. The tissues (brain, kidney, liver, lungs,

spleen, and heart) were collected following a standard surgical procedure. The collected tissues were cleaned with ice-cold formic acid (4 % v/v) solution. The organs were dried using Whatman filter paper (no. 40) and weighed individually. According to the weight, ice-cold formic acid solution was added, 2 mL per gram of tissue, in a 50 mL tarson tube. The organs were thereafter homogenized at 20,000 rpm. The obtained fine homogenate was centrifuged at 7500 rpm for 30 min. The supernatant was collected and processed further for TMZ estimation as described in Chapter 3. TMZ concentration as per gram of tissue, in different organs was estimated using the developed bioanalytical method as described in Chapter 3 [7,8].

7.3.4 Data analysis

The data obtained was evaluated further using the pKsolver Excel-Add In. Various pharmacokinetic parameters were calculated and compared. Data were expressed as Mean ± SD. Statistical significance was determined following One-way ANOVA and multiple comparisons test using Graphpad Prism® with 95 % confidence interval (* $p < 0.05$, ** $p < 0.01$, *** $p < 0.001$, **** $p < 0.0001$)

7.4 Results and discussion

7.4.1. Pharmacokinetic studies

The plasma concentration-time profiles obtained after a single intravenous dose of only TMZ and the selected formulations in rats are represented in **Figure 7.1**. The pharmacokinetic parameters obtained following one compartmental model analysis are represented in **Table 7.1**. The plasma profiles (Figure 7.1) revealed that TMZ loaded PEGylated Liposomes and PEGylated LLCs produced higher plasma concentrations than pure TMZ and remained in plasma for longer period of time. However, uncoated liposomes did not show much difference from pure TMZ solution. This might be attributed to disruption of liposomal structure in system, uptake by macrophages and quick release of the drug. Half-life ($t_{1/2}$) for PEGylated LLCs and PEGylated Liposomes were found to be double (2.609 h) and 1.25 times (1.635 h), respectively, of $t_{1/2}$ for TMZ solution (1.310 h). Here, the $t_{1/2}$ was calculated from the terminal plasma concentrations. It was enhanced, probably due to lower distribution to other tissue/organs, controlled release and extended plasma circulation time. As the TMZ was encapsulated in a nanocarrier, it protected TMZ from plasma pH, slowed its' release and conversion to the metabolites, and lowered elimination of the drug leading to

enhanced plasma circulation time. The inset figure of **Figure 7.1** revealed that significantly higher TMZ concentrations were achieved with PEGylated liposomes and LLCs up to 6 h. A 2.762 fold (1.544 µg/mL) and 1.502 fold (0.840 µg/mL) increase in plasma concentration was achieved at 6 h in comparison to TMZ solution (0.559 µg/mL). Also 80% increase in $AUC_{0-\infty}$ for PEGylated LLCs (45.197 µg/mL*h) and about 25% increase for PEGylated liposomes (32.773 µg/mL*h) were observed compared to TMZ solution (25.958 µg/mL*h). However, uncoated liposome produced same $AUC_{0-\infty}$ as TMZ solution. These results confirmed that encapsulation of TMZ and PEGylation of Liposomes and LLCs led to enhanced plasma circulation time of TMZ and probably lesser distribution to other tissues/organs [9,10].

A 1.3 and 1.8-fold reduction in the Clearance (CL) was observed in case of PEGylated liposomes and PEGylated LLCs respectively in comparison to the TMZ. This confirmed that PEGylation of nanocarriers successfully reduced the clearance from the plasma. It is reported that even a 0.25-fold increase in plasma $t_{1/2}$ or a 0.25-fold decrease in clearance rate for drugs with short half-lives (< 2 h) is of great significance and it helps in dose reduction. The PEGylated LLCs demonstrated better pharmacokinetic parameters in comparison to PEGylated Liposomes. LLCs contain thicker lipid layers in comparison to liposomes. Also, the degree of PEGylation and PEG chain length plays an important role in enhancing the pharmacokinetic parameters [9,10].

The pharmacokinetics of TMZ-loaded liposomes and PEGylated liposomes was compared to evaluate the significance of PEGylation. When administered into the plasma circulation, liposomes are considered foreign particles and taken up by macrophages following opsonization. Opsonins are serum components that bind to the nanoparticle surface and form a protein corona which is recognized by the scavenger receptors of the RES system. This results in shorter plasma circulation time resulting in decreased plasma drug concentration. Organs rich in macrophages like the liver and spleen play an essential role. Only the opsonized liposomes are taken up by these organs and cleared from plasma when compared with the unopsonized liposomes (PEGylated). The uncoated liposomes are easily cleared from the plasma due to opsonization as indicated by the higher CL values for both pure TMZ and uncoated liposomes. Thus, shorter plasma circulation time and faster clearance are achieved. It is reported that PEGylation of liposomes creates a hydrophilic layer around the liposomes which helps escape the opsonization and uptake by macrophages. Although PEGylation does not completely escape the opsonization, it delays the process thus providing

longer circulating nanocarriers in comparison to the uncoated carriers. The extent of circulation time is determined by the length of the PEG chain and the degree of PEGylation. The significance of PEGylation in improving the circulation time was confirmed from the results obtained through the cell-uptake and pharmacokinetic studies [11,12].

Pharmacokinetic studies of TMZ-loaded uncoated LLCs was not conducted due to the possible chances of hemolysis. As the pharmacokinetic profile obtained with the TMZ-loaded uncoated liposomes was more or less similar to the pure TMZ, only the PEGylated nanocarriers were further evaluated for biodistribution studies.

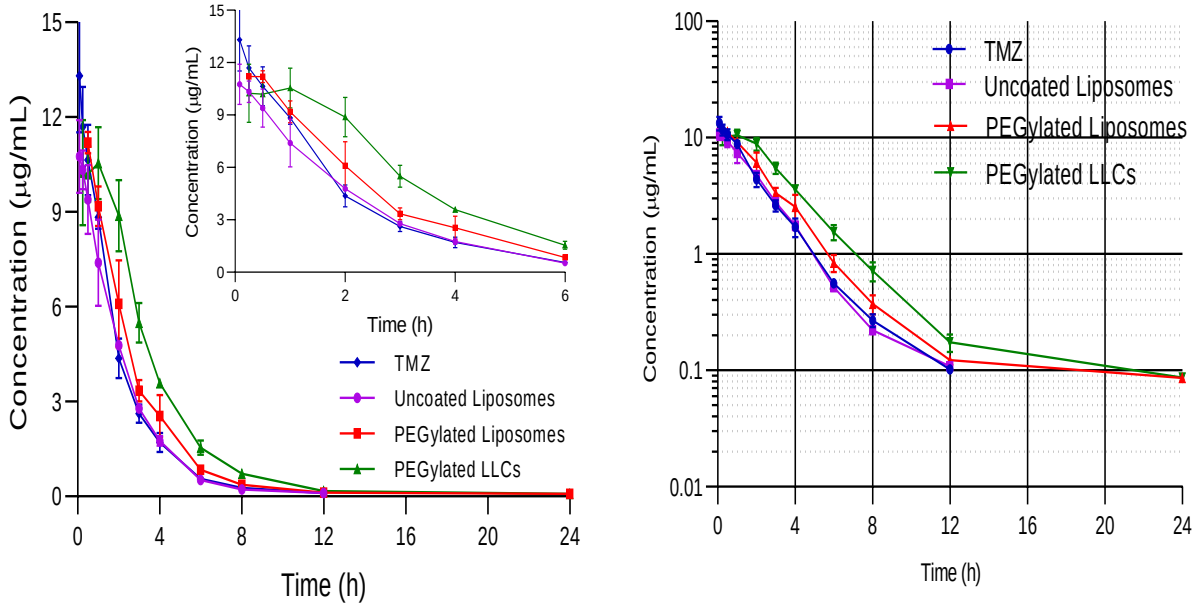

Figure 7.1. Plasma concentration-time profiles obtained for pure TMZ, TMZ-loaded uncoated liposomes, TMZ-loaded PEGylated liposomes, and TMZ-loaded PEGylated LLCs following i.v. administration (n =4 expressed as Mean ± SD).

Table 7.1. Pharmacokinetic parameters obtained for pure TMZ and the selected nanocarriers following i.v. administration (n =4 expressed as Mean ± SD)

	TMZ	**Uncoated Liposomes**	**PEGylated Liposomes**	**PEGylated LLCs**
K (1/h)	0.534 ± 0.067	0.458 ± 0.019	0.428 ± 0.052 *	0.270 ± 0.011 ****
$t_{1/2}$ (h)	1.310 ± 0.145	1.464 ± 0.097	1.635 ± 0.115 **	2.609 ± 0.095 ****
$AUC_{0-\infty}$ (µg/mL*h)	25.958 ± 1.684	25.218 ± 1.176 #	32.773 ± 3.295 *	45.197 ± 4.440 ****
Vd (L/kg)	0.729 ± 0.088	0.869 ± 0.078 **##	0.718 ± 0.021	0.744 ± 0.095
CL (L/kg/h)	0.386 ± 0.025	0.397 ± 0.018 ###	0.307 ± 0.029 **	0.222 ± 0.022 ****
MRT (h)	1.889 ± 0.216	2.185 ± 0.096	2.456 ± 0.310 *	3.703 ± 1.662 ****

* compared with pure TMZ, # comparison between uncoated liposomes and PEGylated liposomes using one-way ANOVA followed by multiple comparison tests (* p < .05, ** p < .01, *** p < .001, **** p < .0001)

7.4.2. Biodistribution studies

Both the PEGylated Liposomes as well as LLCs were found to improve brain bioavailability as indicated by the higher TMZ uptake in the brain **(Figure 7.2)**. A 2.91 and 6.31-fold increase in brain uptake was achieved at 8 h with PEGylated liposomes and PEGylated LLCs respectively in comparison to the free drug. When the biodistribution of PEGylated LLCs was compared with pure TMZ, it was observed that the distribution to brain is maximum enhanced ~ 44 % as observed from the $AUC_{0-\infty}$ values (25.49 µg/mL*h as compared to 14.27 µg/mL*h). For PEGylated liposomes, about 21 % enhancement was observed as indicated by the $AUC_{0-\infty}$ values of 18.20 µg/mL*h in comparison to pure TMZ (14.27 µg/mL*h). The above enhancement suggested that PEGylation enhanced the permeation of TMZ to brain, which was more in case of PEGylated LLCs in comparison to PEGylated liposomes. The enhanced brain bioavailability achieved by LLCs can be correlated to the enhanced plasma pharmacokinetic parameters achieved in comparison to the Liposomes. PEGylated liposomes are well established for other anti-cancer drugs for longer plasma circulation and enhanced brain bioavailability through passive targeting. Longer plasma circulation time allows more time for the drug to permeate the blood-brain barrier. Other possible mechanisms for enhanced brain bioavailability through the PEGylated nanocarriers could be enhanced retention time of nanocarriers in the brain capillaries, fluidization of the

endothelial cell membrane, and opening of tight junctions between the endothelial cells due to the lipidic nature of these carriers [13,14].

At 2 h, PEGylated liposomes showed a higher TMZ concentration in liver as compared to TMZ solution. It is reported that Liposomes are taken up by the reticuloendothelial system rich organs like the liver and spleen. Nanocarriers with size 100-200 nm are majorly taken up by the Kupffer cells of the liver. The uptake by the liver can be prevented through PEGylation of the nanocarrier surface. PEGylation confer hydrophilicity to the carrier surface which prevents the binding of opsonins. This prevents macrophage uptake and lowers the distribution thereby increasing the plasma concentration. Higher uptake of PEGylated liposomes to some extend by liver might have resulted in less plasma concentration than the PEGylated LLCs. However, PEGylated LLCs showed lower concentrations in liver as compared to TMZ solution. It is reported that due to their lipid composition, LLCs are mainly destroyed by the spleen. Nanocarriers with size larger than 400 nm undergo splenic filtration and get destroyed by the macrophages in the spleen. The uptake by the spleen can be reduced by reducing the particle size. As the LLCs particle size was less than 200 nm, they might have escaped the splenic macrophages [15–17].

The nanocarriers of size lower than 15 nm are expected to be eliminated through renal filtration. Not much change was observed in distribution to lungs and kidneys. In highly perfused organs like heart and kidney, in initial 1 h, PEGylated LLCs showed lower TMZ concentration in comparison to PEGylated liposomes and TMZ solution. However, by 4 h, the TMZ concentration attained was similar in TMZ solution, PEGylated liposomes and PEGylated LLCs. This indicates that encapsulation of TMZ in these nanocarriers can help in reduction of side effects and the possible cardiotoxicity. However, from the $AUC_{0-\infty}$ values, distribution to the heart was found to be drastically decreased in PEGylated liposomes but marginally decreased in PEGylated LLCs [15–17].

The disposition of nanocarriers after administration can be regulated by the lipid composition, surface charge, size, and dose. The nanocarrier uptake by organs is likely to be dependent on the blood flow rate, opsonins depletion, or saturation of uptake [15–17].

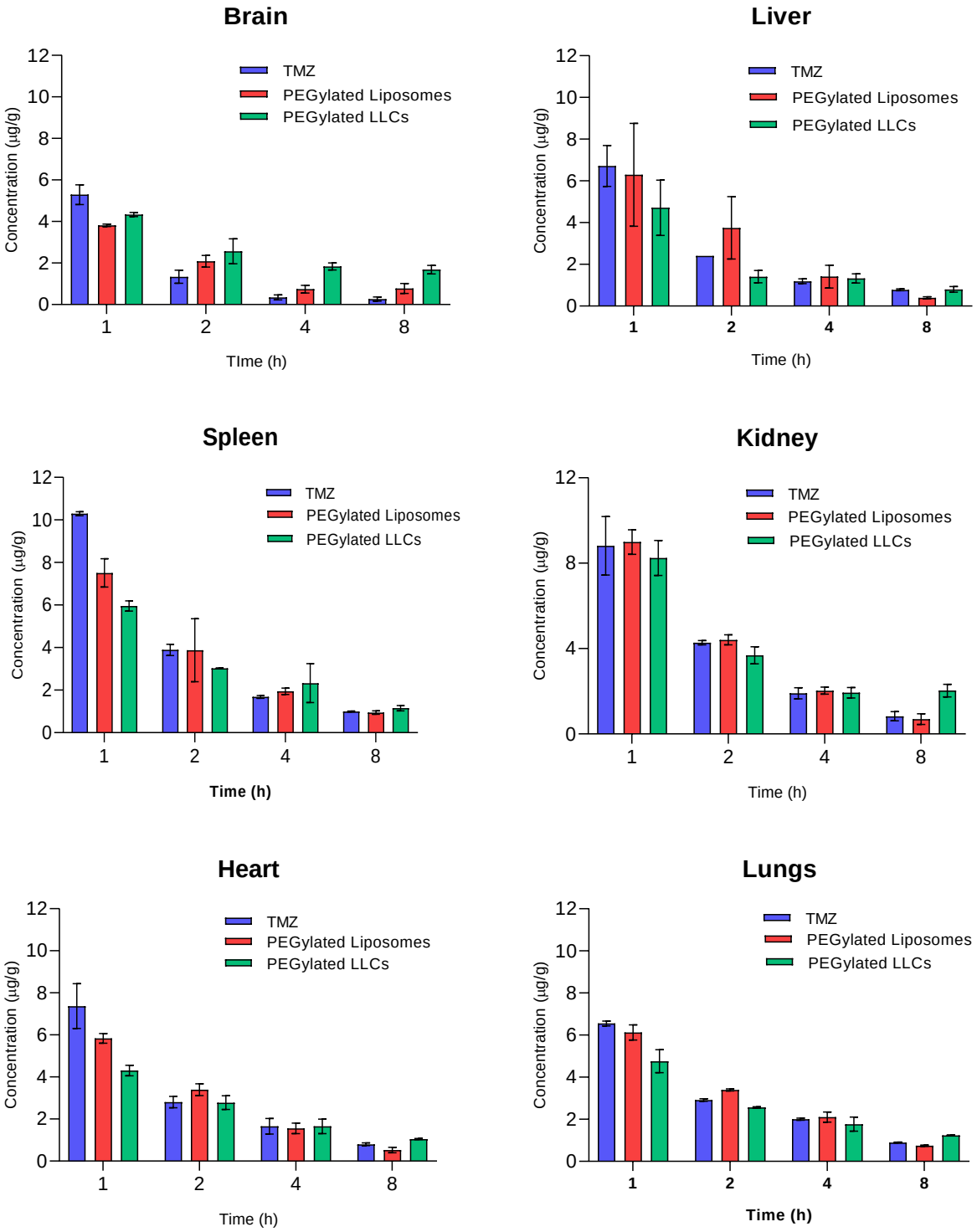

Figure 7.2: TMZ concentration in various organs following intravenous administration (n=3)

Table 7.2. Pharmacokinetic parameters for TMZ, TMZ-loaded PEGylated Liposomes, and TMZ-loaded PEGylated LLCs obtained in various organs following intravenous administration (n=3 expressed as Mean ± SD)

	TMZ		**PEGylated Liposomes**		**PEGylated LLCs**	
	$AUC_{0-\infty}$ (µg/g*h)	MRT (h)	$AUC_{0-\infty}$ (µg/g*h)	MRT (h)	$AUC_{0-\infty}$ (µg/g*h)	MRT (h)
Brain	14.27 ± 1.92	0.76 ± 0.14	18.20 ± 1.09	1.95 ± 0.34	25.49 ± 3.40	5.63 ± 0.60
Liver	18.22 ± 1.61	1.18 ± 0.14	17.94 ± 5.63	1.78 ± 0.39	13.87 ± 1.88	1.52 ± 0.97
Spleen	28.02 ± 0.06	1.20 ± 0.06	24.57 ± 3.52	1.92 ± 0.87	30.17 ± 3.71	3.35 ± 1.09
Kidney	26.64 ± 1.02	1.75 ± 0.33	27.51 ± 0.85	1.89 ± 0.24	24.96 ± 1.46	1.86 ± 0.07
Heart	20.36 ± 1.96	1.38 ± 0.01	9.50 ± 0.32	2.19 ± 0.11	19.61 ± 4.32	2.23 ± 1.45
Lungs	20.73 ± 0.00	2.08 ± 0.04	22.42 ± 1.17	2.63 ± 0.31	20.27 ± 0.95	3.01 ± 0.42

7.5 Conclusion

The pharmacokinetic and biodistribution studies of TMZ and the selected optimized formulations were successfully evaluated following the intravenous administration. Free TMZ was eliminated faster from the systemic circulation. Intravenous administration of TMZ-loaded lipid-based nanocarriers successfully resulted in prolonged residence of TMZ in systemic circulation with higher residence achieved with PEGylated LLCs followed by PEGylated Liposomes. Uncoated liposomes did not show much difference. The nanocarriers protected the entrapped TMZ from the plasma pH and reduced the conversion rate to the metabolites impermeable through BBB. PEGylation successfully resulted in longer plasma circulation time and enhanced brain bioavailability. The studies confirmed the possible potential of both the nanocarriers in the effective treatment of glioblastoma. Overall, the observations from the pharmacokinetic and biodistribution study indicated that modifying the formulation (either liposomes or LLCs) or changing the phospholipids can modify the distribution of drug to different organs with extended plasma circulation time leading to selective distribution to brain. Thus, selection of specific formulation type may make selective distribution to specific organs.

References

1. Serrano DR, Hernández L, Fleire L, González-alvarez I, Montoya A, Ballesteros MP, et al. Hemolytic and pharmacokinetic studies of liposomal and particulate amphotericin B formulations. Int J Pharm. 2013;447(1–2):38–46.

2. Raza K, Kumar P, Kumar N, Malik R. Pharmacokinetics and biodistribution of the nanoparticles. In: Advances in Nanomedicine for the Delivery of Therapeutic Nucleic Acids. Woodhead Publishing; 2017. p. 165–86.

3. Alavijeh MS, Chishty M, Qaiser MZ, Palmer AM. Drug Metabolism and Pharmacokinetics , the Blood-Brain Barrier , and Central Nervous System Drug Discovery. NeuroRx J Am Soc Exp Neurother. 2005;2:554–71.

4. Rosso Lula, Brock C, JM G, Saleem A , Price PM , Turkheimer FE AE. A New Model for Prediction of Drug Distribution in Tumor and Normal Tissues : Pharmacokinetics of Temozolomide in Glioma Patients. Cancer Res. 2009;69(1):120–7.

5. Gao J, Wang Z, Liu H, Wang L, Huang G. Liposome encapsulated of temozolomide for the treatment of glioma tumor : preparation , characterization and evaluation. Drug Discov Ther. 2015;9(3):205–12.

6. Narayan R, Singh M, Ranjan OP, Nayak Y, Garg S, Shavi G V., et al. Development of risperidone liposomes for brain targeting through intranasal route. Life Sci. 2016;163:38–45.

7. Khosa A, Krishna K V., Saha RN, Dubey SK, Reddi S. A simplified and sensitive validated RP-HPLC method for determination of temozolomide in rat plasma and its application to a pharmacokinetic study. J Liq Chromatogr Relat Technol. 2018;41(10):692–7.

8. Tang J, Wei H, Liu H, Ji H, Dong D, Zhu D, et al. Pharmacokinetics and biodistribution of itraconazole in rats and mice following intravenous administration in a novel liposome formulation. Drug Deliv. 2010;17(4):223–30.

9. Chow T, Lin Y, Hwang J, Wang H, Tseng Y, Wang S, et al. Improvement of Biodistribution and Therapeutic Index via Increase of Polyethylene Glycol on Drug-carrying Liposomes in an HT-29 / luc Xenografted Mouse Model. Anticancer Res. 2009;2120:2111–20.

10. Gunaydin H, Altman MD, Ellis JM, Fuller P, Johnson SA, Lahue B, et al. Strategy for Extending Half-life in Drug Design and Its Significance. ACS Med Chem Lett. 2018;9:528–33.

11. Klibanovl AL, Maruyamal K, Torchilin VP, Huangl L. Amphipathic polyethyleneglycols effectively prolong the circulation time of liposomes. 1990;268(1):235–7.

12. Rajamanickam M, Kosuru R. Trans resveratrol loaded DSPE PEG 2000 coated liposomes : An evidence for prolonged systemic circulation and passive brain targeting. J Drug Deliv Sci Technol. 2016;33:125–35.

13. Tian X-H, Lin X-N, Wei F, Feng W, Huang Z-C, Wang P, et al. Enhanced brain targeting of temozolomide in polysorbate-80 coated polybutylcyanoacrylate nanoparticles. Int J Nanomedicine. 2011;6:445–52.

14. Barenholz YC. Doxil ® — The fi rst FDA-approved nano-drug : Lessons learned. J Control Release. 2012;160(2):117–34.

15. Harashima H, Sakata K, Kiwada H. Distinction Between the Depletion of Opsonins and the Saturation of Uptake in the Dose-Dependent Hepatic Uptake of Liposomes. Pharm Res. 1993;10(4):606–10.

16. Cataldi M, Vigliotti C, Mosca T, Cammarota M. Emerging Role of the Spleen in the Pharmacokinetics of Monoclonal Antibodies , Nanoparticles and Exosomes. Int J Mol Sci. 2017;18:1249.

17. Zhang Y, Poon W, Tavares AJ, Mcgilvray ID, Chan WCW. Nanoparticle – liver interactions : Cellular uptake and hepatobiliary elimination. J Control Release. 2016;240:332–48.

Chapter 8
Summary and Future Perspectives

8.1 Summary

Glioblastoma is an abnormal proliferation of the glial cells and has the highest mortality rate. Among the few drugs like carmustine, lomustine, everolimus, bevacizumab, and temozolomide approved for the treatment of glioblastoma, temozolomide (TMZ) is considered a first choice. TMZ is a small molecule amphiphilic in nature. It attains 100 % bioavailability when administered in the form of oral capsules and intravenous infusion. Despite the high permeability through the blood-brain barrier, only 20-30 % brain bioavailability is achieved. This prodrug undergoes non-enzymatic modification at plasma pH. The resulting active metabolites cannot cross the blood-brain barrier due to their hydrophilic nature. The short half-life of TMZ limits the therapeutic efficacy. The limitations of conventional therapies can be tackled with nanomedicine.

We investigated two lipid-based nanocarriers with the aim to prolong the plasma circulation time of TMZ and higher distribution to brain. These nanocarriers entrap TMZ within, protect the drug from outside pH, reduce the conversion to its metabolites, release the TMZ over a prolonged period and thus enhance the plasma circulation time. Lipid-based nanocarriers have gained much attention due to their biocompatible nature. Liposomes are one of the nanocarriers successfully entering the market. These are phospholipid vesicles enclosing an aqueous core. Advanced research led to the discovery of unique structures known as lyotropic liquid crystals (LLCs). This mesophase contains properties of a crystal and liquid simultaneously. Liposomes and Lyotropic liquid crystals are nanocarriers with hydrophilic as well as lipophilic regions thus suitable for entrapment of amphiphilic drugs.

Before starting with the formulation development, an analytical and bioanalytical method was developed successfully for the estimation of TMZ in nanoformulation, release, plasma, and tissue samples. Initially, an analytical method was developed using UV-visible spectroscopy. Based on the solubility and stability of TMZ, 0.1 HCl (pH 1.2) and acetate buffer (pH 4.5) were selected as media for method development. The maximum absorbance of TMZ was found to be at 329 nm. The final stable metabolite, AIC, was found to show maximum absorbance at 267 nm which also indicated that the metabolite did not show any absorbance at drug wavelength (329 nm). The linearity range of TMZ in both media was found to be 4-24 µg/mL. The LOD and LOQ for TMZ in 0.1 N HCl were found to be 0.036 µg/mL and 0.109 µg/mL respectively. The LOD and LOQ for TMZ in acetate buffer were found to be 0.047 µg/mL and 0.144 µg/mL respectively. The

method was validated as per the ICH guidelines for repeatability, intra and inter-day precision, accuracy, specificity, and selectivity. The % RSD was less than 2 %. An analytical method was developed using HPLC with 0.5 % glacial acetic acid and methanol (9:1) as the mobile phase. The system suitability parameters were highly reproducible indicated by the low standard deviation values. The tailing factor was found to be ~ 1.2 which is within the acceptable range (0.8 – 1.5). Linearity was observed in the range of 0.1 to 10 µg/mL. The % RSD obtained was less than 2 %. The % recovery was in the range of 99.874 to 101.527 % which was within the acceptable range (95-105 %). A bioanalytical method was developed using HPLC with 0.5 % glacial acetic acid and methanol (98:2) as the mobile phase to estimate TMZ in plasma and tissue samples. The extraction efficiency obtained in plasma was above 95 %. All the developed methods were found to be reproducible, precise, and accurate.

Further, a few preformulation studies were conducted to assist in formulation development. TMZ was characterized by using ATIR and DSC. TMZ was found to have a solubility of 4.604 ± 0.22 mg/mL in water and aqueous buffers (pH 1-6). It was found to be unstable in pH conditions above 6 which was confirmed through the stability studies. The conversion of TMZ to AIC in alkaline conditions was confirmed through UV-visible spectroscopy. TMZ was found to be stable in normal saline, water for injection, and dextrose injection for up to 48 h. Appropriate pH needs to be maintained during the formulation and storage of TMZ. A partition coefficient of 0.311 was found between lipid (GMO) and water. The drug excipient compatibility studies revealed that refrigerated conditions are required to ensure drug stability. An appropriate dissolution medium was selected based on the stability of the drug and excipients.

During the formulation of liposomes and lyotropic liquid crystals (LLCs), various lipids, methods of preparation, and size reduction techniques were screened. Microfluidics and membrane extrusion techniques were found to produce liposomes with smaller particle sizes in a reproducible manner. From the various phospholipids screened, synthetic phospholipids were found to provide maximum TMZ entrapment. For LLCs, hot melt emulsification followed by probe sonication was found to provide a smaller particle size. Initially, the Quality Target Product Profile was designed and the various critical quality attributes were derived. The designed process flow map and fishbone diagram gave an overview of the entire liposome and LLCs formulation process and the factors/causes likely to cause variability in the quality attributes of the product. With the help of

relative risk-based matrix analysis and failure mode effect analysis, various critical material attributes and critical process parameters were identified. Thereafter, the effect of various material attributes and process parameters on critical quality attributes was studied in detail. During the formulation of liposomes, the temperature has to be maintained above the phase transition temperature of the phospholipids used. For liposomes, less number of factors were found to be critical, thus the effect was studied individually. For LLCs, the effects were studied with the help of experimental design and Design Expert Software. The data was analyzed using statistics and various model graphs. Design space was also established. The entrapment efficiency of TMZ in these nanocarriers was found to be mainly dependent on the internal to external volume ratio. The optimized formulations were further PEGylated using DSPE-PEG 2000. All the nanocarriers were in the 80-150 nm particle size range with narrow size distribution. The PEGylated nanocarriers carried a negative surface charge as compared to the uncoated nanocarriers. The entrapment efficiency obtained with liposomes, PEGylated liposomes, LLCs, and PEGylated LLCs was 45.014 ± 4.835, 42.994 ± 3.303, 37.46 ± 5.481 and 40.451 ± 2.561 % respectively. The morphology of these nanocarriers was confirmed using various microscopic techniques. TMZ was found to follow first-order kinetics whereas the TMZ loaded formulations were found to follow the Korsmeyer Peppas model. The nanocarriers were found to show a prolonged release up to 24-72 h.

PEGylated LLCs were found to reduce the hemolytic potential of GMO. TMZ-loaded Liposomes and TMZ-loaded PEGylated Liposomes were found to show 1.71 and 1.59 fold more cytotoxicity as compared to TMZ alone. TMZ-loaded LLCs and TMZ-loaded PEGylated LLCs were found to show 2.22 and 1.54 fold more cytotoxicity as compared to TMZ alone. The PEGylated nanocarriers were found to follow a different path for uptake in U87 cell lines in comparison to the uncoated nanocarriers. PEGylated LLCs were found to show more cell uptake in U87 glioblastoma cell lines as compared to LLCs. PEGylated nanocarriers were found to significantly reduce the uptake by macrophage cell lines. The pharmacokinetic parameters and biodistribution data confirmed that encapsulation of TMZ within Liposomes and LLCs led to enhanced plasma circulation of TMZ. PEGylated LLCs were able to prolong the plasma circulation time to double whereas PEGylated Liposomes by 1.25 fold in comparison to TMZ solution. The prepared nanocarriers released the encapsulated TMZ in a sustained manner and successfully protected TMZ from plasma pH. This provided delayed conversion of TMZ to the metabolites in comparison

to the TMZ alone. The pharmacokinetic parameters also confirmed the significance of PEGylation. Also, a 1.3 and 1.8-fold reduction in the clearance was observed with PEGylated liposomes and PEGylated LLCs respectively in comparison to the TMZ. Prolonged plasma circulation time along with reduced clearance rate for a drug with short half-life like TMZ is of great significance which was confirmed through biodistribution study. A 2.91 and 6.31-fold increase in brain uptake was achieved at 8 h with PEGylated liposomes and PEGylated LLCs respectively in comparison to the TMZ solution. The PEGylated LLCs were found to show better pharmacokinetics and biodistribution in comparison to PEGylated Liposomes in rats following intravenous injection.

8.2 Outcomes

The principles of Quality by Design and Design Expert software were explored for lipid-based nanocarriers. TMZ-loaded liposomes were investigated using microfluidics and membrane extrusion techniques for the first time. TMZ-loaded PEGylated LLCs were also investigated for the first time in this study. Both the nanocarriers were investigated using industrial feasible techniques which were found to be reproducible. The effect of various material attributes and process parameters on the key characteristics of the liposomes and LLCs were investigated. The nanocarriers were found to improve the plasma circulation time, hence, the pharmacokinetics and biodistribution of TMZ. For different drugs, different types of formulations can be designed to achieve selective distribution to different organs.

8.3 Future perspectives

- The formulations can be further modified/explored with other novel lipids/ surfactants/ coating agents.
- The optimized formulations can be further investigated in disease animal models.
- The optimized formulations can be further investigated for delivery through other routes like nasal administration.
- The information obtained can be used for the formulation design of other drugs with similar physicochemical properties as of Temozolomide.
- The formulations can be further investigated for clinical application.

Appendixes

List of Publications and Conferences

Research articles

1. **Waghule T**, Swetha KL, Roy A, Saha RN, Singhvi G. Exploring temozolomide encapsulated PEGylated liposomes and lyotropic liquid crystals for effective treatment of glioblastoma: in-vitro, cell line, and pharmacokinetic studies. European Journal of Pharmaceutics and Biopharmaceutics. 2023 May 1;186:18-29.

2. Waghule T, Saha RN, Singhvi G. Exploring microfluidics and membrane extrusion for the formulation of temozolomide-loaded liposomes: investigating the effect of formulation and process variables. Journal of Liposome Research. 2022 Nov 11:1-3.

3. Waghule T, Swetha KL, Roy A, Saha RN, Singhvi G. Quality by design assisted optimization of temozolomide loaded PEGylated lyotropic liquid crystals: Investigating various formulation and process variables along with in-vitro characterization. Journal of Molecular Liquids. 2022 Apr 15;352:118724.

4. Waghule T, Saha RN, Singhvi G. UV spectroscopic method for estimation of temozolomide: Application in stability studies in simulated plasma pH, degradation rate kinetics, formulation design, and selection of dissolution media. Spectrochimica Acta Part A: Molecular and Biomolecular Spectroscopy. 2021 Sep 5;258:119848.

5. Waghule T, Rapalli VK, Singhvi G, Gorantla S, Khosa A, Dubey SK, Saha RN. Design of temozolomide-loaded proliposomes and lipid crystal nanoparticles with industrial feasible approaches: comparative assessment of drug loading, entrapment efficiency, and stability at plasma pH. Journal of Liposome Research. 2021 Apr 3;31(2):158-68.

Review articles

1. Waghule T, Saha RN, Alexander A, Singhvi G. Tailoring the multi-functional properties of phospholipids for simple to complex self-assemblies. Journal of Controlled Release. 2022 Sep 1;349:460-74.

2. Waghule T, Dabholkar N, Gorantla S, Rapalli VK, Saha RN, Singhvi G. Quality by design (QbD) in the formulation and optimization of liquid crystalline nanoparticles (LCNPs): A risk based industrial approach. Biomedicine & Pharmacotherapy. 2021 Sep 1;141:111940.

3. Rapalli VK, Waghule T, Hans N, Mahmood A, Gorantla S, Dubey SK, Singhvi G. Insights of lyotropic liquid crystals in topical drug delivery for targeting various skin disorders. Journal of Molecular Liquids. 2020 Oct 1;315:113771.

Book chapters

1. Batra U, Waghule T, Saha RN, Singhvi G. Liposomal Drug Delivery. Nanoparticles and Nanocarriers Based Pharmaceutical Formulations. 2022 Dec 9:303.

Patents filed

1. Temozolomide – Lyotropic Lipid Nanoparticle Composite, 202111026752

2. Prolyotropic liquid crystals and method for preparing the same, 201911016252

Conferences attended and Poster presentations

1. Was selected as Zonal 1st Runner up and Semifinalist (received a cash prize of ₹ 7,000/-) in All India 'DRPI 2021 – Online' under PhD category. It is a scientific research presentation competition for young pharmaceutical researchers across academia and industry, organized by SPDS in association with AAPS and APTI. (Title: Selection of an appropriate dissolution medium and release mechanism from lipid based nanoparticles)

2. Participated and poster presented in "Dissolution Science and Applications, Theme: Ensuring Built-in Quality through Dissolution Studies" organized by National Institute of Pharmaceutical Education and Research (NIPER), SAS Nagar, Chandigarh from 12-13th September, 2019 (Poster details: Tejashree Waghule, Vamshi Krishna Rapalli, Srividya Gorantla, Ranendra N. Saha, Sunil K Dubey, Gautam Singhvi. Enhanced stability and prolonged drug release of temozolomide through lipid based nanocarriers)

Biography of Prof. Ranendra N. Saha

Dr. Ranendra N. Saha is a former Senior Professor of Pharmacy, Former Vice Chancellor (Acting) of BITS PILANI, pilani campus and Former Director of BITS Pilani, Dubai Campus, UAE. In 2011 he has been awarded Shri B. K. Birla and Shrimati Sarala Birla Chair Professorship at BITS Pilani. He has completed his PhD from BITS, Pilani. Prof. Saha has more than 40 years of teaching, research and administrative experience and guided several doctoral, postgraduates and undergraduate students. He has vast experience in the field of Pharmacy especially in Pharmaceutics, novel drug delivery systems and pharmacokinetics. He received "Pharmacy Professional of the Year 2013" award from Indian Association of Pharmaceutical Sciences and Technologists. He has published book, several book chapters, review and research articles in renowned international and national journals and presented papers in conferences conducted in India and abroad. Prof. Saha received 'Pharmacy Teacher of India of the Year- 2005' award given by Association of Pharmaceutical Teachers of India (APTI). Dr. Saha has successfully completed several government and industry sponsored projects. He has obtained patent on novel delivery systems entitled, "Stable Controlled Release Pharmaceutical Composition Comprising Aceclofenac", which is commercialized, and brought to Indian market by Ipca Lab Ltd, Mumbai. He has visited abroad on several occasions on invitation from universities and associations to deliver lectures. He has organized several national and international conferences. He is a passionate teacher who inspires and motivates his students to face the challenges in all aspects of career and life. His way of teaching and explaining the concepts to the students is just admirable.

Biography of Dr. Gautam Singhvi

Dr. Gautam Singhvi is working as an Assistant Professor in the Department of Pharmacy, BITS PILANI, Pilani campus since 2015. He has industrial and research experience in pharmaceutical solid oral, pellets, and nanocarrier development. His major research focus is on developing industrially feasible preparation techniques and pharmaceutical formulation. He has been involved in more than 8 formulations which were successfully scaled-up and commercialized. He has published several mini-reviews, book chapters, review and research articles in reputed international and national peer-reviewed journals. He has also filed 6 patents. He is a peer-reviewer of several national and international journals. He is a passionate teacher who inspires and motivates his students to face the challenges in all aspects of career and life.

Biography of Tejashree Waghule

Ms. Tejashree has completed her B. pharm from Bombay College of Pharmacy, Kalina in 2017. She has completed her M. pharm from Birla Institute of Technology and Sciences (BITS PILANI), Pilani campus in 2019. In 2019, she received vertical transfer from M. pharm to PhD. During her M. pharm and PhD in BITS PILANI, she has published book chapters, several review and research papers in reputed journals. She has attended and presented her research work in several conferences. She has research experience in analytical method development and validation, preformulation, formulation optimization and characterization of various lipid based nanocarriers, Quality by Design, and pharmacokinetic studies. Her name was listed in World's Top 2 % scientists list published in 2022 by Stanford University and Elsevier.